

Techno-economic evaluation of a novel biomass pyrogasification process with an integrated sorption-shift system

Master Thesis

Jesse Buiteveld

February 2021

UNIVERSITY OF TWENTE.

Faculty of Engineering Technology

Techno-economic evaluation of a novel biomass pyrogasification process with an integrated sorption-shift system

A process for the conversion of waste to high-quality biochar and hydrogen with carbon capture and hydrogen upgrading

Faculty of Engineering Technology

Master Thesis

In fulfillment of the requirements for the degree of Master of Science in Mechanical Engineering and Master of Science in Sustainable Energy Technology

Author:

J. Buiteveld (s1495186)

Graduation committee:

Chair:

Prof. dr. ir. G. Brem

Supervisor:

ir. E.A. Bramer

External member:

dr. M.P. Ruiz Ramiro

External member:

dr. E.H.J.M. Coenen

Project started: 17-02-2020

Thesis issued: 09-02-2021

Defence : 16-02-2021

UNIVERSITY OF TWENTE.

Department of Thermal and Fluid Engineering
University of Twente
7500 AE Enschede
the Netherlands
09-02-2021

Abstract

This thesis describes the development of a novel system that produces high-quality biochar and high-purity hydrogen out of biomass. The proposed system uses a combination of pyrolysis in an auger reactor, steam reforming, and a novel Sorption Enhanced Water Gas Shift (SEWGS) system based on Calcium Looping (CaL). This system uses calcium oxide (CaO) for CO_2 capture and to shift the Water-Gas-Shift (WGS) reaction into the direction of hydrogen. A system parameter analysis identified key process parameters for optimal hydrogen/biochar production. Reactor temperature has been identified as the main key process parameter for the pyrolysis (≈ 600 °C) and steam-reforming system (≈ 750 °C), while system configuration is identified as the main key parameter for the sorption-shift system: a decoupled sorption-shift system can produce high purity hydrogen with H_2 Vol % > 99.6%. The figure below displays the system configuration which is analysed in this research.

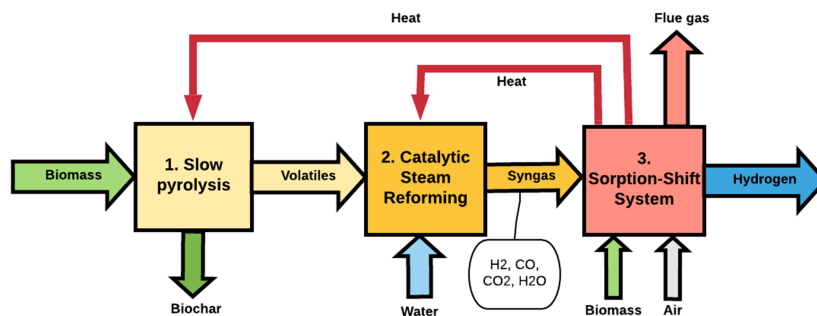


Figure 0.1: General system configuration pyrogasification SEWGS system

An Aspen Plus model is constructed to simulate reactor stoichiometry, develop efficient heat integration, and for system analysis and evaluation. Results from the developed model are used for process optimization. The designed system operates at a reformer temperature of 750 °C, a final sorption shift temperature of 550 °C, and a Steam to Carbon (SC) ratio of 4.6 in the pre-reformer. Process simulations show an overall maximum energy efficiency of 74.9% based on chemical energy. High-quality biochar is produced: HHV=34.2 MJ/kg as well as high-quality hydrogen: 99.7% purity. Per ton of dry and ash-free biomass input (HHV = 18.0 MJ/kg), the system produces 59 kg of hydrogen and 186 kg of biochar. A sensitivity analysis identified (pre-) reformer heating as the main bottleneck in the system.

A financial model is constructed for the designed system based on cash-flow simulations. Biomass input cost and investment cost are identified as the main driver of hydrogen/biochar levelized cost of production. Heat exchanger size optimization is performed with respect to cost efficiency, resulting in a system with a levelized cost of hydrogen of €4.01 per kg combined with a levelized cost of biochar of €668 per ton. The optimized system with respect to cost efficiency has a thermal efficiency of 71.4 %. Subsidies are required for a profitable system. Compared to other sustainable high purity hydrogen production techniques, the designed system is compatible and produces high purity hydrogen at a significantly lower cost than hydrogen production by electrolysis.

A societal analysis is performed which identified the analyzed technology as fitting with future biomass-based policies of western European countries which focus on high quality bio-based raw materials. This analysis shows that there is sustainable biomass potential in Europe and the Netherlands for the developed technology. Biochar has many high-end applications, varying from pollutant removal from gases (activated carbon) to carbon sequestration (soil amendment). A model is designed for CO_2 footprint calculations of the installation under operation, which shows a negative CO_2 footprint -1041 kg CO_2 per ton of biomass input: the process has the potential to reverse global warming.

Further process optimizations and development is recommended for a better understanding of CaL based SEWGS, especially for understanding CaL-based SEWGS kinetics. We wrote a research proposal for a (European) research project to further analyze SEWGS reactor mechanics. Upscaling of auger reactors for slow pyrolysis and implementing oxy-fuel combustion for CaO regeneration are subjects that require further research. The oxy-fuel system is (shortly) analyzed, and shows a large future potential, especially in a combined process configuration with water electrolysis for hydrogen production. This research shows that a pyrogasification sorption enhanced water gas shift system can be a technical, economic, and societal feasible technology that delivers high-quality, sustainable products that fit the needs of the future sustainable economy.

Keywords: hydrogen, biochar, biomass, pyrolysis, gasification, pyrogasification, steam reforming, calcium looping, CO_2 absorption, pre-combustion carbon capture, heat integration, aspen plus modeling, sorption enhanced water gas shift, economic optimization, societal analysis, CO_2 footprint, system optimization

Preface

Sustainability has always been a great interest of mine. After completing my bachelor's in mechanical engineering, I continued my academic career with a Master in Sustainable Energy Technology (SET). Although I enjoyed the courses very much in the SET master, I wanted to learn more in-depth engineering tools to solve sustainable energy-related problems. Therefore, after one year of courses from the SET curriculum, I decided to combine the SET master with a Mechanical Engineering Master in Thermal and Fluid engineering. The mechanical engineering master courses were challenging, and I am proud that I finished all these courses and I can present my master assignment in this work.

My graduation project started in February 2020. At the time, a part of my research would be experimental: to test the novel system discussed in this work. Due to the COVID-19 pandemic, things changed, the university closed down, and I had to work from home. Working from home was hard, especially in the first few months when there was a lot of uncertainty. The COVID-19 pandemic made things much harder in 2020, but I look positive to the future and to a brighter 2021 where hopefully, everything will get slowly back to normal.

First of all, I want to thank Eddy Bramer for all the help and constructive conversations we had during my graduation project. Next, I want to thank Gerrit Brem, who in January 2020 introduced the novel concept discussed in this thesis to me. Finally, I also want to thank Herman Klein Teeselink, who helped me with the economic evaluation discussed in this work. The insights given by Herman, based on full-scale biomass processing experience, improved my work significantly. I also want to thank my family and friends for their unconditional support. I want to give a special thank you to my parents, who always encouraged me to learn more and supported me throughout my studies. I also want to thank Eva, who always supported me, especially when I was struggling.

I've always wanted to contribute to the energy transition, to make the Netherlands and the world a better, cleaner place without fossil fuels. During my internship at HoSt bio-energy installations, I learned a lot about implementing bio-based raw materials (biomass) as a sustainable energy source. I found that there is considerable potential of waste to energy systems for the production of sustainable energy. I want to contribute to these technologies and make sure that these technologies will be implemented on a large scale in the near future. To do so, I will start in March 2021 as a project developer at HoSt, where I want to make a large contribution to the energy transition.

Jesse Buiteveld
February 2021

Nomenclature

<i>BEWCCS</i>	Bio Energy With Carbon Capture and Storage
<i>CaL</i>	Calcium Looping
<i>CAPEX</i>	Capital Expenditure
<i>CFB</i>	Circular Fluidized Bed
<i>daf</i>	dry and ash free
<i>DIC</i>	Direct and Indirect Cost
<i>DPC</i>	Direct Plant Cost
<i>DSM</i>	Demand Side Management
<i>ER</i>	Equivalence Ratio
<i>GH</i>	Greenhouse
<i>GHSV</i>	Gas Hourly Space Velocity
<i>GWP</i>	Global Warming Potential
<i>HEX</i>	Heat Exchanger
<i>HHV</i>	Higher Heating Value
<i>HTS</i>	High Temperature Shift
<i>IRR</i>	Initial Rate of Return
<i>Ktoe</i>	Kilo ton oil equivalent
<i>LCOH</i>	Levelized Cost Of Hydrogen
<i>LHV</i>	Lower Heating Value
<i>LMTD</i>	Log Mean Temperature Difference
<i>LTS</i>	Low Temperature Shift
<i>MSR</i>	Methane Steam Reforming
<i>MSW</i>	Municipal Solid Waste
<i>Mtoe</i>	Mega ton oil equivalent
<i>OPEX</i>	Operational Expenditure
<i>PEM</i>	Polymer Electrolyte Membrane
<i>PGSS</i>	PyroGasification Sorption Shift
<i>PSA</i>	Pressure Swing Absorption
<i>SBR</i>	Steam to Biomass Ratio
<i>SC</i>	Steam to Carbon

<i>SCWG</i>	Super Critical Water Gas Shift
<i>SEWGS</i>	Sorption Enhanced Water Gas Shift
<i>SOM</i>	Soil Organic Matter
<i>SSM</i>	Supply side Management
<i>TCI</i>	Total Capital Investment
<i>TDC</i>	Total Depreciable Cost
<i>TGA</i>	thermogravimetric analysis
<i>TSA</i>	Temperature Swing Absorption
<i>VOC</i>	Volatile Organic Compound
<i>WACC</i>	Weighted Average Cost of Capital
<i>WGS</i>	Water Gas Shift

Contents

List of Figures	xii
List of Tables	xiv
1 Introduction	1
1.1 The big challenge of the energy transition	1
1.2 Supply side management of the future energy economy: hydrogen fuel and carbon capture	2
1.3 Biomass: a dispatchable sustainable energy source and a means for carbon capture	2
1.4 Thermal conversion paths for biomass-based hydrogen production	3
1.5 Pre-combustion carbon capture and gas upgrading	4
1.6 Research goal	4
1.7 Method and outline	5
2 Literature review: system parameter analysis	7
2.1 Pyrolysis system	7
2.1.1 Pyrolysis mechanics	7
2.1.2 Pyrolysis temperature	8
2.1.3 Pyrolysis residence time	9
2.1.4 pyrolysis heating rate	9
2.2 Gasification and steam reforming	10
2.2.1 Gasification mechanics	10
2.2.2 Catalyst type	11
2.2.3 Gasification temperature	11
2.2.4 Steam to carbon ratio	13
2.2.5 Reactor pressure	14
2.2.6 Residence time (specific gasification rate)	14
2.3 Sorption-shift system	14
2.3.1 Temperature and (partial CO ₂) pressure	15
2.3.2 System configuration	15
2.4 Overview key process parameter per system	17
3 Model Design	19
3.1 Process configuration options	19
3.2 Process configuration selection	24
3.3 Reactor options	24
3.4 Reactor selection	26
3.5 Results	27
4 Aspen Plus model pyrogasification SEWGS system	29
4.1 Model assumptions and basic equations	29
4.1.1 Pyrolysis system assumptions	29
4.1.2 Catalytic reforming system assumptions	30
4.1.3 Sorption-Enhanced-Water-Gas-Shift system	31
4.2 Aspen plus pyrolysis model	31
4.2.1 Slow-pyrolysis product composition	32
4.2.2 Modeling slow Pyrolysis stream results	33
4.2.3 Energy flows slow pyrolysis	33
4.3 Aspen plus steam reforming model	34
4.3.1 Stream results steam reforming system	35
4.3.2 Energy flows steam reforming system	36
4.3.3 Reforming model results validation	36

4.4	Aspen plus SEWGS system	37
4.4.1	Stream results sorption-shift system	37
4.4.2	Stream results calcination reactor	38
4.4.3	Energy flows sorption-shift system	39
4.4.4	SEWGS model results validation	40
4.5	System efficiency	41
4.6	Results	42
5	Sensitivity analysis pyrogasification model	43
5.1	Reactor temperature sorption-shift-1	43
5.2	Reactor temperature sorption-shift-2	45
5.3	Reactor temperature regenerator	46
5.4	Pinch point heat exchangers	48
5.5	SC ratio	49
5.6	Results	51
6	Financial model pyrogasification SEWGS system	53
6.1	Weighted Average Cost of Capital	53
6.2	Expected income	54
6.3	CAPEX estimation	54
6.3.1	Reactors	55
6.3.2	Heat exchangers	56
6.3.3	Other process equipment cost	58
6.3.4	Total capital investment	59
6.4	OPEX	60
6.4.1	variable cost	60
6.4.2	Fixed cost	62
6.4.3	Company general operating expenses	62
6.4.4	Results OPEX pyrogasification SEWGS system	62
6.5	Cash flow simulations	63
6.5.1	Scenario 1: no additional subsidies	64
6.5.2	Scenario 2: break even	64
6.5.3	Scenario 3: expected subsidies	65
6.6	Sensitivity analysis and cost optimization	66
6.6.1	Heat exchanger optimization	66
6.6.2	Sensitivity analysis biomass cost and catalyst/sorbent replacement strategies	69
6.7	Discussion	70
6.8	Conclusion	70
7	Societal study on a biomass powered pyrogasification SEWGS system	71
7.1	Future biomass policy guidelines in the Netherlands	71
7.2	Biomass potential in Europe and the Netherlands	72
7.2.1	Europe	72
7.2.2	the Netherlands	73
7.3	Biochar applications	74
7.3.1	Carbon sequestration using biochar as soil amelioration	74
7.3.2	Pollutant removal	75
7.3.3	Carbon black replacement	75
7.3.4	Substitute of fossil fuels	75
7.4	Biomass quality variability	76
7.5	Carbon footprint	77
7.5.1	Model for carbon dioxide footprint calculations	77
7.5.2	Results CO2 footprint	78
7.6	Discussion	79
7.7	Conclusion	79
8	Future perspective: oxy-fuel regeneration and partial combustion reformer	81
8.1	Process simulation results	82
8.2	Pyrogasification SEWGS oxy-fuel system with reduced SC ratio	84
8.3	Cost analysis oxy-fuel system	84

8.3.1	CAPEX	84
8.3.2	OPEX	86
8.3.3	Results and cash flow simulations	87
8.4	Carbon footprint oxy-fuel system	88
8.5	Discussion	88
8.6	Conclusion	89
9	Research proposal	91
9.1	Research up to date in CaL based SEWGS	91
9.2	Research goals	92
9.3	Deliverables	93
9.4	Required resources	93
9.5	Planning	94
10	Discussion	95
10.1	Pyrolysis system	95
10.2	Reforming system	96
10.3	Sorption enhanced gasification system	97
10.4	Socio-economic analysis	97
11	Conclusion and recommendations	99
11.1	Conclusion	99
11.2	Recommendations	100
Bibliography		103
Appendices		111
A	Reactor types for thermal processing of biomass	111
B	Aspen plus flowsheets pyrogasification SEWGS system	113
C	Energy calculations thermal processing of biomass	116
D	Sankey Diagram pyrogasification SEWGS system	120
E	Limitations for carbon capture using metal oxides	121
F	Sensitivity analysis pyrogasification SEWGS system additional graphs	124
G	Hydrogen fuel specifications for fuel cell applications	127
H	Additional cost analysis	128
I	Graphs for cost estimation	129
J	Sensitivity analysis OPEX	131
K	Biomass characteristics related to thermal conversion	134
L	Alternative Hydrogen production processes out of biomass: biological and SCWG	137
M	Societal analysis bar graphs CO2 footprint	140
N	Paper draft: Techno-economic analysis of a novel pyrogasification-sorption-shift system for the production of a high purity hydrogen and high quality biochar out of biomass	141
O	Research proposal for further research	164
P	Proceedings "Young Professionals in Power Engineering" conference, Wroclaw University, Poland	174
	Abstract Young Professionals in Power Engineering conference	175
	Conference Paper	177

List of Figures

Chapter 2

2.1	General reaction mechanism thermal treatment biomass	8
2.2	(a) : Slow pyrolysis product yield as a function of process temperature and (b):Slow pyrolysis product quality as function of process temperature	9
2.3	Influence heating rate and reactor temperature of slow pyrolysis on char yield	9
2.4	Syngas yield for gasification as a function of reactor temperature, using a dolomite catalyst	12
2.5	Representation temperature range and hydrogen yield for 1. sorption enhanced gasification, 2. Catalytic (Steam) gasification	13
2.6	CO ₂ Equilibrium pressure versus CO ₂ partial pressure in typical syngas under ambient pressure	15
2.7	Two possible simplified system configurations for <i>in situ</i> sorption enhanced gasification of biomass	16
2.8	General overview calcium looping system for pre-combustion carbon capture	17

Chapter 3

3.1	General system configuration	19
3.2	Process diagram scenario 1: Sorption enhanced gasification	20
3.3	Process diagram scenario 2: Separate reformers and uncoupled shift-system	21
3.4	Process diagram scenario 3: Coupled SEWGS system with air combustion	22
3.5	Process diagram scenario 4: Coupled SEWGS system with oxy-fuel combustion	23
3.6	Different types of fluidized bed reactors	25
3.7	General schematics auger reactor	25
3.8	Process diagram Coupled SEWGS system with air combustion	27

Chapter 4

4.1	Overview simplified Aspen Plus model	29
4.2	Overview model for Pyrolysis	31
4.3	Sankey diagram pyrolysis system	34
4.4	Overview model for reforming	34
4.5	Sankey Diagram gasification system	36
4.6	Overview model for calcium looping based SEWGS including heat regeneration	37
4.7	Sankey diagram sorption shift system	39
4.8	Sankey diagram downstream gas treatment	40

Chapter 5

5.1	Relative carbon absorption per reactor as function of sorption-shift-1 reactor temperature	44
5.2	Overall system efficiency as function of Shift-1 temperature	44
5.3	Temperature sorption-shift-reactor versus overall system efficiency	45
5.4	Carbonation temperature versus syngas concentrations sensitivity results Aspen Plus	45
5.5	Carbonation temperature versus syngas concentrations sensitivity results Aspen Plus	46
5.6	Regenerator CO ₂ equilibrium pressure and flue gas CO ₂ partial pressure as a function of regenerator temperature	46
5.7	Overall system efficiency as a function of regeneration temperature	47
5.8	Overall system efficiency as a function of lower limit pinch point of gas-gas heat exchanger and boilers	48
5.9	Steam temperature and flue-gas temperature (after heating pre-reformer) as function of the lower limit pinch point of gas-gas heat exchanger and boilers combined with temperature limits given the lower limit pinch point boundary conditions	49

5.10 Overall system efficiency versus SBR	50
5.11 Hydrogen and containment concentration product gas as function of the SC ratio, excluding water	50
Chapter 6	
6.1 System overview with HEX highlighted	57
6.2 Overview operational cost Pyrogasification sorption-shift system	63
6.3 Discounted cumulative cash flows for scenario 1: no subsidies, no CO ₂ taxation	64
6.4 Discounted cumulative cash flows for scenario 3:break even	64
6.5 Discounted cumulative cash flows for scenario 4: with subsidies	66
6.6 Influence pinch points HEX on hydrogen production cost	67
6.7 Influence pinch points HEX on hydrogen production cost without air pre-heating	67
6.8 Influence pinch points air pre-heater HEX on hydrogen production cost, other minimum Pinch Point boundary conditions: 25°C	68
Chapter 7	
7.1 SER classification of biomass utilisation ranging from low end quality applications (bottom) to high end applications (top)	72
Chapter 8	
8.1 General process overview combined PGSS with hydrogen production from electrolysis	82
8.2 Pyrogasification sorption-shift system with oxy-fuel combustion system design	82
8.3 OPEX oxy-fuel system	86
8.4 Cumulative cash flows oxy-fuel system when only subsidies are given for hydrogen production	87
8.5 CO ₂ footprint per ton of biomass input for air combustion systems with and without flue gas greenhouse feeding and oxy-fuel combustion system with carbon capture	88
Chapter 9	
9.1 Test set up for fluidized bed SEWGS reactor	93
9.2 Planning	94
Chapter 11	
11.1 System configuration pyrogasification SEWGS system	99

List of Tables

Chapter 1

1.1 Chemical reactions involved in biomass gasification	4
---	---

Chapter 2

2.1 Thermal treatment of biomass in inert conditions: process conditions and yield fractions	8
2.2 Chemical reactions involved in steam reforming of biomass	13
2.3 Results process parameter analysis	17

Chapter 3

3.1 Advantages and disadvantages of the proposed system configurations	24
3.2 Advantages and disadvantages of different reactor types for biomass pyrolysis, gasification and the sorption-shift-system	26
3.3 Streams in proposed system configuration	27
3.4 Reactor overview with main design characteristics	28

Chapter 4

4.1 Proximate and ultimate analysis biomass input	30
4.2 Pyrolysis product yield	32
4.3 Proximate and ultimate analysis bio-char product	32
4.4 Analysis bio-oil products	32
4.5 Pyrolysis gas yield composition	33
4.6 Stream results Aspen Plus simulations pyrolysis step	33
4.7 Pre-reformer product input and yield	35
4.8 Pre-reformer gas yield composition	35
4.9 Stream results steam reforming step	35
4.10 Simulation results and experimental results found by van Rossum et al.	37
4.11 Syngas stream results sorption-shift system	38
4.12 Solid stream results sorption-shift system	38
4.13 Stream results calcination step	38
4.14 Simulation results validation by results found by Li et al.	40
4.15 Main system input and output	41
4.16 Results Aspen plus simulation results	42

Chapter 5

5.1 Results sensitivity analyses pyrogasification SEWGS system	51
--	----

Chapter 6

6.1 Product prices and estimated system income in 2020	54
6.2 Reactor types pyrogasification-sorption-shift-system	55
6.3 Reactor sizing pyrogasification SEWGS system	55
6.4 Reactor cost	56
6.5 HEX types and characteristics in the system	57
6.6 HEX LMTD and cost characteristics	58
6.7 HEX cost results	58
6.8 Other process equipment cost estimates	59

6.9	Total CAPEX sorption-shift-system based on factorial technique by Peters and Timmerhaus	60
6.10	Raw material cost pyro-gasification sorption-shift system	61
6.11	Utility cost pyrogasification SEWGS system	61
6.12	Fixed cost pyrogasification SEWGS system	62
6.13	Total operational expenditure Pyrogasification SEWGS system	62
6.14	Investment "strategy"	63
6.15	SDE++ subsidies in the Netherlands for sustainable energy production	65
6.16	HEX cost calculations system with decreased air pre heater	68

Chapter 7

7.1	European woody biomass potential in 2020 and 2030	73
7.2	Dutch woody biomass potential in 2020 and 2030	73
7.3	Dutch woody biomass Production,consumption and export for chips/shreds and pellets	73
7.4	CO ₂ footprint pyrogasification sorption shift system per ton of biomass input	78

Chapter 8

8.1	Stream results sorption-shift system with oxy-fuel combustion (1)	83
8.2	Stream results sorption-shift system with oxy-fuel combustion (2)	83
8.3	System results Air combustion versus oxy-fuel combustion	83
8.4	stream results sorption-shift system with oxy-fuel combustion, SC = 2	84
8.5	Total CAPEX sorption-shift-system for the oxy-fuel based system	85
8.6	Total annual OPEX sorption-shift-system	86
8.7	Hourly production rate oxy-fuel system, including expected market prices and expected subsidies	87
8.8	Financial results Air combustion versus oxy-fuel combustion	88

Chapter 9

9.1	Total CAPEX sorption-shift-system for the oxy-fuel based system	93
-----	---	----

Chapter 11

11.1	Main simulation results	99
11.2	Main results cost analysis	100

Chapter 1

Introduction

1.1 The big challenge of the energy transition

The demand for sustainable energy sources is rising globally. There are limited fossil fuel resources available, which are depleting fast, and more importantly, carbon dioxide (CO_2) emissions from the combustion of fossil fuels cause climate change. Due to economic growth and global population growth, energy demand is expected to rise in the foreseeable future: in 2018 the global primary energy consumption increased with 2.1 % to $161.471 \cdot 10^3$ TWh per year [1, 2] and the accompanied CO_2 emissions increased with 1.7% to 36.15 billion tonnes per year [2, 3]. The US Energy Information Administration projects a global increase in the world energy usage of 28% in 2040 compared to 2017 [4]. Fossil fuels are currently (2020) the main energy source used for electricity production, heating, and transportation. In 2018, 84.7 % of the world energy consumption was provided by fossil fuels (excluding nuclear energy) [1]. Fossil fuels need to be replaced by sustainable energy sources to keep up with the energy demand and prevent global temperature rise to an unacceptable level. In 2016 the Paris agreement came into effect, which currently (2020) has been ratified by 187 countries. The Paris agreement strives for climate change mitigation and states that global warming should not exceed the limit of 2 °C compared to the pre-industrial level. Countries that have ratified the Paris agreement have agreed to pursue efforts to keep global temperature increase below 1.5 °C compared to the pre-industrial level [5].

In order to honor the Paris agreement, fossil fuels need to be replaced by sustainable energy sources. In 2018 $0.6 \cdot 10^3$ TWh of the primary energy consumption came from solar energy, $1.3 \cdot 10^3$ TWh from wind energy, and $4.2 \cdot 10^3$ TWh from hydropower compared to $136.6 \cdot 10^3$ TWh coming from fossil fuels [1]. The current share of renewable energy sources is a slim amount compared to the share of fossil fuels, but modern renewable energy, especially solar and wind energy, is increasing rapidly. Other renewable energy sources are biomass (waste to energy, biofuels), geothermal energy, and hydropower, of which the share is also increasing, but not as significant as the share of solar and wind energy [6]. From 2012 until 2017, the global capacity of solar and wind energy increases by 350 % and 115 % respectively [6], while the capacity of hydropower in this period increased only 11%, and the capacity of geothermal/biomass increased by 36% [6].

The main future challenge in the energy transition with increasing shares of solar energy and wind energy is that these are intermittent energy sources: there is a large variability in the electricity production, while electricity demand is relatively constant and predictable [7]. The intermittency problem of solar and wind energy causes an increasing mismatch between supply and demand as the share of renewable energy increases. There are several solutions to deal with this increasing mismatch of energy supply and demand. Solutions are divided into demand-side-based solutions (Demand Side Management: DSM) and supply-side-based solutions (Supply Side Management: SSM). One of the most promising future sustainable energy scenario is a hydrogen energy economy, based on hydrogen production using renewable sources [8]. This research will focus on SSM, using biomass-to-hydrogen systems with Carbon Capture and Storage (CCS).

1.2 Supply side management of the future energy economy: hydrogen fuel and carbon capture

One of the most likely scenarios for a sustainable energy supply in the future is a hydrogen-energy economy based on sustainably produced hydrogen [9], which can be used as an energy storage medium, transportation fuel, and replacement of natural gas. Hydrogen is the smallest element on the periodic table and is a colorless, odorless gas. Due to its low atomic weight, hydrogen gas (H_2) has a low Lower Heating Value (LHV) per nm^3 ($9.9 MJ/nm^3$) compared to natural gas, while the LHV per kg is extremely high ($120 MJ/kg$). Hydrogen can be stored chemically or physiochemically and has several superior properties to conventional fossil fuels, namely rapid burning speeds, a high effective octane number, no toxic and ozone-forming potential, and a wide limit of flammability [10].

Currently, most hydrogen is used in the petroleum industry: 38.2 Mt/year in 2018 [11] and for ammonia production (fertiliser):31.5 Mt/year in 2018 [11], while the share of other hydrogen applications (transport, energy storage etc.) was relatively small:4.2 Mt/year in 2018 [11]. Hydrogen is not a primary form of energy existing freely in nature but is a secondary form of energy that needs to be produced and thus acts as an energy carrier [10]. Hydrogen can be produced in several ways, requiring either hydrocarbons (fossil fuels or biomass), electricity, or heat [9]. Not all of these methods are sustainable, and currently, only 4% of the world hydrogen production is based on sustainable sources (mainly electrolysis with renewable electricity) [12]. The rest of the currently (2020) produced hydrogen is produced out of fossil fuels using Methane Steam Reforming (MSR), steam reforming of oil or coal gasification [11, 13]. Sustainable hydrogen can also be produced out of biomass using thermal or biological conversion methods [14], sustainable hydrogen is expected to be one of the future fuels, and there is a large potential for biomass-based hydrogen production.

The main source of global warming is related to CO_2 emissions from fossil fuels. In order to decrease CO_2 emissions, fossil fuels need to be replaced by sustainable energy sources. A temporal solution to increase the transition time to sustainable energy sources within the Paris agreement's climate change boundaries is CO_2 capture such that carbon dioxide emissions do not enter the atmosphere and do not contribute to global warming. When these carbon capture techniques are used in combination with already sustainable energy production using products from the short carbon cycle such as biomass, systems with negative carbon emissions are achieved, which reverse global warming and produce sustainable energy. These systems are so-called "Bio-Energy With Carbon Capture and Storage" (BEWCCS) systems [15]. There are several promising techniques for carbon capture using biomass: based on algae, biochar, or pre-and post-combustion CO_2 capture, which can be combined with sustainable hydrogen production [15].

1.3 Biomass: a dispatchable sustainable energy source and a means for carbon capture

There are many different types of biomass, Brosowski et al. [16] identified 93 different types which can be utilized for energy production without additional land use (energy crops), these types of "bio-waste" can be categorised into five different categories:

- Agricultural by-products
- Residues of forestry and wood industry
- Municipal waste
- Industrial residues
- Residues from other areas

It is important to note that all these biomass types are biogenic by-products, residues, and waste, which can be utilized without the destruction of ecosystems and that these biomass sources are already available but not yet utilized for energy production [16]. Examples of these forms of biomass are straw, manure, logging residues, waste wood, etc. Most biological waste is currently not processed for energy recovery purposes, if it is processed at all. Good examples of waste being treated without the utilization of its energy potential are sewage sludge (water treatment) and manure(fertilizer), which contain a lot of organic matter, which have a large potential for biogas production, which is not utilized. Logging residues also have a large potential for sustainable energy production, but logging residues are currently mostly left untouched on the logging side. If biomass is used for energy generation, minerals are preserved in the ashes, and carbon can be captured. A promising technique for energy production and carbon capture

out of woody biomass is slow pyrolysis in combination with a separate gasification system. Slow pyrolysis produces biochar, which has many applications varying from soil amendment to pollutant removal agent (activated carbon replacement) in gas cleaning systems, while the released volatile fraction can be upgraded to hydrogen-rich syngas using gasification/ steam reforming. Brosowski et al. [16] analyzed the potential of waste to energy in Germany and estimated that up to 13 % of Germany's primary energy consumption could be supplied by waste to energy systems [16] which can help to overcome the main future challenge in the energy transition: supply-side management based on BEWCCS systems to bridge the gap between sustainable energy supply and demand.

Woody biomass consists out of cellulose (approximately 50 % of dry content), hemicellulose (approximately 25%-35% of dry content), lignin (approximately 15%-25% of dry content), minerals, inert ash, and moisture [6, 17]. Biomass can be classified using either a proximate analysis or an ultimate analysis. A proximate analysis determines the amount of volatile matter, fixed carbon ash, and moisture, while an ultimate analysis determines the chemical composition: mainly hydrogen, carbon, and oxygen, biomass also contains small fractions of nitrogen and sulfur. A relatively large oxygen concentration characterizes biomass compared to fossil fuels. The oxygen to carbon (O/C) ratio of coal is typically in the range of 0,10-0,20 while the typical O/C-ratio for biomass is 0,6-0,8 [18], this large share of oxygen in biomass decreases the Lower Heating Value (LHV) of biomass (typical 10-18 MJ/kg) compared to coal (typical 30 MJ/kg) [19]. Besides the large oxygen content, untreated woody biomass has a large moisture content, which decreases the LHV and energy density. Woody biomass requires pre-treatment before it is processed: drying/torrefaction and/or grinding. Transport of biomass is relatively inefficient since biomass sources are scattered and due to the low energy densities of biomass. This requires biomass installations to be located close to the source. As of February 2020, only 6 BEWCCS projects are in operation worldwide, which focus either on bio-ethanol production in combination with carbon capture (US) or on Municipal Solid Waste (MSW) recycling centers with carbon capture (Europe, UK) [20]. No operational BEWCCS installation has been reported to be operational, which uses the thermal treatment of woody biomass for hydrogen production combined with carbon capture.

1.4 Thermal conversion paths for biomass-based hydrogen production

Different thermochemical conversion methods are used to process biomass: torrefaction, pyrolysis, gasification, reforming, and combustion. Torrefaction and pyrolysis are similar with respect to Equivalence Ratio (ER) = 0. Torrefaction is performed at relatively low temperatures of approximately 250-300 °C, which produces some tars and fuel gas, but the main product is biochar. Typical operation conditions for pyrolysis are 500-700 °C, pyrolysis (biomass cracking and reforming) produces bio-oil, fuel gas, and biochar. Depending on the residence time, large quantities of either oil (tars) or gas can be produced, a short resident time, and fast heating rates (so called flash pyrolysis) can have oil yields up to 70 wt%. Under long residence times, secondary cracking reactions crack the tars into smaller molecules/ gases. Pyrolysis can also be used to produce high quality biochar, which has many applications varying from soil amendment (carbon segregation) to pollutant removal from gases (activated carbon replacement). During gasification/reforming, small quantities of an oxidization agent (oxygen/steam) are added to cause partial combustion or enhance reforming processes, a typical Equivalence Ratio (ER) for gasification is in the range of 0.20, and typical temperatures are between 800-900 °C. During gasification, fuel gases are produced in combination with small fractions of char and oil. Gasification using oxygen as an oxidization agent is exothermic, while reforming, torrefaction, and pyrolysis are endothermic processes.

Different chemical reactions of biomass gasification are displayed in table 1.1, accompanied with the enthalpy changes of the reactions [13] at 650 °C. Biomass gasification produces a gas rich in hydrogen as can be seen from the gasification reactions given in table 1.1, hydrogen production using gasification is expected to have a large future perspective and is expected to become cost-competitive with hydrogen production out of fossil fuels [10]. High purity hydrogen production using the thermochemical conversion of biomass has major challenges, and no complete technology demonstrations are implemented commercially up to date [10].

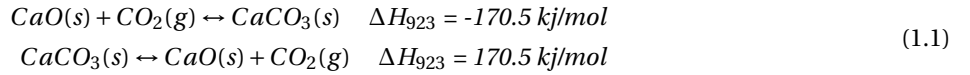
This research will focus on a novel system for both biochar and hydrogen production using a combination of slow pyrolysis followed by steam-gasification (steam reforming), a process labeled as "pyrogasification" from this point on.

Table 1.1: Chemical reactions involved in biomass gasification

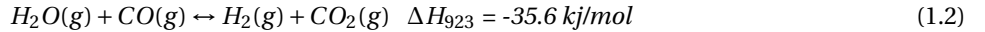
Name of Reaction	Chemical reaction	Enthalpy change: ΔH_{923} (kJ/mol)
Biomass reforming	$C_n H_m O_p + (2n - p) H_2 O \rightarrow n CO_2 + (m/2 + 2n - p) H_2$	Variable, endothermic
Water-gas shift	$CO + H_2 O \rightarrow CO_2 + H_2$	-35.6, exothermic
Methane reforming	$CH_4 + H_2 O \rightarrow CO + 3H_2$	224.8, endothermic
Water-gas (i)	$C + H_2 O \rightarrow CO + H_2$	135.8 endothermic
Water-gas (ii)	$C + 2H_2 O \rightarrow CO_2 + 2H_2$	100.3, endothermic
Oxidation (i)	$C + O_2 \rightarrow CO_2$	-394.5, exothermic
Oxidation (ii)	$C + 0,5O_2 \rightarrow CO$	-111.5, exothermic
Boudouard	$C + CO_2 \rightarrow 2CO$	171.4 endothermic
Methanation	$C + 2H_2 \rightarrow CH_4$	-88.9 exothermic

1.5 Pre-combustion carbon capture and gas upgrading

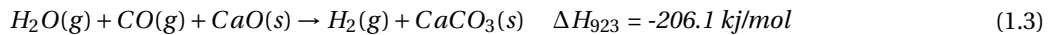
Pre-combustion carbon capture can be applied in gasification systems, where CO_2 is captured from the fuel gas before combustion, resulting in a hydrogen-rich gas which causes minimal CO_2 emissions when utilized. Metal oxides, for example calcium oxide, can be used for carbon capture and storage at high temperatures ($T > 500$ °C), a carbonation reaction, between CaO and CO_2 under specific process conditions (CO_2 equilibrium pressure < gas CO_2 partial pressure respectively) binds carbon dioxide to the CaO forming calcium carbonate ($CaCO_3$): carbonation. Carbonation is an exothermic equilibrium reaction. Under higher temperatures, equilibrium shifts towards the side of CaO and CO_2 while under lower temperatures, the equilibrium lies more to the $CaCO_3$ side. For efficient carbonation, temperatures should be, on the one hand, sufficiently high to have a high enough reaction rate so that CO_2 binds sufficiently fast to the metal oxide, but should not be too high since this will cause calcination (sorbent regeneration), which is the decomposition of a $CaCO_3$ to CaO [13]. The reaction mechanisms for carbonation and calcination of CaO/ $CaCO_3$ are given in equations 1.1.



Recalling the water-gas shift reaction from table 1.1 as shown in equation 1.2 explains how CO_2 capture enhances both the relative and absolute hydrogen yield in syngas from gasification processes.



When CO_2 is captured from a syngas (containing H_2O , CO, CO_2 , H_2) a gas will be produced with almost pure hydrogen (and water vapor) [21]. The two big advantages of calcium oxide as a sorbent for (*in situ*) carbon capture is that it has a relatively high calcination temperature supplying a possibility for high-temperature heat integration and that $CaCO_3$ (limestone) is abundantly available in nature [13]. Combining the water-gas shift reaction with the calcination reaction of calcium oxide yields the exothermic reaction described by equation 1.3 which removes both CO and CO_2 from the system. Once CO_2 is captured in the form of calcium carbonate (limestone), the produced limestone can be regenerated under high temperatures ($T \approx 850-900$ °C), releasing CO_2 and forming CaO, which can be reused in the process: so-called Calcium Looping (CaL). A process which both absorbs CO_2 and causes a shift in the "water-gas-shift reaction": Sorption Enhanced Water Gas Shift (SEWGS), such a system can be applied directly in a gasifier (for *in situ* carbon capture) or can be applied in a separate reactor, a "sorption-enhanced-water-gas-shift-reactor".



1.6 Research goal

This research aims to design and analyze a novel system to produce high purity hydrogen and high-quality biochar out of woody biomass based on Aspen Plus process simulations and to determine the technical, economic, and societal feasibility of this novel system. This novel "pyrogasification sorption-shift" system is based on pyrolysis, steam reforming, and sorption shift mechanics, which are analyzed to produce high-quality products. This research aims to construct a model of this system in Aspen Plus based on thermodynamic equilibrium. This model aims to model reactor stoichiometry and to model efficient heat integration. The Aspen Plus model results serve as input for a financial model, including cash flow simulations to determine the financial feasibility. A societal analysis is performed to analyze the potential of the system in Europe based on biomass availability, CO_2 footprint, and current trends in biomass policies. This research also aims to sketch a future perspective of this technology and to provide subjects for further research. A research proposal for a (European) research project is one of the deliverables of this research.

The main research question and sub-questions of this research are:

Main Research Question

"Determine the feasibility of a pyrogasification sorption-shift system for production of high-quality biochar and high purity hydrogen out of biomass-based on key technical, economic and sustainable parameters using Aspen Plus process simulations"

Sub Question

1. Identify the most important process parameters and system performance for pyrolysis, steam reforming, and of a CaO based sorption-shift system based on literature
2. Model and design an industrial-sized installation for biochar and hydrogen production with a pyrogasification system combined with an integrated sorption-shift system using flow sheeting software (Aspen Plus)
3. Construct a financial model based on cash flow simulations to evaluate the financial feasibility of the pyrogasification sorption-shift system
4. Determine the societal feasibility of the developed system based on raw material availability, CO_2 footprint, and current sustainability policies
5. Provide future perspectives for the pyrogasification sorption-shift system
6. Construct a research proposal for further research for a (European) research project

1.7 Method and outline

To answer this research question, first, an extensive literature study based on key process parameter identification is performed. Next, a system is designed for pyrogasification and CO_2 capture based on the parametric study results. The system is modeled using the flow-sheeting software tool Aspen Plus. Aspen plus is used to perform a technical analysis (stoichiometry and heat integration) of the design and perform a sensitivity analysis on the design to optimize process conditions and test the system's robustness. Once the technical results are gathered, an economical analysis of the design is performed: translating the technical model output data to a cash flow model to determine the economic system's feasibility. A societal study is performed to determine the system sustainability and potential in Europe. Next, a future perspective is given with suggestions for system improvements, and a research proposal is discussed for further research. This thesis is finalized with a discussion and conclusion.

The thesis outline is displayed below:

- **Chapter 2-** Literature review: system parameter analysis
- **Chapter 3-** Design of pyrogasification-sorption-shift system
- **Chapter 4 -** Aspen Plus model construction and results
- **Chapter 5-** Sensitivity analysis pyrogasification sorption-shift model
- **Chapter 6-** Financial model construction and results
- **Chapter 7-** Societal analysis and results
- **Chapter 8-** Future perspective and system improvement suggestions
- **Chapter 9-** Research proposal for further research
- **Chapter 10-** Discussion
- **Chapter 11-** Conclusion

Chapter 2

Literature review: system parameter analysis

This chapter will discuss the system parameter analysis of the three main systems used in the proposed novel pyro-gasification sorption-shift system. This chapter aims to determine the most important process parameters for process design and optimization based on previous research from literature. The results of this chapter are used for the system design in chapter 3. The three systems which are analyzed are:

- Pyrolysis system
- Gasification/reforming system
- Sorption-shift system

2.1 Pyrolysis system

The main goal of the pyrolysis system in the pyro-gasification sorption-shift system is to produce high-quality biochar and maximize volatile matter release from woody biomass. This section will first describe general pyrolysis mechanics before process parameters are analyzed, and key process parameters are identified.

2.1.1 Pyrolysis mechanics

Pyrolysis of biomass can be defined as thermal treatment (heating) of biomass in an inert atmosphere under relative high (>400 °C) temperatures, heating of biomass to sufficiently high temperatures releases volatile matter in the form of permanent gases (CO , CO_2 , H_2 , CH_4 , etc.) and oil (tars), fixed carbon remains solid in the form of biochar (which also contains ash). No oxygen is added to pyrolysis processes, but biomass contains up to 40 wt% oxygen [14] which can enhance (partial) oxidation. Furthermore, biomass also contains water, which can act as an oxidization agent. Pyrolysis is an endothermic process: the process requires external heat. The temperature, residence time, and heating rate of pyrolysis are process parameters that influence the fractions of gas, solids, and liquids produced directly. Depending on the desired products, process conditions can be tuned. Pyrolysis can be used in several ways to produce hydrogen out of biomass. In general, there are three different routes to produce a hydrogen-rich gas out of biomass as described by Kalinci et al. [14]. i) Steam reforming of bio-oil produced by fast pyrolysis. ii) A two-reactor process: pyrolysis in the first reactor, next tar and gas processing in a second reactor with the aid of a catalyst, high temperatures, steam, and possibly oxygen. iii) pyrolysis at relatively high temperatures: 700 °C in a single reactor, incorporating a catalyst in the reactor. This research will focus on option ii). In this system, the main goal of pyrolysis is to produce high-quality biochar. The tars and volatiles released are sent to a gasification system in an additional process step for complete reforming and cracking of pyrolysis gas/liquids into syngas.

The general reaction mechanism of pyrolysis is displayed in figure 2.1 [22] in combination with options for further processing of the pyrolysis products. Note that when biochar is removed from the pyrolysis reactor, char gasification as shown in figure 2.1 will not apply for further processes. Pyrolysis consists out of two stages: primary pyrolysis and secondary pyrolysis. During primary pyrolysis, biomass gets cleaved up: devolatilization, forming different hydroxyl, carboxyl, and carbonyl groups [23]. After primary pyrolysis, secondary pyrolysis occurs: cracking of the heavy oils into char, gases, and a condensable fraction. A simplified reaction of primary biomass pyrolysis is shown in equation 2.1 [24]. A simplified reaction mechanic of secondary pyrolysis is shown in equation 2.2 [23].

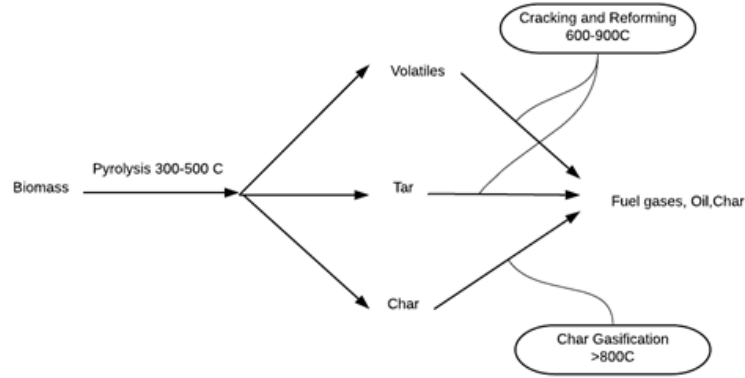
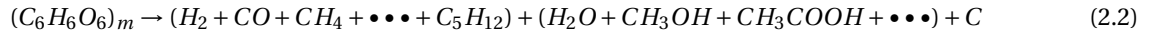
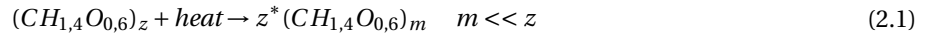


Figure 2.1: General reaction mechanism thermal treatment biomass

Table 2.1 [23–26] describes different types of pyrolysis of biomass and the accompanied process conditions. Torrefaction and carbonization are used to produce solids with a higher energy density than conventional biomass, reducing transportation costs. Fast and flash pyrolysis is used to produce pyrolysis oil, which increases the product energy density significantly, reducing transportation costs. Bio-oil lies at the basis for the development of biofuels and biochemicals.

Table 2.1: Thermal treatment of biomass in inert conditions: process conditions and yield fractions

Process name	Heating rate	Process temperature	Residence time	Liquids[%]	Solids [%]	Gas[%]
Torrefaction	0.1 to 1 °C/s	200 to 300 °C	1 hour	5	85	10
Carbonisation	0.1 to 1 °C/s	350 to 400 °C	>1 hour	20	35	45
Slow Pyrolysis	0.1 to 1 °C/s	400 to 600 °C	5 min to 60 min	35-45	20-30	20-40
Fast Pyrolysis	10 to 200 °C/s	400 to 700 °C	1 to 10 sec	60-75	15-25	10-20
Flash Pyrolysis	>1000 °C/s	700-1200 °C	0.1 to 1 s	75	12	13

For this research, pyrolysis is primarily used for biochar production and secondarily for syngas production as part of a pyrogasification system. For pyrogasification, secondary cracking reactions are desired in order to increase gas yield and reduce oil yield. Under long residence time and intermediate temperatures, biomass is cracked and reformed further into fuel gases as shown in table 1.1. This research will further focus on slow pyrolysis since this will result in high-quality biochar and high conversion to tars and fuel gases. The next section will cover a system parameter analysis with the main focus on char yield and quality. The influence of pyrolysis temperature, residence time, and heating rate on biochar quality and quantity is discussed.

2.1.2 Pyrolysis temperature

The influence of pyrolysis temperature for slow pyrolysis processes on the biochar yield and quality has been studied by many authors[23, 27, 28]. The char yield decreases under higher temperatures due to additional thermal cracking of heavy hydrocarbons into light hydrocarbons. On the other hand, the quality of produced biochar increases under increasing temperature [27] both the HHV as the C/O ratio increases due to the release of more volatiles under higher temperatures. Figure 2.2a displays the product yields of slow pyrolysis of woody biomass (pine wood) as function of temperature [27] and figure 2.2b displays the corresponding biochar quality as function of process temperature [27].

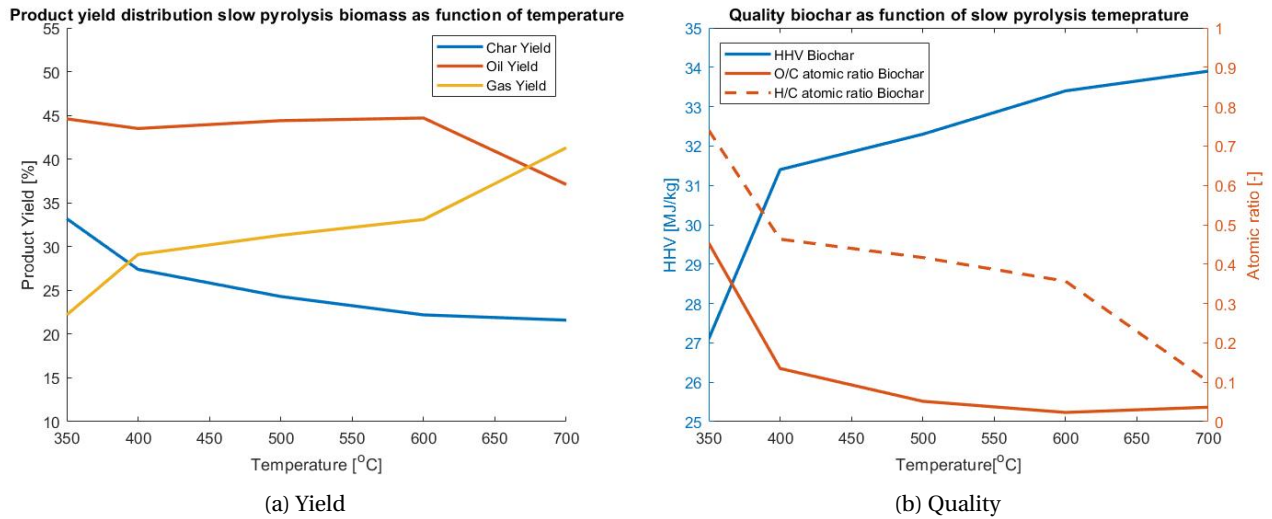


Figure 2.2: (a) : Slow pyrolysis product yield as a function of process temperature and (b):Slow pyrolysis product quality as function of process temperature

2.1.3 Pyrolysis residence time

The residence time of slow pyrolysis has a slight influence on the produced biochar. It has been reported that under longer residence times, biochar quality increased due to the formation of macro- and micro-pores in the produced biochar [23]. Under high process temperatures, for example, during flash pyrolysis, the product oil contains a char fraction. Longer residence times will result in more secondary cracking, resulting in additional biochar production (but lower oil yield). On the other hand, when lower temperatures are used, an increased residence time will decrease the biochar yield due to additional release of volatile matter under longer residence times [23]. Residence time has not been identified as a key process parameter for biochar yield and quality. Process temperature and heating rate have a larger influence on biochar production and quality [23].

2.1.4 pyrolysis heating rate

The heating rate has been identified as a key parameter with respect to biochar yield and quality. Reducing heating rates reduces the secondary reactions and reduces the oil and gas yield, increasing the biochar yield. On the other hand, increasing heating rates will decrease biochar yield and increase the biochar quality (increased HHV and decreases O/C and H/C ratio) [23, 29, 30]. The influence of heating rate of slow pyrolysis on the biochar yield was investigated by Williams et al. [29] is displayed in figure 2.3.

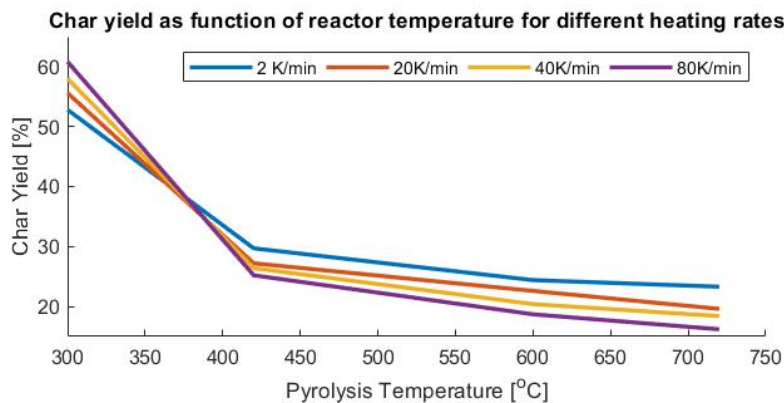


Figure 2.3: Influence heating rate and reactor temperature of slow pyrolysis on char yield

Research by Demirbas et al. [30] showed that the HHV of product biochar increased significantly with increasing heating rates. At a reactor temperature of 800K and a heating rate of 2 K/s, biochar with HHV= 27 MJ/kg was produced, while at a heating rate of 100K/s, biochar with HHV = 35 MJ/kg was produced.

It is important to note that higher-quality biochar can be formed when the produced biochar is kept for a longer time in the specific reactor (increased residence time). In the discussed literature, the used residence time in the experiments was equal to the temperature increase (ΔT) divided by the heating rate. Once the biomass specimen reached the final temperature, biochar was immediately removed from the reactor. When for example, an auger reactor is used, biomass/char can be heated rapidly to the specific reactor temperature, but residence times can be controlled and are depending on the throughput rate (rotational speed and length of the auger), improving biochar quality by releasing additional volatiles under longer residence times [31].

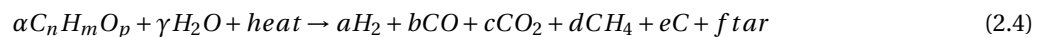
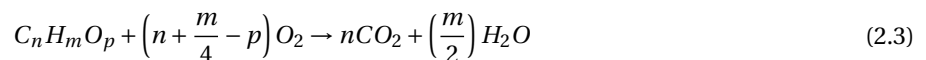
The two key process parameters identified for biochar production are process temperature and heating rate, but process residence times also influence biochar quality and volatile matter depending on the system/reactor configuration.

2.2 Gasification and steam reforming

The gasification system aims to process the released volatiles during pyrolysis and reform and crack the volatiles to a syngas consisting of mainly H_2O , CO , CO_2 and H_2 . First general gasification mechanics are explained before a system parameter analysis is performed to analyze key system parameters to maximize syngas/hydrogen production. In gasification processes, oxygen (or air) is used for partial combustion (oxidation), while in the reforming process, steam is used for reforming reactions. Gasification reactions are exothermic (partial combustion), while reforming reactions are highly endothermic.

2.2.1 Gasification mechanics

Gasification is a thermal treatment method that can produce hydrogen-rich syngas with minimum amounts of methane and higher hydrocarbons. The advantage of biomass gasification for syngas production over biomass pyrolysis for bio-oil production is that gasification produces a more versatile and cleaner fuel than bio-oil, which has a high water content of roughly 25 wt% [14] and contains acids, which cause corrosion problems. Gasification temperatures are higher compared to the pyrolysis process and are in the range of 600-1400 °C [14]. For gasification, an oxidizing agent (oxygen or steam) is required; this results in faster and more complete decomposition of biomass into syngas. When oxygen is used, a so-called Equivalent Ratio (ER) can be calculated to describe the process. The ER is defined as the used O_2 to fuel ratio compared to the stoichiometric O_2 to fuel ratio for complete combustion [13], stoichiometric combustion of biomass is shown in equation 2.3 [13]. Due to partial combustion during gasification, oxygen-based gasification of biomass is an exothermic process, and in general, no additional heat is required for biomass gasification. Steam reforming requires additional heat for both steam production and steam reforming reactions, which are endothermic. The general reaction mechanics of biomass steam gasification are shown in equation 2.4 [32].



There are three main ways of gasification/steam reforming, using either: [14]:

- Pure oxygen
- Air
- Steam

Depending on the type of gas which has to be produced, different gasifying agents are used. Steam can be combined with an oxygen-rich gas to enhance biomass decomposition due to partial combustion with oxygen. Pure oxygen is used to obtain a higher energy-dense gas with a typical HHV of roughly 10-15 MJ/nm³. Using pure oxygen brings, however, issues with respect to safety and cost. The advantage of using air as a gasifying agent is that it is widely available. However, air contains 79% nitrogen, which deludes the produced syngas to HHV values of roughly 4-6 MJ/nm³ since the produced syngas consists of roughly 60 % N_2 [14]. When the syngas is directly utilized in a gas turbine for electricity production, this is not a problem. If the syngas has to be transported, higher energy densities are preferred. Using steam has the advantage that steam favors hydrogen production due to steam reforming of hydrocarbons [13, 14], furthermore using steam does not consume part of the product by combustion. However, steam gasification will lead to an additional energy demand for steam production and can bring problems such as corrosion, poisoning of catalysts, and tar-related problems (coking) [14]. For the designed system, the produced tars and gases from the pyrolysis system are led over a steam gasification system.

The next section discusses a process parameter analysis for steam gasification, emphasizing catalyst selection, reaction temperature, steam to biomass ratio (or steam to carbon ratio), biomass characteristics, and Gas Hourly Space (GHS) velocity.

2.2.2 Catalyst type

Different catalysts can be used in gasification systems to enhance tar cracking and steam reforming to increase syngas (and thus hydrogen) yield and decrease tar-related problems (coking). Two types of catalysts have been studied widely for their tar cracking abilities: Dolomite's and Ni-based catalysts.

Dolomites are most effective in the 800-900 °C range and Ni-based catalysts in the 700-800 °C range [17]. Ni-based catalyst has reported tar cracking efficiencies up to $\approx 100\%$ [33], it is important to note that tars are not per definition cracked to hydrogen and carbon mono/dioxide, but also methane and longer carbon chains are formed. A wide variety of Ni-based catalysts have been the subject of prior research. In general, nickel-based catalysts consists out of the active catalyst (nickel), promoter (optional), and supporter. The promoter increases the catalyst's activity and stability, and the supporter is used for a high surface area, durability, and coking resistance [33]. Aluminium is the most widely used support for nickel-based catalysts: $NiAl_2O_3$. Dolomite has a lower tar conversion rate compared to Ni-based catalyst (in the 95% range) [33, 34], dolomites are, however, widely available and thus cheap and have a high potential out of economic considerations. Dolomite (calcium magnesium carbonate) has a chemical formula of $CaMg(CO_3)_2$ or more accurately $MgCO_3 \cdot CaCO_3$, traces of other materials such as SiO_2 and Fe_2O_3 are commonly found in dolomite's [34]. Calcium oxide can act as a sorbent for carbon dioxide. During the carbonation of calcium oxide, calcium carbonate: $CaCO_3$ is formed, which can acts as a catalyst as discussed by Mahishi et al. [35]. Research performed by Pfeifer et al. [36] on a 100kW dual fluidized bed system which used naturally found dolomite's as bed material/catalyst found that using some species of dolomite's brings problems with attrition and accompanied formed agglomerates, while other types of dolomites did not have the proper mechanical strength resulting in mechanical breakdown and thus blowouts of bed material in the fluidized bed. Herefore not only the tar cracking abilities of (dolomite-based) catalysts are of importance. but also the mechanical properties should be well understood and analyzed before implementation.

Other types of catalysts can also be used to enhance tar cracking and steam reforming. Rhenium bases catalysts, which have a large (technical) potential for tar cracking, and it is shown that gasification with a rhenium catalyst (Rh/CeO_2) has a higher tar cracking conversion rate and hydrogen yield compared to Ni-based, and dolomite catalysts [17, 37]. The main disadvantage of rhenium bases catalysts is the costs, which makes it not economical feasibly. Only when durability is increased significantly, rhenium bases catalysts become a viable option for hydrogen-producing gasification processes.

2.2.3 Gasification temperature

Gasification reactor temperature influences both the fraction of oils and gases (and char for direct biomass gasification) and the gas composition. Higher temperatures correspond to higher gas yield and lower char/oil yield; this is caused by the following processes [13]:

1. Increased gas yield of the pyrolysis process for direct gasification
2. Increased cracking and steam reforming of higher hydrocarbons under higher temperatures
3. Increased gas yield due to char gasification at $T > 800\text{ °C}$ (only for direct gasification)

Process 1 and 3 are not applicable for this research since pyrolysis is performed before gasification in the analyzed system, and chars are removed before gasification. Although the gas yield increases with increasing temperature, the relative amount of hydrogen in the syngas does not per see; this is due to the water-gas shift reaction. The water-gas shift reaction is shown in equation 2.5. Under higher temperatures, the equilibrium of the water-gas shift reaction shifts more to the side of the reactants instead of the products, and therefore an optimum temperature with respect to hydrogen concentration is found. An optimum hydrogen yield for the gasification of biomass is found for a temperature of 756,85 °C by Mahishi et al. [38] based on thermodynamic equilibrium modeling. This balance is reached by steam reforming on the one side, increasing the hydrogen yield under higher temperatures and a shift in the water gas shift reaction to water and carbon monoxide under increasing temperatures, which decreases the hydrogen yield. Note that when a CO_2 sorbent is used, the hydrogen concentration is not limited by the equilibrium of the water-gas shift reaction. In the presence of a CO_2 sorbent, Florin et al. [21] found an optimum temperature range of 527-567 °C

for maximum hydrogen production based on thermodynamic modeling for biomass steam gasification in combination with *in situ* carbon capture. Hanaoka et al. [39] found an optimum temperature of 700 °C for biomass gasification with a CO_2 sorbent based on experimental results (under a pressure of 0,6Mpa).



When literature is studied with respect to the influence of process temperature on the gas yield from steam gasification processes, it becomes clear that with increasing temperature, the (absolute) gas yield increases [13, 39–41]. The results found by Lv. et al. [41] with respect to the gas yield in nm^3 gas per kg of wet biomass are displayed in figure 2.4, which are comparable with, for example, the results found by Turn et al. [13]. The results show a plateau at 700 °C, at this temperature, most tars are reformed to gases, the gas yield starts to increase significantly after 750 °C, related to the char gasification processes, which requires higher temperatures.

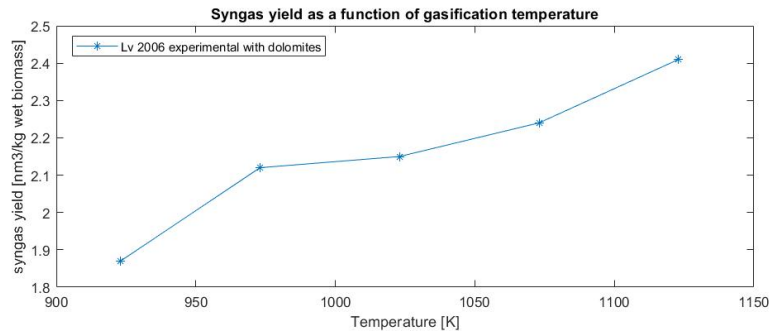


Figure 2.4: Syngas yield for gasification as a function of reactor temperature, using a dolomite catalyst

Based on an extensive literature review, figure 2.5 is made which displays the relative hydrogen yield (Vol%) in the produced syngas as a function of reactor temperature [21, 35, 36, 38–41]. Studies based on thermal equilibrium modeling and experimental studies of biomass steam gasification have been analyzed. Furthermore, studies that use a CO_2 sorbent, catalysts for steam reforming, fluidized beds, and auger reactors have been analyzed with respect to the influence of reaction temperature on hydrogen yield. It becomes clear that there is a large variety of hydrogen yields reported in the literature, and different optimum process temperatures are found. This is because many parameters are influencing the hydrogen yield, which are not constant in the reviewed literature. The general tendency is that relative hydrogen yield in fuel gas increases with increasing temperature up to temperatures of 1050K. The only exception is when a CO_2 sorbent is used in the reactor, which causes a "shift" in the water gas shift reaction. The highest purity of hydrogen has been reported using CaO as CO_2 sorbent (*in situ* carbon capture). Research by Solar et al. [40] on an auger reactor used a reactor that consists of increments that could be heated individually; the temperature displayed in figure 2.5 is the average screw temperature.

In figure 2.5 two different processes with a typical temperature/hydrogen yield range can be observed [21, 35, 36, 40, 41]. The first process type is gasification with *in situ* carbon capture, so-called sorption enhanced gasification; here, the process temperature is relatively low, while the relative hydrogen yield is high. The second process is catalytic (steam) gasification at relatively high temperatures but with a high relative hydrogen yield compared to regular thermal gasification, but with a relative low hydrogen yield compared to sorption enhanced gasification. Figure 2.5 plots the temperature/hydrogen yield data, with the typical operation range of these different gasification types.

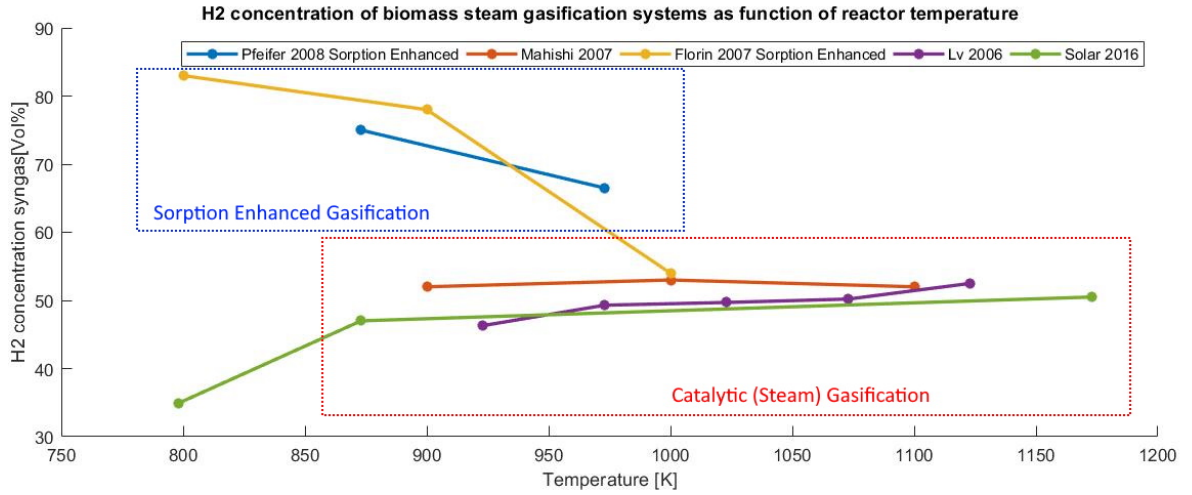


Figure 2.5: Representation temperature range and hydrogen yield for 1. sorption enhanced gasification, 2. Catalytic (Steam) gasification

For sorption enhanced gasification, the relative hydrogen yield is highest at temperatures at roughly 550 °C, but the absolute gas yield is not yet optimized; due to low temperatures, tars are not completely cracked and reformed to syngas. For catalytic based steam gasification, optimal temperatures are in the range of 750-800 °C, van Rossum et al. [42] found that at these temperatures, using a two-step gasification system, all tars and hydrocarbons converged into a syngas. Non-catalytic gasification is of interest at high temperatures: $T > 800$ °C.

2.2.4 Steam to carbon ratio

Steam is used for reforming in many different processes, varying from Methane Steam Reforming (MSR) (a conventional method of hydrogen production) to biomass gasification processes. For biomass steam reforming, biomass, tars, and methane are cracked and reformed using steam. The basic equations for steam reforming are displayed in table 2.2 [13, 34], Steam reforming reactions are endothermic reactions, thus requiring heat.

Table 2.2: Chemical reactions involved in steam reforming of biomass

Name of Reaction	Chemical reaction	Enthalpy change: ΔH_{923} (kJ/mol)
biomass reforming (i)	$C_n H_m O_p + (2n - p) H_2 O \rightarrow n CO_2 + (m/2 + 2n - p) H_2$	Variable, endothermic
biomass reforming (ii)	$C_n H_m O_p + (n - p) H_2 O \rightarrow n CO + (m/2 + n - p) H_2$	Variable, endothermic
Steam dealkylation (i)	$C_n H_m + H_2 O \rightarrow C_x H_y + H_2 + CO$	variable, endothermic
Steam dealkylation (ii)	$C_n H_m + 2H_2 O \rightarrow C_x H_y + H_2 + CO_2$	variable, endothermic
Methane reforming	$CH_4 + H_2 O \rightarrow CO + 3H_2$	224.8, endothermic
Water-gas (i)	$C + H_2 O \rightarrow CO + H_2$	135.8 endothermic
Water-gas (ii)	$C + 2H_2 O \rightarrow CO_2 + 2H_2$	100.3, endothermic

The Steam to Carbon Ratio (SC) is a ratio which is calculated according to equation 2.6. Another term that is widely used to represent the amount of steam used in the process is the Steam to Biomass Ratio (SBR) as displayed in equation 2.7, which represent the ratio between H_2O (mass) and biomass input (mass).

$$SC = \frac{H_2O(moles)}{C(moles)} \quad (2.6)$$

$$SBR = \frac{H_2O(mass)}{Biomass(dry, mass)} \quad (2.7)$$

Florin et al. [21] used thermodynamic equilibrium modeling to analyze the SBR with respect to hydrogen yield. They found that under increased SBR, the absolute hydrogen yield increased, the relative amount of hydrogen in the produced gas decreased due to an increasing fraction of steam in the produced gas. Due to the energy penalty of producing steam, Florin et al. concluded that an SBR of 1.5 would result in the most energy-efficient system. An SBR of 1.5 translates for the used biomass composition by Florin et al. (49.3 %C) to an SC of 2.03.

Mahishi et al. [38] found comparable results also based on thermodynamic equilibrium modeling, with respect to hydrogen yield as a function of SBR. Mahishi et al. found an optimum energy efficiency of 54 % under an SBR of 3

(SC =4.06) using efficiency optimization. Furthermore, they found a reduction of produced methane and solid carbon of $\approx 80\%$ when the SBR increased from 0.5 (SC=0.68) to 1.5 (SC=2.03) at T=1000K. Experimental studies show similar results with respect to SBR/SC in biomass gasification systems with respect to hydrogen yield: a high increase from SBR=0.5 until SBR=1.5, and no significant increase for SBR >3; in practice, an SC between 3 and 4.5 is used most often [13, 14].

2.2.5 Reactor pressure

The reactor pressure influences the production rate of hydrogen out of biomass. The influence of reactor pressure on hydrogen production has been analyzed extensively, both experimental and based on thermodynamic equilibrium modeling, to determine the effect of pressure on absolute and relative hydrogen yield from biomass gasification processes. A thermodynamic equilibrium study performed by Mahishi et al. [38] showed that under higher than atmospheric pressures (10 and 25 atm respectively), the CO and H_2 yield reduced, while low pressures (0.1 atm and 0.5 atm respectively) did not have a significant effect on the hydrogen yield. Hanaoka et al. [39] performed an experimental study on the influence of pressure on the hydrogen production out of gasification of biomass in the presence of a CO_2 sorbent (CaO) and found similar results compared to the study performed by Mahishi et al., concluding that increasing pressure decreases the hydrogen yield. Florin et al. [21] analyzed biomass gasification for hydrogen production with CaO as CO_2 sorbent using thermodynamic equilibrium modeling; they found that for gasification under temperatures up to 950 K pressures of 1 atm are preferred. When gasification of temperatures above 950 K is used, increasing the pressure can be beneficial since this shifts the $CaO/CaCO_3$ equilibrium towards $CaCO_3$, increasing the relative CO_2 capture and shifting the water gas shift reaction. Under low temperatures and elevated pressures, CaO reacts with water forming $Ca(OH)_2$, reducing CO_2 capture and hydrogen production. In general, optimal biomass gasification pressure is 1 atm for optimal hydrogen production; only under specific process conditions can it be beneficial to change the gasification pressure.

2.2.6 Residence time (specific gasification rate)

The flow rate of products leaving a gasifier (or reformer) can be expressed in nm^3/h ; the flow rate depends on reactor dimensions, bed void fraction (for fluidized beds), and biomass throughput rate. The specific gasification rate [m/s] relates the flowrate to the size of the installation. The produced gas contains both combustible and non-combustible gases as well as steam, tars, and dust [14]. The specific gasification rate is expressed according to equation 2.8 where R_{sg} is the specific gasification rate [m/s], V_g the volumetric gas flow [m^3/h], which depend on the pressure, temperature, and produced amount of gas (in accordance to the ideal gas law) and A_t is the effective surface of the reactor. The specific gasification rate and the length of the reactor (L_r) determines the residence time according to equation 2.9 [13]. The residence time influences the produced syngas. If residence times increase, more biomass, tar, and methane is reformed, and the produced syngas will lie closer to thermal equilibrium [35, 38]. Mahishi et al. [35] showed that a residence time of 1.4 compared to 0.4 seconds increased the hydrogen yield by a factor of ± 1.6 from $\pm 30Vol\%$ to $\pm 50Vol\%$ in the produced syngas for steam gasification at 800 °C.

$$R_{sg} = \frac{V_g}{A_t} \quad (2.8)$$

$$\tau = \frac{L_r}{R_{sg}} \quad (2.9)$$

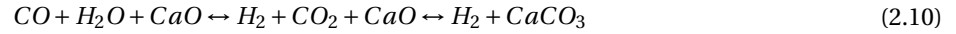
Concluding from this parameter analysis, the reaction temperature is identified as the most important key process parameter for the gasification system. Furthermore, SC ratio, specific gasification rate, catalyst type and loading, and reactor type/configuration influence the product yield. This study shows that a system can be designed which produces a syngas that approaches thermodynamic equilibrium and contains no significant amount of hydrocarbons.

2.3 Sorption-shift system

This section discusses the process parameter analysis of the sorption-shift system, which is used for 1. capturing CO_2 using calcium oxide, and 2. Shifting the syngas towards hydrogen. The influence of reactor temperature and CO_2 partial pressure are discussed. Furthermore, the system configuration is discussed in this section.

2.3.1 Temperature and (partial CO₂) pressure

The equilibrium reaction between calcination, carbonation, and WGS is displayed in equation 2.10. When the equilibrium of calcination/carbonation shifts towards $CaCO_3$, high-quality hydrogen can be produced.



The equilibrium between calcium oxide and calcium carbonate is determined by the CO_2 equilibrium partial pressure, which is a function of temperature. Relations for this partial pressure are given in different forms [43, 44]. The correlation derived by Barker is shown in equation 2.11 [44] and results are displayed in figure 2.6. Under normal process conditions ($T=750\text{ }^\circ\text{C}$, $P = 1\text{ atm}$), it was found that the typical CO_2 concentration lies in the range of 20 Vol% for syngas, using the ideal gas law ($PV=nRT$) results in a partial CO_2 pressure in fuel gases for systems with no pre-combustion CO_2 capture of roughly 20kPa. When the system pressure increases, the CO_2 partial pressure changes accordingly, resulting in increased CO_2 capture performance, which can be of special interest under higher temperatures. Increased pressures for the regenerator would, on the other hand, result in a higher (temperature) heat requirement since calcination would require higher temperatures under increased pressures. Process temperature and pressure are the key parameters for carbon capture using calcium oxide since they directly influence the sorbent's carbon capture ability.

$$\text{Log}(p_{eq}) = 7.079 \times \frac{38000}{4.574 * T[K]} \quad [atm] \quad (2.11)$$

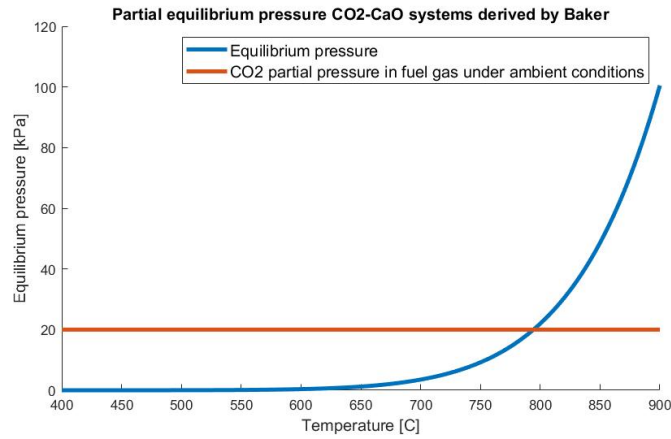


Figure 2.6: CO₂ Equilibrium pressure versus CO₂ partial pressure in typical syngas under ambient pressure

The molecular fractions in the syngas also influence the final gas composition after carbon capture. If, for example, more steam is used, the WGS reaction shifts towards hydrogen and CO_2 and less CO, increasing carbon capture capacity (but of course also increasing heat demand for gasification).

2.3.2 System configuration

Two system configurations are discussed for pre-combustion carbon capture using Calcium Looping (CaL), a system with integrated *in situ* carbon capture and separate carbon capture in a sorption-shift-reactor.

Process configuration for sorption enhanced gasification of biomass

for sorption enhanced *in situ* gasification, two different reactors are required: a gasification/carbonation reactor and a calcination reactor. Under atmospheric pressures, efficient carbonation using CaO is in the 550 °C to 650 °C range, while efficient calcination is in the 800 °C to 900 °C range. Carbonation is exothermic, and calcination is endothermic, resulting in additional heat requirements for the regenerator (calcination). For *in situ* gasification, there are two main reaction in the gasifier: gasification reactions and CO_2 absorption reactions. The CO_2 absorption reaction also causes a shift in the WGS reaction due to a decrease in partial CO_2 pressure by absorption.

Two possible configurations for biomass gasification with *in situ* carbon capture have been analysed by Florin et al. [13] and are shown (simplified) in figure 2.7. The configuration shown in figure 2.7a is a Circulating Fluidized Bed (CFB), which operates continuously. In the gasifier, biomass and steam are added. The gasifier is heated by regenerated CaO together with the exothermic carbonation reaction, which delivers heat required for heating and reforming biomass (steam/water addition can be tuned in such a way that desired reactor temperatures are reached). The bed material is transported (overflow) to the regeneration reactor, which is heated to 900 °C in order to calcinate

the formed calcium carbonate to release CO_2 . Furthermore, ashes, char, and decayed sorbent are collected from the gasifier, and fresh sorbent is added to the regeneration installation. The advantage of such a system is that it is a continuous process, which can reach steady-state conditions. Furthermore, heat is efficiently recycled through the system. Another option for *in situ* CO_2 capture are two parallel beds for respectively gasification and sorbent regeneration as shown in figure 2.7b. This means that both reactors have the function of both gasifier and sorbent regeneration, and the biomass/steam feed switches between reactors; no steady-state conditions are reached in such a system. The main advantage of such a parallel system is that there are no circulating solids, which can result in a decrease of sorbent particle attrition and elongate sorbet durability. [13].

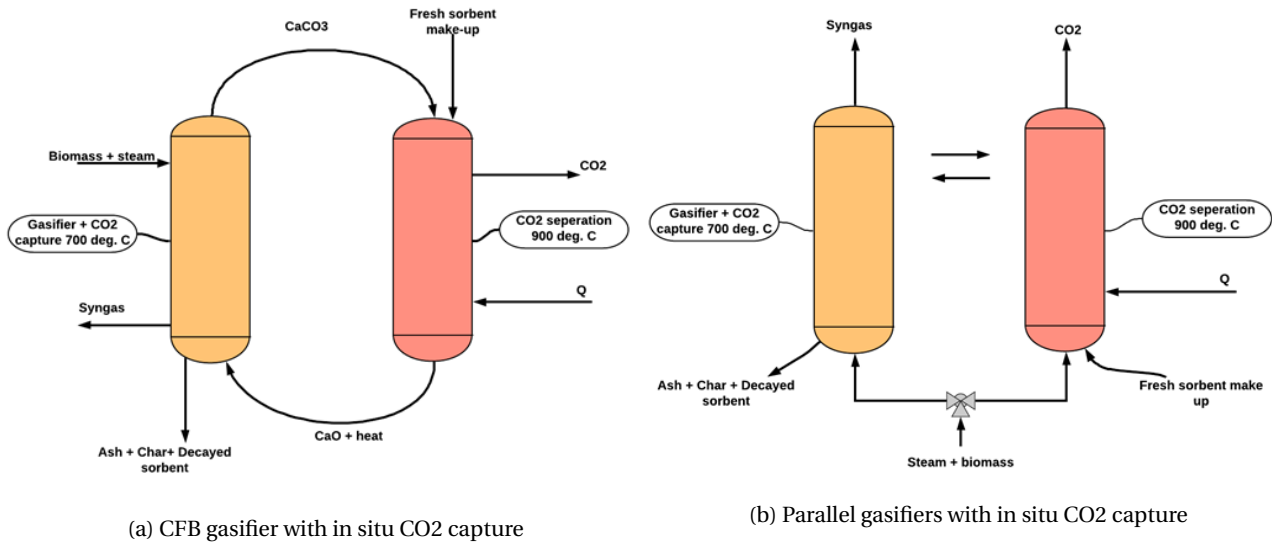


Figure 2.7: Two possible simplified system configurations for *in situ* sorption enhanced gasification of biomass

Limitations for sorption enhanced gasification

Research performed on gasification processes with *in situ* carbon capture using CaO both as sorbent and as catalyst [13, 21, 35, 39] clearly reveal the limitations for *in situ* carbon capture. Ideal process conditions for catalytic steam gasification are between 700 °C to 800 °C which result in a high conversion rate to syngas. In this temperature range and under atmospheric pressures, CaO mostly acts as a catalyst and not as a CO_2 sorbent due to high sorbent CO_2 equilibrium pressure. If temperatures between 550 to 650 °C are selected, this results in a high concentration of hydrogen in the produced syngas, but this is accompanied by high concentrations of methane and tars due to the lack of steam reforming[21]. Under these low temperatures, biomass is not completely reformed, and tars are not cracked, resulting in a relatively low absolute gas yield compared to the oil and char yield as explained in section 2.2.3. Furthermore, when tars are not cracked, this leads to coking and deactivation of the sorbent. Elevated temperatures help with the decomposition of coke. In general, for sorption enhanced gasification, there is a trade-off between relative hydrogen yield (is highest at roughly 550 °C) and absolute hydrogen yield (highest at temperatures of 750-800 °C)

Separate Calcium looping for pre-combustion carbon capture

Separate Calcium looping (CaL) is another method that can be used for pre-combustion carbon capture. While the gasification temperature for *in situ* carbon capture is limited by the maximum carbonation temperature, the gasification temperature for separate CaL is not bound by this limitation. Gasification with separate Calcium looping is a method in which first gasification and reforming of the produced syngas take place before CO_2 is captured in a separate reactor. The main advantage of separate CaL is that during gasification and reforming, optimum conditions ($T > 750$ °C) can be reached, resulting in a syngas which consists mainly out of H_2 , CO, CO_2 and steam with minimal tar and methane concentrations. Due to CO_2 absorption in a separate reactor at lower temperatures, in combination with the water gas shift reaction, almost all CO and CO_2 can be removed, which results in much higher hydrogen quality compared to *in situ* carbon capture as well as higher absolute gas yield. The main disadvantage is the large energy penalty that has to be paid for this system: gasification at a higher temperature, cooling is required between the reforming and carbonation step, while sorbent regeneration (calcination) still requires high-quality heat input. Therefore CaL is interesting for applications that can use heat released by carbonation, for example, for steam production for gasification processes, power production (power plants), or/with residential heating (CHP) [45]. Figure 2.8. gives a general overview of a carbon looping system for pre-combustion carbon capture.

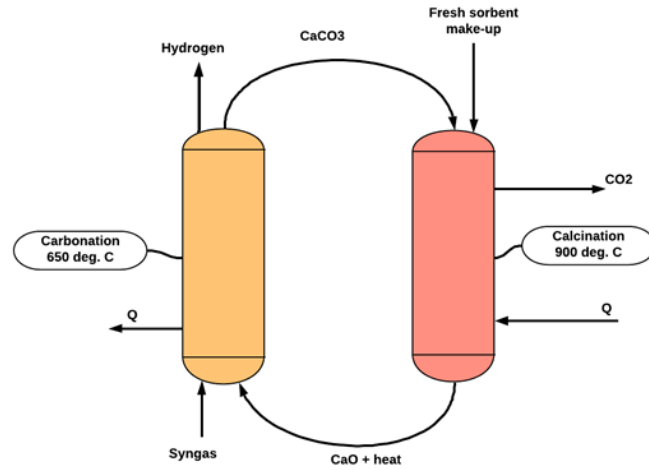


Figure 2.8: General overview calcium looping system for pre-combustion carbon capture

The system configuration is the most important key process parameter for CaL based CO_2 absorption, especially when high purity hydrogen is desired. The system configuration directly influences the possible temperature range and product gases. Given the process configuration, the temperature and pressure are still important process parameters, directly influencing hydrogen quality.

2.4 Overview key process parameter per system

The pyrolysis system aims to produce high-quality biochar and to release volatiles for further processing. Pyrolysis temperature (500-700 °C) combined with biomass heating rate (1-10 °C/s) has been identified as the key process parameters which are required for high purity biochar production. Residence time also influences biochar yield and quality, but temperature and heating rate have been identified as the dominant parameters. Within the given temperature and heating rate range, residence times of 5-10 minutes are recommended. The gasification/reforming system aims to produce hydrocarbon free syngas. It is recommended to use steam as a gasification agent; thus, non of the product is (partially) combusted. Reforming instead of gasification will, however, require external heating. Process simulations are required to analyze the reformer heat demand and analyze if this heat demand can be supplied by internal heat integration using residual heat from the CaL based SEWGS system. The most important key process parameter for reforming is temperature, which should be at least 750 °C in order to produce hydrocarbon free syngas. Catalyst selection, catalyst loading, and residence time also influence the gasification/reforming system. For reforming processes, the SC ratio is also a key process parameter, which is recommended to be in the range of SC=3.0-4.5. The goal of the sorption-shift system is to produce high purity hydrogen. For the sorption-shift system, the process configuration is identified as the most important key process parameter. An uncoupled sorption-shift system is recommended instead of sorption enhanced gasification since this enables the steam reforming process and sorption-shift process to operate at ideal conditions. for the sorption shift system, optimal temperatures are in the 500-600 °C range resulting in high purity hydrogen. Required temperatures for the calcination reaction (regenerator) are in the 850-900 °C range, depending on the CO_2 partial pressure. Table 2.3. displays the key system parameters for each of the analyzed systems.

System	Key process parameters	Specification
Pyrolysis system	1. Temperature 2. Heating rate	500-700 °C 1-10 °C/s
Gasification system	1. Temperature 2. Gasification agent 3. Steam to Carbon Ratio	>750 °C Steam 3.0-4.5
Sorption-shift system	1. System configuration 2. Temperature carbonation 3. Temperature calcination	Separate sorption-shift system 550-650 °C 850-900 °C

Table 2.3: Results process parameter analysis

Chapter 3

Model Design

This chapter will discuss the model which is designed for the pyrogasification-sorption-shift system. First, the process configuration is selected. Next, the reactor selection is discussed before system process parameters are selected based on the process parameter study. The designed model will be translated into an Aspen Plus model in Chapter 4.

3.1 Process configuration options

The goal of this research is to produce high-quality biochar and high purity hydrogen out of biomass. In this research, a combination of pyrolysis, gasification/steam reforming, and sorption enhanced water gas shift is used. The general principle of the proposed system is displayed in figure 3.1

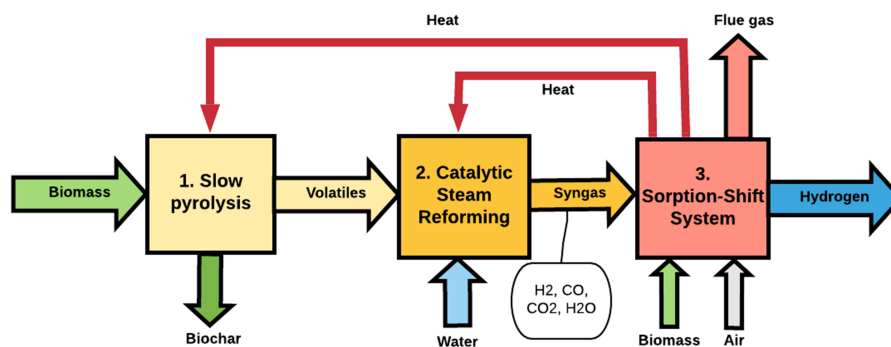


Figure 3.1: General system configuration

Different process configurations can be used to produce high-quality biochar and high purity hydrogen out of biomass, based on the proposed mechanics. These different process configurations are:

1. Pyrolysis followed by sorption enhanced gasification using CaL in a dual circulating fluidized bed
2. Pyrolysis followed by steam reforming followed by a two-step shift system and separate biomass combustion for heat supply
3. Pyrolysis followed by steam reforming followed by a CaL sorption enhanced water gas shift system with air-combustion based regeneration
4. Pyrolysis followed by steam reforming/gasification followed by a CaL sorption enhanced water gas shift system with oxy-fuel combustion based regeneration

The section below briefly explains the different systems. Each system starts with a pyrolysis system. The pyrolysis system aims to maximize the release of volatiles from the biomass species and to produce high-quality biochar. The pyrolysis system and key process parameters for the pyrolysis system have been discussed in section 2.1.

System configuration 1: Pyrolysis followed by sorption enhanced gasification using CaL in a dual circulating fluidized bed

Sorption enhanced gasification based on calcium looping combines gasification and CO_2 absorption in one reactor. This system first contains a pyrolysis step. The volatiles and released moisture are led to a gasifier, together with additional steam. The main reactor operates at 600-700 °C. In this gasifier, volatiles (tars and gases) are reformed into mostly syngas, but due to temperature limitations caused by the sorption system, there is no complete conversion. In the gasifier, CO_2 is absorbed by calcium oxide, forming calcium carbonate. The formed calcium carbonate is led to a regenerator where biomass is combusted to supply heat for regeneration. The regenerated sorbent is led back to the gasifier. The main disadvantage of this system that a temperature compromise in the main reactor is required between optimal temperature for gasification (>750 °C) and carbon capture (<650 °C). This results in sub-optimal conditions for both processes resulting in a product gas with 60-70 % hydrogen as well as contaminants (tars, CH_4 , C_2H_4 , C_2H_6 , etc.) as explained in section 2.3. The process diagram for scenario one is displayed in figure 3.2

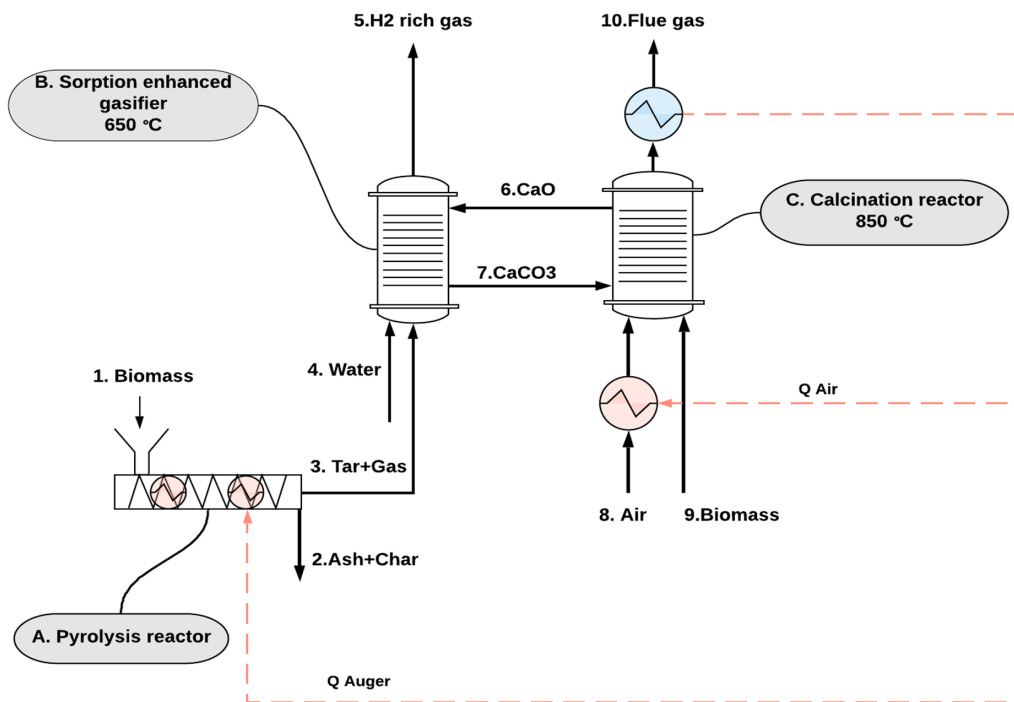


Figure 3.2: Process diagram scenario 1: Sorption enhanced gasification

System configuration 2: Pyrolysis followed by steam reforming followed by a two-step shift system and separate biomass combustion for heat supply

This system also starts with a slow pyrolysis process. Next, two reformers are placed in series; the released volatiles, water, and additional steam are led to the pre-reformer followed by a reformer. Catalytic cracking in the reformers produces hydrocarbon free syngas. Two reformers are used for energy savings and system robustness, comparable to the Methane Steam Reforming (MSR) process. The hydrocarbon free syngas consisting of the species H_2 , CO , CO_2 , and H_2O is led over two shift reactors, the High-Temperature Shift (HTS) contains chromium promoted iron oxide as a catalyst, and the Low-Temperature Shift (LTS) contains copper promoted zinc oxide as catalyst. The HTS and LTS shift the WGS reaction such that (almost) all CO reacts to CO_2 . Finally, a CO_2 removal step is implemented, consisting of a gas scrubber and a Pressure Swing Absorption (PSA) system; this system makes sure high purity hydrogen: Vol %>99.9% can be produced. This system is in many ways similar to the MSR process. The main difference is that in this process, pyrolysis is in place before the reforming process. Furthermore, the heat required for steam generation and the endothermic reforming process is delivered by biomass combustion in a separate reactor. The process diagram for scenario two is displayed in figure 3.3

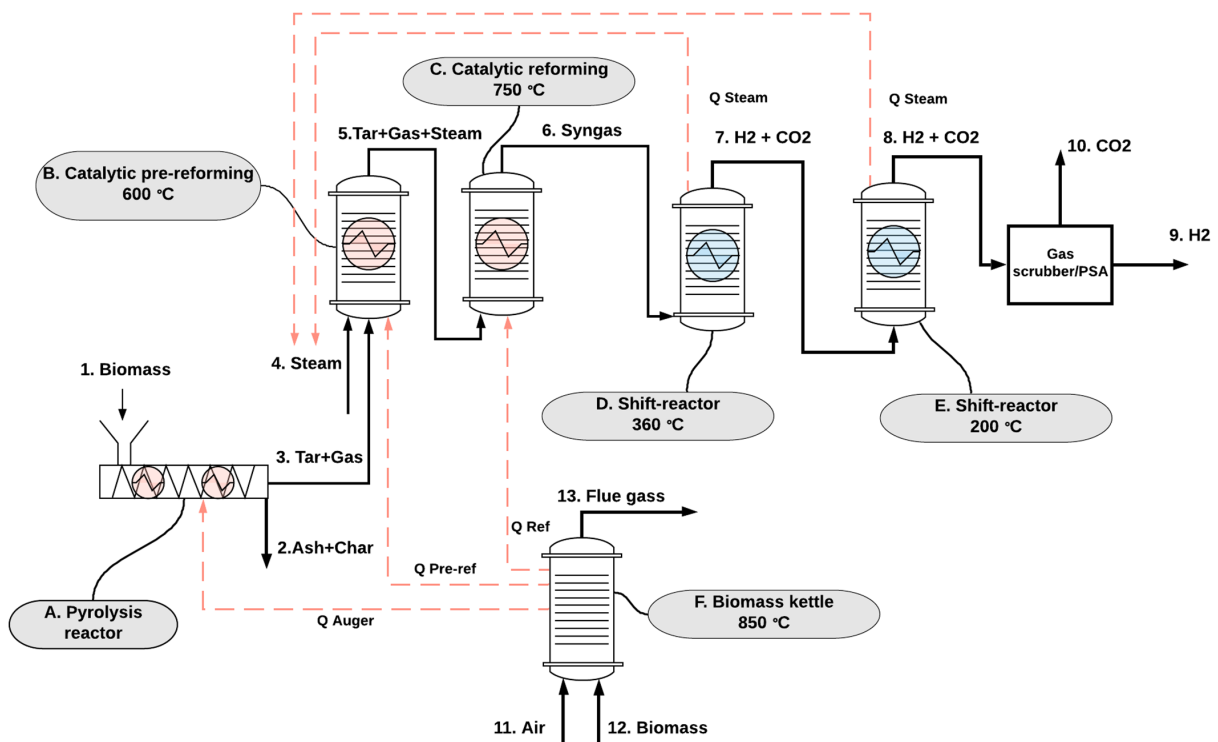


Figure 3.3: Process diagram scenario 2: Separate reformers and uncoupled shift-system

System configuration 3: Pyrolysis followed by steam reforming followed by a CaL sorption enhanced water gas shift system with air-combustion based regeneration

This system uses an auger reactor for pyrolysis as well. The released volatiles are led to a pre-reformer and reformer, respectively, similar to system configuration 2. The reforming system produces hydrocarbon free syngas, which is led to a Sorption Enhanced Water Gas Shift system based on CaL. This system consists of high-temperature sorption enhanced water gas shift system (SEWGS1), and a low-temperature sorption enhanced water gas shift system (SEWGS2), followed by a regenerator for sorbent regeneration. In the sorption shift systems, calcium oxide (CaO) is used to absorb CO_2 ; furthermore, CaO is used as a catalyst to shift the WGS from CO to CO_2 . The formed $CaCO_3$ is led to the regenerator operated at 850 °C; here, biomass is combusted to provide heat for regeneration, which is an endothermic reaction. Carbonation is exothermic; released heat in the sorption-shift reactors is used for high-quality steam generation used for the steam reforming process. The hot flue gases released by the regenerator are used to heat the pyrolysis and reforming system, respectively. The process diagram for scenario three is displayed in figure 3.4

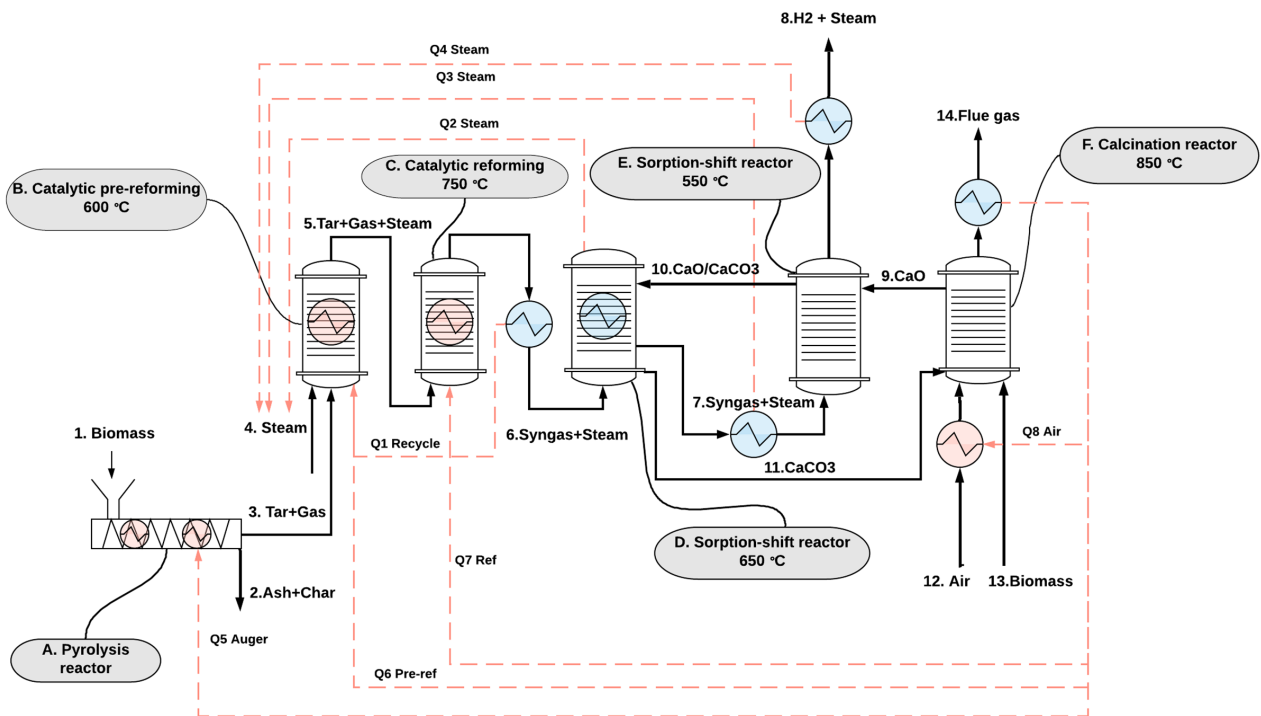


Figure 3.4: Process diagram scenario 3: Coupled SEWGS system with air combustion

3.2 Process configuration selection

The table on the next page displays the advantages and disadvantages of each of the discussed system. Option 1 does not produce high-quality hydrogen. Therefore option one will not further be discussed. Option 2 brings a large energy penalty by introducing an additional biomass kettle to supply sufficient heat for the pyrogasification system; therefore, option 2 will not be further discussed. Options 3 and 4 are in many ways similar; they both contain a separate SEWGS system, enabling high-quality heat integration. Since option 4 combusts part of the product gases in the reformer and higher regeneration temperatures are required, option 3 is selected for further research: A pyrogasification SEWGS system with air combustion in the regenerator. Option 4 still remains a valid option for further research, especially when additional value is given to a pure stream of CO_2 and O_2 is available, for example as by-product of electrolysis.

Table 3.1: Advantages and disadvantages of the proposed system configurations

Option 1	Advantages	Disadvantages
	<ol style="list-style-type: none"> 1. Relative simplicity 2. Proven concept 3. Combustion prevents coking on sorbent 	<ol style="list-style-type: none"> 1. Gasifier temperature limitation 2. The system cannot produce high purity hydrogen 3. Product gas still contains tars and higher order carbons
Option 2	Advantages	Disadvantages
	<ol style="list-style-type: none"> 1. Proven technology 2. Produces high purity hydrogen 3. Produces pure CO_2 for possible CCS 4. CO concentrations are reduced to minimal levels 	<ol style="list-style-type: none"> 1. Required catalysts in HTS/LTS are expensive 2. Additional CO_2 removal steps are required 3. Additional biomass kettle is required 4. Limited amount of heat can be utilised from HTS/LTS
Option 3	Advantages	Disadvantages
	<ol style="list-style-type: none"> 1. High purity ($V\% > 99\%$) H_2 is produced 2. Cost of CaO sorbent is less compared to conventional HTS/LTS catalysts 3. High quality heat is integrated from SEWGS system 	<ol style="list-style-type: none"> 1. Complex heat intergration 2. Solid mass transport is required (sorbent) 3. No pure stream of CO_2 is produced for CCS 4. Calcium oxide required continuously sorbent make up
Option 4	Advantages	Disadvantages
	<ol style="list-style-type: none"> 1. High purity ($V\% > 99\%$) H_2 is produced 2. simple heating mechanics compared to scenario 3 3. Produces pure stream of CO_2 4. Cost of CaO sorbent is less compared to conventional HTS/LTS catalysts 5. High quality heat is intergrated from SEWGS system 	<ol style="list-style-type: none"> 1. Producing oxygen required additional energy 2. Using pure oxygen brings safety issues 3. High calcination temperature brings issues with ash melting and sintering 4. Part of hydrogen product is combusted in the reformer 5. Solid mass transport is required (sorbent) 6. Calcium oxide required continuously sorbent make up

3.3 Reactor options

In this section, reactor types are discussed. The reactor type and the biomass feeding point's location influence the heating rate of biomass, the residence time, the catalyst's effectiveness, and, therefore, the char and syngas yield and quality. Reactor types that can be used for biomass pyrolysis and gasification are fixed bed and fluidized bed reactors; auger reactors can be used for biomass pyrolysis. More detailed information of these reactors can be found in appendix A.

Fixed bed and fluidized beds

Fluidized bed and fixed bed reactors are both reactors that contain a bed of non-reacting particles that act as a heat sink and can have a catalytic function. In both reactors, gases pass through the bed from bottom to top. In a fixed (stacked) bed reactor, gas velocities do not reach the minimum fluidization velocity resulting in plug flow in the reactor. In a fluidized bed, gas velocities are higher than the minimum fluidization velocity. When particle size decreases or particle density increases, a larger minimum gas velocity for fluidization is required.

The different types of fluidized reactors (including fixed bed) are displayed in figure 3.6 [46]. When a circulating fluidized bed is designed, the bed should be characterized as at least turbulent fluidized. A circular fluidized-bed could be desired for solid mass transport or ensure equal heat distribution in the bed when reactions in the bed are

(highly) endothermic or exothermic, for example: char combustion in a biomass pyrolysis twin bed system with a pyrolysis reactor (endothermic) and char combustor (exothermic).

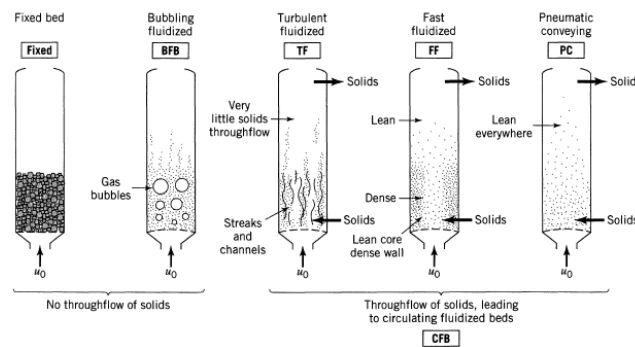


Figure 3.6: Different types of fluidized bed reactors

Plug flow (fixed bed) is desired with respect to contact between gases and active catalyst. If a fluidized bed is used, there is a lot of bypassing of gases due to gas bubbles resulting in a system with a wide residence time distribution, which requires more catalysts for high gas conversion rates [46]. Temperature control can be difficult in fixed beds due to the lack of mixing of solids and thus lower heat transfer rates within the bed. When the reactions in a fixed bed reactor are exothermic, this can cause hot spots, which can result in sintering and deactivation of catalysts [46] while if the reaction is endothermic cold spots can develop at the product inlet, which decreases the reactor activity and can cause accumulation of product (for example biomass) [46]. Fluidized beds are able to use bed material with small particle sizes; this can, however, cause plugging and high pressure drops in fixed beds.

Auger reactor

An auger reactor is another reactor type in which biomass can be thermally treated. Biomass is transported through the reactor using a screw; a schematic overview is given in figure 3.7. The screw can be placed horizontal, vertical, or inclined, and the cross-section of the reactor can be circular or rectangular. An auger reactor is heated externally (the walls of the reactor are heated), but the screw itself could also be heated, for example, with circulating hot fluid through a hollow structure in the screw [47]. An auger reactor can be designed with holes in the reactor wall, making it possible for the gases and tars to escape, which reduces secondary cracking reactions, which is desirable when a high-quality pyrolysis oil is the main system output. An auger reactor's advantages are that there is a reliable mass flow, and different particle sizes can be used. Furthermore, the residence time can be well controlled in a screw reactor, and gases and tars do not quickly leave the reactor (when there are no holes in the reactor wall), resulting in secondary cracking reactions, which can lead to small tar and high gas yields [31]. Disadvantages are limited scaling possibilities due to limited heat transfer (relative wall contact decreases during upscaling). Research performed by Solar et al. [40] and by Efika et al. [48]. found that pyrolysis of woody biomass in an auger reactor followed by catalytic steam reforming or thermal treatment can result in 1. a high-quality char out of the auger reactor and 2. a syngas with a high hydrogen concentration out of the gasifier (reformer).

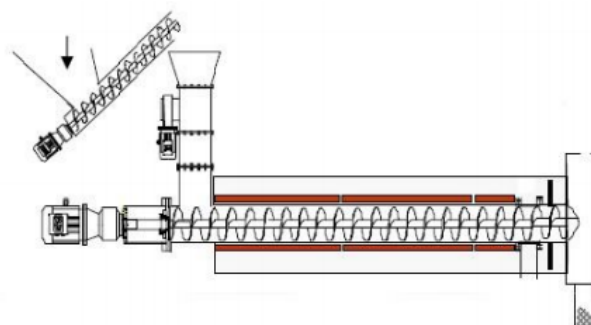


Figure 3.7: General schematics auger reactor

3.4 Reactor selection

Table 3.2 shows the advantages and disadvantages of each of the reactor types [31, 46].

Table 3.2: Advantages and disadvantages of different reactor types for biomass pyrolysis, gasification and the sorption-shift-system

Auger Reactor	Advantages	Disadvantages
	<ol style="list-style-type: none"> 1. Controlled residence time and heating rates 2. High-quality biochar 3. Flexible with biomass particle sizes 4. Enhances secondary cracking reactions 5. Easy char removal 	<ol style="list-style-type: none"> 1. Heating problems with upscaling 2. Requires external heating
Fixed bed reactor	Advantages	Disadvantages
	<ol style="list-style-type: none"> 1. Good contact between gas and solid 2. No blowout 	<ol style="list-style-type: none"> 1. Can have uneven heat distribution 2. Small particles can cause plugging 3. Char removal from bed material is complex 4. External reactor heating is complex
Fluidized bed reactor	Advantages	Disadvantages
	<ol style="list-style-type: none"> 1. Good heat distribution/transport 2. Small particles can be used 3. Easy bed material transport (overflow) 	<ol style="list-style-type: none"> 1. Blowouts, requiring additional bed material 2. High fluidization velocity result in reduced residence time or increased reactor size 3. Char removal from bed material is complex

Pyrolysis reactor

For the pyrolysis system, an auger reactor is selected because an auger reactor is relatively simple to operate, has controlled residence times, contributes to secondary cracking reactions, and char separation is easy since char is not mixed with bed material.

Reformers

Either a fixed (packed) bed or a fluidized bed can be used for catalytic steam reforming. A two-stage reactor concept with two fixed fluidized beds is selected for catalytic steam methane reforming because of better contact between fuel gas and catalysts than for fluidized beds. Gas already enters the gasification system "pre-heated" due to pyrolysis before gasification. Therefore the beds will require less heating, and thus heat distribution becomes less of a problem. Due to the endothermic nature of steam reforming and reformer temperature of 750 °C, the reactors still require additional heat, which can be supplied indirectly by the hot flue gases leaving the regenerator.

Sorption-Shift system

A separate CaL SEWGS system is used. This will increase hydrogen yield and purity, although it comes with an energy penalty and increases complexity. Since CaL requires solid mass transport, and the regenerator and sorption-shift reactor requires a good heat distribution, fluidized beds are selected. The SEWGS reactors will be bubbling fluidized beds, while the regenerator will be a fast fluidized bed due to highly exothermic combustion.

Reactor overview

Concluding the following reactors and configurations are selected:

- Pyrolysis: auger reactor
- Gasification: two-stage fixed bed reactors
- Sorption-shift system: two-stage sorption shift system with bubbling fluidized beds, in combination with a fast fluidized bed for regeneration

3.5 Results

A pyrogasification system combined with a separate SEWGS system based on CaL is selected for further research. Within this system, coupled heat integration is implemented: the SEWGS system delivers high-quality heat to the pyrogasification system. A detailed setup of the mass and heat flows and reactor characteristics are displayed in figure 3.8. All the stream numbers for both mass and heat flow as displayed in figure 3.2 are displayed in table 3.3 with further explanation. These stream numbers are used throughout this research for the given process configuration.

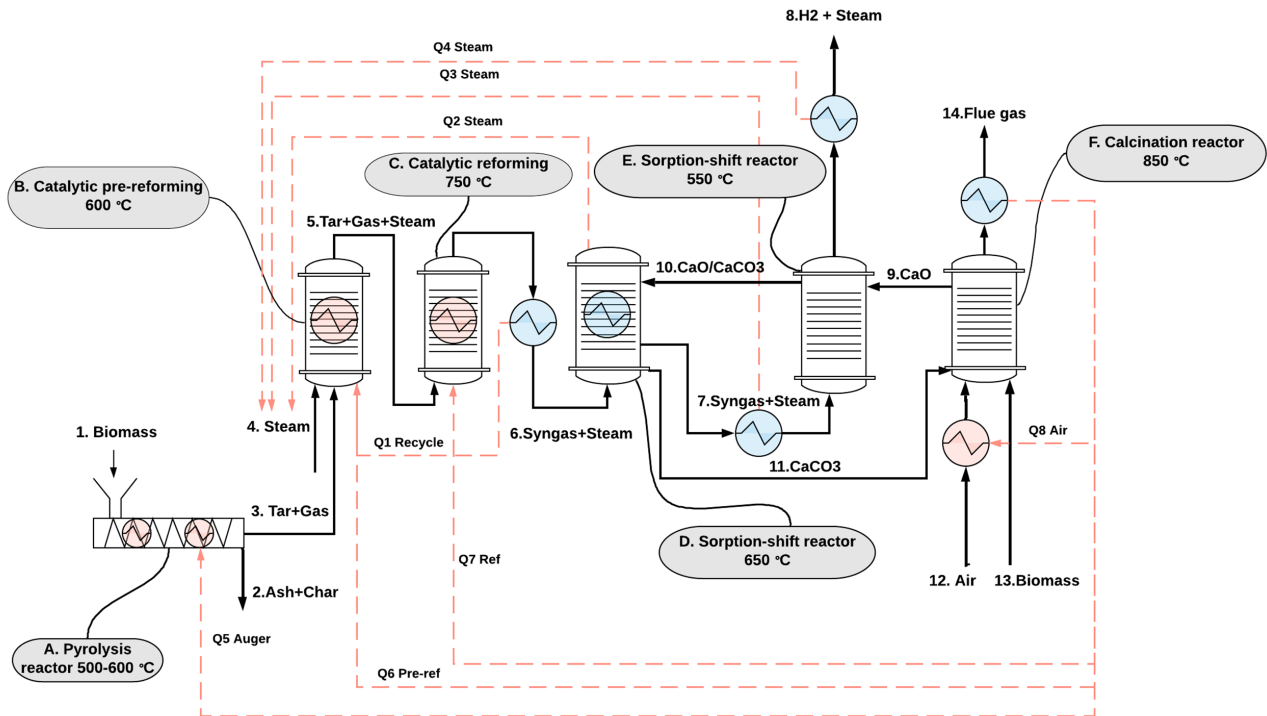


Figure 3.8: Process diagram Coupled SEWGS system with air combustion

Table 3.3: Streams in proposed system configuration

Stream nr.	Mass flow	Stream nr.	Heat flow
1	Biomass input auger	Q1	Pre-reformer heating from hot syngas
2	Biochar + ash	Q2	Steam production from SEWGS 1
3	Tars+volatiles	Q3	Steam production from intermittent gas cooling
4	Steam input pre-reformer	Q4	Steam production from gas cooling
5	Product pre-reformer	Q5	Auger heating from hot fluegas
6	Product reformer (syngas)	Q6	Pre-reformer heating from hot fluegas
7	Product SEWGS reactor 1	Q7	Reformer heating from hot fluegas
8	Product SEWGS reactor 2 (hydrogen)	Q8	Air pre-heating from hot fluegas
9	Regenerated CaO		
10	CaO/CaCO ₃ mixture		
11	CaCO ₃ to regenerator		
12	Air		
13	Biomass input regenerator		
14	Flue gases leaving regenerator		

Table 3.4 shows the design characteristics of each reactor. The design characteristics are based on the literature study performed in chapter 2 and on the reactor selection in this section.

Table 3.4: Reactor overview with main design characteristics

Reactor	Process	Type	Bed material	Key process parameters
A	Slow pyrolysis	Auger reactor	-	T = 500-600 °C Heating rate \approx 1-10K/s
B	Catalytic steam reforming	Packed bed reactor	Ni-based catalyst	T = 600 °C SC=3-4.5
C	Catalytic steam reforming	Packed bed reactor	Ni-based catalyst	T = 750 °C SC = 3-4.5
D	Sorption-shift	Bubbling fluidized bed	CaO/CaCO ₃	T = 650 °C
E	Sorption-shift	Bubbling fluidized bed	CaO/CaCO ₃	T = 550 °C
F	Combustion/calcination	Fast fluidized bed	CaO/CaCO ₃	T = 850 °C

Chapter 4

Aspen Plus model pyrogasification SEWGS system

The pyrogasification SEWGS system as designed and discussed in chapter 3 is simulated in Aspen Plus. Both reaction mechanisms, as well as heat integration, are modeled. The process simulations aim to model heat integration, determine reactor stoichiometry, and determine system operating conditions. The simulations are also used to analyze the system's technical feasibility based on energy efficiency. The entire constructed Aspen plus model is displayed in appendix B. An simplified version is displayed in figure 4.1. The system can be divided into three main sections: pyrolysis, gasification, and the CaL-SWEGS system. The next sections will discuss the modeling and results of each section individually, but first general model input, assumptions, and equations are discussed.

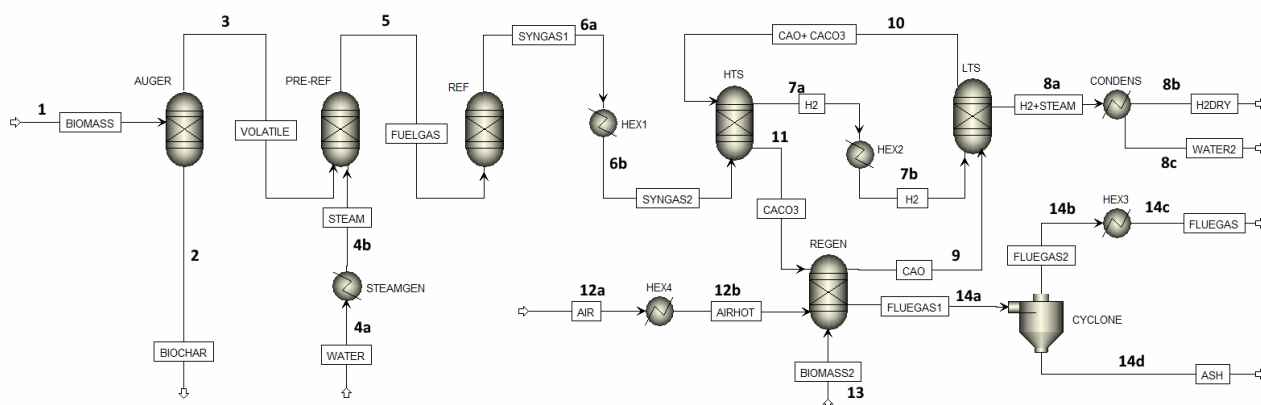


Figure 4.1: Overview simplified Aspen Plus model

4.1 Model assumptions and basic equations

In Aspen plus, a template for working with solids with metric units is used. UNIQUAC is selected as a physical property method since previous research on thermal treatment of biomass in Aspen Plus shows that using this property method results in the most accurate results [49], since pyrolysis liquids are formed (phenol's) which have non-ideal behavior an activity coefficient model like UNIQUAC is used instead of an ideal model.

4.1.1 Pyrolysis system assumptions

Woody biomass is the input of the slow-pyrolysis system. For simulation purposes, biomass is first decomposed based on its elemental composition using a FORTRAN statement in Aspen Plus. Pyrolysis is hard to model due to the complexity and wide variety of pyrolysis products; more than 100 different species have been identified. Complex dynamic modeling is required in order to determine the process kinetics and final yield. Since kinetic pyrolysis modeling is not the aim of this research, experimental yield data of slow pyrolysis of woody biomass is used.

The following data is required in order to construct an accurate slow-pyrolysis model in Aspen Plus:

- Char yield and composition
- Oil yield and composition
- Gas yield and composition
- Biomass specifications (ultimate and proximate analyze)

Research performed by Phan et al. [27] describes all product yields from slow pyrolysis accurately and is used as the basis for pyrolysis modeling. The biomass input data is compared to data for pinewood in the Phyllis database [50], and the Phyllis database is used to determine the proximate analysis of the used biomass since this was not given by Phan et al. [27]. The proximate analysis and the ultimate analyze of biomass input is given in table 4.1.

Table 4.1: Proximate and ultimate analysis biomass input

Prox. analysis	wt%	Ultimate analysis	wt % daf ¹
Moisture	8.0%	C	49.4%
Volatiles	78.7%	H	6.0%
Ash	0.4%	N	0%
Fixed Carbon	12.9%	O	44.6%
HHV = 18.00 MJ/kg		¹ dry and ash free	

The HHV of the biomass used is calculated according to the formula 4.1 given by Gaur and Reed [51] and is 19.56 MJ/kg (dry basis). Since the used biomass has a moisture content of 8 wt%, the HHV of the used biomass can be calculated back to 18.00 MJ/kg according to equation 4.2. Appendix C explains the methods used in this research concerning energy calculations in more detail.

$$HHV = 34,91Y_C + 117,83Y_H + 10,05Y_S - 1,51Y_N - 10,34Y_O - 2,11Y_{ash} \quad (4.1)$$

$$HHV^{wb} = HHV^{db} * (1 - Y_{moisture}) \quad (4.2)$$

4.1.2 Catalytic reforming system assumptions

Studies have been performed on systems that use slow pyrolysis (auger reactor) in combination with a catalytic bed for gas upgrading [27, 40, 52]. The results found in these practical studies are used to determine the yield after the pre-reformer, which will have an increased gas yield with increased hydrogen concentration and a decreased oil fraction. The pre-reformer product will not be hydrocarbon free syngas. For determination of oil and gas yield, and the gas composition research performed by Solar et al. [40] is used to determine the tar/gas yield after the pre-reformer.

The reformer is modeled based on thermodynamic equilibrium: minimizing the Gibbs free energy. The basic equations for thermodynamic equilibrium modeling are given below. The Gibbs free energy is given by equation 4.3.

$$G = U - TS + pV \quad (4.3)$$

Requiring that the Gibbs free energy is minimized: $dG = 0$, the substitution of the first law thermodynamics into the total derivative of the Gibbs free energy yields equation 4.4.

$$dG = -SdT + vdp + \sum_{i=1}^N \mu_i dn_i = 0 \quad (4.4)$$

Assuming constant pressure and temperature in the reformer simplifies the equation to equation 4.5.

$$\sum_{i=1}^N \mu_i dn_i = 0 \quad (4.5)$$

Where n_i is the number of molecules (or moles) of component i and μ_i is the chemical potential of component i .

4.1.3 Sorption-Enhanced-Water-Gas-Shift system

In order to increase hydrogen production and purity, a CaL-SEWGS system is used. The sorption-shift-system contains two SEWGS reactors, one operated at 650 °C and one at 550 °C in order to increase the hydrogen purity. The carbonation reactors (Shift-1 and Shift-2) require cooling due to the exothermic nature of carbonation; therefore, the reactors are also used to supply heat for steam generation. The upgraded syngas (almost pure H_2 with steam) is cooled in a condenser, and the sensible heat is also used for steam production. This combined heating system supplies enough steam at 625 °C for a system with a SBR=1.5 (SC=4.58 in the reformer). The sorbent ($CaO/CaCO_3$) is regenerated at 850 °C. In order to reach this temperature, additional biomass is combusted in the regenerator. The sensible heat in flue gases leaving the regenerator is used to supply heat for the auger reactor, (pre)reformer and are used to pre-heat air prior to combustion, respectively.

The SEWGS reactors (shift-1 and shift-2) and regenerator are modeled on thermodynamic equilibrium with the use of a RGibbs reactor. The mass flow of recirculating $CaO/CaCO_3$ is set at 100 kmol/h, which is 142% of the required calcium oxide for CO_2 capture (depending on sorption-shift-reactor temperatures), a surplus is used to ensure that the capacity loss of calcium oxide is compensated, and to make sure there always is a driving force towards a lower CO_2 partial pressure.

Calcination is an endothermic process; heat is supplied for calcination using biomass combustion. The flue gases from this process are used to supply heat for the pyrolysis and gasification system; therefore, sufficient biomass needs to be combusted so that:

- The calcination reactor reaches the set temperature of 850 °C
- The flue gases contain enough heat to heat the auger reactor to a minimum temperature of 500°C
- The flue gases contain enough heat to heat the pre-reformer to a minimum temperature of 600°C
- The flue gases contain enough heat to heat the reformer to a minimum temperature of 750 °C

The Equivalence Ratio (ER) used for combustion is selected to be 2.5. Air is pre-heated, therefore combustion temperatures of 850 °C can still be achieved. The same type of biomass is used for combustion as is used for pyrolysis. For simulation purposes, biomass is first decomposed based on its elemental composition using a FORTRAN statement in Aspen Plus.

4.2 Aspen plus pyrolysis model

Biomass is modeled as a non-conventional solid. Both the ultimate and proximate analysis are used for model input. The Aspen Plus model, which is constructed to model pyrolysis, is displayed in appendix B. Figure 4.2 displayed the pyrolysis system, which is analyzed in this section. The input of the pyrolysis system is set to be 1kg/s of pinewood as described in the previous section (HHV = 18,0 MW).

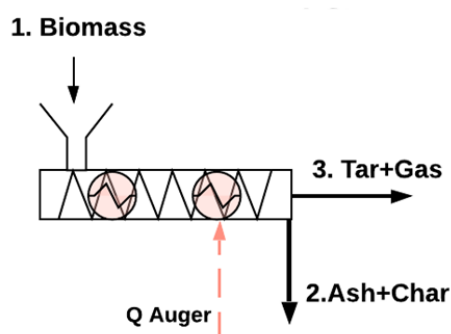


Figure 4.2: Overview model for Pyrolysis

The gas, oil, and char yield found to Phan et al.[27] on slow-pyrolysis of pine wood is displayed in table 4.2 and is used as model output. Research by Phan et al. was performed at 500 °C since, at this temperature, all product compositions are known this temperature is also used in the simulations. Note that under higher temperatures (600 °C), higher quality biochar can be produced under shorter residence time; this data is however not available and should be gathered using experimental research on auger reactor slow pyrolysis.

Table 4.2: Pyrolysis product yield

Pyrolysis product	Yield wt%	stream nr.
Char	24.3 %	2
Oil	44.4%	3
Gas	31.3	3

4.2.1 Slow-pyrolysis product composition

The ultimate analysis of the produced biochar is given as a representative molecular formula: $C_6H_{2,50}O_{0,31}$, it is modeled that all ash and fixed carbon moves from biomass to biochar. Furthermore, it is modeled that all moisture moves with the volatiles. Data for the produced bio-char is given in table 4.3. The HHV is calculated using formula 4.1.

Table 4.3: Proximate and ultimate analysis bio-char product

Prox. analysis bio-char	wt%	Ultimate analysis bio-char	wt %
Moisture	0%	C	89.2%
Volatiles	45.2%	H	3.1%
Fixed Carbon	53.2%	O	6.1%
Ash	1.6%	ash	1.6%
HHV = 34.18 MJ/kg			

The oil yield is characterized as a heavy oil phase and an aqueous phase. The produced bio-oil contains a lot of water, resulting in a low-quality bio-oil; this is expected due to the auger's relatively long residence time (5-10 minutes). The bio-oil characterization is given in table 4.4. [27]

Table 4.4: Analysis bio-oil products

Aqueous phase bio oil		heavy oil phase bio oil	
Mass fraction	78.1%	Mass fraction	21.9%
Empirical formula	$CH_{6,23}O_{2,46}$	Empirical formula	$CH_{2,28}O_{0,59}$

Since no further composition is known of the produced bio-oil, an estimate is made of the bio-oil composition in order to model biomass pyrolysis. The HHV of the produced bio-oil is given to be in the range of 10-12 MJ/kg [27], this indicates that there is a significant amount of water in the produced bio-oil. Analyzing the data given for the aqueous phase confirms this, typical values for moisture content in pyrolysis oil from slow pyrolysis is $\approx 50\%$ [53]. Water concentration is modeled to be 50% of the total oil yield. A major component in pyrolysis oil is levoglucosan ($C_5H_{10}O_5$) [54, 55], which is modeled to make up for most of the pyrolysis oil (80%, excluding water). Besides Levoglucosan, phenol (C_6H_6O) is modeled as the remaining fraction in bio-oil [52, 55]. In order to close the molecular balance (C, H, and O) in Aspen Plus, it is also assumed that small parts of methane and char (pure carbon) are formed.

The gas composition of slow pyrolysis is taken from research by Phan et al. [27], the composition of the higher-order components ($C_2 - C_3$) is, however, not described in this paper and therefore research by Solar et al. [40] is used to describe the fractions of these higher-order components. The model input for gas composition is displayed in table 4.5.

Table 4.5: Pyrolysis gas yield composition

Gas species	Volume %
CO_2	44.7 %
CO	30.5%
H_2	7.0 %
CH_4	14.7%
C_2H_4	1.2%
C_2H_6	1.9%

4.2.2 Modeling slow Pyrolysis stream results

As can be seen in the Aspen Plus flowsheet for pyrolysis in appendix B the auger reactor is modeled using four reactors: "DECOMP", "GAS", "LIQUID" and "OIL" each reactor is an RYield reactor: the yield needs to be specified. Each of the reactors used in Aspen Plus is in practice all part of the same auger reactor; multiple reactors are used for simulation purposes. The first reactor: "DECOMP" is a purely numerical step which decomposes the used biomass into its basic components (H_2O, C, O_2, H_2). In order to do so, a calculation block is programmed using a FORTRAN statement. The produced char is modeled as an unconventional solid according to the ultimate and proximate analysis given in table 4.3.

the pyrolysis system is heated using one heat flow coming from the hot flue gases from the calcination reactor: Q5. The biomass input is set to be 3600 kg/h (1kg/s), biomass specifications are given in table 4.1. The heat requirement for slow pyrolysis is Q5:1.06 MW; this heat is used for heating biomass/products to 500 °C, water evaporation, and heat required for pyrolysis reactions (endothermic). The stream results for the slow-pyrolysis system are given in table 4.6. The results are similar compared to the experimental results found by Phan et al. [27].

Table 4.6: Stream results Aspen Plus simulations pyrolysis step

Bio-char(2)		Oil + Gas(3)		
Mass flow	874 kg/h	Mass flow	2726 kg/h	
Temperature	500 °C	Temperature	500 °C	
Ultimate analysis		Component	Mass flow	molar fraction gas
C	89.2 %	CO_2	699 kg/h	0.342
H	3.1 %	CO	306 kg/h	0.234
O	6.1%	H_2	5.0 kg/h	0.054
Ash	1.6 %	CH_4	259 kg/h	0.348
		C_2H_4	12 kg/h	0.009
		C_2H_6	21 kg/h	0.013
		H_2O	799 kg/h	
		$C_6H_{10}O_5$	558 kg/h	
		C_6H_6O	34 kg/h	
		Char	32 kg/h	
Energy flow rate	8.3 MW			

4.2.3 Energy flows slow pyrolysis

Flue gases are used to heat up the auger reactor. Flue gases enter the HEX at 647 °C and leave at 516°C supplying 1,06 MW of heat for the auger reactor heating the product to 500 °C.

The Sankey diagram of the pyrolysis system is given in figure 4.3. Due to the endothermic nature of pyrolysis, the intermediate results do not seem correct; the products contain 1,9MW of sensible heat, while only 1,1 MW of sensible heat is added to the pyrolysis system. A reason for this deviation can be found in the assumptions which are made for the bio-oil composition. These assumptions are not easily changed due to mass and elemental balances implemented in the designed system. The overall system efficiency is not influenced significantly by this deviation, since the reformer is modeled at thermodynamic equilibrium. The overall heat demand stays the same for the combined pyrogasification system, only the minimum required temperatures of the supplied heat changes slightly: more heat

is required at the auger reactor (held at 500 °C), and less heat is required at the pre-reformer (held at 600 °C) and the reformer (held at 750 °C). Therefore the efficiency (if it is changed at all) will increase slightly compared to the modeled results. Further research with respect to slow pyrolysis yield in auger reactors is required to more accurately model the pyrolysis yield in the constructed model.

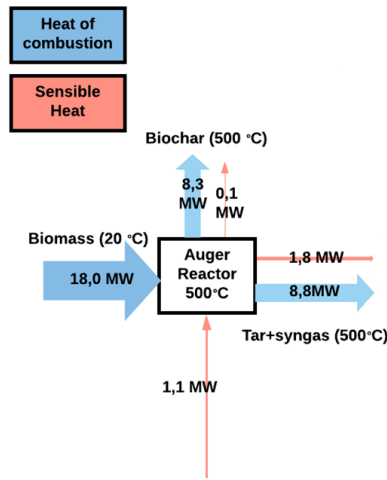


Figure 4.3: Sankey diagram pyrolysis system

4.3 Aspen plus steam reforming model

The gasification system contains two reactors that are used for catalytic steam reforming: a pre-reformer and a reformer. The pre-reformer is modeled as an RYield reactor, with specified product output based on literature [40] while the reformer is a "RGibbs" reactor based on thermodynamic equilibrium modeling (minimizing Gibbs free energy). Heat is supplied from the hot flue gases (850 °C) of the calcination reactor to the reformer, next the produced syngas is used to heat up the pre-reformer. This is beneficial since 1) the pre-reformer requires heat, and 2) the produced syngas requires cooling after the reformer since the carbonation reactor operates at low temperature (550-650 °C). In total, 5400 kg of steam is supplied to the catalytic steam reforming system (SBR=1.5). The flowsheet as designed in Aspen Plus is displayed in appendix B. Figure 4.4 displays the analyzed system in this section with corresponding mass and heat flows.

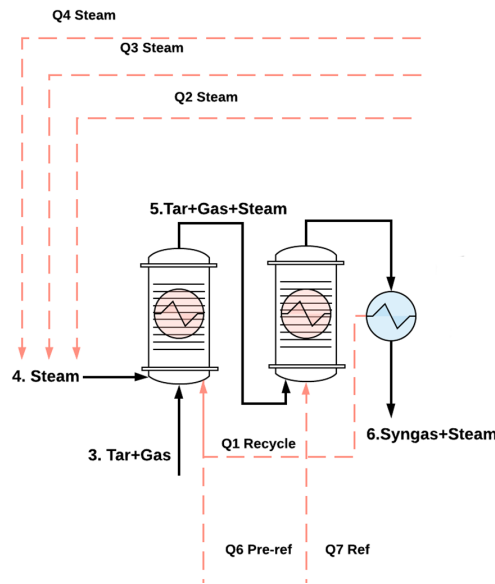


Figure 4.4: Overview model for reforming

The modeled gas yield of the pre-reformer is displayed in table 4.8 [40]. For bio-oil which is not reformed into syngas, it is modeled that the bio-oil composition remains the same (50 wt % water and 50% hydrocarbons) The composition of the product (gas and oils) is displayed in table 4.7 [40].

Table 4.7: Pre-reformer product input and yield

product	Inlet	outlet
Oil	58.7%	32,0 %
Gas	41.3%	68,0 %

Table 4.8: Pre-reformer gas yield composition

Gas species	Volume %
CO_2	19.14 %
CO	23.77%
H_2	37.24 %
CH_4	17.13%
C_2H_4	2,30%
C_2H_6	0.42%

In Aspen Plus, an RGibbs reactor which calculated thermodynamic equilibrium is used to model the reformer at 750 °C. The pre-reformer operates at 600 °C and is modeled as an RYield reactor.

4.3.1 Stream results steam reforming system

The stream results of the catalytic steam reforming system are displayed in table 4.9. For this system, a SC=4.58 in the pre-reformer is used, simulation results show that there is sufficient heat released by the SEWGS system to produce this high-quality steam at 625 °C. A SC=4.58 is on the high end of the optimal SC range: 3-4.5 (as discussed in section 2.2.4). Since there is sufficient heat for steam production, this is not changed in this simulation, but the influence of (lower) SC is further investigated in chapter 5.

Table 4.9: Stream results steam reforming step

Stream nr.	3		5		6a	
Mass flow	2726 kg/h		8126 kg/h		8126 kg/h	
Temperature	500 °C		600 °C		750 °C	
Component	Mass flow	Vol% gas	Mass flow	Vol% gas	Mass flow	Vol% gas
CO_2	699 kg/h	34.2%	1052 kg/h	24.7 %	2353kg/h	28.0 %
CO	306 kg/h	23.4 %	538 kg/h	19.9 %	484 kg/h	9.1 %
H_2	5.0 kg/h	5.4%	90 kg/h	46.2 %	242 kg/h	62.9 %
CH_4	259 kg/h	34.8%	101 kg/h	6.5 %	0 kg/h	0 %
C_2H_4	12 kg/h	0.9 %	62 kg/h	2.3 %	0 kg/h	0 %
C_2H_6	21 kg/h	1.3 %	12 kg/h	0.4 %	0 kg/h	0 %
H_2O	799 kg/h		5835 kg/h		5047 kg/h	
$C_6H_{10}O_5$	558 kg/h		437 kg/h		0 kg/h	
C_6H_6O	34 kg/h		0 kg/h		0 kg/h	
Char	32 kg/h		0 kg/h		0kg/h	
Stream nr.	4					
H_2O	5400 kg/h					
Temperature	625 °C					

4.3.2 Energy flows steam reforming system

Heat is used from the hot flue gases from the calcination reactor (850 °C) to supply heat for the reformer and the pre-reformer. The heat delivered to the reformer is 1512.8 kW and to the pre-reformer is 175 kW. Heat is recycled from the hot syngas (750 °C leaving the reformer to the pre-reformer (600 °C), this is 642 kW, the hot syngases leaving the reformer are cooled from 750 °C to 625 °C. In the model, heat is directly transferred to the pre-reformer, which is operated at 600 °C. In order for a sufficiently large ΔT_{LM} , it is checked that for sufficient heat transfer, the pinch point is at least 25 °C between cold and hot streams. Since there are no phase transitions (except for steam generation), it is expected that the pinpoint P_i for counter-flow heat exchange is:

$$P_i = \min(T_{h,1} - T_{c,2}, T_{h,2} - T_{c,1}) \quad (4.6)$$

The Sankey diagram of the gasification system, displaying both sensible heat and heat of combustion are displayed in figure 4.5. The steam generation is displayed in a simplified manner, 2900 kg/h of steam is generated using heat from the first sorption-shift-reactor using a boiler integrated into the reactor, the total heat supplied to steam from SEWGS-1 is 2.9 MW. The other 2500 kg/h is heated in a two-step system using the hydrogen/steam mixture exiting SEWGS-2 (leaving at 550 °C, 1.4 MW) as well as the hydrogen/steam mixture leaving Shift-1 (leaving at 650 °C, 1.2 MW).

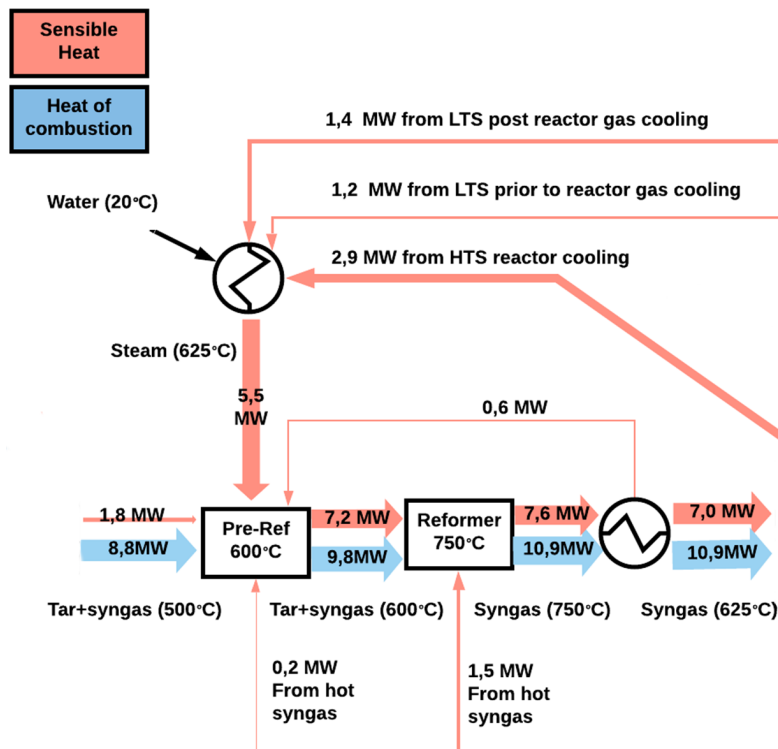


Figure 4.5: Sankey Diagram gasification system

4.3.3 Reforming model results validation

The results are validated with results found by experimental research in the literature. The results by van Rossum [42] are obtained by experiments in a dual bed catalytic gasifier used to process pyrolysis oil at a temperature of 777 °C and steam to carbon ratio of 2.7. The results of van Rossum are displayed in table 4.10 [42], together with the simulation results which have been found using thermodynamic equilibrium modeling. In order for a good comparison, an additional simulation is run at $SC=2.7$ and a reformer temperature of 777 °C. It can be observed that the results are in close agreement, and therefore using thermodynamic equilibrium modeling is a good approach to model the reformer. The difference which is observed can be explained by the fact that van Rossum et al. used pyrolysis oil, derived from pinewood, while this research reformed both oils and gases released by slow pyrolysis: the composition of the input is not exactly similar.

Table 4.10: Simulation results and experimental results found by van Rossum et al.

Gas species	Simulation results	Experimental results
CO_2	21.6%	19.9 %
CO	12.9%	14.3 %
H_2	65.5 %	65.8 %
CH_4	0.0 %	0.0 %
C_2H_4	0.0%	0.0 %
C_2H_6	0.0%	0.0 %

4.4 Aspen plus SEWGS system

The SEWGS system is modeled using two sorption-shift reactors (SEWGS-1 and SEWGS-2) and a regenerator. The sorption-shift reactors require cooling and have a triple function of CO_2 absorption, shifting the WGS-reaction and steam generation. The upgraded syngas (almost pure H_2 with steam) is cooled, and the sensible heat is used for steam production. The sensible heat from flue gases leaving the regenerator is used to supply heat for the auger reactor, (pre)reformer and are finally used to pre-heat air, respectively. The SEWGS reactors and the regenerator are simulated based on thermodynamic equilibrium using an RGibbs reactor. For sorbent regeneration, biomass with the same composition as used as auger input is used as displayed in section 4.1.1, an air-ratio of 2.5 is used in the regenerator. An overview of the system designed in Aspen Plus is given in appendix B. The analyzed system in this section is displayed in figure 4.6

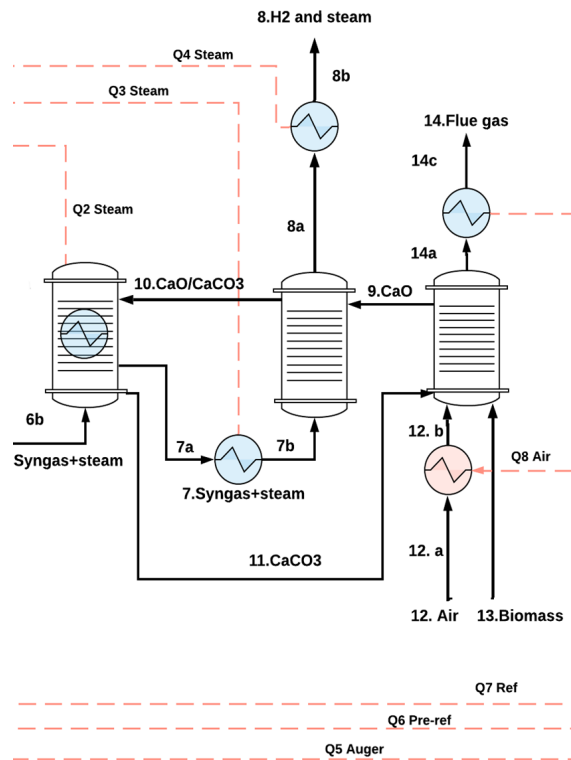


Figure 4.6: Overview model for calcium looping based SEWGS including heat regeneration

4.4.1 Stream results sorption-shift system

The produced syngas enters SEWGS-1, which operates at 650 °C; next, the gas is led to SEWGS-2, which operates at 550 °C. The mass flows and volume fractions of the SEWGS system derived from the Aspen Plus model are displayed in 4.11. The solid mass flows from the CaL looping system are displayed in table 4.12, regenerated sorbent (100% CaO) first enters SEWGS-2 before it is led to SEWGS-1. A surplus of CaO is used (142 %) to compensate for sorbent activity loss.

Table 4.11: Syngas stream results sorption-shift system

Stream nr.	6b		7a		8a	
Mass flow	8126 kg/h		5339 kg/h		5033 kg/h	
Temperature	625 °C		650 °C		550 °C	
Component	Mass flow	V% gas[DB]	Mass flow	V% gas [DB]	Mass flow	V% gas[DB]
<i>CO</i> ₂	2352 kg/h	28.0%	261 kg/h	4.1 %	15,9 kg/h	0,266 %
<i>CO</i>	485 kg/h	9.1 %	41 kg/h	1.0 %	1,4 kg/h	0,038 %
<i>H</i> ₂	242 kg/h	62.9%	274 kg/h	94.9 %	276,3 kg/h	99,670 %
<i>CH</i> ₄	0,2 kg/h	0.0%	0,4 kg/h	0 %	0,6 kg/h	0,028 %
<i>C</i> ₂ <i>H</i> ₄	0 kg/h	0.0 %	0 kg/h	0 %	0 kg/h	0 %
<i>C</i> ₂ <i>H</i> ₆	0 kg/h	0.0 %	0 kg/h	0 %	0 kg/h	0 %
<i>H</i> ₂ <i>O</i>	5048 kg/h		4763 kg/h		4738 kg/h	

Table 4.12: Solid stream results sorption-shift system

Stream nr.	9	10	11
Mass flow	5587 kg/h	5894 kg/h	8681 kg/h
Temperature	850 °C	550 °C	650 °C
CaO	5587 kg/h	5196 kg/h	1645 kg/h
<i>CaCO</i> ₃	0 kg/h	697 kg/h	7035 kg/h

The results displayed in table 4.11 show that high purity hydrogen is produced by the SEWGS system: vol % = 99.67%. Compared to conventional gasification (*H*₂ vol% in the 40-50% range) or sorption enhanced gasification (*H*₂ vol% in the 70-80% range), this is a large improvement. The produced hydrogen purity is comparable to an industrial-sized PEM electrolysis system, which produces hydrogen with a purity in the range of 99.5-99.9 vol % (Siemens Silyzer 200)[56].

4.4.2 Stream results calcination reactor

The calcination reactor is used for the regeneration of calcium carbonate to calcium oxide. The calcination reactor is modeled using thermodynamic equilibrium modeling. Air is pre-heated to 495 °C using sensible heat remaining in the flue gases after heat is supplied to all heat demanding reactors (pinch point > 25 °C). In order to supply sufficient heat, 1540 kg/h additional biomass is combusted in order to supply heat for sorbent regeneration and pyrogasification systems.

The stream results of the regeneration system are displayed in table 4.13. Note that in the simulations, ash is first separated before flue gases are cooled, as displayed in the constructed Aspen Plus flow sheet in appendix B.

Stream nr.	12b	13	11	9	14a
Mass flow	20327 kg/h	1540 kg/h	8681 kg/h	5587 kg/h	24961 kg/h
Temperature	495 °C	20 °C	650 °C	850 °C	850 °C
<i>CO</i> ₂	0kg/h	0 kg/h	0 kg/h	0 kg/h	5648 kg/h
<i>O</i> ₂	4729 kg/h	0 kg/h	0 kg/h	0kg/h	2832kg/h
<i>N</i> ₂	15598 kg/h	0 kg/h	0 kg/h	0kg/h	15598kg/h
<i>H</i> ₂ <i>O</i>	0 kg/h	0 kg/h	0 kg/h	0 kg/h	878 kg/h
Biomass	0 kg/h	1540 kg/h	0 kg/h	0 kg/h	0 kg/h
<i>CaO</i>	0 kg/h	0 kg/h	1645 kg/h	5587 kg/h	0kg/h
<i>CaCO</i> ₃	0 kg/h	0 kg/h	7073 kg/h	0 kg/h	0 kg/h
Ash	0 kg/h	0 kg/h	0 kg/h	0 kg/h	5.9 kg/h

Table 4.13: Stream results calcination step

4.4.3 Energy flows sorption-shift system

Heat is recovered from the flue gases in order to supply heat for the pyrolysis system and gasification system, respectively. First, the flue gases are used to heat up the reformers (gasification) since this system requires the highest temperature. Next, the flue gases are used to heat up the auger reactor (pyrolysis); for simulation purposes, this is done with two heat flows, while in practice, there is only one heat flow, the reason being that the pyrolysis step is split up into multiple reactors in the model. The heat flows are designed in such a way that:

- There is always a temperature difference of 25 °C between the hot stream and the cold stream: Pinch point > 25 °C
- The heat flow supplies sufficient heat in order to heat the products of pyrolysis to at least 500 °C, the products of the pre-reformer to at least 600 °C, and the products of the reformer to at least 750 °C.

In order to reach these design specifications, the amount of biomass for combustion and heat recycles can be tuned given the above specifications. A Sankey diagram is made of the SEWGS, which is shown in figure 4.7. The approach used for the calculation of carbonation energies and sensible heat of sorbents is explained in appendix C.

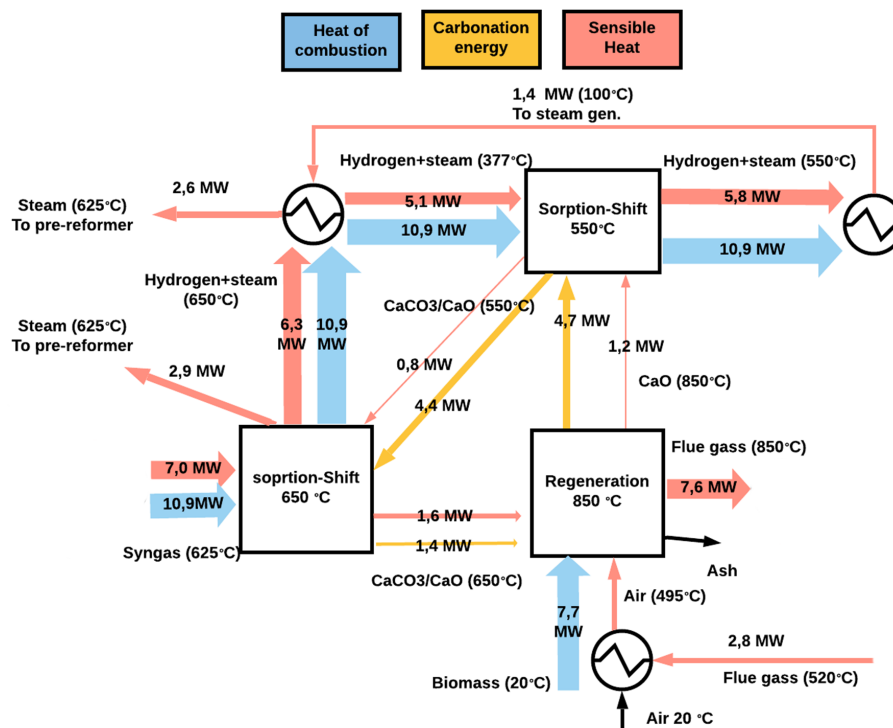


Figure 4.7: Sankey diagram sorption shift system

The Sankey diagram of downstream gas process steps: hydrogen cooling/drying and heat regeneration from the syn-gas is shown in figure 4.8.

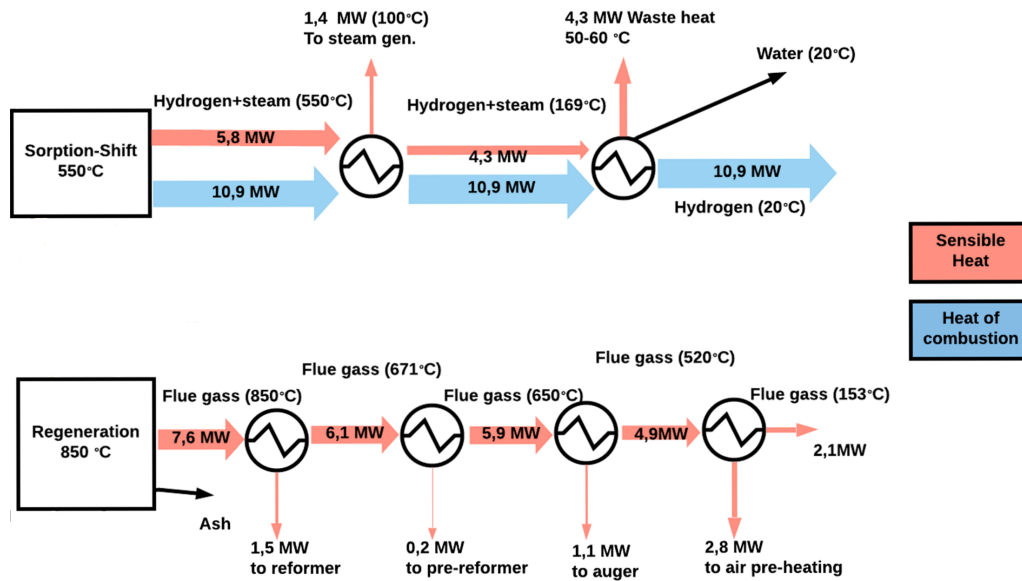


Figure 4.8: Sankey diagram downstream gas treatment

The complete Sankey diagram of the system can be found in appendix D. For the hydrogen gas, during the final cooling step, a lot of sensible heat is lost; this is due to the latent heat of condensation of water. Due to low partial water pressure, this heat is released at a low exergy level below 100 °C. The hydrogen/steam product, after steam generation has a temperature of 169 °C, the flue gases after air-preheating have a temperature of 153 °C. Remaining heat in these gas flows can be used, for example, for residential heating, further heat integration of these streams in the analyzed system is not possible. When lower qualities of biomass are used with higher moisture content, this waste heat can be used for biomass drying.

4.4.4 SEWGS model results validation

The results of the SEWGS system are compared with results found in the literature. CaL based SEWGS has not been the subject of many studies. The only similar study which has been found was by Li et al. [57], which recently (July 2020) published results. These results are also based on thermodynamic equilibrium modeling in Aspen Plus. Li et al. directly gasified biomass (no pyrolysis step) followed by a SEWGS at 550 °C. The results found by Li et al., as well as the results from this research, are displayed in table 4.14. Similar hydrogen purity's are obtained. There is, however, a difference in CO, CO₂, and CH₄ concentrations. This difference is caused by the difference in SC ratio. This research uses a SC ratio of 4.58, while Li et al. used a SC ratio of 1.64. The influence of SC ratio on final product yield and composition is further analyzed in chapter 5 (sensitivity analysis). It can be seen that under lower SC CO₂ concentrations decrease while CO and CH₄ concentrations increase.

Table 4.14: Simulation results validation by results found by Li et al.

Gas species	simulation results	Results Li et al. (2020)
CO ₂	0.266 %	0.1 %
CO	0.038%	0.1 %
H ₂	99.67 %	99.7 %
CH ₄	0.028 %	0.1 %

4.5 System efficiency

The stream results have been presented in the previous sections. The main technical characteristic which determines the technology is the system's overall efficiency. In order to calculate the system efficiency, the energy input and usable energy output have to be determined. The overall system efficiency η_{tot} , based on chemical energy, is determined according to equation 4.7, the cold-gas efficiency is calculated according to equation 4.8. In this equation, the subscript B represents biomass, C represents Biochar and H represents Hydrogen. The HHV of biomass and biochar is calculated according to equation 4.1 and 4.2. The HHV of hydrogen is given by 141.7 MJ/kg [1].

$$\eta_{tot} = \frac{En_{char} + En_{H_2}}{En_{biomass}} \quad (4.7)$$

$$\eta_{cold-gas} = \frac{En_{H_2}}{En_{biomass}} \quad (4.8)$$

The system results are displayed in figure 4.15. Using this data in combination with equations 4.7 and 4.8 results in a cold gas efficiency of 42.2 % and an overall system chemical efficiency of $\eta_{tot} = 74.4 \%$. Comparing the thermal efficiency of the pyrogasification SEWGS system with conventional gasification systems, it can be seen that there is a small decrease in thermal efficiency. Prins et al. found that for conventional biomass gasification, with biomass with an atomic O/C ratio of 0.68 (comparable with this study), the chemical energy efficiency is in the 76% -78 % range [58]. It is important to note, however, that the analyzed system produces high-quality products and not syngas.

Species	Mass flow	HHV
Biomass	5140 kg/h	18.0 MJ/kg
Biochar	874 kg/h	34.2 Mj/kg
Hydrogen	276 kg/h	141.7 MJ/kg

Table 4.15: Main system input and output

The exergy efficiency is calculated according to equation 4.9. Note that in equation 4.11 the mass ratio's are used (and not molar ratio's). The used exergy content of hydrogen fuel is 134.78 MJ/kg [59].

$$\eta_{ex} = \frac{Ex_{H_2} + Ex_{char}}{Ex_{biomass}} \quad (4.9)$$

The exergetic value of both biomass and biochar is calculated according to equation 4.10 and 4.11. Using the ultimate analysis data of both biomass and biochar as discussed in this chapter results in a system exergetic efficiency of $\eta_{ex} = 68,1 \%$.

$$Ex_{biomass} = \beta LHV_{biomass} \quad (4.10)$$

$$\beta = \frac{1.0414 + 0.0177[H/C] - 0.3328[O/C](1 + 0.0537[H/C])}{1 - 0.4021[O/C]} \quad (4.11)$$

In total, 6.3 MW of sensible/latent heat, which is 24.9% compared to the chemical energy input (biomass), leaves the system in the form of flue gas (153 °C) and sensible/latent heat in the hydrogen/steam mixture (before gas drying). Both streams contain water vapor, which largely contributes to the relatively high energy content (latent heat). Both streams have a significantly lower partial water pressure than 1 atm.: the hydrogen/steam mix has a water vapor pressure of 66.8 kPa, the flue gas contains large quantities of CO₂ and nitrogen, resulting in a water vapor pressure of 5.9 kPa. Therefore when cooling these gases, the latent heat is released at temperatures below 100 °C. Especially the steam/hydrogen mixture contains a lot of latent heat due to large quantities of steam which are added to the reforming process. Most of this latent heat will be released at temperatures in the 90°C (water vapor pressure: 70.1 kPa)-60°C (water vapor pressure:19.9 kPa) range. This relatively low quality of heat cannot be used for reactor heating but can be used for biomass drying purposes when high moisture biomass is used or for residential heating.

4.6 Results

An Aspen Plus model has been constructed to model the pyrogasification SEWGS system. Reactor stoichiometry has been determined using A: experimental research from literature and B: Thermal equilibrium modeling. Efficient heat integration is designed. The advantage of combining pyrogasification with SEWGS is heat integration of high-quality heat of the SEWGS system, which can be used for steam production and reactor heating. The model which is designed is dynamic and forms a basis for further system design improvement, system analysis, and optimization of process conditions.

The analyzed system produced high-quality biochar (HHV=34 MJ/kg) combined with high purity hydrogen (V% = 99,67 %). Per ton of daf (dry and ash-free) biomass input, the analyzed system produced 59 kg of hydrogen and 186 kg of biochar. The chemical efficiency of the designed system is 74.4 %, slightly lower compared to conventional biomass gasification. System optimization with respect to cost and efficiency is required, which will be discussed in chapter 5 and 6, respectively. The results of the reforming system and SEWGS system have been validated by literature [42, 57]. The chemical efficiency found in by simulations is slightly lower compared to conventional gasification systems [58], but the quality of the products is much higher. The model also showed that the hot flue gases leaving the regenerator (calcination) contain sufficient heat to heat the reforming system. Table 4.16 displays the main system results found by analysis of the designed Aspen plus system for the pyrogasification SEWGS system

Table 4.16: Results Aspen plus simulation results

Chemical efficiency	74,4 %
Cold-gas efficiency	42.2 %
Hydrogen production rate	59 kg/ton biomass input (daf)
Biochar production rate	186 kg/ton biomass input (daf)
Hydrogen purity	99.7 %
Biochar HHV	34.2 MJ/kg

In order to more accurately model pyrolysis in an auger reactor, experimental research is required. Data found by experimental research can be implemented in the auger reactor model, giving more accurate results for the heat demand and product quality of the auger reactor. The SEWGS reactors are modeled at thermodynamic equilibrium. Experimental research is required to determine if a thermodynamic equilibrium is approached at the used reactor temperatures (650-550 °C) without the addition of an additional catalyst. There has not been a lot of research based on the kinetics for calcium oxide/calcium carbonate related to CaL based SEWGS systems for the production of high purity hydrogen. The kinetics of CaO as a catalyst on the WGS combined with absorption kinetics of CaO for CO₂ capture requires better understanding. Once the kinetics of CaL based SEWGS are better understood, they can be implemented in the designed Aspen Plus model to more accurately model the system.

Sorbent deactivation is one of the main disadvantages of using CaO as CO₂ sorbent. In order to compensate, a surplus of CaO is modeled in the constructed Aspen Plus model. More accurate modeling of the required sorbent make up based on the replacement strategy is required. Replacement strategies are discussed in appendix E which can further improve the accuracy of the process simulations. Furthermore, more research is required with respect to reducing sorbent deactivation, research on sorbent hydration or using calcined dolomite's show promising results [21], these techniques can also be integrated into the designed model.

The process parameters used in this initial Aspen Plus model require better understanding and optimization. Reducing the SC ratio can increase the system efficiency but also may alter the final product composition. The system contains a lot of heat exchangers that require size optimization based on hydrogen/biochar levelized cost of production. Furthermore, the effect of reactor temperature of both the SEWGS reactors and the calcination reactor has to be better understood. In order to determine the influence of these process parameters, a sensitivity analysis is performed, which will be discussed in chapter 5.

Chapter 5

Sensitivity analysis pyrogasification model

This section will cover the sensitivity analysis of the designed system in Aspen Plus discussed in chapter 4. The goal of the sensitivity analysis is to:

1. Determine maximum efficiency points of reactors
2. Determine the model reliability (test robustness)
3. In combination with the financial model find optimal cost-efficiency points (discussed in chapter 6)

The sensitivity of the variables listed below are tested with respect to system output and system efficiency.

- The temperatures of Shift-1 and Shift-2
- The temperature of the regenerator
- SBR
- Pinch point in heat exchangers

5.1 Reactor temperature sorption-shift-1

The temperature of the "SEWGS-1" (Shift-1) reactor is varied between 600 °C and 700 °C with increments of 25 °C. The temperature of Shift-1 influences the temperature of produced steam. Due to high-quality steels' temperature limitations, steam temperatures higher than 625 °C will not be applicable in the system since higher temperatures will result in creep and low cycle fatigue to even high-quality steel. The 2.25Cr-1 Mo and 9Cr-1Mo alloys are types of ferritic steels that can be applied at steam temperatures up to 625 °C [60]. The maximum acquired steam temperature can then be calculated using formula 5.1 assuming that heat exchangers require a minimum pinch point of 25 °C.

$$T_{steam} = \text{Min}((T_{shift-1} - 25^{\circ}\text{C}), 625^{\circ}\text{C}) \quad (5.1)$$

The results with respect to (maximum) steam temperatures are displayed in appendix F. Under reactor temperatures of 650 °C, lower steam temperatures are obtained, while at higher temperatures (>650 °C), the steam temperature is limited at 625 °C. If steam below 625 °C is used, more additional heating of the pre-reformer system is required.

For the system operating at a shift-1 temperature of 700 °C the system has to be modified slightly. Due to the increased temperature of the first shift reactor, relatively a lot of the CO_2 is captured in the second sorption-shift-reactor. This causes a shift in the steam generation system: more steam is generated using heat from SEWGS-2, and less steam is generated from released heat by SEWGS-1.

The system operated at a shift-1 temperature of 700 °C requires additional cooling at the shift-2 reactor in order to operate the shift-2 reactor at 550 °C. The change in carbon capture per reactor as a function of temperature is displayed in figure 5.1. In this figure, the amount of captured carbon (relative to the total amount of carbon in the syngas coming from the gasification system) is displayed for both the first and second sorption-shift-reactor. As a rule of thumb, it is desired that roughly 90 % of the carbon is captured in the first reactor and 10 % of the carbon is captured in the second reactor. This is comparable to CO conversion rates in HTS reactors (≈ 375 °C) compared to LTS reactors (≈ 225 °C) used in conventional methane reforming systems for hydrogen production [61]. This ratio of 9:1 corresponds with an sorption-shift-1 temperature of 650 °C and a sorption-shift temperature ≤ 550 °C as can be seen in figure 5.1, at a sorption-shift-2 temperature of 550 °C only 0.6 % of carbon is not captured and remains as pollutant in the hydrogen gas.

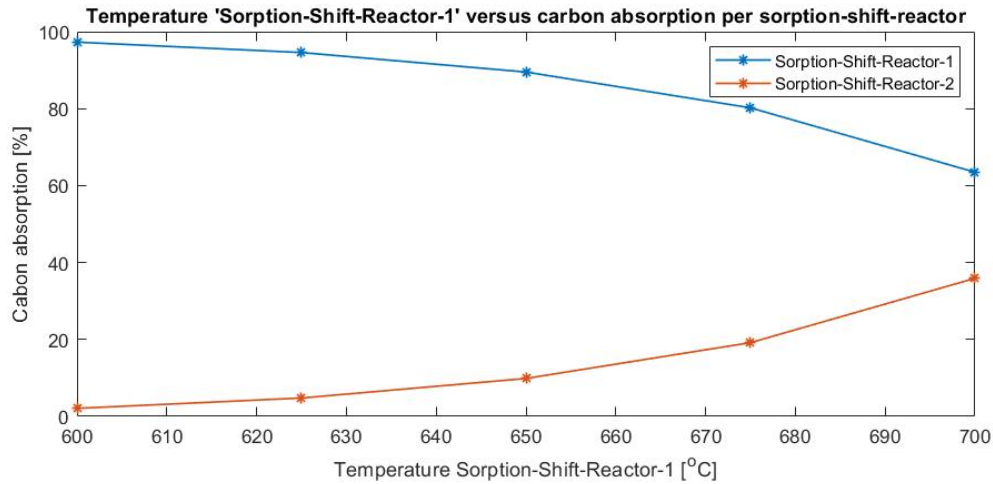


Figure 5.1: Relative carbon absorption per reactor as function of sorption-shift-1 reactor temperature

The total system efficiency as function of the shift-1 reactor temperature is displayed in figure 5.2. The system efficiency varies a bit from 73.39% at 600 °C to 74.93 % at 700 °C. The efficiency is influenced by two main mechanisms, which are dependent on the reactor temperature:

1. Under higher reactor temperatures (up to 650 °C), higher-quality steam can be generated, resulting in less additional required heat input to the gasification system from additional biomass combustion, increasing the system efficiency
2. Under higher temperatures CaO/CaCO₃ leaving Shift-1 enters the generator at higher temperatures; thus less heat is required in this reactor to heat up this mixture for regeneration resulting in less additional biomass combustion, and thus increasing the efficiency.

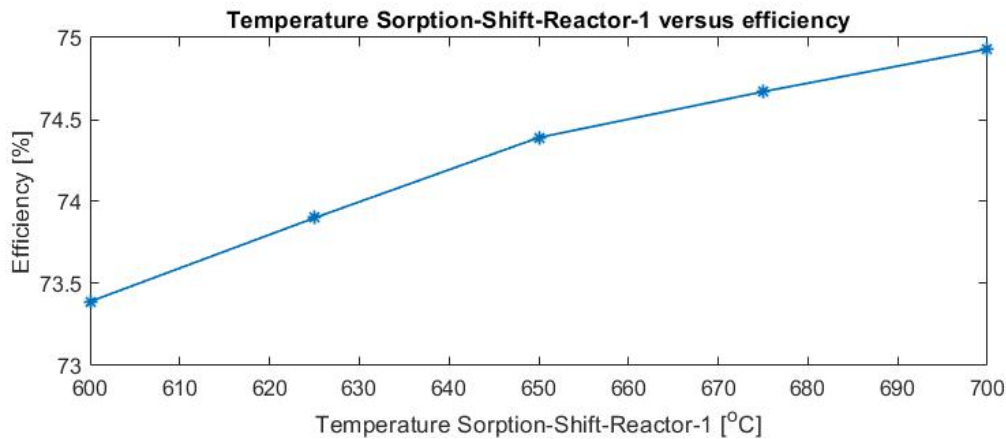


Figure 5.2: Overall system efficiency as function of Shift-1 temperature

The efficiency increases as reactor temperature increases, until 650°C, there is a relatively sharp increase, which is a result of both generated steam temperature increase and Shift-1 solid product temperature (CaO/CaCO₃) increase. After 650 °C, the efficiency increase is only due to Shift-1 solid product temperature (CaO/CaCO₃) increase. The final gas quality is not altered by the Shift-1 temperature since Shift-2 operates at constant conditions in this analysis (550 °C). However, at higher Shift-1 temperatures, more CO₂ needs to be captured in Shift-2 at a relatively low temperature. Therefore it becomes less likely with increasing Shift-1 temperatures that Shift-2 reaches thermodynamic equilibrium; therefore, a 9:1 (Shift-1:Shift-2) carbon-capture ratio is used and recommend, resulting in a SEWGS-1 temperature of 650 °C. This system can produce high-quality steam (625 °C) combined with the desired ratios for carbon capture in both SEWGS reactors (9:1).

5.2 Reactor temperature sorption-shift-2

The temperature of the low-temperature SEWGS reactor is varied between 500-600 °C with increments of 25 °C. Due to constant temperatures of Shift-1 (650 °C) and the regenerator (850 °C), the quality (temperature) of heat, cycled from the SEWGS system to the pyrogasification system does not change, flue gases of 850 °C and (the product from) Shift-1 (650 °C) can still be used in the same way for heat integration (steam generation and reactor heating). More CO_2 is absorbed in Shift-2 at a temperature of 500 °C, so the regenerator requires more heat since more $CaCO_3$ needs to be regenerated. On the other hand, more hydrogen is produced in the second shift reactor with a higher purity under lower reactor temperatures, and hence more CO is shifted towards CO_2 . The influence of the reactor temperature on the overall system efficiency is plotted in figure 5.3. It becomes clear that an increase in temperature has a slightly positive influence on the system efficiency; less biomass is required at the regenerator (less $CaCO_3$ requires regeneration due to less carbon capture). The slight absolute increase of hydrogen production at lower temperatures does not outweigh the decrease in biomass input with respect to chemical energy efficiency. The "contaminant" (CO_2 , CO, CH_4) concentration in the hydrogen gas are, however, influenced significantly by the sorption-shift-reactor-temperature, which can decrease the energy consumption of upstream gas-cleaning. Upstream gas-cleaning is not considered in the efficiency calculations. The change in energy efficiency is not significant (74.35 % at 500 °C and 74.61% at 600 °C).

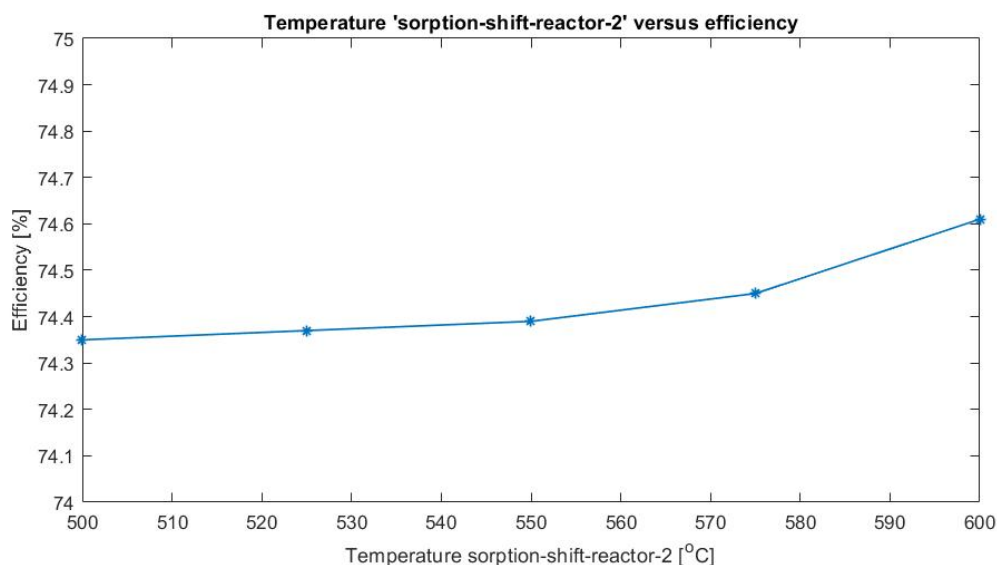


Figure 5.3: Temperature sorption-shift-reactor versus overall system efficiency

Hydrogen quality is influenced significantly by the carbonation temperature, as can be shown from a sensitivity analysis performed in Aspen Plus of a simplified pyro-gasification-shift model as shown in figure 5.4 where temperatures are varied between 550 °C and 750 °C of a sorption-shift reactor.

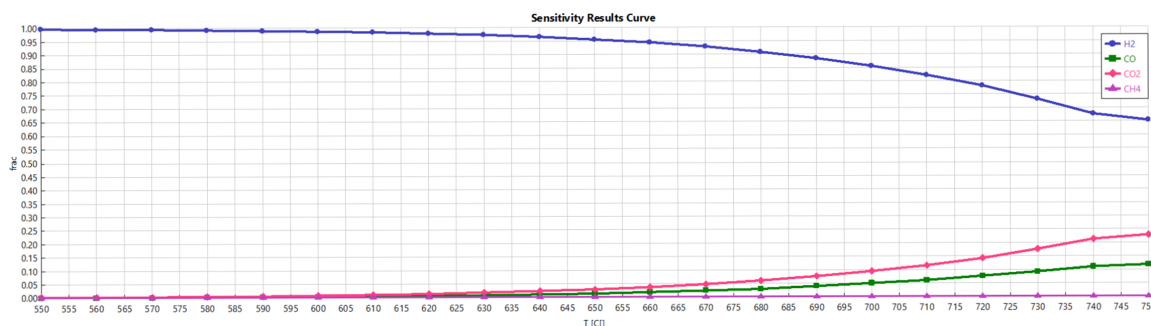


Figure 5.4: Carbonation temperature versus syngas concentrations sensitivity results Aspen Plus

For the temperature range of 500 °C to 600 °C, "Shift-2" is analyzed with respect to product gas. The results are displayed in figure 5.4. The relative hydrogen purity increases significantly with a temperature decrease. At 600 °C, the hydrogen gas has 98.638 % purity, while at 500 °C, the gas has a 99.915 % purity. For fuel cell applications, a hydrogen purity of 99.97 % is required (see appendix G), and therefore even at sorption-shift temperatures of 500°C, upstream upgrading/ gas cleaning is still required to reach this hydrogen purity and to remove CO (max 0.2 ppm) and CO_2

(max 2 ppm), for example with Temperature-Swing-Adsorption (TSA) or Pressure-Swing-Absorption (PSA). Further research is required with respect to SEWGS kinetics using CaL; it is unknown at what temperatures thermodynamic equilibrium is still approached in a SEWGS reactor without the addition of a WGS catalyst (iron oxide or zinc oxide).

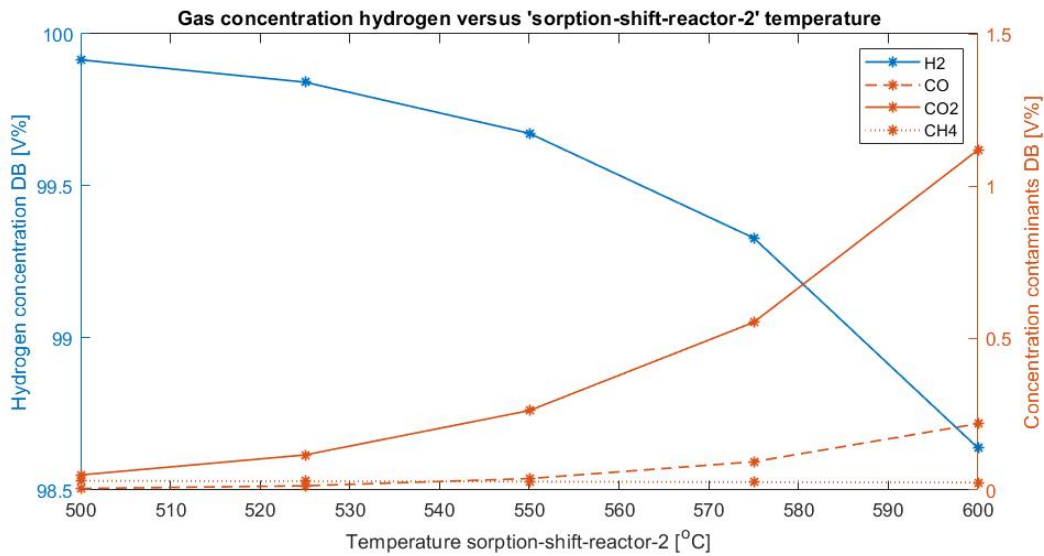


Figure 5.5: Carbonation temperature versus syngas concentrations sensitivity results Aspen Plus

5.3 Reactor temperature regenerator

The regenerator temperature is varied between 800 °C and 900 °C with increments of 25 °C. Between 825 °C, and 850 °C the regenerator is analyzed in more detail, additional analysis of the regenerator at 840 °C and 830 °C are performed. The regenerator is optimized as a function of operation temperature versus efficiency. Air is used for biomass combustion in the regenerator; an equivalence ratio of 2.5 is used, resulting in partial CO_2 pressure below 1 bar in the flue gas. Meaning that at a lower temperature, regeneration can still be complete since there will be a driving force for calcination at CO_2 equilibrium pressures below 1 bar (as long as the CO_2 partial pressure in the flue gas below the CO_2 equilibrium pressure). The CO_2 partial pressure of the flue gases and the CO_2 equilibrium pressure of the CO_2 sorbent (CaO) [44] is displayed in figure 5.6. It can be seen that at all regenerator temperatures, the partial pressure is less than the equilibrium pressure, ensuring complete regeneration of $CaCO_3$ to CaO. If regeneration is performed with pure oxygen, which ensures a concentrated CO_2 stream (for carbon capture), regeneration temperatures should be higher: approximately 850-900 °C (depending on the amount of moisture and hydrogen in the used biomass species), as can be seen in figure 5.6.

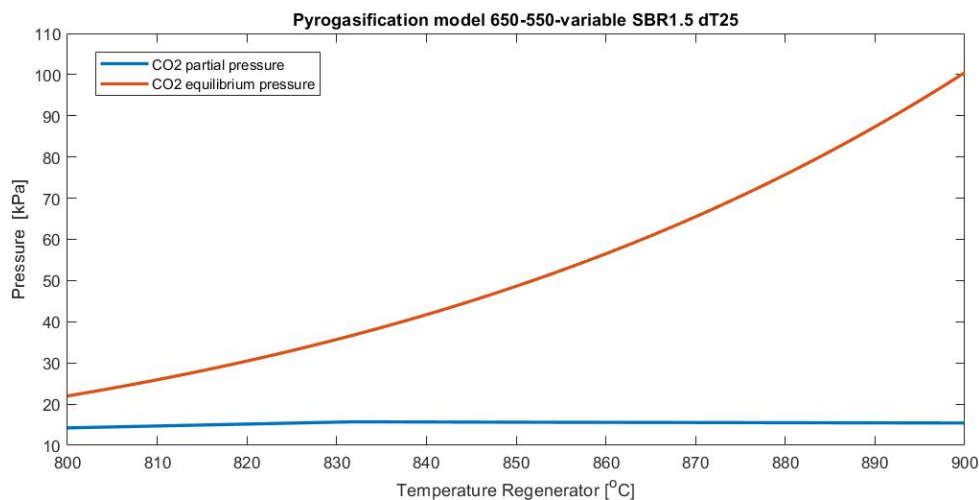


Figure 5.6: Regenerator CO_2 equilibrium pressure and flue gas CO_2 partial pressure as a function of regenerator temperature

In order to model the system within the set boundaries for heat transfer: pinch point $\geq 25\text{ }^{\circ}\text{C}$ for all heat exchangers, the following boundary conditions are set with respect to flue gas temperature, which is used for heating of the pyrogasification system:

- 1. T flue gas after heating Ref $\geq 650\text{ }^{\circ}\text{C}$
- 2. T flue gas after heating Pre-ref $\geq 625\text{ }^{\circ}\text{C}$
- 3. (T flue gas after heating auger- T hot air) $\geq 25\text{ }^{\circ}\text{C}$

These boundary conditions ensure that the hot flue gases can supply sufficient heat to the pyrolysis, gasification, and air pre-heating process. Optimization of the model (650-550-var-1.5SBR-dT25) results in an optimum regenerator temperature of $832\text{ }^{\circ}\text{C}$ with the highest efficiency. The temperature distribution of the flue gases with a regenerator temperature of $900\text{ }^{\circ}\text{C}$ and the temperature distribution of the flue gases with a regenerator temperature of $800\text{ }^{\circ}\text{C}$ are displayed in appendix F.

At a regenerator temperature below $832\text{ }^{\circ}\text{C}$, boundary condition 1 limits the process; this results in additional biomass combustion to increase the mass flow such that enough heat can be delivered to the reformer. At temperatures above $832\text{ }^{\circ}\text{C}$, boundary condition 3 limits the process. At $832\text{ }^{\circ}\text{C}$, the exit temperature of the flue gases is lowest, as can be seen in appendix F, minimizing exergy losses.

The overall system efficiency is plotted in figure 5.7. It can be seen that at temperatures below $832\text{ }^{\circ}\text{C}$, the efficiency drops dramatically, this is due to the exergy loss of the flue gases (for heating of the reformer flue gases can be cooled only to $650\text{ }^{\circ}\text{C}$ given the system boundary conditions). At temperatures above $832\text{ }^{\circ}\text{C}$, additional biomass is used for recirculating sorbents at higher temperature through the system, resulting in slightly lower efficiencies. Higher regenerator temperatures result, however, in larger temperature differences in "flue gas-powered" heat exchangers, decreasing surface area and thus cost. Furthermore, when pure oxygen is used for regeneration (for carbon captures), temperatures should increase to $880\text{-}900\text{ }^{\circ}\text{C}$ to ensure sufficient sorbent regeneration due to higher CO_2 partial pressures.

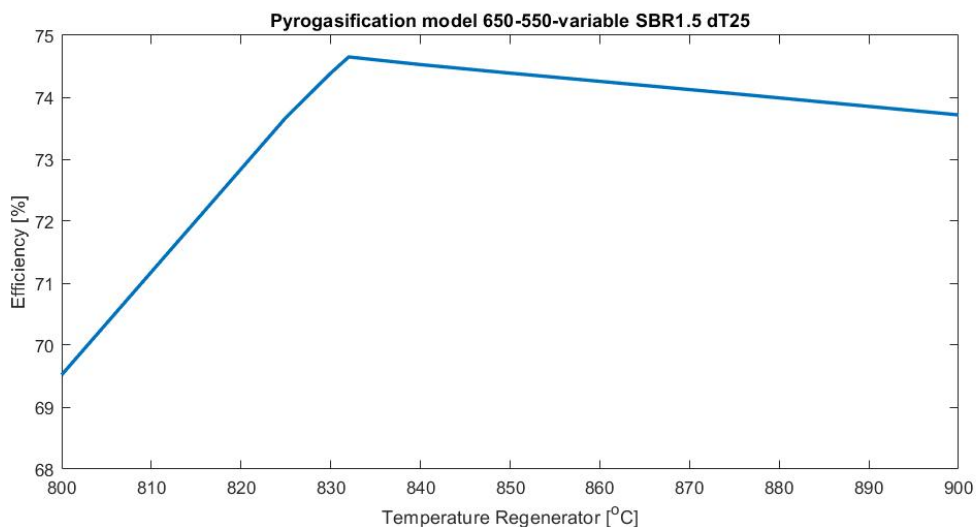


Figure 5.7: Overall system efficiency as a function of regeneration temperature

Reformer heating limits heat generation in the system; when less or no heat is required by the reformer, the regenerator can operate at lower temperatures without an efficiency loss. The reformer requires relatively high-temperature heat ($>750\text{ }^{\circ}\text{C}$), which is in the designed system delivered by flue gases with a maximum temperature of $900\text{ }^{\circ}\text{C}$. Another option for reformer heating can be to add a small fraction of oxygen to the reformer, resulting in partial combustion.

5.4 Pinch point heat exchangers

The "standard" system is modeled with a minimum pinch point (dT_{min}) in each heat exchanger of 25 °C. A sensitivity analysis is performed using minimum pinch points varying from 15 °C to 60 °C in order to analyze the influence of the pinch point on the overall system efficiency. On the one hand, it is expected that lower pinch points will lead to higher efficiencies, but lower pinch points will also require larger heat exchanger surface areas, increasing CAPEX and OPEX (higher pressure drops, more surface area for cleaning). The (boundary) stream temperatures influenced by changing the minimum pinch point are:

- Steam temperature: $\text{Min}(625\text{ °C}, 650\text{ °C} - dT_{min})$
- Syngas temperature before shift 1 ($600\text{ °C} + dT_{min}$)
- Flue gas after heating pre-reformer ($600 + dT_{min}$)
- $(T\text{ flue gas before air heating} - T\text{ air after pre-heating}) = dT_{min}$

The influence of lower limit pinch point of all the gas-gas exchanges is displayed in figure 5.8. At a pinch point up to 40 °C, the influence on overall efficiency is limited and is mainly due to additional heat required for the pre-reformer due to steam which is generated at lower temperatures, and less heat being recycled from the hot syngases coming from the reformer. When the lower limit pinch point increases above 40 °C, the flue gases do not contain enough heat to power the steam reforming system at the set temperatures (600 °C and 750 °C, respectively). Therefore, the only option is to combust a considerable amount of additional biomass, to increase mass flows and deliver the required heat.

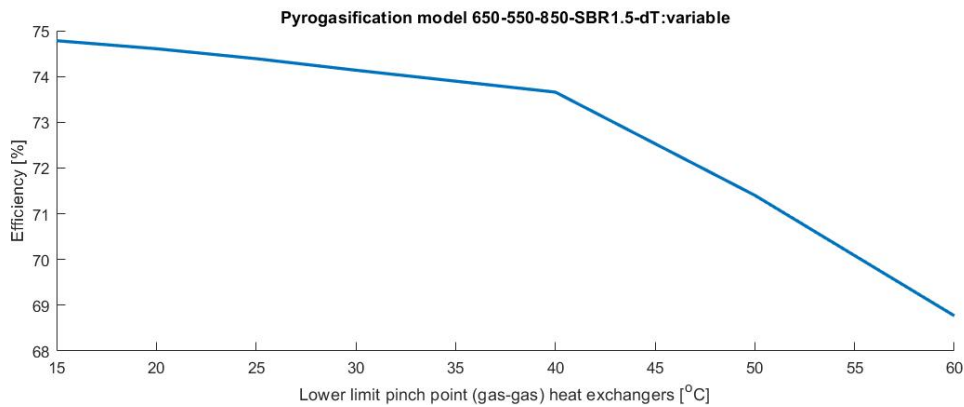


Figure 5.8: Overall system efficiency as a function of lower limit pinch point of gas-gas heat exchanger and boilers

Under the "standard" conditions (minimum pinch point 25 °C), the pre-reformer does not require a significant amount of heat from the flue gases. A lot of heat is recycled from the hot syngas after the Reformer (750 °C), and steam is generated at 625 degrees C. As the pinch point increases, steam of lower temperatures can be generated, in combination with less heat being recycled from the syngas resulting in a rapid increase in additional heat demand from the flue gases. At a minimum pinch point of 60 °C, 2.7 times more heat is required at the pre-reformer. The heat demand for the pre-reformer as a function of pinch point is displayed in appendix F.

The temperatures of generated steam (in combination with the steam temperature limits) and the flue gas temperature after pre-reformer heating (in combination with this stream temperature limit) are displayed in figure 5.9, explaining the transitions in the efficiency curve (figure 5.8) and heat supply curve (figure .18).

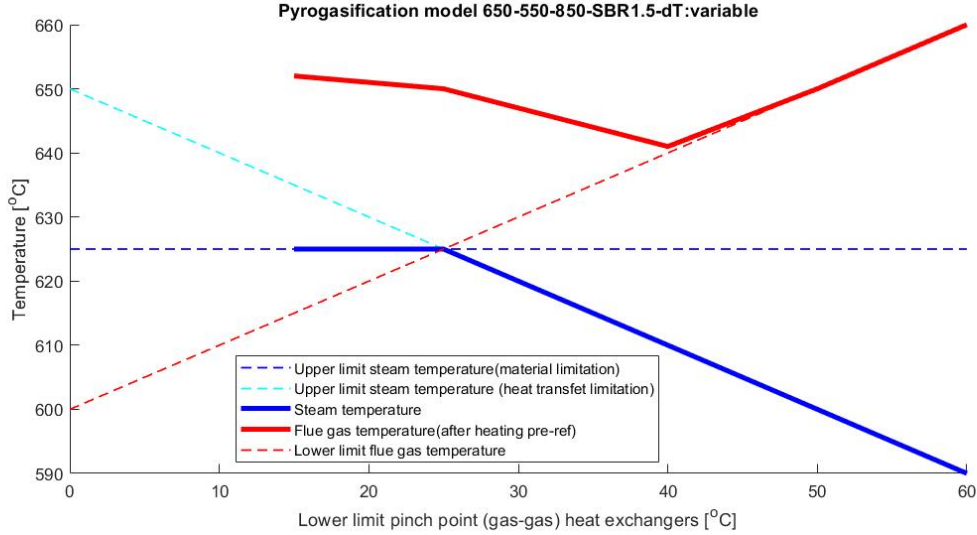


Figure 5.9: Steam temperature and flue-gas temperature (after heating pre-reformer) as function of the lower limit pinch point of gas-gas heat exchanger and boilers combined with temperature limits given the lower limit pinch point boundary conditions

5.5 SC ratio

The Steam to Carbon Ratio (SC) represents the amount (moles) of steam in the fuel gas compared to the amount of moles carbon in the fuel gas. The definition used for the SC in this analysis is given in equation 5.2. Roughly 25% of the biomass is converted into biochar in the auger reactor, which is collected and not sent over the reforming system. This results in less steam being required in order for optimal conversion in the gasification system. Char reforming uses steam according to equations 5.3. Initially, a SBR of 1.5 (SC = 4.58) is used in the process simulations. This section will focus on the influence of SC on main system characteristics: gas quality and efficiency.

$$SC = \frac{[H_2O]}{[C]} \quad (5.2)$$



Simulations have been performed for varying SC: from 3.2 to 6.0 (SBR=1.0 to 2.0) The results with respect to efficiency are displayed in figure 5.10. Up until an SC of 4.6, the overall system efficiency slightly increases as the SC increases; this might look counter-intuitive. This can, however, be explained by the fact that steam is generated at 625 °C given the standard conditions, the pre-reformer operated at 600 °C, and therefore steam provides heat to the gasification system, at an SC of 3.2-4.6 the SEWGS system can provide enough heat for steam generation without additional heating requirements. Therefore the efficiency increases slightly up to SC = 4.6 due to effective heat utilization. For SC > 4.6, additional biomass is combusted for steam generation, resulting in lower overall system efficiency. Research by van Rossum et al. [42] showed that from an SC of 2.2 and higher, it is possible to get hydrocarbon free syngas. It is important to note that under SC ratios of 4.6, there is a high-quality waste heat stream from the SEWEGS system since the SEWEGS reactors require cooling due to exothermic absorption reactions/endothermic WGS. This high-quality heat can be utilized, for example, for power generation. In this case, it is (thermodynamic) beneficial to reduce the SC below 4.6. If waste heat is not utilized, maximum system efficiency is at SC=4.6. Another point of attention is that under a high SC ratio, volume flow increases, resulting in larger reactor volume requirements. The influence of SC ratio on efficiency is further explained in appendix F.

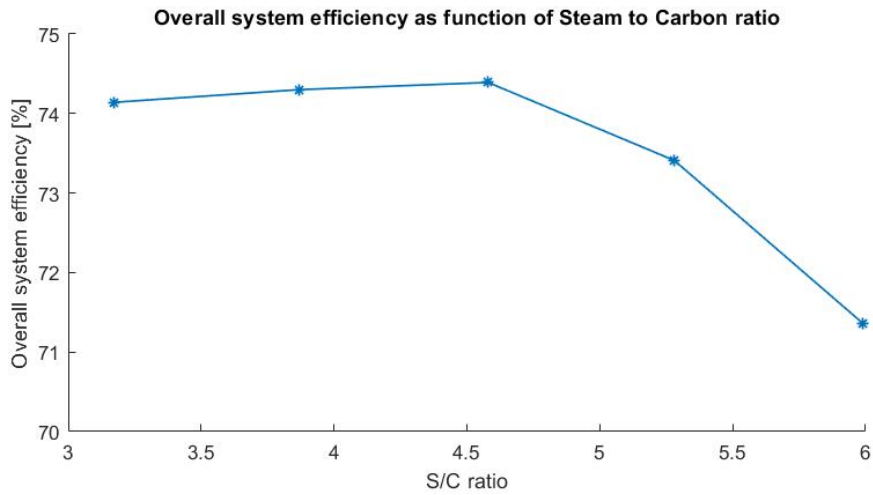


Figure 5.10: Overall system efficiency versus SBR

Figure 5.11 displays the influence of the SC on the final product gas concentrations; this is all based on thermodynamic equilibrium modeling performed in Aspen plus. The equilibrium constant is given by equation 5.4, which is constant under constant temperature. Under higher SBR, the amount of CO_2 increases, and the amount of CO decreases. For methane steam reforming, a similar equilibrium constant applies (equation 5.5), which explains the exponential behavior of CH_4 as a function of the SBR. Carbon monoxide is the species that is hardest to remove from the syngas; therefore, with respect to downstream treatment expenses for hydrogen purification, a high SC is desired since this reduces CO concentrations.

$$K_{wgs} = \frac{[H_2][CO_2]}{[CO][H_2O]} \quad (5.4)$$

$$K_{mr} = \frac{[CO][H_2]^3}{[CH_4][H_2O]} \quad (5.5)$$

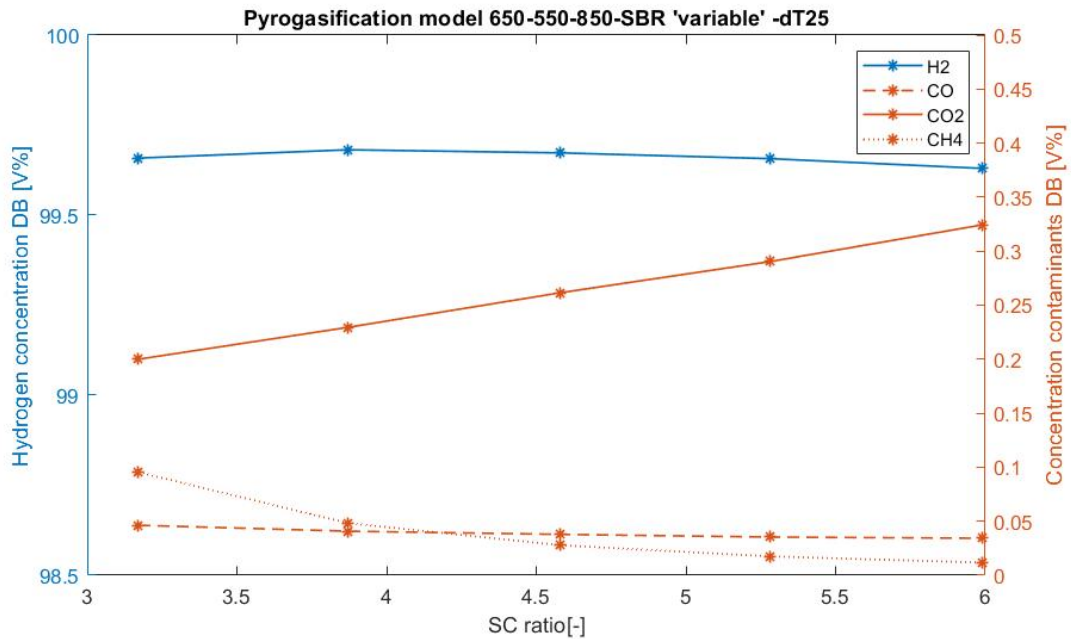


Figure 5.11: Hydrogen and containment concentration product gas as function of the SC ratio, excluding water

5.6 Results

Multiple sensitivity analyses have been performed on the design pyrogasification SEWGS system. The temperature of the high-temperature SEWGS (shift-1) reactor has been analyzed. The optimum shift-1 temperature has been determined to be 650 °C since this temperature will result in the desired ratio of carbon capture between Shift-1 and Shift 2 (9:1). The optimum temperature of Shift-2 can be stated as: "As low as thermodynamic possible". Reducing Shift-2 temperature will increase the hydrogen purity of the product gas (assuming thermodynamic equilibrium); it is, however, not sure at what temperatures thermodynamic equilibrium is still approached in Shift-2 since lower temperatures reduce reaction rates. This subject is further discussed in chapter 9 and requires further research. Varying Shift-1 and the shift-2 temperature does not significantly change the system efficiency (73.4-74.9%).

The regenerator temperature has been optimized at 832 °C using a sensitivity analysis resulting in a system efficiency of 74.7 % based on chemical energy. Below temperatures of 832 °C, reformer heating has been identified as the main bottleneck since this will cause an energy shortage at the reforming system. Other process configurations, with, for example, addition of a small fraction of oxygen in the reformer, should be further analyzed.

The minimum pinch points of heat exchanges in the system have been varied. Results found in this research will be used in section 6 for cost optimization with respect to HEX size. A minimum pinch point (15 °C) resulted in the highest system efficiency: 74.8 %, while a minimum pinch point of 60 °C results in system efficiency of 68.8 %. Reduced pinch points will increase HEX costs. This sensitivity analysis showed that (pre-reformer) heating is a system bottleneck, once again stressing that (pre)reformer heating requires further research and other process configurations should be investigated.

The optimum SC ratio has been set at 4.6, up to an SC ratio of 4.6 all steam can be produced using "waste" heat from the SEWGS system. When lower SC ratios are used, a high-temperature waste stream is present. When this waste stream is utilized (for example, for power production), the optimum SC ratio will reduce. An increase in SC will shift equilibrium reactions such that less CO and CH_4 is in the final product.

Table 5.1 displayed the results of the sensitivity analysis. Further research is required with respect to the kinetics of Calcium oxide in the SEWGS reactor and different process configurations with alternative reformer heating mechanisms. The process conditions as sketched in chapter 3 lies close to the optimal process configuration with respect to maximum efficiency based on chemical energy. Further research concerning cost optimization is required, which will be discussed in chapter 6

Table 5.1: Results sensitivity analyses pyrogasification SEWGS system

Variable	Range	Efficiency range	Conclusions
Shift-1 temperature	600-700 °C	74.35% - 74.61 %	Shift-1 temperature of 650 °C recommended.
Shift-2 temperature	500-600 °C	73.39 % - 74.93 %	Further research for optimal shift-2 temp. is required
Regenerator temperature	800-832 °C	69.52 % - 74.65 %	Reformer heating is identified as bottleneck
	832-900 °C	74.65 % - 73.72 %	Optimal temp = 832 °C
Min pinch point	15-60 °C	74.78 % - 68.77 %	(Pre-) reformer heating identified as bottleneck
SC-ratio	3.2-4.6	74.14 % - 74.39 %	SC of 4.6 maximizes waste heat utilization
	4.6-6.0	74.39 % - 71.36 %	SC<4.6 results in high quality waste heat

Chapter 6

Financial model pyrogasification SEWGS system

This chapter will discuss the design and results of a financial model constructed for the pyrogasification SEWGS system. In the financial model, cash flows are simulated over the lifespan of the installation. The financial analysis goal is to gain insight into the required costs for sustainable hydrogen and biochar production and to determine the production cost of both biochar and hydrogen for the designed pyrogasification SEWGS system. First, the Weighted Average Cost of Capital (WACC) is determined; next, the expected income is discussed before investment cost (CAPEX), and operational costs (OPEX) are determined. The technical model results are used to construct a model to analyze cash flows and for cost efficiency optimization. The results of this analysis have been discussed with an industrial party (HoSt bioenergy installations, Enschede, the Netherlands) to validate/improve the results and give more insight into the (financial) feasibility of the system.

6.1 Weighted Average Cost of Capital

The WACC represents a firm's cost of capital; in this analysis, the before-tax WACC is used; if there are significant profits, the WACC will reduce due to taxes that have to be paid over the profit. Once the economic feasibility is established, the profitability can also be determined using taxation rates. The before-tax WACC is represented in formula 6.1. The after-tax WACC is represented in formula 6.2. Where E is the amount of equity used for financing a specific project, D is the amount of debt used for financing of this specific project, C_E is the cost of equity, C_D is the cost of debt, and T_c is the taxation rate.

$$WACC = \frac{E}{E+D} C_E + \frac{D}{E+D} C_D \quad (6.1)$$

$$WACC = \frac{E}{E+D} C_E + \frac{D}{E+D} C_D * (1 - T_c) \quad (6.2)$$

For this analysis, data is used from the KPMG Cost of Capital study from 2019 [62], where the WACC of different industries in Austria, Germany, and Switzerland is investigated. In this study, the "energy and natural resources" industry have, among others, been investigated. The cost of debt has been found to be: $D=2,6\%$, and the cost of equity was found to be $E=7,4\%$. The average debt ratio of the "energy and natural resources" was found to be $38,1\%$. Applying equation 6.1 results in a WACC of $5,2\%$ for the "energy and natural resources" industry. This WACC has been validated by the consulted industrial party.

The analyzed technology is a novel technology, high purity hydrogen production out of biomass will be a niche market once implemented. The cost of debt can be higher due to higher risks accompanied by an "unproven technology" and the debt share can be smaller, both will increase the WACC.

6.2 Expected income

The income is dependent on the two products: biochar and hydrogen.

Hydrogen price

Currently, most hydrogen is produced using "Grey" Steam Methane Reforming (SMR), the production cost of hydrogen are in between €1/kg and €2/kg [63, 64], depending on natural gas prices, when analyzing the estimated cost of European natural gas for the period 2022-2024, which are in the range of 16-19 €/MWh [65]. This corresponds with hydrogen production prices of €1.40 - €1.50 [63]. For this research, a market price of €1.50 per kg of hydrogen is used. A CO_2 tax will make grey hydrogen more expensive due to the large greenhouse gas emissions from the production process. A CO_2 tax will be introduced in the Netherlands in 2021 for industry, increasing yearly up to 2030, which is expected to increase hydrogen market prices.

Biochar prices

The bio-char which is produced has similar qualities compared to conventional coal. The estimated market price of coal in 2022 is between €50 and €75 per ton. Biochar can be used for agricultural markets for soil enhancement (replacing conventional fertilizer), as fuel (energy production), and for high-end applications: as industrial absorbent [66]. Because of this wide variation of applications and wide variety in biochars, it is hard to estimate biochar sales prices. Cambell et al. [66] showed that biochar prices vary between 87 \$ and 2512 \$ per ton. The mean biochar retail price was 545 €/per ton on the European market in 2014 [66]. In this research, a biochar sales price of 250 €/ton is used in 2022, comparable to the low-end range of prices given in literature [66].

It is assumed that the installation will run at 85% of the time at full capacity on a yearly basis. Assuming constant prices for the produced product (the prices are not compensated for inflation since the WACC is not inflation-adjusted). It is safe to assume that hydrogen and biochar prices will increase faster than average inflation rates due to change in policies. Two different scenarios will be modeled:

1. Scenario 1: Constant hydrogen and biochar prices(inflation-adjusted): €1.50 per kg for hydrogen and €0.25 per kg for biochar
2. Scenario 2: An estimated hydrogen and biochar price increase of 10% per year in between 2020 and 2030 due to CO_2 taxations

For scenario 1 This will lead to a yearly income as shown in table 6.1. , assuming no subsidies and no increased product prices compared to average inflation rates. Scenario 2 is further discussed in appendix H

Table 6.1: Product prices and estimated system income in 2020

Product	production rate	price per kg	income/year
Hydrogen	276.3 kg/h	€1.50	€3.085.000 / year
Biochar	874 kg/h	€0.25	€1.627.000 / year
Total income			€4.713.000 / year

6.3 CAPEX estimation

For cost estimation, the main process equipment in the designed installation needs to be listed. The system as designed in chapter 3, and modeled in chapter 4 is used for cost analysis. Results from Aspen Plus are used for size estimation of reactors and heat exchangers. The size of the equipment is required and is used to estimate the process equipment costs. Next, the total capital expenditure (CAPEX) is estimated using (updated) factorial techniques (based on the Lang-factor technique [67]). This technique uses the calculated CAPEX for the main equipment (reactors, heat exchangers, pumps, etc.) and multiplies this with a factor (Lang-factor) to determine the project's total CAPEX.

for the analyzed system, the following equipment types are mapped in order to get an accurate estimate of the capital expenditure (CAPEX):

- Reactors
- Heat Exchanges, including boilers and condensers
- Other process equipment: feeding system, separators, conveyor belts, conveyor screws, denox system, and start-up burners.

6.3.1 Reactors

The main reactors in combination with their characteristics are listed in table 6.2.

Table 6.2: Reactor types pyrogasification-sorption-shift-system

Reactor type	Reactor temperature [°C]	Residence time	product flow rate
Auger reactor	500	5-10 minutes	3.6 t/h
Pre-reformer: fixed bed	600	2 seconds	394.5 kmole/h
Reformer: fixed bed	750	2 seconds	423.2 kmole/h
Shift-1 : bubbling bed	650	2 seconds	470.9 kmole/h
Shift-2 : bubbling bed	550	2 seconds	407.5 kmole/h
Regenerator: fast fluidized bed	850	1 second	822.3 kmole/h

The reactor volumes are determined using the following assumptions and simulation for the fluidized bed reactors

- Volume flows are calculated at the given temperature, at 1 atm.
- The bed void fraction is assumed to be $\mu = 0.50$
- The additional reactor height is 70 % above the bed height. [68]

The reactor volume can be calculated using equation 6.3, with n the number of moles, R is the ideal gas constant, P is the pressure (pa), T temperature (K), τ the residence time, μ the void fraction and the factor 1.7 is used to include additional reactor length above the bed.

$$V = \frac{nRT}{P} * \frac{\tau}{\mu} * 1.7 \quad (6.3)$$

Using equation 6.3 leads to the total reactor volumes as displayed in table 6.3.

Table 6.3: Reactor sizing pyrogasification SEWGS system

Reactor type	Total volume [m3]
Pre-reformer: Fixed bed	53.5
Reformer: Fixed bed	67.2
Shift-1 : Bubbling bed	67.5
Shift-2 : Fixed bed	52.1
Regenerator: Fast fluidized bed	71.7

In order to determine the price of the fluidized/packed bed reactors, data from Chemical Engineering Economics [69] is used to determine the equipment cost. The prices used are published in 1989; in order to compensate for changing prices over the years, price indexes are used for " Oil and Gas Field Machinery, and Equipment Manufacturing" [70]. The cost index of 1989 is "126.5" and the cost index of 2020 is "268.8". The cost can be calculated using equation 6.4. In equation 6.4 factor f corresponds for the steel type and insulation which is used for the fluidized beds. $f=1.00$ for 304 steel and $f=1.30$ for 316 steel.

After consulting with an industrial partner (Host bio Energy Installations, the Netherlands), the factor f was determined to be 3.0 due to additional insulation (concrete walls). The factor 3.0 is based on the experience of HoSt on fluidized bed reactors for biomass gasification. Due to the highly corrosive favorable process conditions (high temperature/steam), 316 stainless steel is used due to its higher resistance for corrosion. In equation 6.4 the factor "E" represent exchange rate from dollars to euros and is $\frac{1}{1.18}$ corresponding to 2020 exchange rates.

$$C = C_i * \frac{Index_{2020}}{Index_{1989}} * f * E \quad (6.4)$$

The capital expenditure of an auger reactor is set to be dependent on input: 3.6t/h. Since no supplier data is available with respect to auger reactors, cost information of screw-presses is used as the basis. Cost data is acquired from "Chemical Engineering Economics" [69]. The obtained cost is then multiplied with a factor of 2.0 to compensate for increased material requirement (increased size). The cost of the required heat exchanger for heating the auger is calculated separately. The cost of the auger is multiplied with a factor $f=1.3$ to compensate for high-quality steel [69]. Finally, prices are compensated using cost indexes and exchange rates according to equation 6.4. The basis of the cost C_i are taken from "Chemical Engineering Economics" [69], of which figures are retrieved which can be found in appendix I

Table 6.4 displays the calculated capital cost for the reactors present in the system. The total capital cost for the reactors is €2.910.600. This excludes heat exchanger mechanisms that are included in the auger reactor, pre-reformer, reformer, and shift-1 reactor. The additional cost of these heat exchanger devices will be calculated in the next section.

The maximum volume of a reactor is set at 40 m^3 due to transportation limitations with larger sizes. The large SC and ER ratios cause large volume flows in reactors, resulting in relatively large (expensive) reactors. S/C and ER can be further optimized with respect to cost efficiency.

Table 6.4: Reactor cost

Reactor	# reactors	cost per reactor	total cost
Auger reactor	1	€156.666	€156.666
Pre-ref	2	€248.505	€497.011
Reformer	2	€291.724	€583.447
Shift-1	2	€297.126	€594.252
Shift-2	2	€237.701	€475.402
Regenerator	2	€301.902	€603.803
Total reactor cost			€2.910.582

6.3.2 Heat exchangers

In order to determine the cost of the heat exchangers, the size (surface area), type, and construction material have to be determined. All heat exchangers in the system will be based on shell in tube heat exchangers. Due to high temperatures and dust in the syngas/flue gas, gas-gas-based HEX cannot be constructed out of plate heat exchangers due to problems with cleaning. "Coulson Richardson's chemical engineering design" [71] is used to determine the size and cost of the heat exchangers. In order to determine the effective surface area, the Log Mean Temperature Difference (LMTD) of each reactor is determined using data retrieved from the constructed model in Aspen Plus. The LMTD is calculated according to equation 6.5 for counterflow heat exchanges, where T_1 is the inlet hot fluid temperature, T_2 is the outlet hot fluid temperature, t_1 is the inlet cold fluid temperature and t_2 is the cold fluid outlet temperature.

$$LMTD = \frac{(T_1 - t_2) - (T_2 - t_1)}{\ln\left(\frac{T_1 - t_2}{T_2 - t_1}\right)} \quad (6.5)$$

The HEX present in the pyrogasification SEWGS system are displayed in table 6.5 together with the estimated overall heat transfer coefficient based on literature [71], the calculated LMTD and simulated heat duty Q. The process overview is once more given in figure 6.1 to clarify the HEX numbers as used in this section.

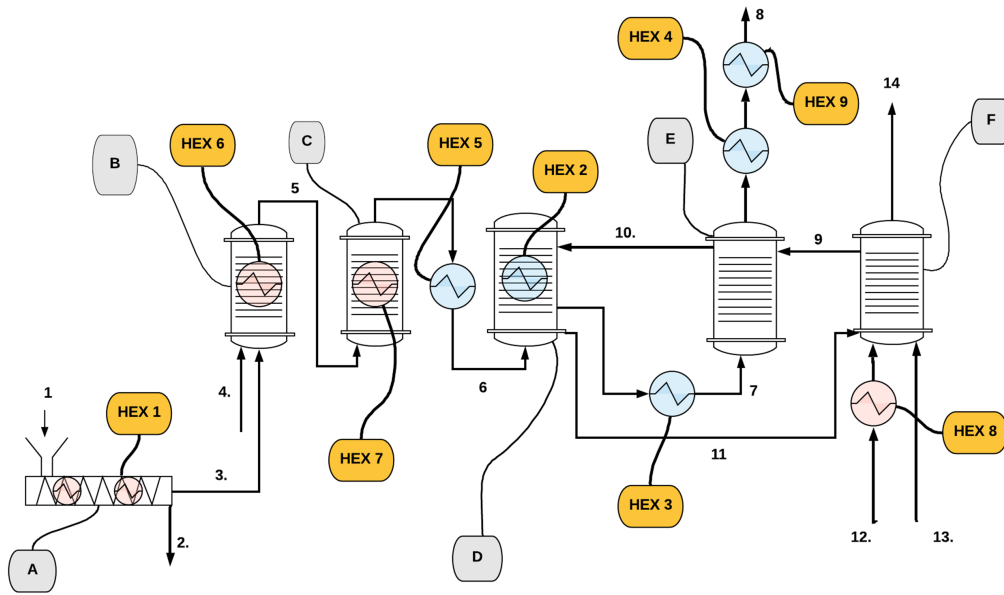


Figure 6.1: System overview with HEX highlighted

Table 6.5: HEX types and characteristics in the system

HEX	Application	type	Q [MW]	U [W/m ² *K]
1	Heating auger	Gas-oil	1.06	150
2	Boiler	Steam-"fluid-bed"	2.86	500
3	Boiler	Syngas-steam	1.21	150
4	Boiler	Syngas-steam	1.45	150
5	Pre-ref heating	Gas-"fluid-bed"	0.64	50
6	Pre-ref heating	Gas-"fluid-bed"	0.18	50
7	Reformer heating	Gas - "fluid-bed"	1.51	50
8	Air pre heating	Gas-gas	2.81	25
9	Condenser	Steam-water	3.73	2000

The required heat exchanger area is calculated according to equation 6.6.

$$A = \frac{Q}{U * LMTD} \quad (6.6)$$

The calculated surface areas for each HEX are displayed in table 6.6 [71]. This table also presents the number of required HEX where the maximum surface area per HEX is set to be 500 m². All HEX will be made out of high-quality stainless steel. For conventional shell and tube HEX, a type factor of 1 is used, while for HEX mounted in fluidized bed reactors, a type factor of 1.3 is used.

Table 6.6: HEX LMTD and cost characteristics

HEX	T_2 [°C]	T_1 [°C]	t_1 [°C]	t_1 [°C]	LMTD [°C]	A [m ²]	Type factor
1	650	520	550	350	132	53.4	1
2	650	650	625	20	187	30.5	1
3	650	350	625	100	97.7	82.5	1
4	550	171	100	20 C	274	35.2	1
5	750	625	600	600	69.8	184	1.3
6	671	650	600	600	59.9	58.4	1.3
7	850	671	750	600 C	84.7	357	1.3
8	520	153	495	20	64.6	1736	1
9	171	20	80	10	36.7	50.9	1

The HEX cost is determined using Coulson Richardson's chemical engineering design [71]. The prices used are from mid-2004; therefore, prices are compensated using price indexes and exchange rates similar to reactor cost calculations in the previous section. Cost are also multiplied with the type factor " T_f " [71] which is 1 for "normal" heat exchangers and 1.3 for HEX placed in fluidized beds. The total cost per HEX is calculated according to equation 6.7. The cost index of 2020 is set to be 268.8, and the cost index of mid-2004 to 178.2 [4].

$$C = C_i * \frac{Index_{2020}}{Index_{2004}} * T_f * E \quad (6.7)$$

The calculated cost per HEX are displayed in table 6.7 [71], the total HEX cost are estimated to be €3.156.800. Note that HEX 5,6, and 7 are mounted in fluidized bed reactors and can be allocated to the reactor cost.

Table 6.7: HEX cost results

HEX	A per HEX [m ²]	C_1	Cost per HEX	Total cost
1	53.4	\$ 79.250	€101.307	€101.307
2	30.5	\$ 50.550	€64.619	€64.619
3	82.5	\$106.875	€136.620	€136.620
4	35.2	\$ 55.720	€71.228	€71.228
5	92.0	\$ 114.000	€189.447	€378.894
6	29.2	\$ 48.880	€81.230	€162.459
7	178.7	\$ 171.155	€284.428	€568.856
8	434.1	\$ 286.935	€366.795	€1.467.179
9	50.9	\$ 76.125	€97.312	€97.312
Total cost				€3.048.474

6.3.3 Other process equipment cost

The additional cost estimations for process equipment listed below are required. The system cost (except cyclone cost) are based on consultation with an industrial partner (HoSt bioenergy installations, the Netherlands) and form an estimate for system costs in 2020.

- Biomass feeding system (moving floor)
- Belt conveyors for char/ash transport
- Denox + scrubber system for flue gas cleaning
- Start up burners
- CaO transport system (screw conveyors)
- Cyclone

Cyclone normalized cost is assumed to be \$6000 per sm³/s in accordance to research by Wang et al. [72]. The volume flow rate of flue gases through the cyclone is 5.60 sm³/s, using price indexes from 2002 (169.6) and 2020 (268.8), and an exchange rate of 1.18 results in an estimated cyclone cost of 45100 euro. The other cost estimated is displayed in table 6.8

Table 6.8: Other process equipment cost estimates

Type	year	cost	source
Biomass feeding system	2020	€100.000	Industry
Belt conveyors	2020	€100.000	Industry
Denox reactor+ scrubber	2020	€200.000	Industry
Start up burners	2020	€420.000	Industry
CaO transport mechanism	2020	€100.000	Industry
Cyclone	2020	€45.101	Wang et al.
Total cost		€965.101	

6.3.4 Total capital investment

The (total) equipment cost as calculated in the previous section is displayed in table 6.9 in combination with the total system Capital Expenditure (CAPEX).

In order to determine the CAPEX based on equipment cost, factorial cost estimation techniques are used derived from the Lang-factor technique. The factorial method derived by Peters and Timmerhaus [73] for solid processing plants is used: $F = 4.55$ to determine the Total Capital Investment (TCI). The required working capital is factorized to be 0.68 of the total equipment cost, resulting in a factor of 3.87 is used to determine the Total Depreciable Cost (TDC).

After consulting with the industry, an additional contingency for this kind of novel technologies should be taken into account for unexpected costs. For a new installation, an additional contingency fee of 40% should be worked with. After the construction of 8 similar installations, the consulted industrial partner estimated that no additional contingency fee would be required (learning curve). The general formula of a learning curve (exponential decay) is given in equation 6.8, where Z_u is the cost of installation number u , K is the cost of the initial installation (1.4 of the estimated TDC excluding the additional contingency fee), and n is the learning curve factor. Given that after $u=8$, the Z_u is expected to be 1, results in a learning curve factor $n = -0.162$. This results in equation 6.9 which can be used to calculate the cost factor Z_u as a function of the number of installations constructed.

$$Z_u = CAPEX * K * u^n \quad (6.8)$$

$$Z_u = CAPEX * 1.4 * u^{-0.162} \quad (6.9)$$

Table 6.9: Total CAPEX sorption-shift-system based on factorial technique by Peters and Timmerhaus

Cost item	Cost	factor
Total cost reactors	€2.911.000	-
Total cost HEX	€3.048.000	-
Total cost other process equipment	€965.000	-
Total equipment cost	€6.924.000	1
Equipment installation labour	€3.116.0000	0.45
Instrumentation and controls	€623.000	0.09
Piping	€1.108.000	0.16
Electrical installations	€692.000	0.10
Buildings	€1.731.000	0.25
Yard improvements	€900.000	0.13
Service facilities	€2.770.000	0.40
Land	€415.000	0.06
Direct Plant Cost(DPC)	€18.280.000	2.64
Engineering and supervision	€2.285.000	0.33
Construction expenses	€2.700.000	0.39
Direct and Indirect Cost (DIC)	€23.265.000	3.36
Contractor's fee	€1.177.000	0.17
Contingency	€2.354.000	0.34
Additional contingency new technology (40%)	€10.719.000	1.55
Total Depreciable cost (TDC)	€37.515.000	3.87+1.55
Working capital	€4.708.000	0.68
Total Capital Investment (TCI)	€42.224.000	4.55+1.55

6.4 OPEX

The system operating expenditure (OPEX) is split up into three different sections:

1. Variable cost
2. Fixed cost
3. Company general operating expenses

For the calculations in this section, a cost model proposed in Richard and Coulson Chemical Engineering design is followed [71], in combination with consultations with an industrial partner (HoSt bioenergy installations, the Netherlands). It is assumed that the system has 7447 full-load hours per year (85% capacity).

6.4.1 variable cost

The variable costs are split into four different categories:

1. Raw material cost
2. Utility Cost
3. Miscellaneous operating materials
4. Shipping and packaging

Miscellaneous operating materials (safety clothing, etc.) are estimated to be 10% of the maintenance costs. Shipping and packaging costs are not applicable to the analyzed system. The raw material and utility cost will be further explained in the next section.

Limestone

Limestone is continuously used in the system as a sorbent make up for the sorption shift system. Limestone prices are relatively low, but large quantities are required. Limestone prices are set to be 10 €/ton [74]. Limestone consumption is calculated using a 10 % replacement strategy per cycle. Further analysis of different sorbent replacement strategies is given in appendix E.

Biomass prices

The biomass prices are depended on the biomass type: chips or pallets. And the quality (moisture content, HHV) of the used biomass. in 2017 ECN and DNVGL published a report with estimates for dutch biomass prices [75] varying from 5.6 €/ GJ to 9.1 €/ GJ. For this research, a biomass price of 6.5 €/ GJ is used, which is comparable to other studies [76]. A price of €6.5 per GJ translates to a price of €118 per ton for the used biomass type, which is comparable to wood pellet prices, which are in the range of 120 €/per ton. The biomass consumption of the analyzed plant is 5.14 ton/h (18,00MJ/kg).

Catalysis costs

The catalytic bed in the pre-reformer and reformer are replaced once in a set amount of time. Nickel bases catalysts are used in both the reformer and pre-reformer, similar to the MSR process. Estimates give that yearly costs for an MSR system producing 100.000 H_2 nm³/h will be 420.000 \$ per year [77]. Extrapolating to the size of the analyzed system, which produces 276,3 kg H_2 /h = 3.356 nm³ H_2 /h results in yearly catalyst costs of 14.103 \$ or 12.054 €/per year given 2020 exchange rates. Research on nickel-based catalyst cost ($NiAl_2O_3$) has been performed, published catalyst prices vary a lot, depending on catalyst quality and order size, ranging from \$2.000 per ton [78] ($\approx 1 \$ lb^{-1}$) up to \$ 145.15 lb^{-1} [79]. Catalyst prices are set at €5.000 per ton, it is assumed that catalyst is replaced four times per year (significantly more compared to MSR), total catalyst volume (bed volume) is 71.0 m^3 , and catalyst density is set to be $0.65 * 10^3$ kg/m³ [80].

The raw material cost per unity, raw material consumption, and annual raw material cost are displayed in table 6.10.

Table 6.10: Raw material cost pyro-gasification sorption-shift system

Raw material	Cost per unity [€/ton]	Annual consumption [ton]	Annual cost
Biomass	118	38272	€4.478.000
Catalyst	5000	184,6	€923.000
Limestone	10	21538	€215.000
Total raw material cost			€5.616.000

It is assumed that the system requires 7m³ of process water per hour, which is mainly used for steam generation (5.4 tons). Water prices are set to be €0.80 per ton according to dutch water prices [3]. Furthermore, the system requires electricity; it is estimated that electricity requirements are 2 % of the thermal system input, electricity prices are set at €80/ MWh. The annual system utility cost are displayed in table 6.11. Miscellaneous operating materials are assumed to be 10% of the maintenance cost = 0.3% of the CAPEX.

Table 6.11: Utility cost pyrogasification SEWGS system

Utility	Cost per unity	Annual consumption	Annual cost
Water	€0.80/ton	52.122 ton	€42.000
Electricity	€80/ MWh	3827 MWh	€306.000
Total utility cost			€348.000

6.4.2 Fixed cost

The fixed cost are displayed in table 6.12. Labor cost and maintenance cost can be identified as the two main fixed cost drivers. The fixed cost is determined using Coulson Chemical Engineering design [71] and consultation with the industry (HoSt bioenergy installations, the Netherlands)

Table 6.12: Fixed cost pyrogasification SEWGS system

Fixed cost	Annual cost	Assumption
Maintenance	€803.895	3% of direct capital cost
Labour	€800.000	10 FTE, €80.000 per FTE
Laboratory cost	€160.000	20 % of operating labour
Supervision	€80.000	1FTE, 80.000 euro per FTE
Plant overhead	€528.000	50% of operation labour
Capital charges	€0	Are already in WACC
Local taxes	€53.593	0.2 % of total capital investment
Insurance	€160.389	0.3 % of total capital investment + 1% profit loss
Licence fee/Royalty payments	€0	Side specific
Total Fixed		€2.585.877

6.4.3 Company general operating expenses

The company general operating expenses are set to be 10% of the direct production cost (fixed cost+ variable cost) and are **€863.049**. The general operating expenses include the R&D cost and the general overhead cost.

6.4.4 Results OPEX pyrogasification SEWGS system

The results of the OPEX analyses are displayed in table 6.13. Biomass is the largest contributor to the OPEX (47.2%), followed by labor cost (16,5 %) and catalyst cost (9,7 %).

Table 6.13: Total operational expenditure Pyrogasification SEWGS system

Variable cost	€6.045.000
Fixed cost	€2.586.000
Company general operating expenses	€863.000
OPEX	€9.493.000

Figure 6.2 gives an overview of the annual operational expenditure. In this overview, labor costs and utility costs are grouped.

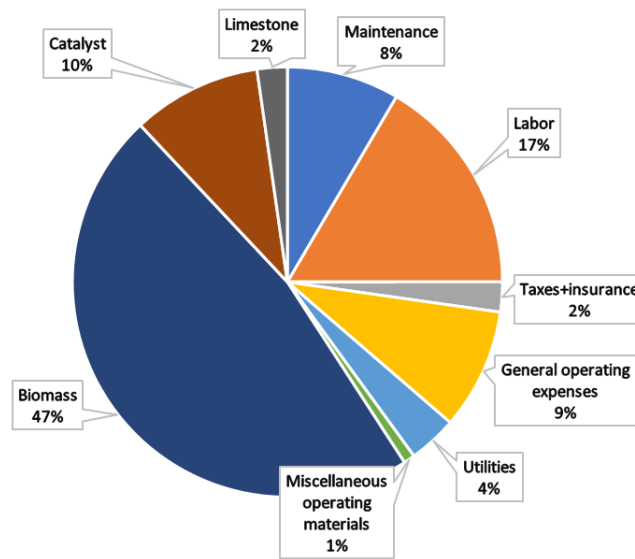


Figure 6.2: Overview operational cost Pyrogasification sorption-shift system

6.5 Cash flow simulations

This section will discuss the cash flow simulations obtained from the financial model. Three different scenarios are discussed. Another scenario, based on upcoming CO_2 taxation's is discussed in appendix H. The first two scenarios modeled are based on a "mature" technology, meaning that the additional 40% contingency for new technologies is not taken into account. For the subsidies based cash flow simulations, emerging technology is assumed, taking into account the 40% additional contingency.

1. No subsidies
2. Break even scenario
3. Expected subsidy scenario

The investment strategy of the capital investment is displayed in table 6.14. Plantlife is assumed to be 12 years (after three years of design/construction), resulting in a total model period of 15 years. Twelve years is relatively short, and it is estimated that the lifetime of the installation is at least in the 20-30 year range. Twelve years is selected after consulting an industrial party exploiting biomass installations (HoSt bioenergy installations, the Netherlands) who always work with 12 years since this is the period over which subsidies are given. The main cost driver of the installation is OPEX (more than 70%), so increased lifetime will not have a large influence on the levelized cost of hydrogen/biochar, furthermore when lifetimes longer than 12 years are taken into account, additional (large) maintenance cost should be considered.

Table 6.14: Investment "strategy"

Year	Investment
1	0.08 of TDC
2	0.60 of TDC
3	0.32 of TDC + working capital

6.5.1 Scenario 1: no additional subsidies

When no additional subsidies or a CO_2 taxation is implemented, the designed system will not be compatible with current hydrogen production technologies. The cumulative discounted cash flows over a 12 years time period (plus 3 years of construction) for the designed 26 MWt (biomass input) pyrogasification SEWGS plant is displayed in figure 6.3. This scenario is not profitable, having a cumulative discounted cash flow over an operational time period of 12 years (plus 3 years construction) of €-65.603.471. This shows that the designed installation is not cost compatible compared to fossil fuel-based hydrogen production when only looking at the market value of the produced products. The strength of the designed system lies, however, within the sustainable character of the installation, which also brings a lot of added value. Therefore subsidies for the system are expected and required, similar to other biomass-based energy production technologies all over the world. At a point in time, the produced products should become cost compatible; subsidies are required to mature the technology, but not to maintain the technology. Therefore an increase in product prices is required over time (or a decrease in production cost). In the next section, a break-even analysis is performed to analyze if these required prices are within reach.

Analyzes of the total cost over the total time span of the installation (12 years operational + 3 years construction) concludes that 23.6 % of the total costs are related to the initial capital expenditure, and 76.4 % is related to the operational expenditure. When the additional contingency is taken into account, 32.0 % of the total costs are related to the CAPEX, and 68.0% of the total cost is related to the OPEX.

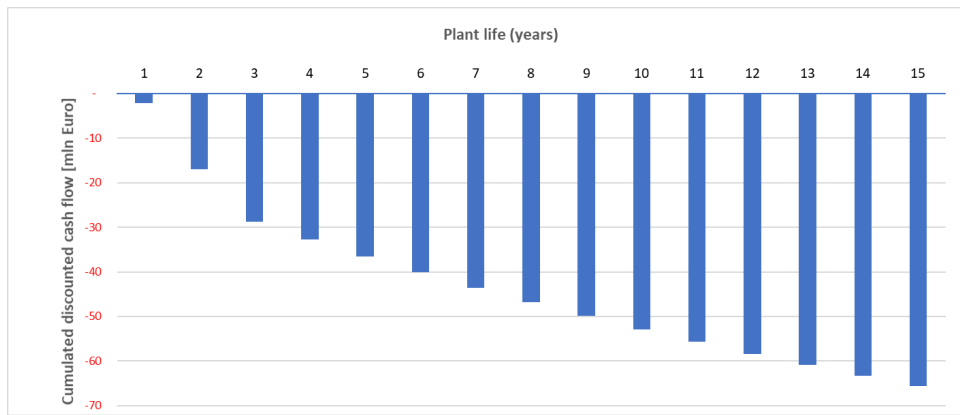


Figure 6.3: Discounted cumulative cash flows for scenario 1: no subsidies, no CO_2 taxation

6.5.2 Scenario 2: break even

A break-even scenario is modeled to determine break-even hydrogen and biochar prices. The results of the break-even analysis with respect to cumulative discounted cash flow over the operational period for 12 years (+3 years start-up) are displayed in figure 6.4 showing the break-even point after 12 years under operation.

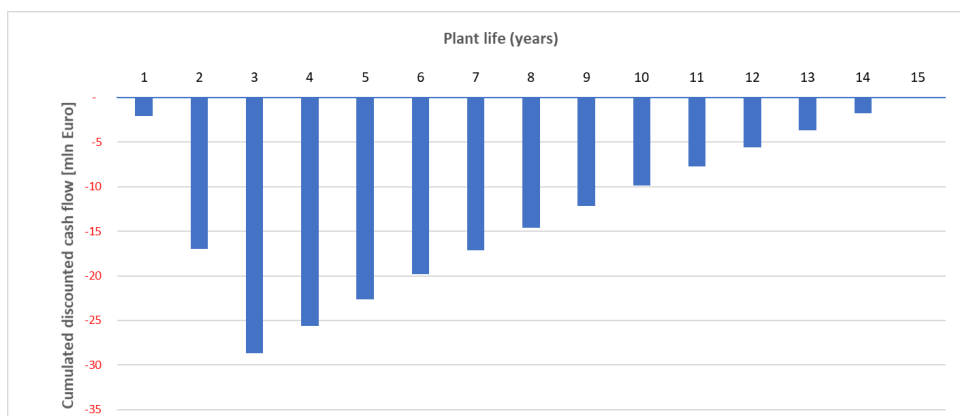


Figure 6.4: Discounted cumulative cash flows for scenario 3: break even

The analysis results in the following coupled break-even prices:

- **Hydrogen break even price: €4.20 per kg**
- **Biochar break even price: €700.7 euro/ton**

The determined coupled break-even prices are based on the current market price of biochar of €250 / ton and €1.50 for hydrogen prices. Both prices are multiplied with the same factor (1.80) such that a break-even point is reached. When Biochar prices remain at €250 per ton, the hydrogen break-even price increases to €5.63 per kg for the analyzed system. Future sustainable hydrogen production by PEM electrolysis produces hydrogen by a cost price in the €6-€7 per kg range [81], current hydrogen production prices by PEM electrolysis are around €10 per kg, depending on electricity prices. The designed pyrogasification SEWGS can cost competitively produce hydrogen compared to other sustainable hydrogen production methods for high purity hydrogen, even when additional value (subsidies) on biochar is not taken into account.

6.5.3 Scenario 3: expected subsidies

The designed system produced sustainable fuels: biochar and hydrogen. The flue gases of the system could also be captured and fed to greenhouses. In order to determine the amount of subsidies, the preliminary rapport for sustainable energy subsidies in the Netherlands (SDE++) for the year 2021 is used.

Due to the novelty of the discussed technology, there are not yet standardized subsidies for biochar/ high purity hydrogen out of biomass. The following (comparable) methods for sustainable fuel production/ carbon capture are standardized in the proposed Dutch SDE++ subsidies:

Table 6.15: SDE++ subsidies in the Netherlands for sustainable energy production

Hydrogen	(equivalent) Subsidies	Purpose
	€3.39 / kg H_2	Gasification of biomass
	€4.06 / kg H_2	Biofuel out of pyrolysis oil
	€5.83 / kg H_2	Ethanol out of biomass
	€10.35 / kg H_2	Hydrogen from electrolysis
Biochar		
	€345.8 / ton biochar	CCS
	€882.6 - €1404.5 / ton biochar	Advanced renewable fuels

Note: 1 ton biochar contains 892 kg of pure carbon, which is equivalent to $892 * \frac{44,01}{12,01} = 3.269$ tones of CO_2 . One ton of biochar contains 34.18GJ of energy = 9.49 MWh.

The assumed subsidies for hydrogen and biochar are listed below, which are based on the SDE++ subsidy regulations for 2021. Note that it is expected that expected subsidies for hydrogen are higher compared to subsidies for biomass gasification. This is due to the fact that his process produces high purity hydrogen (compared in quality to electrolysis products) and not a syngas for power generation.

- Hydrogen subsidies: €5.83/kg
- Biochar subsidies: €345.8/ ton

The simulation results of the cash flow under this scenario is displayed in figure 6.5, in this case, the additional contingency (40%) for the CAPEX is taken into account corresponding to a novel technology.

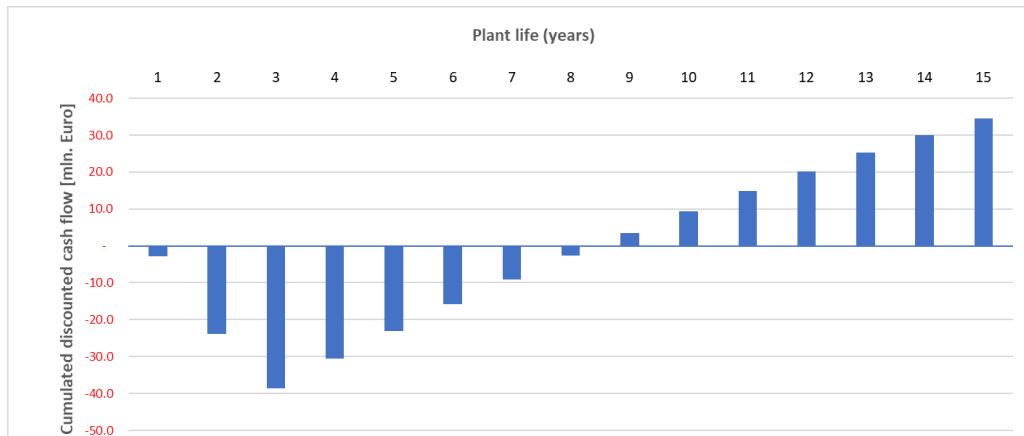


Figure 6.5: Discounted cumulative cash flows for scenario 4: with subsidies

The payback time of the system (after taken in operation) is five years and five months. The Initial Rate of Return (IRR) is 14.8%.

6.6 Sensitivity analysis and cost optimization

This section will cover the sensitivity analysis with respect to system cost and income. Furthermore, process conditions are optimized with respect to cost, with the focus on heat exchanger surface area.

6.6.1 Heat exchanger optimization

As can be seen in section 6.3, heat exchangers contribute significantly to total capital investment: 44,0 % of all capital cost are heat exchanger cost. Due to dust in flue gases/syngas and relatively high temperatures, gas-gas heat exchangers cannot be constructed as plate heat exchangers, but either tube in tube/ shell in tube heat exchangers are required. At high operating temperatures, a plate heat exchanger is a welded box, which is impossible to open for maintenance/cleaning (remove dust).

A sensitivity analysis is performed with respect to the minimal pinch point in all HEX, a boundary condition which is used during the simulations. The results are displayed in figure 6.6. where the hydrogen break-even price is displayed on the left y-axis and the total capital investment on the right y-axis. When the minimum pinch point increases, the efficiency of the system decreases: more biomass is combusted in the regenerator to supply sufficient heat for heat integration. A decrease in CAPEX, on the one hand, results in an increase in OPEX(biomass purchasing cost). The sudden drop in hydrogen production cost from $dT=40\text{ }^{\circ}\text{C}$ to $dT = 50\text{ }^{\circ}\text{C}$ is caused by a large pinch point increase in the air pre-heating system. Due to limiting factors of reformer heating at these pinch points, the LMTD of the air-pre heater drastically increased; this is, however, accompanied by an efficiency loss and OPEX increase. This is why there is no further drop in production cost from pinch point = $50\text{ }^{\circ}\text{C}$ to $60\text{ }^{\circ}\text{C}$.

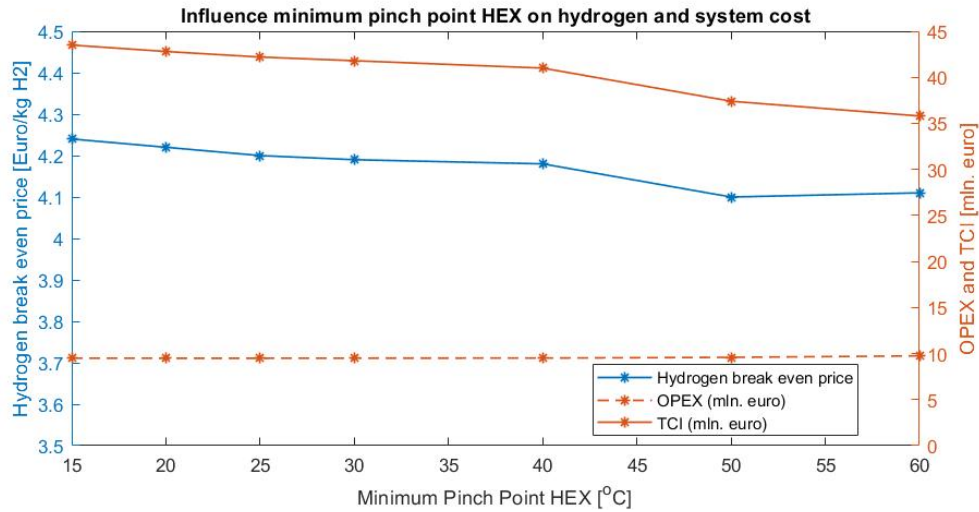


Figure 6.6: Influence pinch points HEX on hydrogen production cost

When analyzing the main system (min $P_i=25\text{ }^\circ\text{C}$). The air pre-heater has a relatively large surface area due to limited heat transfer coefficients for gas-gas shell in tube heat exchangers, the relatively large duty, and the low LMTD. Under the initial operating conditions, the air-pre heater costs are 48.1 % of the total HEX cost, which is not proportional and thus requires optimization. In order to get a better insight into the effect of minimum pinch point on hydrogen production cost, the production cost without air pre-heater is calculated as shown in figure 6.7. This simulation shows that without air pre-heating, a minimum pinch point of 20-30 $^\circ\text{C}$ results in the most cost-effective system. Under lower pinch points, heat exchanger cost increases, while at higher pinch points, the efficiency decreased, requiring additional biomass for sorbent regeneration increasing (OPEX) and increased CAPEX (increased reactor size). Due to the reactor cost increase under higher pinch points, the TCI is hardly influenced by pinch points up from 20 $^\circ\text{C}$.

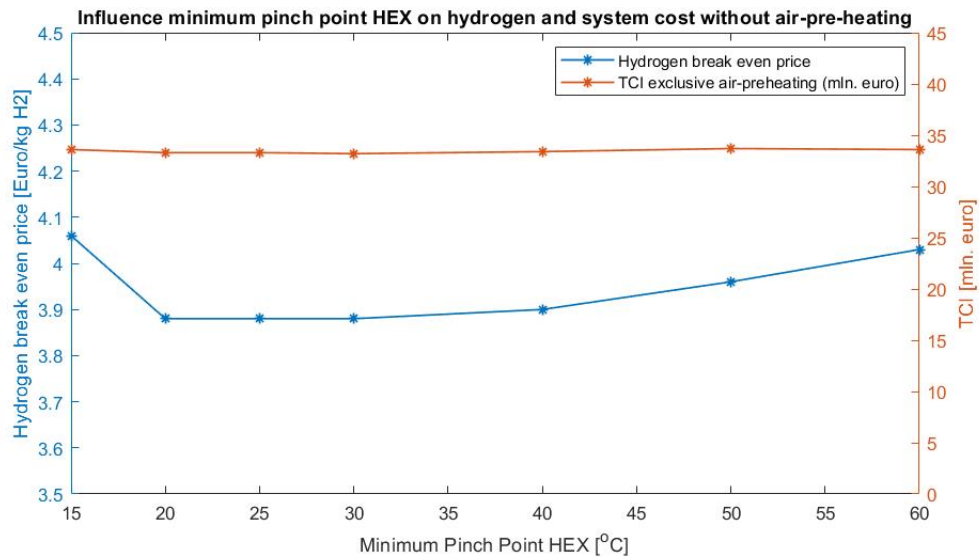


Figure 6.7: Influence pinch points HEX on hydrogen production cost without air pre-heating

In order to determine the optimal size of the air pre-heater, additional simulations are run. for this system, the standard pinch point in the system remains 25 $^\circ\text{C}$, but the pinch point of the air pre-heater is varied. figure 6.8 shows the results of this analysis. Under a pinch point of 200 $^\circ\text{C}$, hydrogen production cost are optimized: 4.01 € per kg H₂, coupled with a biochar break-even price of 668 € per ton, which is significantly lower compared to the optimum found in figure 6.6: 4.10 € per kg H₂. These optimized conditions are minimum pinch point for all HEX (except air pre-heater): 25 $^\circ\text{C}$) and a pinch point for the air pre-heater of 200 $^\circ\text{C}$.

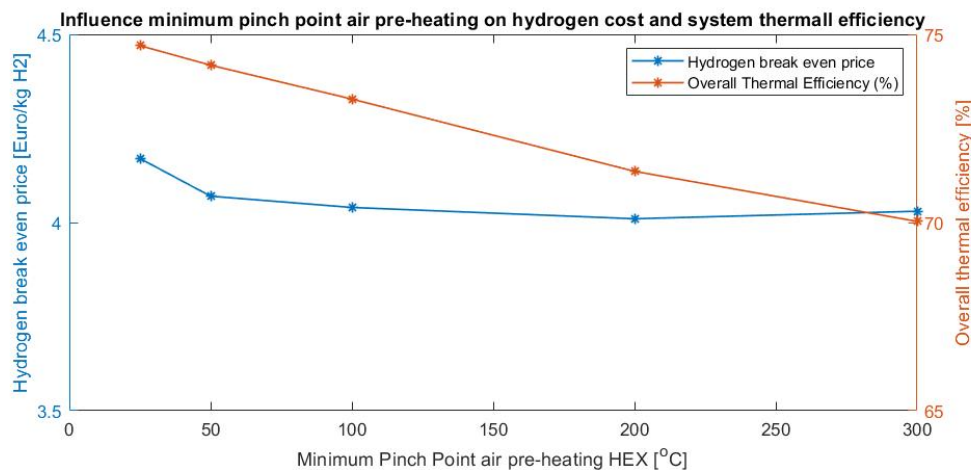


Figure 6.8: Influence pinch points air pre-heater HEX on hydrogen production cost, other minimum Pinch Point boundary conditions: 25°C

The heat exchanger cost for this 25-200 °C system is displayed in table 6.16. HEX costs are decreased by 37.9 % by optimizing the pre-heater. Using the same method, other HEX surface area's could also be further optimized, figure 6.7 show, however, that this will result in a nonsignificant reduction in TCI. Table 6.16 shows that reformer heating requires a relatively large and expensive HEX; the technical system analysis also showed that reformer heating could be a system bottleneck with respect to system efficiency. An alternative system where a small fraction of oxygen is added to the reformer for reactor heating can solve this problem.

The levelized cost of production of the produced hydrogen drops from €4.20 to €4.01 coupled with a biochar price of 668 €/per ton. The payback time of the optimized installation is 5 years and 0 months, and the IRR is 18.7%. The system efficiency decreased from 74,4% to 71.4% due to less "efficient" air pre-heating. In the new system, more biomass is required in the regenerator since air is pre-heated to a lower temperature. On the other hand, the CAPEX is reduced significantly, as well as maintenance cost.

Table 6.16: HEX cost calculations system with decreased air pre heater

HEX	A	Total cost	percentage of total HEX cost
1	60.35 m2	€112.364	5.9 %
2	30.5 m2	€64.619	3.4 %
3	82.5 m2	€136.620	7.2%
4	35.2 m2	€71.228	3.8 %
5	184 m2	€378.894	20.0 %
6	72 m2	€188.118	9.9 %
7	383.5 m2	€596.941	31.5 %
8	250.30 m2	€246.288	13.0 %
9	50.9 m2	€97.312	5.1 %
Total cost		€1.892.384	100 %

6.6.2 Sensitivity analysis biomass cost and catalyst/sorbent replacement strategies

An elaborate analysis of the sensitivity of biomass purchasing cost, catalyst replacement strategy, and limestone replacement strategy can be found in appendix J.

From the sensitivity analysis, the following conclusions can be drawn:

Biomass purchasing cost

- Biomass purchasing cost has the largest influence on the Levelized Cost Of Hydrogen (LCOH), which is expected due to the relatively large contribution of biomass on the OPEX.
- A decrease of 100 % in biomass prices reduced the LCOH by 40.3 % while an increase of 100 % in biomass prices increases the LCOH by 28.9 %
- Even when biomass prices increase by 100%, the required subsidies (€3.89 per kg H_2) to reach break-even are still lower compared to the expected subsidies (€5.83 per kg), meaning the system will be economically feasible even under this (unexpected) price increase of biomass

Catalyst replacement strategy

- There is an exponential relationship between catalyst replacement time and LCOH, when replacement time decreases, LCOH increases exponentially
- When catalyst replacement is performed once every month instead of once every three months, LCOH increases by 15.5% when catalyst replacement is performed once every nine months, LCOH reduces only by 5.0%.

Limestone replacement strategy

- There is only a small influence of limestone replacement strategy with respect to LCOH: when a 2% sorbent make-up is used instead of a 10% sorbent make-up, LCOH reduced by only 0.95%, while an increase from 10% sorbent make-up to 50% sorbent make up per cycle increases LCOH by 3.1%.
- When limestone prices double, LCOH only increases by 1.9%.
- Limestone replacement strategy has a large influence on (average) sorbent activity, influencing the limestone throughput rate through the CaL system. It is expected that this cycle rate influences system efficiency and LCOH due to larger mass flows in the system, which requires heating/cooling. This influence should be further analyzed and simulated.

The sensitivity analysis shows that given the novel design's expected subsidies, the analyzed system is financially feasible. Biomass purchasing costs have been identified as the largest operational expenditure of the system; decreasing biomass purchasing costs can significantly influence the levelized cost of hydrogen.

6.7 Discussion

Of the total system cost over the life span of the installation (12 years + 3 years construction), 23.6 % is related to CAPEX, and 73.4% is related to the OPEX. The main contributors to the OPEX are biomass (47 %) followed by labor cost (17%) and catalyst cost (10 %). The sensitivity analysis showed that biomass purchasing prices and catalyst replacement strategy (catalyst lifetime) significantly influence the levelized cost of hydrogen. However, even under extreme scenarios (100% biomass price increase and 300% catalyst replacement increase), the system is still cost compatible compared to other sustainable high purity hydrogen production techniques.

A financial model has been designed to simulate cash flows of the novel pyrogasification SEWGS system. After optimizing the design, concerning heat exchanger size, the financial model showed that the designed system's hydrogen and biochar break-even prices are €4.01/kg and €668 per ton respectively. These break-even prices are significantly lower compared to expected hydrogen prices produced by sustainable water electrolysis for hydrogen production (€6-7 per kg H_2). When simulating expected subsidies for hydrogen and biochar, respectively (€5.83 kg H_2 and €345.8 per ton biochar), the installation's payback time under these subsidies is 5 years and 0 months; the IRR is 18.7 % of the analyzed installation.

6.8 Conclusion

The cost analysis shows that the designed system is cost-competitive compared to other sustainable, high-quality hydrogen production methods, producing high purity hydrogen at a significantly lower cost than PEM electrolysis, while a similar hydrogen quality is obtained.

It is recommended to also analyze an oxy-fuel powered system, where a fraction of oxygen is added to the regenerator and the reformers; this will simplify heating mechanics even further, reducing HEX cost. Furthermore, this system will require less steam, resulting in reduced reactor volumes and reducing reactor and catalyst cost.

Chapter 7

Societal study on a biomass powered pyrogasification SEWGS system

Biomass, especially woody biomass, has been the subject of many discussions in recent years with respect to sustainability. There is no environmental benefit when biomass is not harvested sustainably. Due to high CO_2 emissions from woody biomass and deforestation, biomass for energy utilization can even contribute to global warming. For biomass-to-energy systems to be sustainable, biomass has to be harvested sustainably: a policy is required to ensure the preservation of forests and nature. The future biomass policy guidelines for the Netherlands are shortly discussed in this chapter. Using biomass sustainably brings the question of how much biomass can be harvested sustainably for energy production. A study is conducted to map sustainable biomass potential in Europe, and especially the Netherlands. Applications of biochar will also be further analyzed in this chapter. Biochar is one of the main products of the analyzed system, but the potential of biochars is not well known. This research analyses other high-end applications of biochar that add value to the overall system.

The analyzed system can run on variable biomass input with respect to biomass quality. Using lower quality biomass (more moisture and more ash) can result in a more sustainable system since lower quality biomass is more abundantly available: logging residues, municipally waste, etc. The influence of different biomass types on the system is shortly discussed in this chapter. Finally, the CO_2 footprint of the designed process is modeled.

7.1 Future biomass policy guidelines in the Netherlands

In 2020 the Dutch "Social Economical Council" (SER) published a report which contained the future perspective of biomass and advice for further biomass energy policies [82]. The general tendency of this report, in combination with shifting policies of other western European countries, implicates that biomass should be utilized for "high-end applications". A categorization has been made for biomass utilization from low-end applications to bridging applications and finally to high-end applications. Low-quality heat production, electricity production, and light road transport fuels are seen as "low-end applications," and future policies should focus on facing out these applications. Bridging applications are high-quality heat and transportation fuels for heavy transport, as well as dispatchable heat and electricity to cope with peak loads. Policies from 2020 to 2050 should commit to these types of solutions and are required to bridge the gap to temporarily replace fossil fuels, but after 2050 bridging applications should also be phased out. High-end applications are described as the production of bio-based raw materials, for example, raw materials for industry (tailored syngas, hydrogen, biochar) building materials, but also carbon Capture and Storage (CCS) techniques.

Figure 7.1 shows the classification published by the Dutch SER ranging from low-end applications (bottom) to high-end applications (top).

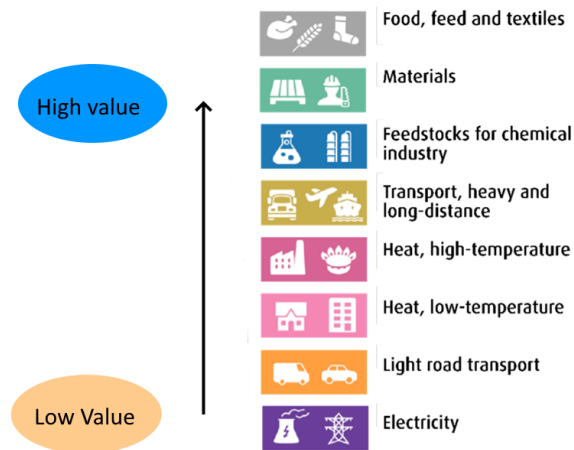


Figure 7.1: SER classification of biomass utilisation ranging from low end quality applications (bottom) to high end applications (top)

7.2 Biomass potential in Europe and the Netherlands

This section will discuss both the biomass potential in Europe as well as for the Netherlands, which can be harvested sustainably. This research will focus on woody biomass potential. Biomass can be divided into the following categories [83]:

1. Biomass from forests
2. Biomass from landscape care
3. Post-consumer wood

Biomass from forests can be divided into the following categories [83]:

- 1.1 Stem wood currently harvested for industry
- 1.2 Additional potential for stem wood within the sustainable harvestable limit
- 1.3 Primary forestry residues
- 1.4 Secondary forestry residues (sawdust/black liquor)

Stem wood derived biomass is a type with generally a high calorific value, low ash, and low moisture content. While the primary forest residues generally have lower calorific values and high ash and high moisture content. Primary forest residues are categorized as logging residues (branches/tops), early thinning, and extracted tree trunks. Secondary residues are derived from processing in the wood industry. Extracting, for example, softwood from stem wood in the Netherlands has an average conversion factor of 1.64, meaning that 1.64m³ of stem wood is required for the production of 1m³ of softwood [84], the remaining 0.64 m³ are residues categorized under secondary forest residues.

7.2.1 Europe

In 2016, 64.1% of sustainable energy produced in Europe came from biomass and waste, which was estimated to be 140 Mtoe (Mega tone oil equivalent). Of this 140 Mtoe, 82 Mtoe came from woody biomass. Agricultural residues and manure were the main contributors to the remaining sustainable production from biomass sources [85]. The European sustainable woody biomass potential in 2020 and 2030 is displayed in table 7.1 [83]. Data is obtained from the Atlas of EU biomass potentials, published by the European commission[83]. Note that round wood is currently harvested mostly for construction material and the paper industry; therefore, woody biomass potential for energy production should be calculated, excluding primary harvested round wood for the industry.

The European potential for sustainable energy production using woody biomass in 2020 is equal to 136.557 Mtoe [5.717 PJ] and in 2030 133.367 Mtoe [5.584 PJ]. Compared to 82 Mtoe, which is currently utilized, there is the potential to sustainably increase Europe's woody biomass consumption by 63% in 2030 compared to 2016.

Table 7.1: European woody biomass potential in 2020 and 2030

Type	Potential 2020 [Ktoe]	Potential 2030 [Ktoe]
Round wood	56.115	56.115
Additional harvestable Round wood	37.871	38.529
Primary forestry residues	41.186	41.842
Black liquor	16.751	8.742
Sawmill byproducts/residues	20.538	23.410
Biomass from landscape care	11.419	11.002
Post consumer wood potential	8.791	9.842
Total	192.671	189.482

7.2.2 the Netherlands

The potential of woody biomass in the Netherlands a published by the European commission is displayed in table 7.2. Excluding round wood, the dutch woody biomass potential was estimated to be 692.3 Ktoe in 2020 (29.0PJ) and is expected to be 756.3 Ktoe (31.7 PJ) in 2030. In 2019 Dutch woody biomass consumption is equal to 51.31 PJ, 177 % of the Dutch biomass potential [86].

Table 7.2: Dutch woody biomass potential in 2020 and 2030

Type	Potential 2020 [Ktoe]	Potential 2030 [Ktoe]
Round wood	137.8	137.8
Additional harvestable Round wood	60.8	78.9
Primary forestry residues	71.5	77.4
Black liquor	0	0
Sawmill byproducts/residues	31	47
Biomass from landscape care	149	144
Post consumer wood potential	380	409
Total	830.1	894.1

The main reason why more biomass is consumed in the Netherlands than produced is due to co-firing of wood pellets in coal-fired powerplants. In 2019 the Netherlands consumed 830 kton of wood pellets, mostly from Baltic states and the USA. When analyzing biomass produced in the Netherlands the following data is obtained [87, 88]:

Table 7.3: Dutch woody biomass Production,consumption and export for chips/shreds and pellets

Type	Produced	consumed	Exported	Imported
Pellets	250 kton	829 kton	162 kton	741 kton
Chips+shreds	1200 kton	987 kton	516 kton	303 kton

Pellets are identified as high-quality biomass with low moisture and ash content, while chips and shreds generally have a higher moisture and ash content. There is a large unharvested potential of woody biomass in the Netherlands, which translates to mostly forest residues (chips and shreds). Additional installations with new technologies are required in the Netherlands, which can process chips and shreds to a high-end application in accordance with the SER rapport on bio-based raw materials [82]. Furthermore, processing biomass close to its source will reduce transportation costs and related CO₂ emissions.

Using pellets for co-firing in coal-fired power plants for the production of heat and power is not a high-end application. Using wood pellets for the production of a high-quality biochar/ high purity hydrogen using a pyrogasification sorption-shift system is a high-end application: hydrogen can be used as (transportation)fuel, for residential heating, to cope with peak demands and can be used in the chemical industry, biochar can be used for soil amendment, carbon capture of even as high-quality sorbent. Therefore the use of pellets should shift from heat/electricity production and the metal industry to the production of high-quality materials and chemicals. Furthermore, most of the unharvested potential of biomass in Europe/the Netherlands is lower quality biomass (chips/shreds). In the Netherlands, a surplus of chips and shred is produced and exported to Belgium and Germany. Technology that can convert lower quality biomass to high-end products (biochar/hydrogen) is desired above conventional technology of conversion of chips/shreds to heat and power.

7.3 Biochar applications

One of the main products of the analyzed pyrogasification sorption-shift system is biochar. Biochar is produced in an auger reactor; depending on biomass input quality, temperature, heating rate, and residence time, the biochar quality is influenced. Besides acting as a carbon sink, biochar can also be used for other applications, which are classified as high-end applications in section 7.1 (except biochar as fuel). Different applications of biochar are listed below.

- Carbon sequestration and soil amelioration
- Pollutant removal from soil, gas and water
- Carbon black substitute
- Substitute for charcoal in blast furnaces

7.3.1 Carbon sequestration using biochar as soil amelioration

In the designed pyrogasification system, biochar is produced in an auger reactor where a high-quality wood (pine wood, 0,4% ash content, HHV=18,0 MJ/kg) is used as input. Of all carbon, 47,9% moves with the produced biochar, the remainder moves with the volatiles to the gasification process. When biochar is stored, carbon is stored, resulting in carbon sequestration, which reverses global warming: carbon from the short-term carbon reservoir is put in the long-term reservoir (fossil fuels). Biochar can be used as a soil amendment, which brings additional benefits besides carbon sequestration with respect to soil quality and pollutant removal from water and soil. When biochar is used as a soil amendment, carbon mass loss of biochar derived from woody biomass within an incubation time of 500 days is in the 5-10 % range, compared to value up to 80 % carbon mass loss when biomass is directly used for soil amendment [89]. Complete degradation of biochar takes a significant amount of time: with estimations of the mean residence time in the millennial time scale, with estimates ranging from 1.000 years to 4.000 years [90].

When biochar is stored in soil, part of the carbon in biochar is biological degradable, causing CH_4 , N_2O and CO_2 emissions [91]. CH_4 emissions are mostly caused by the volatile C fraction due to degradation of the material; on the other hand, biochar reduces CH_4 emissions from the soil due to the increase of methanotrophic proteobacteria. Biochar can have both a negative effect on CO_2 emissions from soil (C mineralization) as well as a positive effect (C stabilization). Biochar produced under low temperatures (250°C-400 °C) typically cause additional CO_2 emissions from soil compared to untreated soil, while "high temperature biochars" (525°C-600°C) reduce CO_2 emissions [91]. For both the high-temperature and low-temperature biochar, net. CO_2 emissions are negative due to carbon storage in soil. Biochar reduces N_2O emissions from the soil due to reduced denitrification and increases nitrogen immobilization [91]. Research by Zhang. et al. [92] found that the Global Warming Potential (GWP) per ha. of soil treated with biochar was lower compared to the control soil. Reduced GWP was mainly caused by reduced N_2O and CH_4 emissions.

Biochar improves soil quality by highly increasing soil fertility, caused by a high Soil Organic Matter (SOM) and a high level of nutrients (N, P, Ca) in soil amendment by biochar since minerals are leached from biochar. Furthermore, biochar is characterized by a large specific surface area (400-800 m²/g), providing a habitat for microorganisms [90].

7.3.2 Pollutant removal

Biochar can act as a sorbent for the removal of both organic and inorganic pollutants from soil, water, and gas. Biochar obtained from high-temperature pyrolysis (> 500 °C) is typically characterized by high microporosity, high specific surface area, high C/N ratio, and low dissolved organic carbon, which makes this type of biochar suitable for the removal of organic compounds such as agrochemicals, pesticides, VOCs, and aromatic dyes [93]. Biochar produced at high temperatures contains less H and O, resulting in mainly hydrophobic interactions. Biochar can serve as a substitute for activated carbon. [93].

Biochar obtained from low-temperature pyrolysis <500 °C on the other hand, is characterized by a relative high dissolved concentration of organic carbon, a low microporosity, relative low specific surface area, and contains functional groups with oxygen, which makes this type of biochar more suitable for the removal of inorganic pollutants like sulfides, heavy metals, ammonia, etc. due to high affinity of these pollutants towards polar components. [93].

The above implementations for pollutants removal are mainly for the removal of pollutants in soil, which gives an additional benefit when biochar is used as a soil amendment. Biochar can also be used for pollutant removal in highly polluted wastewater, for example, from the paramedical, metal processing, petrochemical, and chemical industry [93]. Furthermore, biochar can be used to remove pollutants from gases, for example, removal of H_2S out of biogas: for the removal of H_2S a biochar with pH>7, COOH and OH groups and a moisture content of >80v/w% showed best results up to a removal efficiency of 95% [93]. Currently, activated carbon is used derived from fossil fuels for the removal of H_2S from biogas, which can be replaced by high-quality biochar.

7.3.3 Carbon black replacement

Carbon black is used in pigments, but mostly as filler in rubber. Conventional carbon black is produced by partial combustion of heavy oils, where carbon black particles are filtered out of the flue gases. The specific surface area of carbon black is lower compared to active carbon, but carbon concentrations are higher >95 % carbon black compared to >90% for active carbon. The most important property of a filler is particle size, which influences polymer-filler interaction; carbon black particle sizes are typically in the 20-250 nm range. If biochar is used as carbon black replacement, post-processing is required (milling/grinding) in order to obtain sufficiently small particle sizes [94]. Research by Peterson et al. [94] showed that a low ash (<2%) biochar could partly substitute (up to 50Vol%) of carbon black in styrene-butadiene rubber when low filler concentrations (10%) are used without degradation of mechanical properties. This kind of rubber is typically used for applications that require flexibility yet require improved tensile properties and thus filler.

Biochar can be used to partly (up to 50Vol%) replace carbon black as filler for flexible rubber compounds (10% filler) under the following conditions [94]:

- Low ash content < 2%
- high carbon content 90-95 %
- Small (mean) particle size < 1 μ m

Carbon black prices are in the range of \approx €1000 per ton [95]. Activated carbons have a price range of €500-1000 per ton, meaning there is a large opportunity to add additional value to the pyrogasification SEWGS system when these high-quality products are produced. Note that for both the production of activated carbon black and carbon black, post-processing is required. For activated carbon, high-temperature steam (> 600°C) can be used for activation. For carbon black, small particle sizes are required, requiring an additional fine milling/grinding step.

7.3.4 Substitute of fossil fuels

Biochar can be used as fuel, for example, for the (co-firing) of power plants, metal industry, as barbecue coals, and as input for gasification systems replacing conventional fossil fuels. High-quality biomass used as input in this research can already be used for gasification systems or the co-firing of biomass. When biochar is produced to serve as fuel, relative low pyrolysis temperatures are sufficient <400 °C (carbonization). This results in a moisture-free product with still quite some volatile matter and with relatively low fixed carbon concentration. Using biochar as fuel can be seen as a bridging application, while the other applications discussed in this chapter can be seen as a high-end application under the definitions given in chapter 7.1.

7.4 Biomass quality variability

This study analyzed a biomass powered system with a high-quality biomass input: Pinewood with 8% moisture, 0.4% ash, and a HHV of 18,0 MJ/kg. Woody biomass like pinewood is characterized by a high lignin content, relatively high fixed carbon content, and low ash and moisture content. Lignin is relatively stable under higher temperatures, having a relatively low carbon conversion efficiency when thermally treated: lignin has a high fixed carbon concentration; thus, biomass with high lignin concentrations have a relative high biochar yield [96]. A detailed analysis of biomass characteristics related to thermal conversion is given in appendix K, and alternative hydrogen production methods out of biomass are explained in appendix L.

The analysis in chapter 7.2 based on the Dutch and the European biomass potential showed a large potential for a lower quality of biomass, coming from forest residues and municipal waste. This kind of biomass generally contain more cellulose and hemicellulose [96], corresponding with relative "green" biomass: leaves, small branches, etc. Furthermore, these low-quality biomass types have a high ash concentration (up to 40%), can contain sand (especially shreds), and have a high moisture content [97].

Treating lower quality types of biomass will not have a significant influence on the performance of the reforming system and the sorption-shift-system: the produced volatiles can still be reformed to a hydrocarbon free syngas, CO_2 can be captured, and the gas can be shifted towards pure hydrogen and steam. When ash and moisture content increase, the volume input of a system (under the same thermal input) increases, and therefore a larger pyrolysis system with a larger throughput rate is required to release the same amount of volatiles.

Low-quality biomass with low lignin concentrations and high ash concentration influences the pyrolysis system and system output in several ways:

- + Ash has a catalytic function: enhancing secondary cracking reactions in the auger reactor
- Due to lower lignin (fixed carbon) concentrations, the carbon conversion rate in the pyrolysis reactor is higher, resulting in a relatively reduced biochar yield.
- High ash concentrations lead to a higher energy penalty in the auger, reducing overall system efficiency
- A high ash concentration in biochar reduces biochar applications, "high ash biochar" cannot be used for carbon black and activated carbon replacement. High ash biochar can, however, still be used as a soil amendment and for carbon sequestration.

Additional moisture content in biomass is not a problem per se, since steam reforming requires a lot of water (up to an S/C ratio of 4.6, no significant efficiency decrease has been noted in the sensitivity analysis of the model), meaning that if more moisture is present in biomass, less additional steam has to be generated for steam reforming. This is up to the limit of $S/C = 4.6$ in the pre-reformer. The heating configurations needs to be altered however, when high moisture biomass is used, more heat is in this case required in the auger reactor. An easy switch between biomass types cannot be made since this requires different heat exchange characteristics in the SEWGS and auger reactor.

Although using lower quality biomass results in an energy penalty and lower quality biochar, there still is a large potential for this kind of biomass due to the wide availability and reduced cost for this feedstock. The main reason why this kind of biomass is not used for pyrolysis is due to the high energy penalty due to high moisture concentrations. The designed system requires a significant amount of steam, and therefore this disadvantage does not apply to the pyrolysis SEWGS system. Pyrolysis of low-quality biomass in an auger reactor using, for example, municipal solid waste or waste from landscape care has not yet been studied by many authors. A study performed by Yang et al. [98] in 2018 on pyrolysis in an auger reactor using the organic fraction of municipal solid waste as input material is the only study found using an auger reactor for low-quality biomass processing. The remaining studies using an auger reactor focused on high-quality types of biomass [31, 99]. Therefore it is recommended to perform further research on the application of high moisture, high ash biomass for (slow) pyrolysis in auger reactors. In such research, both the released volatiles and produced biochar are of interest and require detailed analysis. When lower quality biomass is used, problems are expected with respect to auger reactor heating since a lot of heat is required for water evaporation. Furthermore, the biochar quality decreases under high ash concentrations.

7.5 Carbon footprint

In order to get an idea of the CO_2 footprint of the designed installation, a simple model is constructed which covers the main CO_2 emissions of the system under operation. Note that CO_2 emissions could also be negative. This analysis is simplified and is performed to get an idea of the order of magnitude of the CO_2 footprint of the installation under operations.

7.5.1 Model for carbon dioxide footprint calculations

The following CO_2 emissions are taken into account in the model for CO_2 footprint calculations:

- Biomass harvesting
- Biomass transportation
- Biomass chipping
- Plant electricity consumption
- Carbon capture in biochar
- Carbon capture of flue gases

For a complete life cycle assessment, construction and end-of-life decommissioning should also be included, as well as a more detailed analysis of other factors that influence CO_2 footprint: the so-called cradle to grave approach. For a more detailed life cycle assessment of the installation, simulations in GABI can be performed.

Biomass harvesting

Energy cost during biomass harvesting: energy cost for logging and wood extraction is estimated to be between 1 and 1.3 L diesel per m³ of biomass [100]. The system requires 5,14 tones of biomass per hour, assuming a biomass bulk density of 500 kg/m³ [101], results in 10,28 m³ of biomass being harvest per hour of system operations. Assuming diesel consumption of 1.15 L per m³ and 2,9 kg of CO_2 emissions per liter results in a CO_2 footprint of logging of: 34,28 kg CO_2 per hour of operation: 6.67 kg CO_2 per ton of biomass input .

Biomass transport

It is assumed that biomass is transported over an average distance of 50km by truck (100 km total distance). Assuming a truck loading of 40 m³ and a density of 500 kg/m³ results in a truck loading of 20 tones. When the truck is 50 % of the time empty (returning to logging side) the CO_2 emissions per ton*km of biomass are 0.0830 kg CO_2 /km*ton [102]. When the system requires 5,14 tones of biomass input per hour, this translates to 42.66 kg CO_2 emissions per hour: 8.30 kg CO_2 per ton of biomass input.

Biomass chipping

When biomass chipping is done on-side, this can be done with an electrical chipper, which has high efficiencies compared to a diesel-powered chipper. The electricity requirement for biomass chipping depends on the desired particle size and size of the chipper. An energy requirement of 10 kWh per m³ of biomass is assumed for chipping biomass [103]. 10.28 m³ of biomass is chipped per hour, resulting in an electricity requirement of 102.8 kW. The average European energy mix contributes in 0.407 kg CO_2 emissions per kWh [104]: on average, 40% of electricity is produced by fossil fuels, 33% by sustainable energy sources, and 27% from nuclear energy. This results in a CO_2 footprint for chipping of: 41.84 kg CO_2 emissions per hour: 8.14 kg CO_2 per ton of biomass input .

Plant electricity consumption

In the economic analysis, it was assumed that the plant consumes an hourly 2 % of electricity compared to thermal input. This is equal to 514 kW. Using the same assumptions for electricity mix made for the CO_2 footprint of biomass chipping results in a CO_2 footprint of used plant electricity of: 209,20 kg CO_2 /hour: 40.7 kg CO_2 per ton of biomass input .

Carbon capture by biochar

Produced biochar contains carbon; when this char is stored, used as a soil amendment, used as activated carbon, or as carbon black, this will result in negative carbon emissions caused by carbon sequestration. When biochar is used as a replacement for coal in, for example, the steel industry, CO_2 emissions from biochar do not contribute to global warming, but in this case, biochar does not store carbon (carbon neutral). In this research, system boundaries are set around the pyrogasification system, including pre-processing: logging/chipping/transport, but excluding post processes. Since carbon in biochar does not leave the system as atmospheric CO_2 , negative system carbon emissions are allocated to the system from biochar.

Per hour, the analyzed system produces 874 kg of biochar, of which 89,2% is carbon. this is equivalent to: -2857 kg CO_2 per hour : -528.1 kg CO_2 per ton of biomass input .

Carbon capture and/or emissions by flue gases

The produced flue gases can either be discarded to the atmosphere or fed to greenhouses for CO_2 enrichment resulting in additional carbon capture and storage. The designed system produces a flue gas deluded with air. The CO_2 mass flow rate of the produced flue gas is 5648 kg/h. Carbon dioxide enrichment of greenhouses has an efficiency of around 50%, due to CO_2 leakage half of the fed CO_2 still enters the atmosphere directly [105]. When flue gases are directly discarded to the atmosphere, CO_2 emissions are 0 kg due to the short carbon cycle of biomass (only when biomass is harvested sustainably). When flue gases are fed to greenhouses, the CO_2 emissions of the system are negative and equal to -2824 kg/h: -549.4 kg CO_2 per ton of biomass input.

A system which uses pure oxygen for combustion produces a stream of CO_2 and water vapor, water vapor can easily be separated from CO_2 resulting in a concentrated stream of CO_2 which is suited for carbon storage in, for example, old gas fields.

7.5.2 Results CO2 footprint

The CO_2 emissions for each process within the system boundaries per ton of biomass input are displayed in table 7.4. It becomes clear that for both scenarios: including and excluding greenhouse (GH) CO_2 feeding, the designed system is carbon negative. For the system including greenhouse feeding, CO_2 emissions are -1041 kg/ton biomass input, and for the scenario excluding greenhouse feeding, the CO_2 emissions are -492 kg/ton biomass.

Table 7.4: CO_2 footprint pyrogasification sorption shift system per ton of biomass input

Process	CO_2 footprint per ton biomass
Harvesting and extraction	6.7 kg CO_2
Transport	8.3 kg CO_2
Chipping	8.1 kg CO_2
Plant electricity consumption	40.7 kg CO_2
Output	
Biochar	-556 kg CO_2
Flue gases (GH feeding)	-549 kg CO_2
Total CO2 footprint	
Excluding GH feeding	-492 kg CO_2
Including GH feeding	-1041 kg CO_2

Appendix M displays bar charts for different scenarios regarding the carbon footprint of the designed pyrogasification SEWGS system for different scenarios.

7.6 Discussion

The results for the CO_2 footprint show that most CO_2 leaves the system in the flue gases: 1098 kg CO_2 per ton biomass input compared to 556 kg CO_2 equivalent, leaving the system in the form of biochar. When a pure stream of CO_2 is produced (using oxy-fuel combustion), a highly concentrated stream of CO_2 can be produced suitable for CCS decreasing the carbon footprint. To further increase the accuracy of the CO_2 footprint calculations and determine the greenhouse warming potential of this technology, a complete cradle to grave life cycle assessment, for example, in GABI software, can be performed.

There are a lot of different applications for the produced biochar. Two high-end applications use biochar as activated carbon and use biochar as a carbon black replacement. When these types of applications are utilized, post-processing steps (steam activation and/or grinding) are required. Steam activation should be integrated into the Aspen plus model to analyze the possible utilization of high-temperature waste heat under SC ratios < 4.6. Biochar grinding would require additional electricity, influencing the system efficiency, production cost, and carbon footprint. On the other hand, these high-value products will result in higher revenue streams, influencing the analyzed system's cost efficiency in a positive way. The designed models can be extended when biochar is used for either of these two high-end applications to more accurately determine the system's feasibility and potential.

Using lower qualities of biomass as feedstock material for the auger reactor can increase the system sustainability and result in wider usability for different types of biomass: there is a lot of available low-quality bio-waste material, for example, municipal solid waste and forest residues, which have relatively high moisture and ash content. However, using high moisture feedstock will lead to an increased heat demand in the auger reactor (more moisture is evaporated in the auger), which can bring problems concerning auger reactor heating and upscaling. There has been no research up to date on slow pyrolysis in auger reactors using high moisture, high ash biomass feedstock. Additional experimental research is required. Results can be incorporated in the pyrolysis model in Aspen Plus and can give insight into reactor mechanics and possibilities (and barriers) for upscaling.

7.7 Conclusion

The designed pyrogasification SEWGS system provides sustainable high-end products for the future energy economy, following Western European countries' biomass policies. In Europe, there is both the sustainable potential of high and low qualities biomass, which can both be used as a system input. In the Netherlands, there is a large potential of forest residues and municipal waste (low-quality biomass) for the designed system, but the Netherlands also produces high-end biomass (wood pellets), which are preferably used for high-end applications, and not for co-firing in powerplants. Biochar has multiple high-end applications, varying from fuel (bridging application) to soil amendment, pollutant removal agent (can be used as activated carbon substitute), and even as (partial) carbon black replacement for elastic rubbers. The CO_2 footprint of the designed installation has been calculated for scenarios including and excluding greenhouse feeding of the produced flue gases. In both cases, the system is carbon negative. For the model, which includes greenhouse feeding with flue gases, the CO_2 footprint of the pyrogasification SEWGS system was calculated to be -1041 kg CO_2 per ton biomass input.

Chapter 8

Future perspective: oxy-fuel regeneration and partial combustion reformer

Due to bottlenecks identified in the technical and economic analysis of the system, an alternative design is proposed for further research. Bottlenecks were identified for air pre-heating (large capital cost) and reformer heating. Furthermore, large reactors are required (high CAPEX) with respect to large volume flows due to large S/C ratios. This chapter shortly describes the process and shows the perspective of an alternative system. The designed models in Aspen Plus, data processing modeling Excel and Matlab, the designed financial model and model for the carbon footprint can easily be altered for other process configurations. This section discusses simulation results that have been obtained by changing the already designed models, resulting in a short technical, economic and societal analysis of this alternative system.

An alternative system is suggested which used oxy-fuel combustion in the regenerator and used a small fraction of oxygen in the reformer to supply heat for reforming. This chapter is meant to give a future perspective of the analyzed technology, supplying an improved concept for further research. The proposed improved system based on oxy-fuel combustion in the regenerator and oxygen addition to the reformer(s) has the following advantages and disadvantages:

- + Pure stream of CO_2 leaving the regenerator: increasing possibilities for carbon capture
- + Less biomass for heat generation is required in the regenerator
- + Reformer heating was identified as a system bottleneck. By adding oxygen to the reformer, heat is supplied by partial combustion, reducing system complexity, and CAPEX
- + A system configuration parallel to a hydrolysis system for hydrogen/oxygen production gives a function of the produced oxygen
- + Reactor sized decrease due since less steam is required in the reforming system, and air is replaced by oxygen in the regenerator
- Part of the product is burned in the reformer, reducing hydrogen yield per unit input of the auger reactor
- Regeneration at higher temperatures is required due to increased CO_2 partial pressure in the reformer
- Oxygen production requires additional cost

A pyrogasification sorption-shift (PGSS) system combined with an electrolysis system for hydrogen production could be of great interest for further development, especially when oxy-fuel combustion in the regenerator is implemented and additional oxygen is fed to the reformer/gassier. This is because electrolysis for hydrogen production has oxygen as a by-product, which could be fed directly to the PGSS system. Hydrogen production using electrolysis is a form of energy storage, storing the surplus of wind and solar energy in the form of hydrogen, providing a sustainable dispatchable energy source, similar to the hydrogen produced by the proposed PGSS system. Furthermore, for a hydrogen energy economy, a hydrogen gas grid is required to transport large quantities of hydrogen, comparable to the current natural gas grid [64]. Feeding points for this grid are next to hydrogen production systems; placing a pyrogasification sorption system next to an electrolysis system gives the benefit that one more centralized entry point is required. Hydrogen production using PEM electrolysis system provides hydrogen with 99,5-99,9 % purity [64], comparable to the produced hydrogen in the PGSS system; therefore, no further upgrading of the produced hydrogen is required. A general overview of the combined PGSS/electrolysis system configuration is given in figure 8.1.

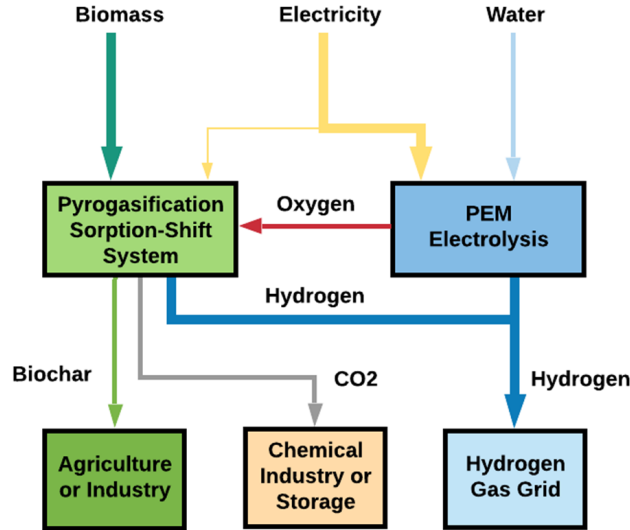


Figure 8.1: General process overview combined PGSS with hydrogen production from electrolysis

A system variation is designed which uses oxy-fuel combustion in the regenerator and with oxygen addition the reformer for heating. This system is based on the original PGSS system. The main differences are that additional pre-reformer and reformer heating from the flue gases is no longer required. Furthermore, the regenerator operates at 900 °C due to increased partial CO_2 pressures in the regenerator, which increases the required temperature for calcination. The designed system is displayed in figure 8.2. We wrote a draft for a research paper concerning the concept and results as discussed in this chapter. This draft can be found in appendix N.

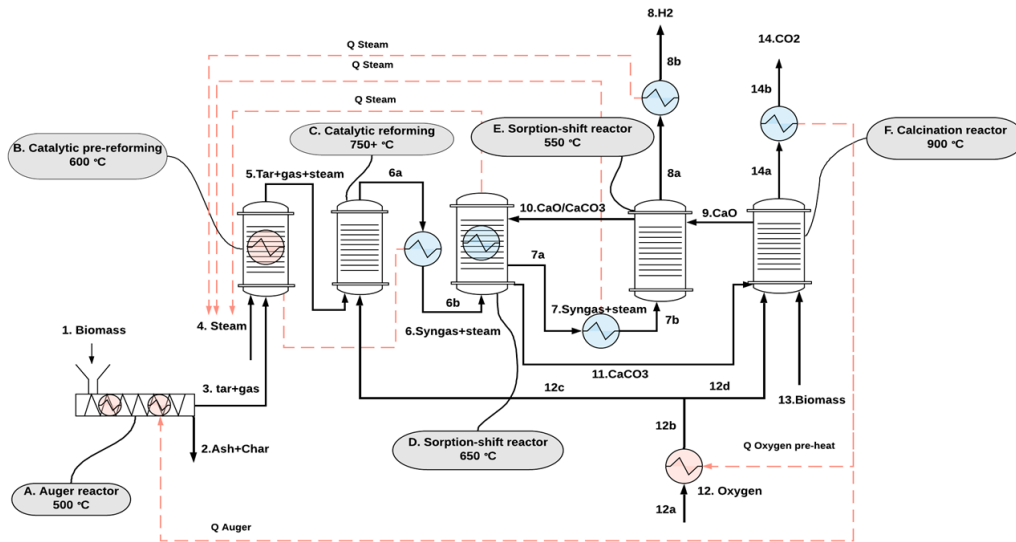


Figure 8.2: Pyrogasification sorption-shift system with oxy-fuel combustion system design

8.1 Process simulation results

The PGSS system, as originally designed and modeled in Aspen Plus, is altered to model oxy-fuel combustion. The heat exchangers to heat the pre-reformer and reformer are removed. Air is replaced by oxygen, and additional oxygen is added to the reformer, in such a way that: a) the reformer has a minimum temperature of 750 °C and b) enough heat is recycled from the syngas leaving the reformer so that the pre-reformer operates at a minimum temperature of 600 °C. These boundary conditions lead to an air ratio of 0.18 in the reformer. Furthermore, the regenerator is now modeled at 900 °C due to increased CO_2 partial pressure. An air ratio of 1.1 is used in the regenerator to prevent partial combustion. The amount of steam that is added to the reformer is initially not adjusted compared to the original system: 5400kg/h: an S/C of 4.58 in the pre-reformer.

The stream results of stream 1,2,6 and 8 are displayed in table 8.1 and the stream results of stream 12,13 and 14 are displayed in table 8.2.

Table 8.1: Stream results sorption-shift system with oxy-fuel combustion (1)

Stream nr.	1	2	6a		8a	
Mass flow	3600 kg/h	874 kg/h	8522 kg/h		5427 kg/h	
Temperature	20 °C	500 °C	782 °C		550 °C	
Component	Mass flow	Mass flow	Mass flow	V% gas[DB]	Mass flow	V% gas[DB]
CO ₂	0 kg/h	0 kg/h	2444 kg/h	33.0 %	16 kg/h	0.31 %
CO	0 kg/h	0 kg/h	426 kg/h	9.1 %	1 kg/h	0.03 %
H ₂	0 kg/h	0 kg/h	196 kg/h	57.9 %	227 kg/h	99.64 %
CH ₄	0 kg/h	0 kg/h	0 kg/h	0.0%	0 kg/h	0.01 %
C ₂ H ₄	0 kg/h	0 kg/h	0 kg/h	0.0 %	0 kg/h	0.00 %
C ₂ H ₆	0 kg/h	0 kg/h	0 kg/h	0.0 %	0 kg/h	0.00 %
H ₂ O	0 kg/h	0 kg/h	5456 kg/h		5182 kg/h	
Biomass	3600 kg/h	0 kg/h	0 kg/h		0 kg/h	
Char	0 kg/h	874 kg/h	0 kg/h		0 kg/h	

Table 8.2: Stream results sorption-shift system with oxy-fuel combustion (2)

Stream nr.	12c	12d	13	14a		
Mass flow	396 kg/h	1450 kg/h	1073 kg/h	5618 kg/h		
Temperature	357 °C	357 °C	20°C	900 °C		
Component	Mass flow	Mass flow	Mass flow	mass flow	V% gas	V% gas[DB]
CO ₂	0 kg/h	0 kg/h	0 kg/h	4875 kg/h	74.5%	96.5 %
O ₂	396 kg/h	1450 kg/h	0 kg/h	128 kg/h	2.7 %	3.5 %
H ₂ O	0 kg/h	0 kg/h	0 kg/h	612 kg/h	22.8 %	-
Biomass	0 kg/h	0 kg/h	1073 kg/h	0 kg/h		
Ash	0 kg/h	0 kg/h	0 kg/h	4 kg/h		

The results of the PGSS system with air combustion versus the PGSS system with oxy-fuel combustion are displayed in table 8.3 with respect to input, output, and efficiencies. There is a small reduction in overall energy efficiency since part of the hydrogen product is combusted in the reformer; on the other hand, less biomass is required for regeneration, partly balancing out this energy loss. The mass-ratio between char/hydrogen does change however, in the original system, this ratio is 3.16, while in the oxy-fuel system, this ratio is 3.86, meaning that in the oxy-fuel system, relative more chemical energy moves with the biochar, which can be seen in the relatively large drop of the cold-gas efficiency of the oxy-fuel system. The reason why the amount of produced biochar is similar for both processes is because the pyrolysis process is unaltered by the modification: 3600 kg/h biomass input, same temperature, same product output distribution. An option can be to add part of the produced biochar to the reformer, such that this char is partially combusted, providing additional energy for the reforming system. Depending on the produced char/hydrogen value, this can be cost-efficient and should be further investigated.

Parameter	Air combustion	Oxy-fuel combustion
Biomass input auger	3600 kg/h	3600 kg/h
Bio char output	874 kg/h	874 kg/h
Biomass input regenerator	1540 kg/h	1073 kg/h
Hydrogen output	276.3 kg/h	226.7 kg/h
CO ₂ concentration flue gas(dry)	16.6 %	96.5 %
Overall energy efficiency	74.4 %	73.4 %
Cold gas Efficiency	42.2 %	38.1 %

Table 8.3: System results Air combustion versus oxy-fuel combustion

8.2 Pyrogasification SEWGS oxy-fuel system with reduced SC ratio

Steam is used as an oxidator in the reformer and pre-reformer in the "conventional" system. When oxygen is added to these systems, oxygen acts as an oxidator as well, reducing the steam requirements of the system. Steam is still required for reforming reactions and for the water-gas shift reaction. Herefore a system with oxy-fuel combustion with an SC ratio of 2.0 is analyzed. van Rossum et al. [42] found hydrocarbon free syngas at S/C ratio's as low as 2.2, without the addition of oxygen to the system. Since less steam is required for the reforming system, a high-temperature stream is left unused within the system (steam at 625 °C); this heat can be utilized in, for example, a steam turbine for electricity production while remaining heat can be used in, for example, a heat network, or for biomass drying. The utilization of remaining heat is outside the scope of this research.

Since steam also provides heat to the pre-reformer, additional heat (oxygen) is required in the system in order to keep the pre-reformer at a minimum of 600 °C and the reformer at a minimum of 750 °C, this will slightly decrease the hydrogen yield of the system. This alternative system is simulated, and stream results of streams 6a and 8a and 12c are displayed in table 8.4, the remaining streams displayed in the previous section stay unaltered.

The air ratio used in the reformer is 0.196, slightly higher compared to the previous system. This system's overall system efficiency is equal to 72.5 %, and the cold gas efficiency is equal to 37.1 %. The high temperature (625 °C) residual heat is, however, significant in this system: 12.6% compared to the thermal input. If, for example, 30% of this energy is converted into electricity in a steam turbine, this would result in an overall system efficiency of 76.3 % as well as a reduction in carbon footprint, since required electricity can now be produced on-side, with no additional emissions of greenhouse gases. The ratio between hydrogen produced from electrolysis: hydrogen produced by pyrogasification SEWGS in the proposed combined set up is 1000kg H_2 (electrolysis) :937kg H_2 (pyrogasification SEWGS).

Table 8.4: stream results sorption-shift system with oxy-fuel combustion, SC = 2

Stream nr.	12c	6a		8a	
Mass flow	430 kg/h	5282 kg/h		2187kg/h	
Temperature	358 °C	898 °C		550 °C	
Component	Mass flow	Mass flow	V% gas[DB]	Mass flow	V% gas[DB]
CO_2	0 kg/h	2484 kg/h	27.0 %	9 kg/h	0.18 %
CO	0 kg/h	837kg/h	19.8 %	2 kg/h	0.05 %
H_2	0 kg/h	162 kg/h	53.2 %	221 kg/h	99.63 %
CH_4	0 kg/h	0 kg/h	0.0%	0 kg/h	0.14 %
C_2H_4	0 kg/h	0 kg/h	0.0 %	0 kg/h	0.00 %
C_2H_6	0 kg/h	0 kg/h	0.0 %	0 kg/h	0.00 %
O_2	358 kg/h	0 kg/h	0.0 %	0 kg/h	0.00 %
H_2O	0 kg/h	2484 kg/h		1953 kg/h	

8.3 Cost analysis oxy-fuel system

A model is constructed for cost analysis of the oxy-fuel pyrogasification SEWGS system with SC=2, similar to the original system's model. Within this model, the capital investments and operational expenses are calculated as well as expected income. This section will discuss the results of the model. Results are obtained by the same method as discussed in chapter 6.

8.3.1 CAPEX

The CAPEX of the oxy-fuel system is calculated, and the system capital expenditure decreases significantly due to two main reasons:

1. Reactor size decrease: The volume flows in reactors are significantly decreased due to slower SC ratios and the use of pure oxygen instead of air
2. Size of HEX decrease: Due to oxygen addition, no heat exchangers are required in the reformer/pre-reformer. Furthermore, oxygen pre-heating requires just a fraction of heat compared to the original air-pre-heating.

The budget for the oxy-fuel system is displayed in table 8.5.

Table 8.5: Total CAPEX sorption-shift-system for the oxy-fuel based system

Cost item	Cost	factor
Total cost reactors	€1.476.000	-
Total cost HEX	€849.000	-
Total cost other process equipment	€928.000	-
Total equipment cost	€3.253.000	1
Equipment installation labour	€1.464.000	0.45
Instrumentation and controls	€293.000	0.09
Piping	€520.000	0.16
Electrical installations	€325.000	0.10
Buildings	€813.000	0.25
Yard improvements	€423.000	0.13
Service facilities	€1.301.000	0.40
Land	€195.000	0.06
Direct Plant Cost (DPC)	€8.588.000	2.64
Engineering and supervision	€1.073.000	0.33
Construction expenses	€1.269.000	0.39
Direct and Indirect Cost (DIC)	€10.930.000	3.36
Contractor's fee	€553.000	0.17
Contingency	€1.106.000	0.34
Additional contingency new technology (40%)	€5.042.000	1.55
Total Depreciable Ccost (TDC)	€17.630.000	3.87+1.55
Working capital	€2.212.000	0.68
Total Capital Investment (TCI)	€19.842.000	4.55+1.55

Compare to the original system, reactor costs are decreased by a factor of 1.97, and HEX costs are decreased by a factor of 3.59. It is important to note that the thermal input (biomass) of the system is also decreased. The CAPEX per MWth input is €1.64 mln. per MWth for the original system versus €0.85 mln. per MWth for the oxy-fuel system.

8.3.2 OPEX

The oxy-fuel system's operational expenses are also significantly different compared to the original system: reactor sizes are decreased; thus, less catalysts for the reformer is required, less (and smaller) equipment is used, so less maintenance is required, and biomass input is reduced. Table 8.6 displayed the annual operating expenditure of the analyzed oxy-fuel system. Compared to the original system OPEX is reduced by 18% compared to the original system, mainly due to lower maintenance and biomass cost.

Table 8.6: Total annual OPEX sorption-shift-system

Cost item	Annual Cost
Maintenance	€377.656
Labor	€1.568.000
Taxes + insurance	€142.943
General operating expenses	€733.405
Utilities	€320.059
Miscellaneous operating materials	€377.766
Biomass	€4.071.034
Catalyst	€601.213
Limestone	€215.376
Total OPEX	€8.067.450

Figure 8.3 displays the distribution of the OPEX.

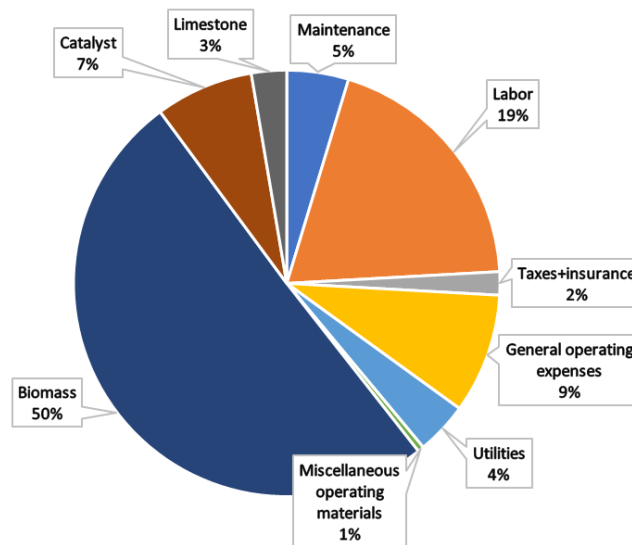


Figure 8.3: OPEX oxy-fuel system

8.3.3 Results and cash flow simulations

For the oxy-fuel system, there are three sources of income: biochar and hydrogen, comparable to the conventional system, but now also a pure stream of CO_2 suited for CO_2 capture. The products hourly produced by the system are displayed in table 8.7, including prices without subsidies and expected subsidies.

Table 8.7: Hourly production rate oxy-fuel system, including expected market prices and expected subsidies

Product	Hourly Production [kg/h]	Expected market price	Expected subsidies
Hydrogen	221	€1.50/kg	€5.83 per kg
Biochar	874	€250/ton	€345.8 per ton biochar
CO_2	4874	€25/ton CO_2	€105.8 per ton CO_2

Using cash flow simulation the combined break even prices for each of the products are calculated as:

- Hydrogen: €3.12/kg H_2
- Biochar: €520/ton biochar
- CO_2 : €52/ton CO_2

When no subsidies are given for biochar, the CO_2 break-even price of the produced hydrogen is: €4.42/kg H_2 . Assuming only the expected subsidies on hydrogen as given in table 8.7 results in the simulated cash flows as displayed in figure 8.4 resulting in a break-even point after 3.47 years in operation, resulting in an IRR of 26.1 %. When subsidies are also taken into account for biochar and CO_2 capture, the IRR increases to 47.2 %, and the break-even time is reduced to 21 months.

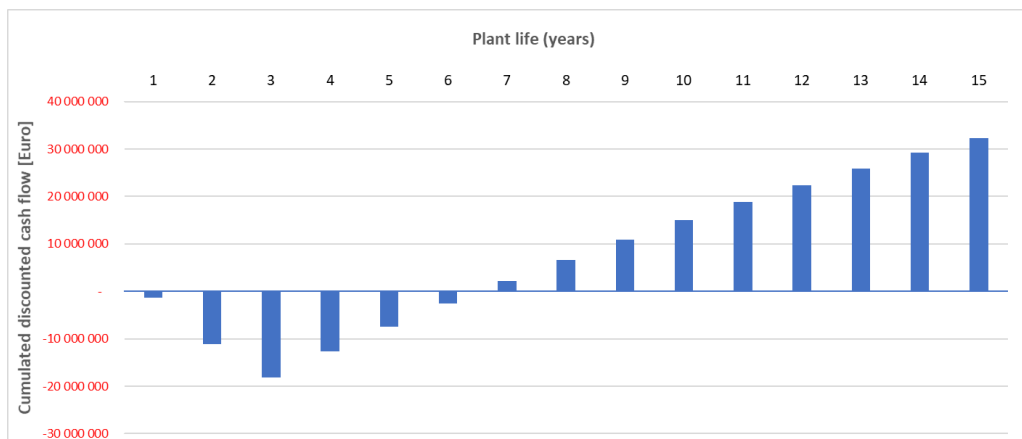


Figure 8.4: Cumulative cash flows oxy-fuel system when only subsidies are given for hydrogen production

Table 8.8 displays the comparison between the original system and the PGSS oxy-fuel system. Using oxy-fuel combustion results in a large increase in cost efficiency. Note that the assumptions made in this analysis are that oxygen is a "waste" product from electrolysis, which can be used without additional purchasing cost. Furthermore, CCS subsidies for CO_2 also require that the pure stream of CO_2 is stored, for example in old gas fields. This also brings additional costs.

Parameter	Air combustion	Oxy-fuel combustion
Hydrogen break even price	€4.01 /kg	€3.12 /kg
Biochar break even price	€668/ton	€520/ kg
CO ₂ break even price	-	€52 / ton
Payback period	8.0 years	4.8 years
Including construction		
IRR	18.7 %	47.2 %

Table 8.8: Financial results Air combustion versus oxy-fuel combustion

8.4 Carbon footprint oxy-fuel system

The carbon footprint of the oxy-fuel system is determined in a similar manner as for the previous system. The oxy-fuel system's carbon footprint with an SC ratio of 2.0 in the pre-reformer is used in this analysis since this is expected to be the most cost-effective system (reduced reactor size due to decreased steam flow rates). The main difference with respect to carbon footprint is the fact that a relatively pure stream of CO₂ is produced, which can be captured and stored (CCS), while the only option for the flue gases in the conventional system is greenhouse feeding, with a carbon capture efficiency of roughly 50 %.

The CO₂ footprint of the analyzed system is -1591 kg CO₂ per ton biomass, which increased significantly compared to the system which uses air combustion since, in this case, all CO₂ in flue gases can be captured. The CO₂ footprint compared to the two other analyzed systems: no greenhouse feeding with flue gases and with greenhouse feeding of flue gases is displayed in figure 5.6.

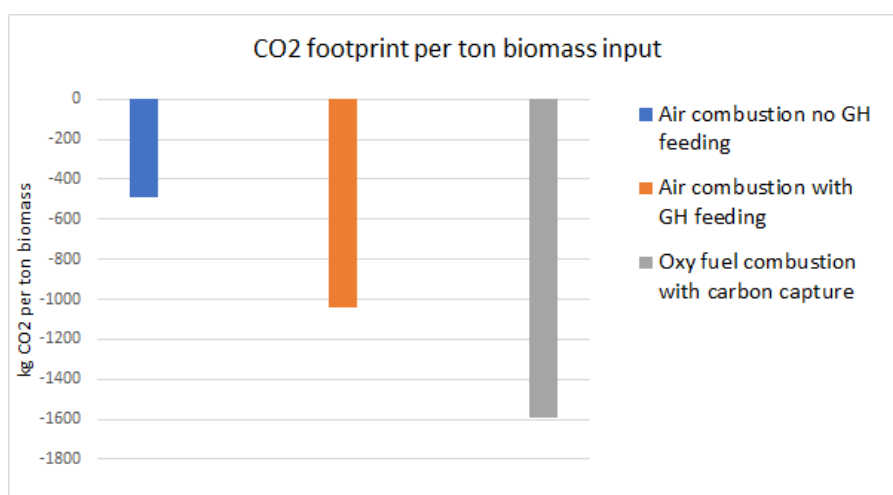


Figure 8.5: CO₂ footprint per ton of biomass input for air combustion systems with and without flue gas greenhouse feeding and oxy-fuel combustion system with carbon capture

8.5 Discussion

Using oxy-fuel combustion instead of air-combustion in the regenerator/calculator and oxygen addition to the reformer solves the identified heating issues for the reforming system. The proposed oxy-fuel system results in an improved process concerning cost efficiency and carbon footprint.

The designed system has an increased biochar/hydrogen product ratio since part of the hydrogen product is combusted in the reformer. Due to cost-efficiency reasons, it can be desired to combust part of the produced biochar in the reformer as heat supply since the market value of biochar in €/MJ is lower compared to the current market value of hydrogen: €0.0073/MJ for biochar (€250 / ton, HHV=34.2 MJ/kg) versus €0.0106/ MJ for hydrogen (€1.5/kg, HHV=142 MJ/kg). It is suggested to simulate a model where part of the produced biochar is fed to the reformer. For char reforming temperatures of >800 °C are desired; therefore, it is recommended for such a system the have reforming temperature in the 800-900 °C range since reforming reactions will still have an impact on the gasifier/reformer due to relative low ER.

The analyzed system still contains a pre-reformer and a reformer. For the oxy-fuel system (and for the original system as well), it can be investigated if only a reformer/gasifier is sufficient. Since the auger reactor enhances secondary cracking reactions, catalytic gasification/reforming in one reactor at temperatures of 750-900 °C can be sufficient to obtain hydrocarbon free syngas. The pre-reformer operates at 600 °C; which possibly brings issues related to coking on the catalyst, resulting in catalyst deactivation and increased cost. Using only one reformer/gasifier also reduces system cost and system complexity. Van Rossum et al. [42] used a dual reactor set up to produce a hydrocarbon free syngas, the first reactor (operated at ≈ 600 °C) was, however, mainly in place to evaporate pyrolysis oil and not for reforming reactions. Experimental research is required to identify possible coking issues in the pre-reformer system when placed post auger for processing the released volatiles of a slow pyrolysis process. Another option to solve the possible coking problems is to supply a fraction of oxygen to the pre-reformer to increase reactor temperature and solve coking issues. This method is only a good option when experimental research shows that using one gasifier with a relative low ER: $ER < 0.2$ and an SC of 2.0 cannot produce hydrocarbon free syngas.

The oxy-fuel system showed a large decrease in the payback period compared to the original system as well as a large increase of the IRR. The main reason for this is the significant decrease in CAPEX and a new revenue stream from the concentrated CO_2 suited for CCS. For CCS, the CO_2 also has to be transported and stored, for example in old gas fields. Transportation of CO_2 as well as storing has not been taken into account in the financial model. The financial model can be extended to also take these costs into account. Furthermore, it is assumed that oxygen is a by-product of electrolysis that can be used without additional cost. A sensitivity analysis is required to determine the influence of possible oxygen purchasing cost on the system feasibility.

The oxy-fuel system produced high-quality waste heat; due to the relatively low SC ratio, a surplus of high quality (625 °C) is produced: 12.6 % of the chemical energy system input (biomass) is released in the form of high-quality steam. This steam can be used for heating the auger reactor instead of using the hot CO_2 syngases. Such a system can then have an integrated form of thermal energy storage: regeneration can take place using electrical power when there is a surplus of solar and wind energy. During these moments, a surplus of $CaCO_3$ is regenerated to CaO using heat derived from electric power. The surplus of calcium oxide is stored (at elevated temperatures to increase system efficiency), providing thermal energy storage, similar in some extent to using salt hydrates for thermal energy storage. However, in this case, heat is released at significantly higher temperatures: 650 °C. When there is no surplus of solar and wind power, the stored CaO is used for the SEWGS system; the formed $CaCO_3$ is stored, waiting to be regenerated when there is an electricity surplus. Such a system will require two large isolated storage tanks, increasing system complexity, requires a larger regenerator capacity, and will have heat losses. Analysis of this modification of the oxy-fuel system can be a subject for further research. The big advantage of this system is that no biomass is required for regeneration, significantly increasing hydrogen/biochar yield per ton of biomass input. Furthermore, a pure stream of CO_2 is produced, without water vapor or a small fraction of oxygen.

8.6 Conclusion

The oxy-fuel powered pyrogasification SEWGS system shows superior results compared to the "conventional" system. The levelized cost of hydrogen decreased by 22.2%. The carbon footprint is 52.8 % more negative for the analyzed oxy-fuel system than the main system discussed in this research. Furthermore, heating problems are solved in the reformer and pre-reformer in this design. The system efficiency decreased slightly compared to the air-powered system: from 74.4 % to 73.4 % under the same process conditions. When the pyrogasification SEWGS system can be situated next to an electrolysis system for hydrogen production (with oxygen as a waste product) it is recommended to use this system. For a stand-alone system, additional oxygen purchasing costs have to be taken into account. For further research, it is recommended to work with this oxy-fuel based system. The designed models in chapters 3,4,6 and 7 showed that they could easily be adjusted to fit alternative system designs.

Chapter 9

Research proposal

This chapter will contain part of the research proposal constructed for further research of this project. The complete research proposal can be found in appendix O. Since a system introduction and simulation results have already been discussed in this thesis, they will not be repeated in this section. This section will focus on research up to date on pyrogasification SEWGS for high purity hydrogen production. Next, research goals, deliverables, required resources, and global planning for the research are discussed. Preliminary results have also been presented during the "Young professionals in Power Engineering" conference on 9-11 December from the Wroclaw University, Poland. A conference paper is written, which can be found in appendix P.

9.1 Research up to date in CaL based SEWGS

Producing high purity hydrogen from biomass feedstock using a calcium looping based SEWGS system has not been the subject of many studies up to date. Li et al. [57] published in October 2020 process simulation results of a CaL looping based SEWGS system combined with biomass gasification, of which results were very similar to the results discussed in chapter 4. Both CaL and SEWGS have been studied in the last 20 years, but a combination for high-quality hydrogen production using syngas from biomass gasification in a separate reactor has not been experimentally validated. To determine the system's technical and economic feasibility and to give proof of concept, further research of this proposed novel system is required. This section discusses the most relevant research up to date on SEWGS and CaL and discusses research subjects that have not been studied yet, which are required to better understand the system.

CaL looping has been the subject of many studies. In the last 20 years, CaL is mainly studied for two types of applications:

1. Sorption enhanced hydrogen production [22, 106]
2. Post-combustion carbon capture [107, 108]

In recent years research is focused on CaL systems for post-combustion carbon capture for coal and gas-fired power plants [107]. Due to relative high carbonation (500 °C - 700 °C) and calcination temperatures (800 °C - 900 °C) there is the possibility of high quality heat integration [107]. The downside of calcium-based sorbents is reduced sorbent multi-cycle activity, as has been described by many authors [108–110] and has been identified as the main bottleneck of CaL based CO_2 capture techniques. Due to the reduced surface area of CaO particles over multiple cycles, the particles' structure changes: micropores are replaced by macropores, which decreases effective surface area. Furthermore, the sintering of CaO particles also causes a reduction in effective surface area over multiple cycles. Multiple methods for sorbent multi cycle activity enhancement have been proposed: sorbent hydration, using calcined dolomite's ($MgCO_3$ - $CaCO_3$), using nano-sized particles, introducing mild calcination conditions (700 °C) and using tailored sorbents which incorporate CaO in an inert porous matrix (Al_2O_3 - 3, $CaTiO_3$) [22]. Out of cost considerations using calcined dolomite and sorbent hydration are the most promising techniques to increase sorbent durability for the proposed novel CaL SEWGS system. Especially since preliminary simulation results show steam generation potential for sorbent hydration without additional energy cost due to exothermic carbonation reactions.

SEWGS is a subject of some ongoing studies, but with the main focus on "low temperature" applications, which in many cases uses both a sorbent and catalyst to shift the WGS reaction [111, 112]. : Boon et al. [113] analyzed potassium-promoted hydrotalcite (K-HTC) as CO_2 sorbent in the 300-500 °C domain. 400 °C steam is used to regenerate the sorbent. Potassium promoted sorbents have been the subject of many recent studies up to date [111, 113, 114].

The big advantage of using K-HTC is durability: while CaO deactivates fast over multiple cycles, potassium promoted sorbents have demonstrated to operate stably in over 4,000 carbonation/calcination cycles. However, purchasing costs are significantly higher of the sorbent, and regeneration requires relatively low-temperature steam compared to CaL, which results in an energy/cost penalty when high-quality heat for pyrolysis/gasification is required. Current research's main focus is not on biomass processing but on the processing of gas from blast furnaces, and CCS in general [113].

Zivkovic et al. [112] designed kinetic models for CaO based SEWGS system. In this research, experimental results at a relatively low-temperature range (250 - 525 °C) were validated with the designed kinetic model. Due to the low carbonation temperatures, a catalyst was used (iron-chromium-based) in order for a sufficiently fast WGS reaction. Li et al. [115] showed that under high temperature operating conditions (500-700 °C), CaO has an enhancing effect on the WGS, acting as both a catalyst and sorbent. Further kinetics of CaO and (partly) deactivated CaO/CaCO₃ should be further investigated to obtain accurate dynamic models for CaL based SEWGS systems. Zivkovic et al. used a shrinking core model to model CO₂ absorption kinetics of CaO. A shrinking core model was proposed to cope with the increased diffusion residence of CO₂ through the formed CaCO₃ layer. A regression analysis was used to determine the kinetic parameters. This research shows a good framework for further fundamental research, where increased temperatures (with no catalyst) and sorbent deactivation and sorbent hydration on catalytic function is further analyzed and modeled.

9.2 Research goals

Additional understanding of the CaL SEWGS system is required, as described in the previous sections. Further fundamental research and proof of concepts are required. The insights gained by fundamental research can be implemented in the already designed model. The following research area's should be further investigated:

- **Fundamental:** Obtain a better understanding of the kinetics of the CaL SEWGS system, including multicyclic sorbent deactivation, sorbent hydration strategies, and alternative calcium-based sorbents.
- **Applied:** Provide proof of concept of the proposed pyrogasification sorption-shift system.
- **Applied:** Improve process simulations and use process simulations for further technology upscaling.

The proposed SEWGS system operates at relatively high temperatures (500-650 °C). Both limestone and calcined dolomite's kinetics can be further investigated for high-temperature SEWGS due to the wide availability and low cost of these materials. Fundamental research is required to analyze the effect of sorbent deactivation and sorbent hydration on WGS kinetics. Furthermore, experiments should be used to design a dynamic model for CaL based SEWGS systems for CaO/calcined dolomites, including sorbent hydration as a possible reactivation step. After constructing this kinetic model, a proof of concept should be given for a pyrogasification SEWGS system on a lab-scale. Prove of concept of heat integration should also be given for the SEWGS reactor. Finally, the already designed simulations should be revisited and fitted to newly found (experimental) data to more correctly simulate the total process and give a more accurate estimation of the system cost.

More concrete research goals of the proposed research are listed below:

1. Construct a kinetic model of CaO and calcined dolomite's to predict CO₂ absorption and WGS reaction kinetics based on TGA test results of sorbents to determine kinetic parameters based on a regression analysis
2. Design and build a fluidized bed based SEWGS reactor, validate kinetic models for CaL based SEWGS
3. Test and optimize different sorbents concerning durability: test different hydration strategies for CaO and calcined dolomite's.
4. Expand kinetic model to also account for sorbent deactivation
5. Provide proof of concept of continuous operating SEWGS system
6. Gain insight in heat transport in a SEWGS reactor due to exothermic carbonation and WGS
7. Design operating conditions and dimensions for a continuous operating SEWGS reactor, based on heat/mass transport requirements as well as sorbent kinetics
8. Use results to simulate the SEWGS in more detail in Aspen Plus by incorporating the newly found kinetic models.

If this research yields positive results, the system can be tested and build as a semi industrial scale installation to upgrade flue gasses and provide carbon capture. This is, however, outside the scope of the proposed research.

9.3 Deliverables

The proposed research has the following deliverables:

1. Improved kinetic model for a CaL SEWGS system, taken into account sorbent deactivation to accurately predict cycling operating conditions
2. Proof of concept for continuous, high-quality hydrogen production using a CaL based SEWGS reactor
3. Improved process simulations incorporated with kinetic models
4. Advise and suggestions for technology upscaling possibilities to a (semi) industrial scale

9.4 Required resources

The research described in this report consists of experimental research on two different test setups. The first set of experiments should be performed using a TGA to analyze a SEWGS system's kinetics. A TGA system is already present at the University of Twente. The second set of experiments should be performed in a lab-scale fluidized bed. A lab-scale bed is already present at the University of Twente, but this test set up is used intensively for other research. A proposed test set up for experimental research is displayed in figure 9.1.

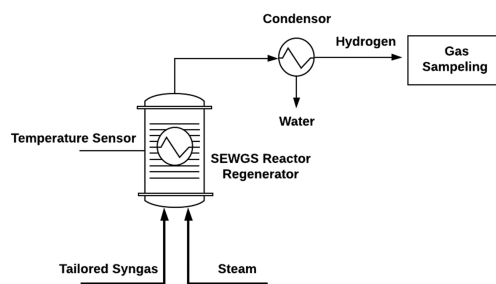


Figure 9.1: Test set up for fluidized bed SEWGS reactor

Concerning required materials, it is recommended that a new (lab scale) fluidized bed, including a heater for the bed, is purchased. Furthermore, sample gases (tailored syngases) are required as well as different sorbent materials. The most important resource which is required for this research are human resources. The proposed research is well suited for a PhD project of 4 years. An associate professor needs to supervise the PhD candidate, and lab assistance is also required. It is estimated that the project required 1.5 FTE per year at €80.000 per FTE/year. The main required resources, with estimated cost, are displayed in table 9.1.

Table 9.1: Total CAPEX sorption-shift-system for the oxy-fuel based system

Resource	estimated Cost
Human resources	€480.000
New equipment purchasing	€100.000-€200.000
Material (sorbents/syngas)	€50.000-€100.000
Depreciation equipment	€50.000-€100.000
Total Estimated cost	€680.000-€880.000

9.5 Planning

It is recommended for the proposed research to make it a PhD project, corresponding with a duration of 4 years. A preliminary planning for this research is shown in figure 9.2.

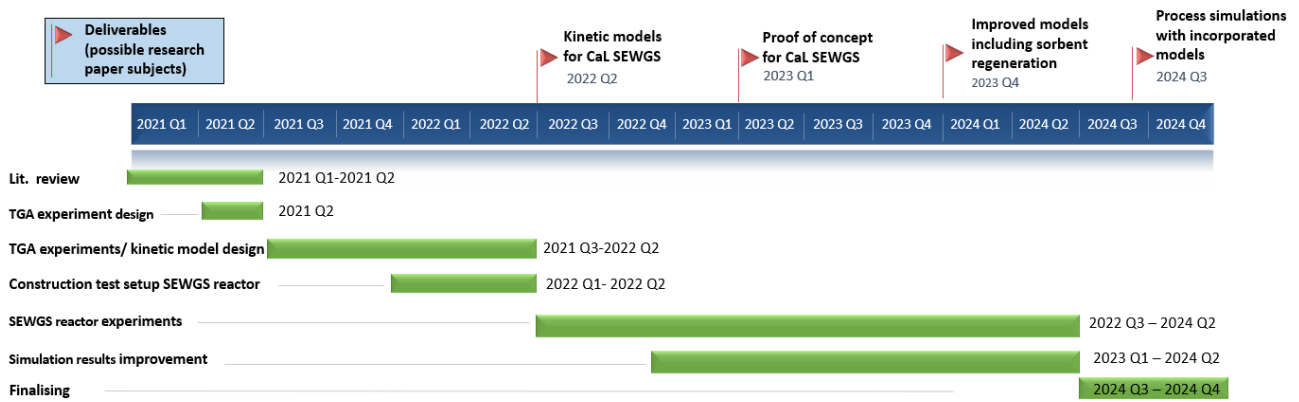


Figure 9.2: Planning

Chapter 10

Discussion

A novel system producing high-quality biochar and high purity hydrogen out of biomass has been developed. The proposed system is a combination of pyrolysis, reforming, and calcium looping based SEWGS. The results discussed in this thesis show promising results and show a technical, economic, and societal feasible system. Before the designed system can be implemented, further research is required, as discussed in section 9. This section critically reviews the work presented in this thesis and discusses possible ways to improve the presented work and additional research directions for further research.

10.1 Pyrolysis system

For the process simulations, the results of the auger reactor (pyrolysis) and pre-reformer were based on experimental research. Experimentally found product yields have been simulated in "RYield" reactors in Aspen Plus; by doing, so insight is obtained concerning the reactors' heat demand without the construction of complicated kinetic models for slow pyrolysis. For the auger reactor, a product yield distribution was hard to find, especially data that described both char, gas, and oil yield accompanied with a detailed analysis of the composition of both oil, gas, and char, respectively. Finally, research was found and implemented by Phan et al. [27]. This research was, however, performed using a batch reactor, operating at 500 °C, while research has shown (discussed in section 2.1) that ideal operating conditions for the production of high-quality biochar are > 600 °C. Because of the long residence times use by Phan et al. (60 minutes) high-quality biochar was obtained in this study. For further analysis, it would be desired to use experimental data of pyrolysis in an auger reactor operating at the desired operating conditions to produce high-quality biochar and release a large volatile fraction as explained in section 2.1. These operating conditions are in the range of $T > 600^{\circ}\text{C}$, residence time 5-10 minutes, medium heating rates in the range of 1-10K/second. Data is required, which describes both the gas, char, and oil product of slow pyrolysis in detail, including a proximate and ultimate analysis of biochar and composition of oils and gases. Such accurate output data of slow pyrolysis products from an auger reactor are not yet published, and therefore experimental research would be required, which can be used as input for the designed model. Furthermore, this data can be used to construct kinetic models for pyrolysis in auger reactors, which is different from pyrolysis in bed reactors due to other different heating mechanics and increased residence time (enhanced secondary cracking) of released volatiles in the auger reactor.

Pyrolysis is simulated in Aspen plus to obtain insight in heat requirements of this sub-system. However, the simulation results show that more heat is released during pyrolysis than is supplied (based on energy balances). Since pyrolysis is an endothermic process, this is not expected. The assumed bio-oil composition could cause this error in the reactor's energy balance. Although the research by Phan et al. [27] gives a good insight into the produced oil (heavy oil fraction, aquatic fraction, ultimate analysis), the exact composition is not given. For simulation purposes, it is assumed the 50% of the produced oil is water (corresponding to the large aquatic fraction), and the remaining parts are either phenol (C_6H_6O) and levoglucosan ($C_6H_{10}O_5$), in order to close elemental balances a small fraction of char is also added to the produced oil in the simulations.

It is expected that the produced oil will contain less water and more hydrocarbons. Due to elemental and mass balances implemented in Aspen Plus, this cannot be changed easily in the simulations. Since the reformer is modeled on thermodynamic equilibrium, the pyrogasification system's total energy requirement does not change. It is only expected that more heat is required for pyrolysis (relative low-temperature reactor) and that less heat is required for gasification (relative high-temperature reactor). Therefore it is not expected that this error has a large influence on the results; if it influences at all, it would slightly increase the system efficiency since less high-temperature heat is required for reforming while this amount of heat is moved to the pyrolysis process, which operates at lower temperatures. This unexpected energy balance coming from the process simulations is another reason for further research of pyrolysis products of pyrolysis in an auger reactor, as discussed in the previous paragraph.

Upscaling limitations of auger reactors is identified as one of the main disadvantages of an auger reactor since this brings problems with respect to reactor heating. The designed system desirably operates at auger temperatures of approximately 600°C to produce high-quality biochar. An auger can be internally heated (using heating oil in the screw) or externally heated by heating the "shell" of the auger by, for example, hot flue gases. Another option is to add a hot material (for example, hot sand at 900 °C) together with biomass to the auger; this will, however, dilute the biochar product and is thus not desirable. Conventional heating oils can be heated to a maximum of 350-400 °C, and therefore for the designed system, external heating is the most feasible solution, but it is expected that this brings heating problems when upscaling due to the decreased surface area/volume ratio's. A solution for this heating problems can be to add two pyrolysis reactors in series, a reactor operating at 350 °C, which is both internally and externally heated, followed by an auger reactor which is externally heated to 600 °C. Moisture will evaporate in the first reactor, combined with biomass heating to 350°C. It is expected that this low-temperature reactor has a higher heat demand compared to the high-temperature auger. An additional option for this configuration can be to place a grinder between the first and second auger; the produced char in the first pyrolysis reactor (or carbonation reactor) is brittle, which makes grinding energy inexpensive. Grinding of char increases the surface area of produced biochar, enhancing pyrolysis reactions and increasing both the amount of released volatiles in the second auger reactor as well as the biochar product quality. Placing a grinder between the first and second auger also makes it possible to feed relatively large particles to the first auger. Such a "dual-auger" placed in series has not been a subject of research up to date and can be further investigated since a dual-auger configuration can provide a solution when upscaling.

10.2 Reforming system

Two reformers are used in the reforming system, a pre-reformer (600 °C) and a reformer (750 °C) in a similar fashion to Methane Steam Reforming (MSR). The reason why a two-stage system is selected is because of 1. Energy efficiency and 2. system robustness. For the low-temperature reformer, coking (deactivation of catalyst) can become a significant problem. The severity of coking related problems in the designed model is, however, not known. Due to relative long residence times in the auger reactor and enhanced secondary cracking reactions in the auger, it is expected that the heavy oil fraction (tars) in produced pyrolysis oil is relatively low, resulting in a low char and ash content in the released volatiles and thus less coking related problems. If coking becomes a problem, an option can be to only introduce a reformer at 750-800 °C. Another option can be to use calcined dolomite's as sorbent in the Sorption shift system and give a double function to these calcined dolomite's: use spend sorbent from the SEWGS system to the reformer system as a catalyst. Since dolomite's also have good tar cracking abilities (have a catalytic function), they can be used in the reformer system. Calcined dolomites are cheap compared to Ni-based catalysts. A continuous and relative large sorbent make-up is required for the SEWGS system, meaning that in this configuration, catalyst in the reformer system can continuously be replaced with fresh catalyst. Experimental research is required to determine the degree of coking on Ni-based catalyst when a catalytic bed is placed after an auger reactor for slow pyrolysis. When coking becomes a significant issue, this results in increased catalyst cost (and thus increased OPEX) as described in section 6.6.2. However, solutions can be implemented as described in this paragraph to deal with potential coking issues. The addition of a small fraction of oxygen (the oxy-fuel system) to the pre-reformer can also help to cope with coking and solves heating problems that have been identified in the system sensitivity analysis.

10.3 Sorption enhanced gasification system

As discussed in section 9 there are still many unknowns concerning the designed SEWGS system. In the designed process simulations, the system has been analyzed at thermodynamic equilibrium. Two shift reactors are used, a high-temperature shift reactor to capture the bulk of CO_2 at 650 °C, at these relatively high temperatures, the catalytic effect of CaO on the WGS (shifting CO to CO_2) should lead to thermodynamic equilibrium. It is assumed that at the low-temperature shift (LTS), thermodynamic equilibrium is also approached; how close actual product yield is to thermodynamic equilibrium is unknown; therefore, the catalytic effect of CaO on the WGS should be better understood. If product yield lies far away from thermodynamic equilibrium, a solution can be to add another catalyst to the sorbent or to add an additional catalytic bed of iron oxide (a conventional WGS enhancing catalyst) between the HTS and LTS for sufficiently fast WGS.

Multi-cyclic deactivation of calcium-based sorbents is one of the main disadvantages of calcium looping based systems for CO_2 capture. Because of multi-cyclic deactivation: 1. a surplus of CaO has to be cycled through the system because of decreased sorbent activity, and 2. a continuous sorbent make-up is required. In appendix E a model is discussed which calculates the required sorbent make-up and the amount of cycled CaO/ $CaCO_3$ through the system. Within the simulations, a sorbent surplus of $\approx 40\%$ has been assumed to compensate for sorbent deactivation. A sensitivity analysis using the designed Aspen Plus model combined with the designed sorbent replacement model can be used to determine the effect of the CaO replacement strategy on system efficiency, which would provide a better understanding of the effect of multi-cyclic deactivation and replacement strategy on the overall system performance.

The energetic system analysis shows two significant heat losses in the system. The first heat loss is due to the steam hydrogen mixture leaving the system at 169 °C, which contains 16.9 % of sensible and latent heat compared to the chemical energy input. The second heat loss is in the flue gases leaving the system at 153 °C, which also contain water vapor. The flue gases contain 8.1% of sensible and latent heat compared to the chemical energy input. Since both streams are mixtures of water vapor and other gases, water condenses at temperatures below $< 100^\circ\text{C}$, and this heat cannot be used in, for example, steam generation. This low-quality heat can be utilized in, for example, biomass drying process or for residential heating applications. If an SC ratio < 4.6 is used, there is a surplus of high-quality heat (steam at 625 °C) available. This steam can be used in, for example, power generation, such system configurations have potential when there is a significant amount of high-quality heat available and can be a subject for further research. The remaining high-quality steam can also be used to activate biochar to produce activated carbon or be used for sorbent hydration, which increases the lifetime of the calcium-based sorbent.

10.4 Socio-economic analysis

Cost optimization has been performed with respect to heat exchanger size and minimum pinch points in heat exchangers. Cost optimization with respect to reactor size has not been performed. The alternative design based on an oxy-fuel system shows that when lower C/S ratios are used, the volume flows in bed reactors reduces significantly, reducing reactor sizing and overall CAPEX. A lower S/C ratio is used in the oxy-fuel system; in this system, a small fraction of oxygen is added to the reformer; therefore, less steam (also an oxidant) is required. For the main system, it is questionable if the S/C (4.58) can be reduced significantly without a reduction in gas quality. Research by van Rossum et al. [42] showed, however, that it was possible at S/C ratios of 2.2 and 2.7 to produce hydrocarbon free syngas (at a slightly higher temperature, however, in the 800 °C range). A sensitivity analysis with respect to the S/C ratio can be performed to further optimize the analyzed system's levelized cost of hydrogen. A lower S/C ratio, combined with a higher reformer temperature, can be more cost-effective; these mechanics can be further analyzed with respect to cost optimization.

The cost analysis results showed that most expenses are related to the OPEX (73.4 %). Within the OPEX, biomass purchasing cost is the largest contributor (47%), followed by labor cost (17%). The break-even prices for the analyzed pyrogasification SEWGS system concerning hydrogen and biochar are optimized at 4.01 €/kg and 668 €/ton, respectively. An alternative design that uses oxy-fuel combustion in the regenerator/reformer showed a significant improvement with respect to hydrogen and biochar production costs. For this alternative system, hydrogen production costs were €3.12/kg, and biochar production costs were calculated at €520 per kg, showing the potential for this alternative system configuration. The main drivers of these reduced costs are less complex heating systems, reactor size decrease (decreased volume flows), reduced maintenance cost, and reduced catalyst cost (due to reduced reactor size). For the oxy-fuel system, 77.5% of the cost is related to the OPEX and 22.5 % to CAPEX. It is recommended for further research to use this alternative design.

The cost of auger reactors are not yet widely known. Therefore assumptions have been made in the cost determination, which is one of the reasons why a 40% contingency is used in the cost estimations due to this large unknown. Further research concerning cost determination and industrial applications of auger reactors is required.

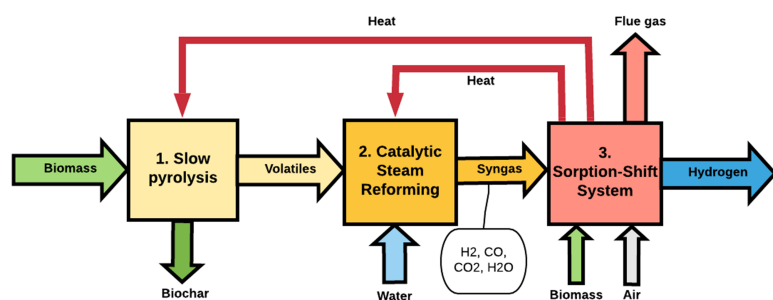
An analysis with respect to CO_2 footprint has been performed, at which a model is developed which determined the system footprint under operation. In order to get a better understanding of the CO_2 footprint of the system a complete life cycle analysis (a "cradle to grave" analysis) should be performed, this can be done in life cycle assessment software, in which unconventional actions (logging, wood chipping) can be added/modified based on the already calculated CO_2 footprint.

Chapter 11

Conclusion and recommendations

11.1 Conclusion

A pyrogasification sorption-shift system for the production of high purity hydrogen and high-quality biochar out of biomass has been analyzed and modeled in Aspen Plus. The analyzed system uses an auger reactor for pyrolysis for the production of high-quality biochar. A two-stage reforming system produces hydrocarbon free syngas. Finally, a Sorption Enhanced Water Gas Shift (SEWGS) system is designed and modeled based on calcium looping to produce high purity hydrogen and for pre-combustion carbon capture. Heat integration is modeled, which shows a large potential for implementing high-temperature waste heat from the SEWGS system, consisting of two SEWGS reactors operated in series. Sorption-Shift reactors have a double function in the designed system: increase hydrogen purity (hydrogen upgrading) and act as a steam generator providing steam for the reforming processes. Simulation results are validated with the literature. Optimization with respect to energy efficiency shows an overall system energy efficiency up to 74,9%, the recommended system configuration with respect to SEWGS reactor temperature (650 °C and 550 °C respectively) yields a system efficiency of 74,4 %. The overall system efficiency is comparable to conventional biomass gasification systems. Higher quality products are obtained with much more versatile high-end applications. Sensitivity analyses identified reactor heating and air pre-heating as system bottlenecks. Figure 11.1 displays the general process configuration which is analysed in this research, and table 11.1 displays the most important data obtained from the process simulations performed in Aspen Plus.



System parameter	Value
Hydrogen production per ton biomass (daf)	59 kg/ton
Biochar production per ton biomass (daf)	186 kg/ton
Hydrogen purity	99.7 %
Biochar HHV	34.2 MJ/kg
Efficiency	74.4 %

Figure 11.1: System configuration pyrogasification SEWGS system

Table 11.1: Main simulation results

A financial model is designed for cash flow simulations of the designed pyrogasification SEWGS system. This model is used to optimize hydrogen and biochar production costs based on simulation results from the Aspen Plus simulations. In order to do so, the system is analyzed in more detail to determine the capital expenditure using factorial techniques. The financial model is constructed after consulting an industrial partner. Cash flows (CAPEX and OPEX) are simulated in the designed dynamic model. The financial model shows that hydrogen and biochar costs can be reduced significantly by heat exchanger size optimization. The optimized system based on cost shows the production cost of high purity hydrogen of €4.01 per kg combined with a biochar production cost of €668 per ton. This system configuration has a slightly lower efficiency (71.4%) than the maximum efficiency, mainly due to decreased heat exchanger surface area. Table 11.2 contains the main results from the financial analysis performed on the designed pyrogasification SEWGS system.

Table 11.2: Main results cost analysis

System parameter	Value
Hydrogen production cost	€4.01 /kg
Biochar production cost	€688 /ton
System efficiency after cost optimisation	71.4 %
System initial rate of return (including expected subsidies)	18.7 %
System payback time (including expected subsidies)	5.0 years
Fraction OPEX of total cost	73.4 %
Fraction CAPEX of total cost	26.6 %

The societal analysis shows that there is a shift towards high quality "bio-based raw materials" like hydrogen and biochar in bioenergy policies from Western European countries. In Europe, there is a large untouched potential for both high-quality biomass (pellets) and lower types of biomass (forest residues, municipal waste). In the Netherlands, there is mainly untouched potential for low-quality biomass: chips and shreds derived from forest residues and municipal waste. The CO_2 footprint of the analyzed system shows a negative CO_2 footprint of maximal -1041 kg CO_2 per ton biomass input: the system has the potential to reverse global warming when biomass is harvested sustainably.

Multiple models are designed in this research: Aspen Plus models with accompanied data processing models in Excel and Matlab and models for cash flow simulations and carbon footprints. These dynamic models can be altered easily when future model adjustments are considered. Furthermore, these models can be altered easily to fit other research on biomass processing.

This research showed, based on process simulations, that a pyrogasification sorption enhanced water gas shift system can be a technical, economic, and societal feasible technology. The pyrogasification SEWGS system can deliver high-quality biochar and high purity hydrogen out of biomass: sustainable products that fit within the needs of the future sustainable economy.

11.2 Recommendations

Further research is required for the analyzed system. It is proposed that further research is performed concerning an oxy-fuel powered system. Simulations on an oxy-fuel based system show promising results with respect to hydrogen and biochar leveled cost of production and carbon footprint. Furthermore, auger reactor mechanics for slow pyrolysis should be better understood. Fundamental research is required with respect to the SEWGS reactor and kinetics in CaL based SEWGS system. For further research, a research proposal is written for a (European) research project, which is discussed in this Master Thesis in chapter 9. The new insights found by this fundamental research can be used to model the process more accurately, using the already designed models in this research as a basis. Further research is required to increase the technology readiness level of auger reactors for slow pyrolysis and the CaL based SEWGS system. Furthermore, several model improvements can be considered, as discussed in this thesis. Recommendations for further research are listed below, where the recommendations are grouped in recommendations for fundamental research, simulation improvement, system improvement, and technology upscaling.

Fundamental research

- Determine sorbent kinetics of CaO on the WGS reaction in a SEWGS reactor
- Determine the influence of sorbent deactivation on sorbent kinetics
- Obtain insight in heat and mass transfer in CaL based SEWGS reactors
- Determine yield (gases, char, and oil accompanied with proximate and ultimate analysis) of auger reactors for slow pyrolysis of different biomass species, including low quality biomass

Simulation improvements

- Implement sorbent kinetics in the SEWGS reactor in the process simulations
- In the process simulations, implement experimentally found yield from slow pyrolysis in an auger reactor
- Simulate sorbent replacement strategies

System improvements

- Expand the model with (waste) steam utilization: use steam for sorbent reactivation (hydration) and/or steam activation of biochar for activated carbon production
- Analyse a system with only one reformer/SEWGS reactor
- Analyse and model the possibilities for thermal heat storage implemented in the oxy-fuel based system

Upscaling

- Analyse and model the option of using two auger reactors in series: a low-temperature auger and a high-temperature auger, to solve part of the heating issues accompanied with auger reactor upscaling

Bibliography

- [1] Our World in Data. Our world in data - energy, 2019. URL <https://ourworldindata.org/energy>.
- [2] Enerdata. Global energy statistical yearbook 2019, 2019. URL <https://yearbook.enerdata.net/total-energy/world-consumption-statistics.html>.
- [3] Our World in Data. Our world in data - co2 and greenhouse gas emissions, 2019. URL <https://ourworldindata.org/co2-and-other-greenhouse-gas-emissions>.
- [4] EIA. Today in energy - eia projects 28% increase in world energy use by 2040, 2017. URL <https://www.eia.gov/todayinenergy/detail.php?id=32912>.
- [5] unfccc. Paris agreement - status of ratification, 2020. URL <https://unfccc.int/process/the-paris-agreement/status-of-ratification>.
- [6] Our World in Data. Renewable energy - global renewable energy consumption, 2019. URL <https://ourworldindata.org/renewable-energy>.
- [7] William F Pickard and Derek Abbott. Addressing the intermittency challenge: Massive energy storage in a sustainable future. *Proceedings of the IEEE*, 100(2):317, 2012.
- [8] Sean B Walker, Ushnik Mukherjee, Michael Fowler, and Ali Elkamel. Benchmarking and selection of power-to-gas utilizing electrolytic hydrogen as an energy storage alternative. *International Journal of Hydrogen Energy*, 41(19):7717–7731, 2016.
- [9] Marc A Rosen and Seama Koochi-Fayegh. The prospects for hydrogen as an energy carrier: an overview of hydrogen energy and hydrogen energy systems. *Energy, Ecology and Environment*, 1(1):10–29, 2016.
- [10] Havva Balat and Elif Kirtay. Hydrogen from biomass—present scenario and future prospects. *International Journal of Hydrogen Energy*, 35(14):7416–7426, 2010.
- [11] IEA. The future of hydrogen, 2019. URL <https://www.iea.org/reports/the-future-of-hydrogen>.
- [12] IRENA. Hydrogen from renewable power: technology outlook for the energy transition, 2018.
- [13] Nicholas H Florin and Andrew T Harris. Enhanced hydrogen production from biomass with in situ carbon dioxide capture using calcium oxide sorbents. *Chemical Engineering Science*, 63(2):287–316, 2008.
- [14] Yildiz Kalinci, Arif Hepbasli, and Ibrahim Dincer. Biomass-based hydrogen production: a review and analysis. *International journal of hydrogen energy*, 34(21):8799–8817, 2009.
- [15] MA Quader and S Ahmed. Bioenergy with carbon capture and storage (beccs): future prospects of carbon-negative technologies. In *Clean Energy for Sustainable Development*, pages 91–140. Elsevier, 2017.
- [16] André Brosowski, Daniela Thrän, Udo Mantau, Bernd Mahro, Georgia Erdmann, Philipp Adler, Walter Stinner, Gerd Reinhold, Thomas Hering, and Christian Blanke. A review of biomass potential and current utilisation—status quo for 93 biogenic wastes and residues in germany. *Biomass and Bioenergy*, 95:257–272, 2016.
- [17] RC Saxena, Diptendu Seal, Satinder Kumar, and HB Goyal. Thermo-chemical routes for hydrogen rich gas from biomass: a review. *Renewable and Sustainable Energy Reviews*, 12(7):1909–1927, 2008.
- [18] Marliati Ahmad and Handoko Subawi. New van krevelen diagram and its correlation with the heating value of biomass. *Journal of Agriculture and Environmental Management*, 2(10):295–301, 2013.
- [19] European Biomass Industry Association. Biomass characteristics, 2020. URL <https://www.eubia.org/cms/wiki-biomass/biomass-characteristics-2/>.

- [20] Bioenergy Europe. Bioenergy carbon capture and storage, 2019. URL <https://bioenergyeurope.org/article/206-bioenergy-explained-bioenergy-carbon-capture-and-storage-beccs.html>.
- [21] Nicholas H Florin and Andrew T Harris. Hydrogen production from biomass coupled with carbon dioxide capture: the implications of thermodynamic equilibrium. *International Journal of Hydrogen Energy*, 32(17):4119–4134, 2007.
- [22] Nicholas H Florin and Andrew T Harris. Enhanced hydrogen production from biomass with in situ carbon dioxide capture using calcium oxide sorbents. *Chemical Engineering Science*, 63(2):287–316, 2008.
- [23] Manoj Tripathi, Jaya Narayan Sahu, and P Ganesan. Effect of process parameters on production of biochar from biomass waste through pyrolysis: A review. *Renewable and Sustainable Energy Reviews*, 55:467–481, 2016.
- [24] E. Bramer. Pyrolysis of biomass - 3tu energy from biomass. University Lecture, 2017.
- [25] D Vamvuka. Bio-oil, solid and gaseous biofuels from biomass pyrolysis processes—an overview. *International journal of energy research*, 35(10):835–862, 2011.
- [26] Li Li, Jack S Rowbotham, Christopher H Greenwell, and Philip W Dyer. *An introduction to pyrolysis and catalytic pyrolysis: versatile techniques for biomass conversion*. Elsevier, 2013.
- [27] Anh N Phan, Changkook Ryu, Vida N Sharifi, and Jim Swithenbank. Characterisation of slow pyrolysis products from segregated wastes for energy production. *Journal of Analytical and Applied Pyrolysis*, 81(1):65–71, 2008.
- [28] Ozlem Onay and O Mete Kockar. Slow, fast and flash pyrolysis of rapeseed. *Renewable energy*, 28(15):2417–2433, 2003.
- [29] Paul T Williams and Serpil Besler. The influence of temperature and heating rate on the slow pyrolysis of biomass. *Renewable energy*, 7(3):233–250, 1996.
- [30] Ayhan Demirbas. Determination of calorific values of bio-chars and pyro-oils from pyrolysis of beech trunk-barks. *Journal of analytical and applied pyrolysis*, 72(2):215–219, 2004.
- [31] Felipe Campuzano, Robert C Brown, and Juan Daniel Martínez. Auger reactors for pyrolysis of biomass and wastes. *Renewable and Sustainable Energy Reviews*, 102:372–409, 2019.
- [32] A Abuadala, I Dincer, and GF Naterer. Exergy analysis of hydrogen production from biomass gasification. *International Journal of Hydrogen Energy*, 35(10):4981–4990, 2010.
- [33] Samsudin Anis and ZA Zainal. Tar reduction in biomass producer gas via mechanical, catalytic and thermal methods: A review. *Renewable and sustainable energy reviews*, 15(5):2355–2377, 2011.
- [34] Md Waliul Islam. A review of dolomite catalyst for biomass gasification tar removal. *Fuel*, 267:117095, 2020.
- [35] Madhukar R Mahishi and DY Goswami. An experimental study of hydrogen production by gasification of biomass in the presence of a co2 sorbent. *International Journal of Hydrogen Energy*, 32(14):2803–2808, 2007.
- [36] Christoph Pfeifer, Bernhard Puchner, and Hermann Hofbauer. In-situ co2-absorption in a dual fluidized bed biomass steam gasifier to produce a hydrogen rich syngas. *International Journal of Chemical Reactor Engineering*, 5(1), 2007.
- [37] Yohan Richardson, Joël Blin, and Anne Julbe. A short overview on purification and conditioning of syngas produced by biomass gasification: catalytic strategies, process intensification and new concepts. *Progress in Energy and Combustion Science*, 38(6):765–781, 2012.
- [38] Madhukar R Mahishi and DY Goswami. Thermodynamic optimization of biomass gasifier for hydrogen production. *International Journal of Hydrogen Energy*, 32(16):3831–3840, 2007.
- [39] Toshiaki Hanaoka, Takahiro Yoshida, Shinji Fujimoto, Kenji Kamei, Michiaki Harada, Yoshizo Suzuki, Hiroyuki Hatano, Shin-ya Yokoyama, and Tomoaki Minowa. Hydrogen production from woody biomass by steam gasification using a co2 sorbent. *Biomass and Bioenergy*, 28(1):63–68, 2005.
- [40] J Solar, I De Marco, BM Caballero, A Lopez-Urionabarrenechea, N Rodriguez, I Agirre, and A Adrados. Influence of temperature and residence time in the pyrolysis of woody biomass waste in a continuous screw reactor. *Biomass and Bioenergy*, 95:416–423, 2016.

- [41] Pengmei Lv, Zhenhong Yuan, Chuangzhi Wu, Longlong Ma, Yong Chen, and Noritatsu Tsubaki. Bio-syngas production from biomass catalytic gasification. *Energy Conversion and Management*, 48(4):1132–1139, 2007.
- [42] G. van Rossum. *Steam reforming and gasification of pyrolysis oil : Reactor and process development for syngas production from biomass*. PhD thesis, University of Twente, Netherlands, 10 2009.
- [43] JM Valverde, PE Sanchez-Jimenez, and Luis A Pérez-Maqueda. Limestone calcination nearby equilibrium: kinetics, cao crystal structure, sintering and reactivity. *The Journal of Physical Chemistry C*, 119(4):1623–1641, 2015.
- [44] EH Baker. 87. the calcium oxide–carbon dioxide system in the pressure range 1–300 atmospheres. *Journal of the Chemical Society (Resumed)*, pages 464–470, 1962.
- [45] JC Abanades. Calcium looping for co2 capture in combustion systems. In *Fluidized bed technologies for near-zero emission combustion and gasification*, pages 931–970. Elsevier, 2013.
- [46] Octave Levenspiel. Chemical reaction engineering. *Industrial & engineering chemistry research*, 38(11):4140–4143, 1999.
- [47] Anthonia E Eseyin, Philip H Steele, and Charles U Pittman Jr. Current trends in the production and applications of torrefied wood/biomass—a review. *Bioresources*, 10(4):8812–8858, 2015.
- [48] Chidi E Efika, Chunfei Wu, and Paul T Williams. Syngas production from pyrolysis–catalytic steam reforming of waste biomass in a continuous screw kiln reactor. *Journal of Analytical and Applied Pyrolysis*, 95:87–94, 2012.
- [49] Kristin Onarheim, Yrjo Solantausta, and Jani Lehto. Process simulation development of fast pyrolysis of wood using aspen plus. *Energy & Fuels*, 29(1):205–217, 2015.
- [50] ECN Phyllis. Ecn phyllis classification. *Forest residue chips, pine spruce*, 3156, 2013.
- [51] Siddhartha Gaur and Thomas B Reed. An atlas of thermal data for biomass and other fuels. Technical report, National Renewable Energy Lab., Golden, CO (United States), 1995.
- [52] Bosong Li, Wei Lv, Qi Zhang, Tiejun Wang, and Longlong Ma. Pyrolysis and catalytic upgrading of pine wood in a combination of auger reactor and fixed bed. *Fuel*, 129:61–67, 2014.
- [53] AV Bridgwater, P Carson, and M Coulson. A comparison of fast and slow pyrolysis liquids from mallee. *International journal of global energy issues*, 27(2):204–216, 2007.
- [54] Qi Zhang, Jie Chang, Tiejun Wang, and Ying Xu. Review of biomass pyrolysis oil properties and upgrading research. *Energy conversion and management*, 48(1):87–92, 2007.
- [55] Gaojin Lyu, Shubin Wu, and Hongdan Zhang. Estimation and comparison of bio-oil components from different pyrolysis conditions. *Frontiers in Energy Research*, 3:28, 2015.
- [56] E. Wolf. Silyzer 200 (pem electrolysis system). Conference Lecture, 2015.
- [57] Bin Li, Christian Fabrice Magoua Mbeugang, Dongjing Liu, Shu Zhang, Shuang Wang, Qian Wang, Zhixiang Xu, and Xun Hu. Simulation of sorption enhanced staged gasification of biomass for hydrogen production in the presence of calcium oxide. *International Journal of Hydrogen Energy*, 45(51):26855–26864, 2020.
- [58] Mark J Prins, Krzysztof J Ptasinski, and Frans JGG Janssen. From coal to biomass gasification: Comparison of thermodynamic efficiency. *Energy*, 32(7):1248–1259, 2007.
- [59] Zhiquan Wu, Shaoxiang Zhou, and Liansuo An. The second law (exergy) analysis of hydrogen. *Journal of Sustainable Development*, 4(1):260–263, 2011.
- [60] Baldev Raj, BK Choudhary, and RK Singh Raman. Mechanical properties and non-destructive evaluation of chromium–molybdenum ferritic steels for steam generator application. *International journal of pressure vessels and piping*, 81(6):521–534, 2004.
- [61] Vlad C Sandu, Ionela Dumbrava, Ana-Maria Cormos, Arpad Imre-Lucaci, Calin C Cormos, Paul D Cobden, and Robert de Boer. Computational fluid dynamics of rectangular monolith reactor vs. packed-bed column for sorption-enhanced water-gas shift. In *Computer Aided Chemical Engineering*, volume 46, pages 751–756. Elsevier, 2019.

- [62] M Castedello and S Schöniger. Cost of capital study 2019: The calm before the storm, rising profits and deflates values?, 2019.
- [63] Machiel Mulder, Peter Perey, and José L Moraga. Outlook for a dutch hydrogen market, 2019.
- [64] Ad van Wijk. *The green hydrogen economy in the Northern Netherlands*. Noordelijke Innovation Board, 2017.
- [65] ABN AMRO. Energy monitor - gas market has turned global depressing prices, 2020. URL <https://insights.abnamro.nl/en/2020/01/energy-monitor-gas-market-has-turned-global-depressing-prices/>.
- [66] Robert M Campbell, Nathaniel M Anderson, Daren E Daugaard, and Helen T Naughton. Financial viability of biofuel and biochar production from forest biomass in the face of market price volatility and uncertainty. *Applied energy*, 230:330–343, 2018.
- [67] H.J. Lang. Simplified approach to preliminary cost estimates. *Chemical Engineering*, 55:112–113, 1948.
- [68] Abhijit Dutta, Joshua A Schaidle, David Humbird, Frederick G Baddour, and Asad Sahir. Conceptual process design and techno-economic assessment of ex situ catalytic fast pyrolysis of biomass: A fixed bed reactor implementation scenario for future feasibility. *Topics in Catalysis*, 59(1):2–18, 2016.
- [69] Donald E Garrett. *Chemical engineering economics*. Springer Science & Business Media, 2012.
- [70] Producer price index by industry: Oil and gas field machinery and equipment manufacturing, 2020. URL <https://fred.stlouisfed.org/series/PCU333132333132>.
- [71] Ray Sinnott, John Francis Richardson, and JM Coulson. *Chemical engineering: An introduction to chemical engineering design*. Elsevier, 2013.
- [72] Applicable Pollutants. Air pollution control technology fact sheet, 2005.
- [73] Max Stone Peters, Klaus D Timmerhaus, Ronald Emmett West, et al. *Plant design and economics for chemical engineers*, volume 4. McGraw-Hill New York, 1968.
- [74] YA Criado, B Arias, and JC Abanades. Calcium looping co₂ capture system for back-up power plants. *Energy & Environmental Science*, 10(9):1994–2004, 2017.
- [75] Kostenonderzoek verbranding en vergassing van biomassa sde+ 2018, 2017. URL <https://publicaties.ecn.nl/PdfFetch.aspx?nr=ECN-N--17-009>.
- [76] C Bang, A Vitina, JS Gregg, and H Henrik Lindboe. Analysis of biomass prices, future danish prices for straw, wood chips and wood pellets “final report”. *Copenhagen, Denmark: Ea Energy Analyses*, 2013.
- [77] Guido Collodi, Giuliana Azzaro, Noemi Ferrari, and Stanley Santos. Techno-economic evaluation of deploying ccs in smr based merchant h₂ production with ng as feedstock and fuel. *Energy Procedia*, 114:2690–2712, 2017.
- [78] Estimates-Wood Feedstock. Equipment design and cost estimation for small modular biomass systems, synthesis gas cleanup, and oxygen separation equipment. *Nat Renew Energy Lab*, 2006.
- [79] Yangyang Deng, Prem B Parajuli, and Hakkwan Kim. Cost analysis model for catalytic conversion of syngas in to light hydrocarbon gases. *Information Processing in Agriculture*, 2(1):37–50, 2015.
- [80] Eugenio Meloni, Marco Martino, and Vincenzo Palma. A short review on ni based catalysts and related engineering issues for methane steam reforming. *Catalysts*, 10(3):352, 2020.
- [81] Francesco Calise, Massimo Dentice D’Accadia, Massimo Santarelli, Andrea Lanzini, and Domenico Ferrero. *Solar Hydrogen Production: Processes, Systems and Technologies*. Academic Press, 2019.
- [82] Sociaal Economische Raad. *Biomass in the balance -A sustainability framework for high-value use of bio-based raw materials*. SER, 2020.
- [83] BS Elbersen, IG Staritsky, GM Hengeveld, MJ Schelhaas, HSD Naeff, and H Böttcher. Atlas of eu biomass potentials: Spatially detailed and quantified overview of eu biomass potential taking into account the main criteria determining biomass availability from different sources. Technical report, Alterra/IIASA, 2012.
- [84] EJMM Arets, PJ Van der Meer, CC Verwer, GM Hengeveld, GW Tolcamp, GJ Nabuurs, and M Van Oorschot. Global wood production: assessment of industrial round wood supply from forest management systems in different global regions. Technical report, Alterra, Wageningen-UR, 2011.

- [85] N Scarlat, JF Dallemand, N Taylor, M Banja, J Sanchez Lopez, and M Avraamides. Brief on biomass for energy in the european union. *European Commission's Knowledge Centre for Bioeconomy*, 2019.
- [86] Centraal Bureau voor de Statistiek. *Hernieuwbare energie in Nederland 2019*. Centraal Bureau voor de Statistiek, 2019.
- [87] M.Boosten. *Beschikbaarheid van Nederlandse verse houtige biomassa in 2030 en 2050*. Probos, Wageningen University, 2018.
- [88] M. Gortworst J.W.A. Langeveld, P.M.F. Quist-Wessel. *Gebruik van houtige biomassa voor energieopwekking*. Platform Bio Economie, 2019.
- [89] Veronika Hansen, Dorette Müller-Stöver, Lars Juhl Munkholm, Clément Peltre, Henrik Hauggaard-Nielsen, and Lars Stoumann Jensen. The effect of straw and wood gasification biochar on carbon sequestration, selected soil fertility indicators and functional groups in soil: an incubation study. *Geoderma*, 269:99–107, 2016.
- [90] Sunil Kumar and Ajay Bharti. *Management of Organic Waste*. BoD–Books on Demand, 2012.
- [91] Supriya Majumder, Surama Neogi, Tanushree Dutta, Michael A Powel, and Pabitra Banik. The impact of biochar on soil carbon sequestration: Meta-analytical approach to evaluating environmental and economic advantages. *Journal of environmental management*, 250:109466, 2019.
- [92] Afeng Zhang, Rongjun Bian, Genxing Pan, Liqiang Cui, Qaiser Hussain, Lianqing Li, Jinwei Zheng, Jufeng Zheng, Xuhui Zhang, Xiaojun Han, et al. Effects of biochar amendment on soil quality, crop yield and greenhouse gas emission in a chinese rice paddy: a field study of 2 consecutive rice growing cycles. *Field Crops Research*, 127: 153–160, 2012.
- [93] Fernanda R Oliveira, Anil K Patel, Deb P Jaisi, Sushil Adhikari, Hui Lu, and Samir Kumar Khanal. Environmental application of biochar: Current status and perspectives. *Bioresource technology*, 246:110–122, 2017.
- [94] Steven C Peterson. Utilization of low-ash biochar to partially replace carbon black in styrene–butadiene rubber composites. *Journal of Elastomers & Plastics*, 45(5):487–497, 2013.
- [95] ECHEMI. Carbon black price analysis, 2021. URL <https://m.echemi.com/productsInformation/pd20150901230-carbon-black.html>.
- [96] Vamsee Pasangulapati, Karthikeyan D Ramachandriya, Ajay Kumar, Mark R Wilkins, Carol L Jones, and Raymond L Huhnke. Effects of cellulose, hemicellulose and lignin on thermochemical conversion characteristics of the selected biomass. *Bioresource technology*, 114:663–669, 2012.
- [97] L Plass, J Albrecht, and JC Loeffler. Processing of residues and municipal waste in circulating fluidized beds: Operating experience, design concepts and future developments. Technical report, American Society of Mechanical Engineers, New York, NY (United States), 1997.
- [98] Yang Yang, Sonia Heaven, Nikolaos Venetsaneas, CJ Banks, and AV Bridgwater. Slow pyrolysis of organic fraction of municipal solid waste (ofmsw): Characterisation of products and screening of the aqueous liquid product for anaerobic digestion. *Applied energy*, 213:158–168, 2018.
- [99] Patrick Brassard, Stéphane Godbout, and Vijaya Raghavan. Pyrolysis in auger reactors for biochar and bio-oil production: A review. *Biosystems engineering*, 161:80–92, 2017.
- [100] Mohammad Reza Ghaffariyan, Robin Apolit, and Martin Kuehmaier. Analysis and control of fuel consumption rates of harvesting systems: A review of international studies. *Industry Bulletin*, 15:1–4, 2015.
- [101] Nike Krajnc. *Wood fuels handbook*. FAO, 2015.
- [102] ECTA Cefic. Guidelines for measuring and managing co2 emission from freight transport operations. *Cefic Report*, 1(2011):1–18, 2011.
- [103] Dan Bergström and Fulvio Di Fulvio. Review of efficiencies in comminuting forest fuels. *International Journal of Forest Engineering*, 30(1):45–55, 2019.
- [104] Alberto Moro and Laura Lonza. Electricity carbon intensity in european member states: Impacts on ghg emissions of electric vehicles. *Transportation Research Part D: Transport and Environment*, 64:5–14, 2018.
- [105] Takeshi Kuroyanagi, Ken-ichiro Yasuba, Tadahisa Higashide, Yasunaga Iwasaki, and Masuyuki Takaichi. Efficiency of carbon dioxide enrichment in an unventilated greenhouse. *Biosystems engineering*, 119:58–68, 2014.

- [106] Charles C Dean, John Blamey, Nicholas H Florin, Mohamad J Al-Jeboori, and Paul S Fennell. The calcium looping cycle for co₂ capture from power generation, cement manufacture and hydrogen production. *Chemical Engineering Research and Design*, 89(6):836–855, 2011.
- [107] Dawid P Hanak, Sebastian Michalski, and Vasilije Manovic. From post-combustion carbon capture to sorption-enhanced hydrogen production: A state-of-the-art review of carbonate looping process feasibility. *Energy Conversion and Management*, 177:428–452, 2018.
- [108] Isabel Martinez, Gemma Grasa, Jarno Parkkinen, Tero Tynjälä, Timo Hyppänen, Ramon Murillo, and Matteo C Romano. Review and research needs of ca-looping systems modelling for post-combustion co₂ capture applications. *International Journal of Greenhouse Gas Control*, 50:271–304, 2016.
- [109] Ronald Barker. The reversibility of the reaction $\text{CaCO}_3 \rightleftharpoons \text{CaO} + \text{CO}_2$. *Journal of applied Chemistry and biotechnology*, 23(10):733–742, 1973.
- [110] Li Zhen-shan, Cai Ning-sheng, and Eric Croiset. Process analysis of co₂ capture from flue gas using carbonation/calcination cycles. *AIChE journal*, 54(7):1912–1925, 2008.
- [111] ER Van Selow, PD Cobden, RW Van den Brink, JR Hufton, and A Wright. Performance of sorption-enhanced water-gas shift as a pre-combustion co₂ capture technology. *Energy Procedia*, 1(1):689–696, 2009.
- [112] Luka A Živković, Andrej Pohar, Blaž Likozar, and Nikola M Nikačević. Kinetics and reactor modeling for cao sorption-enhanced high-temperature water–gas shift (se–wgs) reaction for hydrogen production. *Applied Energy*, 178:844–855, 2016.
- [113] Jurriaan Boon, Kai Coenen, Eric van Dijk, Paul Cobden, Fausto Gallucci, and Martin van Sint Annaland. Sorption-enhanced water–gas shift. In *Advances in chemical engineering*, volume 51, pages 1–96. Elsevier, 2017.
- [114] Hyun Min Jang, Ki Bong Lee, Hugo S Caram, and Shivaji Sircar. High-purity hydrogen production through sorption enhanced water gas shift reaction using k₂co₃-promoted hydrotalcite. *Chemical engineering science*, 73:431–438, 2012.
- [115] Bin Li, Liangyuan Wei, Haiping Yang, Xianhua Wang, and Hanping Chen. The enhancing mechanism of calcium oxide on water gas shift reaction for hydrogen production. *Energy*, 68:248–254, 2014.
- [116] G. Brem. Fluidized bed conversion. University Lecture, 2017.
- [117] EnggCyclopedia. Types of gasifiers, 2020. URL <https://www.enggcyclopedia.com/2012/01/types-gasifier/>.
- [118] Simona Ciuta, Francesco Patuzzi, Marco Baratieri, and Marco J Castaldi. Enthalpy changes during pyrolysis of biomass: Interpretation of intraparticle gas sampling. *Applied Energy*, 228:1985–1993, 2018.
- [119] NIST. Calcium oxide, 2020. URL <https://webbook.nist.gov/cgi/cbook.cgi?ID=C1305788&Mask=1000>.
- [120] Gary K Jacobs, Derrill M Kerrick, and Kenneth M Krupka. The high-temperature heat capacity of natural calcite (CaCO₃). *Physics and Chemistry of Minerals*, 7(2):55–59, 1981.
- [121] Jan Szargut, David R Morris, and Frank R Steward. Exergy analysis of thermal, chemical, and metallurgical processes. *web*, 1987.
- [122] Jonatan D Durán-Martín, Pedro E Sánchez Jimenez, José M Valverde, Antonio Perejón, Juan Arcenegui-Troya, Pablo García Triñanes, and Luis A Pérez Maqueda. Role of particle size on the multicycle calcium looping activity of limestone for thermochemical energy storage. *Journal of Advanced Research*, 22:67–76, 2020.
- [123] Gemma S Grasa and J Carlos Abanades. Co₂ capture capacity of cao in long series of carbonation/calcination cycles. *Industrial & Engineering Chemistry Research*, 45(26):8846–8851, 2006.
- [124] Hydrogen Tools. Hydrogen fuel quality standards, 2020. URL <https://h2tools.org/hyarc/hydrogen-data/hydrogen-fuel-quality-standards>.
- [125] Carlos A Grande, Filipe VS Lopes, Ana M Ribeiro, José M Loureiro, and Alírio E Rodrigues. Adsorption of off-gases from steam methane reforming (h₂, co₂, ch₄, co and n₂) on activated carbon. *Separation Science and Technology*, 43(6):1338–1364, 2008.
- [126] Wiebren De Jong and J Ruud Van Ommen. *Biomass as a sustainable energy source for the future: Fundamentals of conversion processes*. John Wiley & Sons, 2014.

- [127] Toshiaki Hanaoka, Seiichi Inoue, Seiji Uno, Tomoko Ogi, and Tomoaki Minowa. Effect of woody biomass components on air-steam gasification. *Biomass and bioenergy*, 28(1):69–76, 2005.
- [128] Jimin Zeng, Rui Xiao, Huiyan Zhang, Xing Chen, Dewang Zeng, and Zhong Ma. Syngas production via biomass self-moisture chemical looping gasification. *Biomass and Bioenergy*, 104:1–7, 2017.
- [129] Javier Herguido, Jose Corella, and Jose Gonzalez-Saiz. Steam gasification of lignocellulosic residues in a fluidized bed at a small pilot scale. effect of the type of feedstock. *Industrial & engineering chemistry research*, 31(5):1274–1282, 1992.
- [130] Yildiz Kalinci, Arif Hepbasli, and Ibrahim Dincer. Biomass-based hydrogen production: a review and analysis. *International journal of hydrogen energy*, 34(21):8799–8817, 2009.
- [131] S Venkata Mohan and Ashok Pandey. Biohydrogen production: an introduction. In *Biohydrogen*, pages 1–24. Elsevier, 2013.
- [132] Debabrata Das and T Nejat Veziroglu. Hydrogen production by biological processes: a survey of literature. *International journal of hydrogen energy*, 26(1):13–28, 2001.
- [133] Y Guo, SZ Wang, DH Xu, YM Gong, HH Ma, and XY Tang. Review of catalytic supercritical water gasification for hydrogen production from biomass. *Renewable and Sustainable Energy Reviews*, 14(1):334–343, 2010.

Appendices

A Reactor types for thermal processing of biomass

The reactor type and the location of the biomass feeding point influence the heating rate of biomass, the residence time, and the effectiveness of the catalyst, and therefore the syngas yield and quality. Reactor types which can be used for biomass gasification are fixed bed and fluidized bed reactors, downdraft and updraft gasifier. Another option for biomass gasification, which will be discussed in this section, is an auger reactor (screw reactor).

Fixed bed and fluidized beds

Fluidized bed and fixed bed reactors are both reactors which consists out of non-reacting particles, which can act as catalyst. In both reactors gases pas through the bed. In a fixed bed reactor gas velocities do not reach the minimum fluidization velocity resulting in plug flow in the reactor. In a fluidized bed gas velocities are higher than the minimum fluidization velocity. When particle size decreases or particle density increases, a larger minimum gas velocity for fluidization is required. The minimum fluidization velocity is given by the Ergun relation [116]:

$$(\rho_p - \rho_f) g = \frac{\rho_f u_{mf}^2}{\phi_s D_p \epsilon_{mf}^3} \left[\frac{150(1 - \epsilon_{mf}) \mu}{\phi_s D_p \mu_{mf} \rho_f} + 1,75 \right] \quad (1)$$

The different types of fluidized reactors (including fixed bed) are displayed in figure .2. When a circulating fluidized bed is designed, the bed should be characterized as at least turbulent fluidized. A circular fluidized-bed could be desired for catalyst regeneration or for heating of the bed material when reactions in the bed are endothermic: for example, char combustion in a biomass pyrolysis twin bed system with a pyrolysis reactor (endothermic) and char combustor (exothermic).

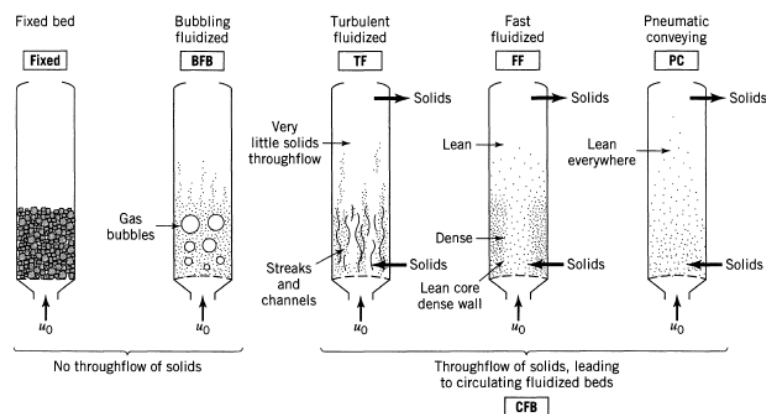


Figure .2: Different types of fluidized bed reactors [46]

Plug flow (fixed bed) is desired with respect to contact between gases and active catalyst. If a fluidized bed is used, there is a lot of bypassing of gases due to gas bubbles resulting in a system that requires much more catalytic material for high gas conversion [46]. Temperature control can be difficult in fixed beds due to the lack of the mixing of solids. When the reactions in a fixed bed reactor are exothermic, this can cause hot spots, which can result in sintering and deactivation of catalysts [46] while if the reaction is endothermic cold spots can develop at the product inlet, which decreases the reaction rate and can cause accumulation of product (for example biomass) [46]. Fluidized beds are able to work with small particle sizes, while this will cause plugging and high pressure drops in fixed beds.

Downdraft and updraft reactors

In both updraft and downdraft gasifiers, the feed is added from the top. In updraft gasifiers, the gas also leaves at

the top, while in downdraft gasifiers, the gas leaves at the bottom. figure .3. shows the working principle of updraft and downdraft gasifiers. The advantage of the updraft gasifier is that it is a simple system. Using an updraft gasifier will, however, have a large tar yield since the formed tars during primary cracking leave the system relatively quickly, preventing further cracking. In a downdraft gasifier, the formed tars in the pyrolysis zone pass through the combustion and reduction zone, which causes further cracking/oxidation of the tars reducing the total tar yield and increasing the gas yield [117]. Another type of gasifier that can be used for biomass gasification is a crosscurrent gasifier, where the produced syngas leaves in the middle of the reactor.

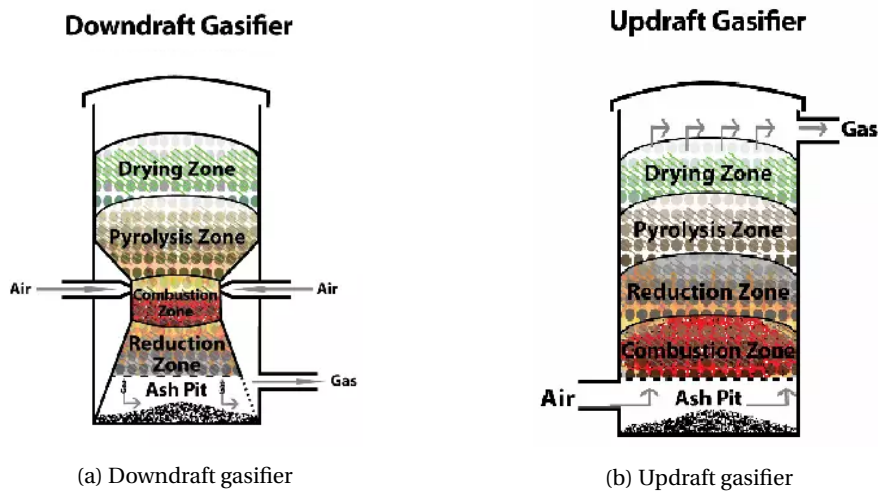


Figure .3: Downdraft gasifier versus updraft gasifier

Auger reactor

A screw reactor is another reactor type in which biomass can be thermally treated. Biomass is transported through the reactor using a screw. A schematic overview is given in figure .4. The screw can be placed horizontal, vertical, or inclined, and the cross-section of the reactor can be circular or rectangular. A screw reactor is heated externally (the walls of the reactor are heated), but the screw itself could also be heated, for example, with circulating hot fluid through a hollow structure in the screw [47]. A screw reactor can also be designed with holes in the reactor wall, making it possible for the gases and tars to escape. The advantages of a screw reactor are that there is a reliable mass flow, and different particle sizes can be used. Furthermore, the residence time can be well controlled in a screw reactor. If gases and tars are not able to "escape" the reactor secondary cracking reactions are enhanced, which can lead to small tar and high gas yield under anaerobic conditions. Disadvantages are limited heat transfer in a screw reactor and limited scaling possibilities due to limited heat transfer (relative wall contact decreases during upscaling). Research performed by Solar et al. [40] and by Efika et al. [48]. found that pyrolysis of woody biomass in a screw reactor followed by catalytic steam reforming or thermal treatment can result in a high-quality char yield out of the screw reactor, and syngas with a high hydrogen concentration, a syngas yield up to 75 wt% has been measured by Solar for a residence time of 64 minutes and reactor temperature of 900 °C without the addition of steam or the use of a catalyst.

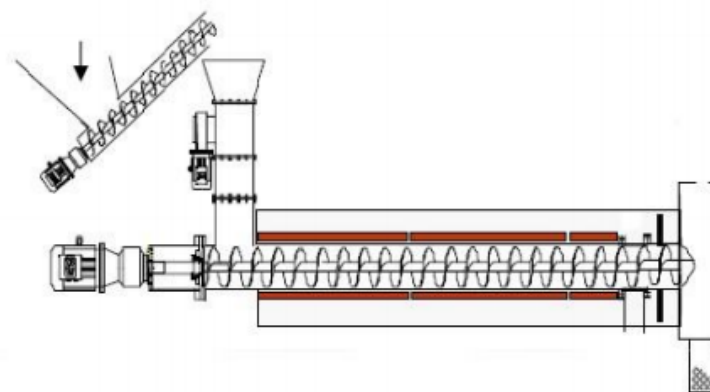


Figure .4: Screw reactor [47]

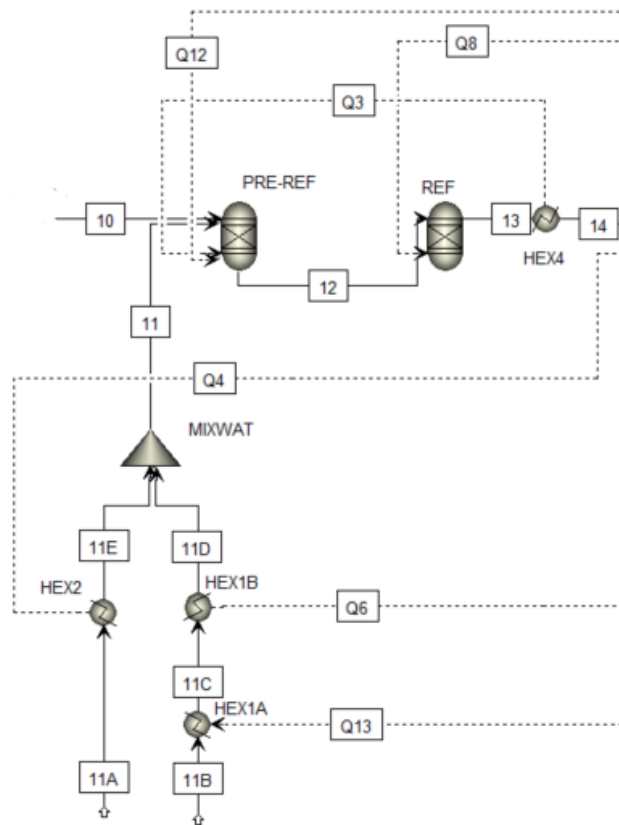


Figure .7: Aspen Plus flowsheet for steam reforming

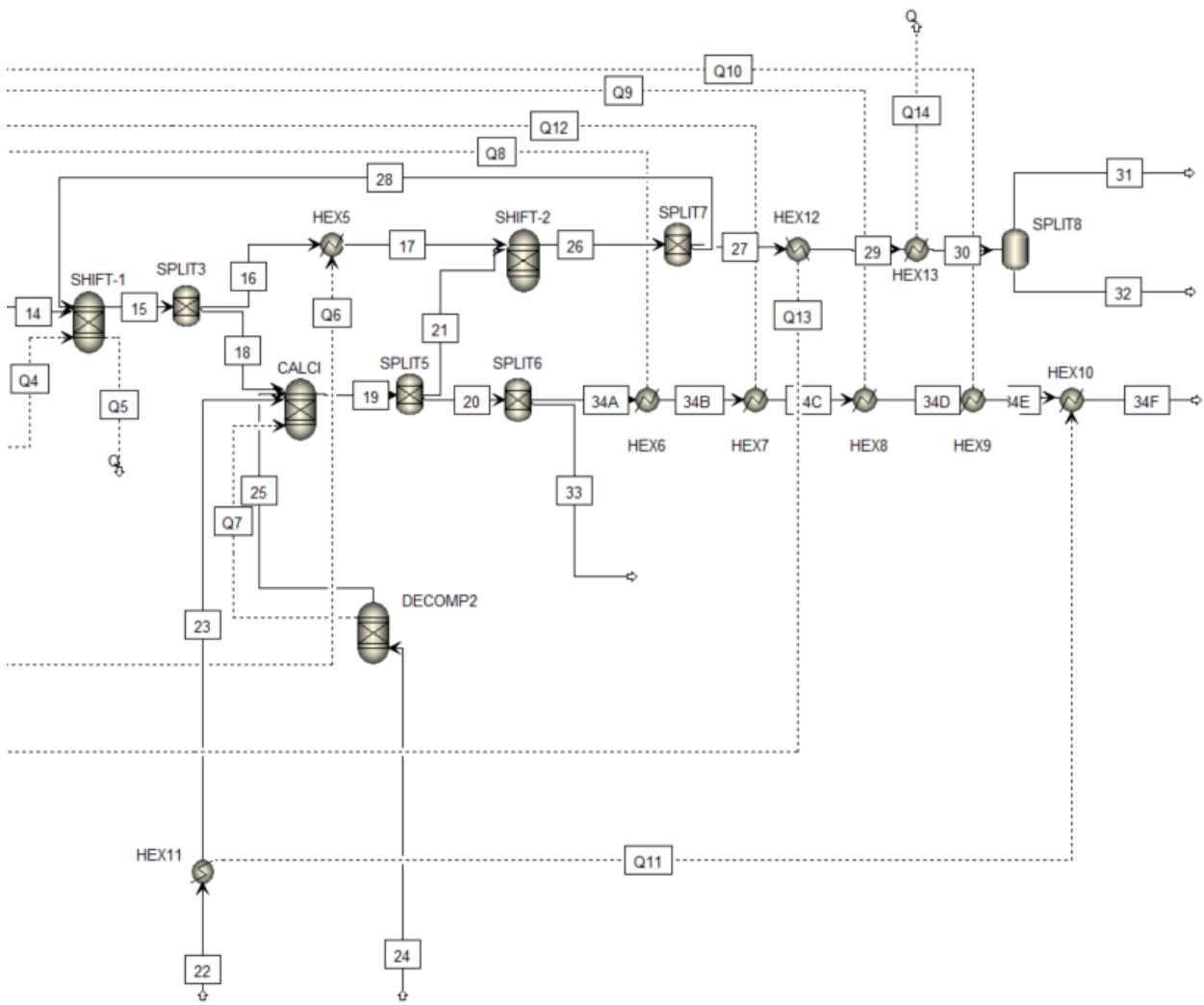


Figure .8: Aspen Plus flowsheet for CaL SEWGS including heat integration

C Energy calculations thermal processing of biomass

The next section will discuss the heating values of biomass and produced products during pyrogasification. Furthermore, exergy evaluation is discussed as well as system efficiencies.

Heating values of biomass

Heating values or calorific values represent the amount of heat which is released during complete combustion; there are both Higher Heating Values (HHV) and Lower Heating Values (LHV), an HHV corresponds to all the energy which is released during combustion while the LHV already compensates the released energy for the required latent heat for water vaporization. A simplified example of combustion under stoichiometric conditions is given in equation .2.



When an ultimate analysis is performed of a biomass sample, the HHV can be accurately be determined according to equation .3 [51] where Y_i represents the mass fraction of the given component.

$$HHV = 34,91Y_C + 117,83Y_H + 10,05Y_S - 1,51Y_N - 10,34Y_O - 2,11Y_{ash} \quad (.3)$$

The LHV of dry based biomass: LHV^{DB} can be calculated according to equation .4 where 2,4 MJ/kg corresponds to the latent heat of evaporation of water at 25 °C 8,9 corresponds to the relative amount of water which is formed during stoichiometric combustion of one kg of hydrogen, which comes down to the molar mass of water divided by the molar mass of hydrogen in water (18,016/2,016) and Y_H is the mass fraction of water. When wet biomass is used, the LHV of the dry based biomass needs to be compensated since part of the mass of the biomass does not contribute to the LHV. Furthermore, the additional latent heat of evaporation of the extra water content needs to be subtracted from the LHV^{DB} in order to obtain the LHV of the wet based biomass LHV^{WB} according to equation .5.

$$LHV^{DB} = HHV - 2,4 * 8,9 * Y_H \quad [Mj/kg] \quad (.4)$$

$$LHV^{WB} = LHV^{DB} * (1 - Y_{moisture}) - Y_{moisture} * 2,4 \quad [MJ/kg] \quad (.5)$$

Heating values of produced products

There are three products that are produced during pyrogasification: syngas, bio-char, and oil. The aim of pyrogasification is to maximize syngas yield. However, a fraction of biochar and bio-oil will also be present as a product if a conventional route of gasification is taken. The higher heating value of (bio)char can be calculated in the same way as the HHV of biomass. Performing an ultimate analysis will result in the chemical composition, which can be used to calculate the HHV of biochar according to equation .3. The produces syngas and bio-oil are mixtures of different gases/oils, and therefore to determine the HHV of these mixtures, the mass fraction of each component x_i is multiplied with the HHV of the given component HHV_i according to equations .6 and .7 [118].

$$HHV_{syngas} = \sum_{i=1}^n x_i HHV_i \quad \text{with } i = H_2, CH_4, CO, C_2H_4, C_2H_6 \text{ etc.} \quad (.6)$$

$$HHV_{bio-oil} = \sum_{i=1}^n x_i HHV_i \quad \text{with } i = C_6H_7O, C_{10}H_8, C_{11}H_{10} \text{ etc.} \quad (.7)$$

Enthalpy change during pyrogasification

During pyrogasification, biomass is converted into syngas, biochar, and bio-oil. This process is endothermic, meaning that additional heat is required for biomass cracking, tar cracking, steam reforming, etc. The energy required for pyrogasification reactions is called the enthalpy for the reaction: h_r , since it is hard to model all the reactions during the process (some reactions are endothermic, some are exothermic), the best way to determine h_r is to look at the deficit of HHV of the products compared to the reactants according to formula .8 where j stands for the produced products: oil, char, and syngas.

$$h_r = \sum_{j=1}^n (x_j \times HHV_j) - HHV_{biomass} \quad (.8)$$

Besides heat which is required for the endothermic pyrogasification reactions, heat is also required to heat biomass and to evaporate moisture out of the processed biomass, which leads to a certain amount of sensible heat which is required for pyrogasification h_s , which can be calculated by multiplying the mass fractions of water and dry biomass with their corresponding specific heat and multiplying it with the temperature difference dT. Additionally, the latent heat of evaporation of water needs to be added to the total sensible heat requirement. Note that the specific heat of steam and water different; therefore, it is assumed that water is heated to 100 °C resulting in a temperature difference

$T^* = 100\text{ }^\circ\text{C} - T_0$ with T_0 the biomass inlet temperature. Next, water is turned into steam (assuming ambient pressure) before steam is heated to the reactor temperature resulting in a temperature difference $T^{**} = T_g - 100\text{ }^\circ\text{C}$ with T_g the reactor temperature.

$$h_s = x_{dry-biomass} * c_p * dT + x_{water} * c_p * dT^* + x_{steam} * c_p * dT^{**} + x_{water} * L_{water} \quad (.9)$$

The heat for pyrogasification can be calculated by adding the heat of reaction and the sensible heat requirement according to equation .10.

$$h_p = h_r + h_s \quad (.10)$$

Figure .9 shows the energy balance of a gasification system when the gasification reactor is modeled as an open system, assuming biomass and heat enters the system, and heated products leave the system. In figure .9. circulating bed material is not taken into account, and reference temperatures are taken at ambient conditions, meaning biomass entering the system only contains chemical energy and no sensible heat. Assuming no work is done by (or on) the system, the kinetic and potential energy of the flows do not change; this will result in an energy balance according to equation .9 when the first law of thermodynamics is used, where ΔT is the difference between gasifier temperature (it is assumed that all products leave the gasifier at the same temperature as the gasifier) and ambient conditions: $\Delta T = T_g - T_0$. The specific heat: $c_{p,j}$ of the produced gases and liquids are a mixture of different species. The specific heat can be calculated in the same manner as the HHV according to equations .6 and .7, replacing the HHV by the c_p .

$$HHV_{biomass} + h_p - \sum_{j=1}^n (x_j \cdot (HHV_j + \Delta T \cdot c_{p,j})) = 0 \quad (.11)$$

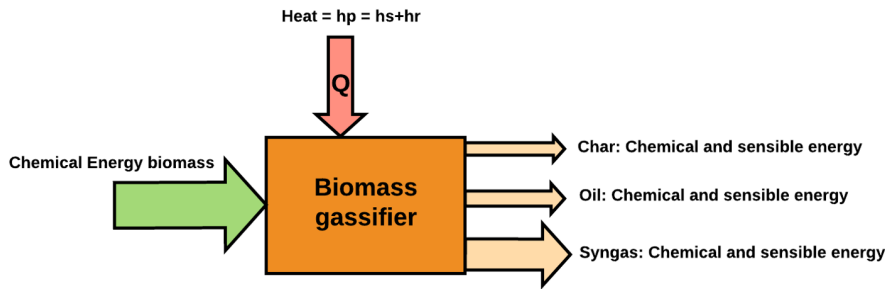


Figure .9: Gassifier energy balance

Enthalpy change during carbon capture

Carbonation is an exothermic reaction, while calcination is endothermic. During the calculations it is assumed that the enthalpy change during carbon capture = $\Delta H = -170,5\text{ kJ/mol}$ and during calcination $\Delta H = 170,5\text{ kJ/mol}$. The chemical potential of a mass flow containing CaO is calculated by multiplying the molar flowrate (moles/s) by the chemical potential per mole (170,5 kJ/mol).

The sensible heat in CaO is calculated according to formula .12 retrieved from the NIST database [119].

$$H^0 - H_{298,15}^0 = A * T + \frac{B * T^2}{2} + \frac{C * T^3}{3} + \frac{D * T^4}{4} + F - H \quad (.12)$$

The sensible heat for $CaCO_3$ is calculated by integration of the specific heat using formula .13 [120] for the specific heat of $CaCO_3$ under high temperatures.

$$C_p = A + B * T + C * T^{-2} + DT^2 + ET^{-0.5} \quad (.13)$$

Integration over the temperature range, where $T=293\text{K}$ is the base value results in equation .15 which is used to calculate sensible heat flowrate of $CaCO_3$

$$H^0 - H_{293}^0 = \int_{293}^T C_p \quad (.14)$$

$$H^0 - H_{293}^0 = \left[A * T + \frac{B * T^2}{2} - C * T^{-1} + \frac{D * T^3}{3} + 2E * T^{0.5} \right]_{293}^T \quad (.15)$$

Table .3: Constants used for calculation of sensible heat in CaO and $CaCO_3$

Constant	CaO	$CaCO_3$
A	49.954020	-184.79
B	4.887916	0.32322
C	-0.352056	-3688200
D	0.046187	$1.9274 * 10^{-4}$
E	-0.825097	3883.5
F	-652.9718	
G	92.560960	
H	-635.0984	

Exergetic analysis of the biomass pyrogasification process

Exergy, and especially exergy efficiency is an important measure of performance for a biomass pyrogasification system. Similar to energy flows, exergy enters the system in the form of biomass and steam. Exergy leaves the system in char, fuel gases, and heat.

Just like the HHV and LHV values, there are correlations to calculate the exergy value of biomass as a function of hydrogen, oxygen, and carbon content, in combination with the Lower Heating Value (LHV). The correlations found by Szargut et al. [121] to calculate the exergy value of biomass is given in equation .16 and .17. Note that in equation .17 the mass ratio's are used (and not molar ratio's).

$$Ex_{biomass} = \beta LHV_{biomass} \quad (.16)$$

$$\beta = \frac{1.0414 + 0.0177[H/C] - 0.3328[O/C](1 + 0.0537[H/C])}{1 - 0.4021[O/C]} \quad (.17)$$

The physical exergy of the steam entering the system, as well as the physical exergy of all the products leaving the system, can be calculated according to equation .18

$$Ex_{ph} = (h - h_0) - T_0(s - s_0) \quad (.18)$$

Furthermore, the chemical exergy of the gases can be calculated according to equation .19 where X_i is the molar fraction of component i, and $Ex_{0,i}$ is the standard chemical exergy of component i.

$$Ex_{ch} = \sum_i X_i Ex_{0,i} + RT_0 \sum_i X_i \ln X_i \quad (.19)$$

The fuel gases leaving the system both contain physical and chemical exergy, and therefore, the total exergy can be calculated according to equation .20.

$$Ex_{fuel-gas} = Ex_{ch} + Ex_{ph} \quad (.20)$$

The exergy value of the char leaving the system can be calculated in a similar fashion compared to the exergy value of biomass. Char leaves the system at elevated temperatures. The thermal energy present will not be used in the system since the char is solid (relative small heat transfer rate), and the relative amount of thermal energy will be neglectable in the char.

There are different forms of the exegeric efficiency of the gasification process of biomass, which is used in literature [32]. A couple of different forms are displayed in the equations listed below. Depending on the desired products (Hydrogen, fuel gas, Fuel gas and char, Fuel gas, Char and heat, etc.), a different form can be used. The exegeric values of the products are chemical exergy, only equation .24 takes heat flows into account, where Ex_{lost} represents the exegeric value of heat losses in the system. Since the main aim of this research is to produce hydrogen with negative carbon emissions, either formula .21 or .23 will be used in the system analyses. Other produced gases (for example, methane) are undesired, and the system will not be designed for residential heating, and therefore heat losses will not be utilized.

$$\eta_{ex,1} = \frac{Ex_{H_2}}{Ex_{biomass} + Ex_{steam}} \quad (.21)$$

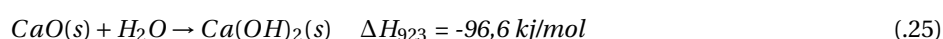
$$\eta_{ex,2} = \frac{Ex_{fuelgas}}{Ex_{biomass} + Ex_{steam}} \quad (.22)$$

$$\eta_{ex,3} = \frac{Ex_{H_2} + Ex_{char}}{Ex_{biomass} + Ex_{steam}} \quad (.23)$$

$$\eta_{ex,4} = \frac{Ex_{H_2} + Ex_{char} + Ex_{lost}}{Ex_{biomass} + Ex_{steam}} \quad (.24)$$

E Limitations for carbon capture using metal oxides

A general problem that can occur during both sorption enhanced gasification as well as during calcium looping using metal oxides is the formation of low-temperature melts. Melts cause agglomeration of particles, which can cause problems with circulating fluidized beds. Furthermore, agglomeration decreases carbon capture reaction rates due to a decrease in surface area [13] CaO melts at a temperature of 2927 °C and $CaCO_3$ melts at a temperature of 1339 °C. Therefore it is expected that these substances do not form a problem with respect to the formation of melts. The formation of $Ca(OH)_2$ according to equation .25 can cause problems with respect to low temperature melts since $Ca(OH)_2$ decomposes at 385 °C[13]. The formation of $Ca(OH)_2$ compared to the formation of $CaCO_3$ is, however, unfavorable due to the high equilibrium pressure of CaO with H_2O , only at low temperatures (<600 °C) and high partial water pressures (>5 atm.) $Ca(OH)_2$ is formed [13] these process conditions are only reached under pressurized gasification with a high SBR. When process temperatures reach 750 °C the partial water equilibrium pressure, resulting in the decomposition of CaO and water to $Ca(OH)_2$ is close to 100 atm [13], under these process conditions, the formation of low-temperature melts will only occur under extreme process conditions (pressure and SBR), these process conditions are not expected in the designed system, and therefore it is expected that the formation of melts will not cause any problems in the designed system.



Further limitations with respect to carbon capture using CaO is the sintering of particles, which is temperature-dependent and becomes a significant problem at $T > 750$ °C, sintering will cause agglomerates of calcium oxide particles, resulting in a surface area reduction and incomplete conversion of CaO to $CaCO_3$ due to reduced particle surface area. Incomplete conversion of CaO to $CaCO_3$ is a problem that can be attributed to the large volume increase when CO_2 is absorbed, resulting in the closure of small pores in the particle, making CO_2 absorption diffusion-controlled towards the center of the particle instead of kinetically controlled [13]. Decreasing the particle size may solve this problem and also leads to increased reaction speeds due to the surface area increase. Using smaller particles requires additional pre-treatment of calcium carbonate (grinding), which is energy-intensive. On the other hand, using smaller particles can result in plugging of equipment and will increase the minimum fluidization/bubbling velocity for fluidized bed reactors.

Sintering, the production of low temperature melts the formation of coke on particles and the decrease of pore volume result in a decreased activity of the CO_2 sorbent over time, which results in a system which requires continuously fresh sorbent. Luckily CaO is abundantly available in nature (limestone) and is therefore relatively cheap. Florin et al. [13] discussed several methods to increase the multi-cycle reactivity of calcium oxide CO_2 sorbents as listed below. These methods will not be discussed in detail in this report.

- The use of mild calcination conditions $T \approx 700^\circ\text{C}$
- Sorbent hydration
- The use of nano sized particles

The decrease in sorbent activity is displayed in figure .11 as measured by Florin et al. [21], which results are similar to results found by Duran et al. [122]. In figure .11 the weight is plotted, each experiment starts with $CaCO_3$ (100% weight), next $CaCO_3$ is heated such that all CO_2 is removed and only CaO remains (roughly 55 weigh %), next temperatures are dropped, and CO_2 is added, this time mass increases are less than 100% due to sorbent activity decrease. Figure .11 clearly shows the two phases of CO_2 absorption, the relative fast kinetically controlled absorption followed by the relatively slow diffusion-controlled absorption.

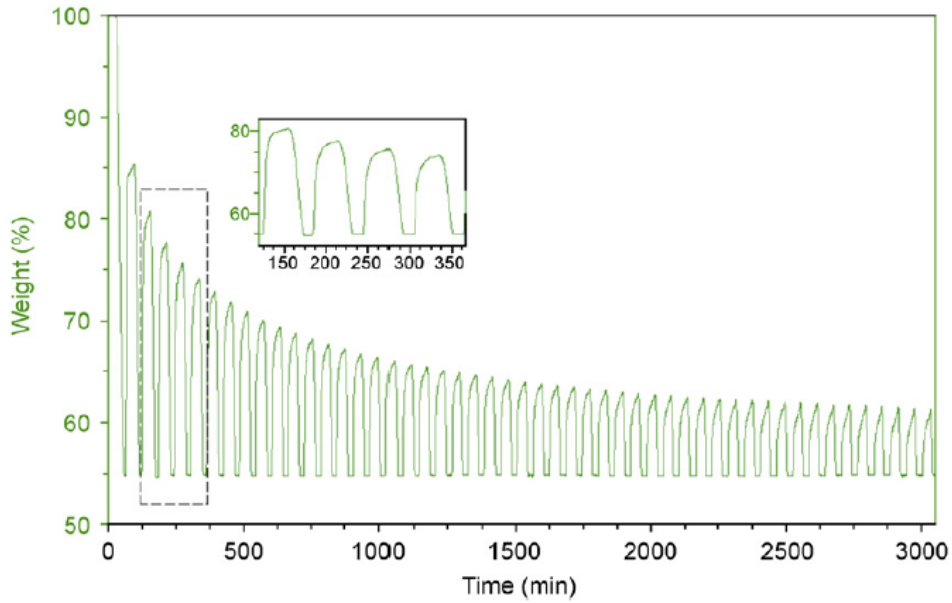


Figure .11: Decrease in sorbent (CaO) activity over multiple recycles [21]

The rapid decrease in sorbent activity requires accurate modeling of sorbent activity to determine the required amount of sorbent make up, in combination with the required sorbent flow rate to the sorption-shift reactors and regeneration reactors. In each cycle, a fraction "m" of the used sorbent is removed from the system and replaced by a sorbent makeup "m" (similar molar flows). It is assumed that sorbent is removed at random (independent of particle size, hence sintering), and therefore, the "particle age" (number of absorption/regeneration cycles) is distributed according to

$$P_N = m(1 - m)^{N-1} \quad (26)$$

$$\sum_{N=1}^{\infty} P_N = 1$$

So of the present sorbent 10 % has been through 1 cycle, 9% through 2 cycles. 8,1% through 3 cycles etc. The activity of the sorbent as a function of the number of cycles can be expressed by a formula derived by [123] given in formula .27.

$$X_N = X_r + \left(\frac{X_1}{K(N-1) + \left(1 - \frac{X_r}{X_1}\right)^{-1}} \right) \quad (27)$$

In this formula X_r is the residual conversion, which is the "minimal" conversion after a large number of cycles (related to the asymptotic value displayed in figure .11). X_1 is the conversion after one cycle (Amount of CaCO₃ relative to 100 % CaCO₃), K represents the deactivating constant, and N is the number of cycles. Duran et al. [122] performed experimental research on CaCO₃ sorbent activity as a function of a number of cycles, they fitted their results with equation .27, the results found by Duran et al. are displayed in table .4.

Table .4: Calcination conditions for limestone [122]

Species	Limestone (CaCO ₃)
Particle mean diameter	900 μm
X_1	64 %
X_r	7 %
K	0,56

The average conversion \bar{X} is calculated by taking the sum of the probability of a particle being through N cycles (P_N) times the activity at cycle N (X_N), resulting in equation .28

$$\bar{X} = \sum_{N=1}^{\infty} (P_N * X_N) \quad (28)$$

The average sorbent activity as function of the fractional sorbent make up "m" according to equation .28 is plotted in figure .12.

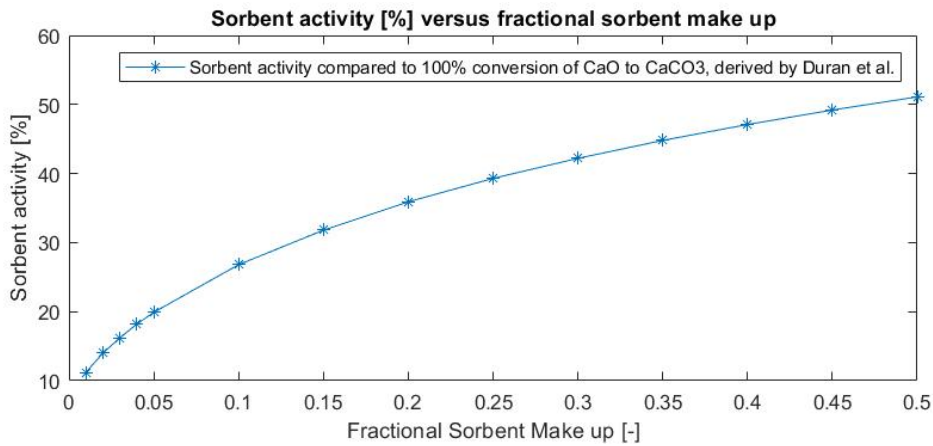


Figure .12: Sorbent activity, compared to 100 % conversion of caO to CaCO₃ as function of the fractional sorbent make up [122]

In order to calculate the required amount of sorbent equations .27 and .26 needs to be substituted in equation .28. The amount of CO₂ which needs to be captured is required : V_{CO₂}, in combination with a safety factor "s". The total flowrate of sorbent in the system (in moles/h) can then be calculated as a function of the fractional sorbent make up "m" compared to total molar flow according to:

$$V_{CaO} + V_{CaCO_3} = \frac{V_{CO_2} * f}{\bar{x}} \quad (.29)$$

An increased sorbent make up will result in smaller solid mass flows through the system due to a relatively high sorbent activity. This will also increase system efficiency since less heat is required in the generator, and less cooling is required in the sorption-shift reactor. The results of equation .29 are displayed in figure .13 in combination with the absolute required amount of sorbent makeup.

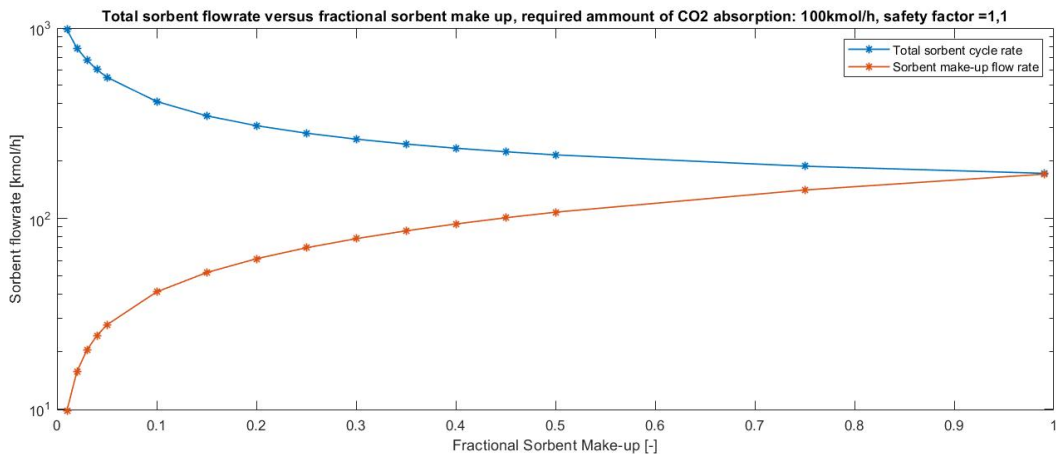


Figure .13: Total sorbent cycle rate and sorbent make up rate, assuming 100 kmol/h CO₂ absorption and safety factor of 1.1, using data from Duran et al. [21]

F Sensitivity analysis pyrogasification SEWGS system additional graphs

Sensitivity analysis Shift 1 Temperature

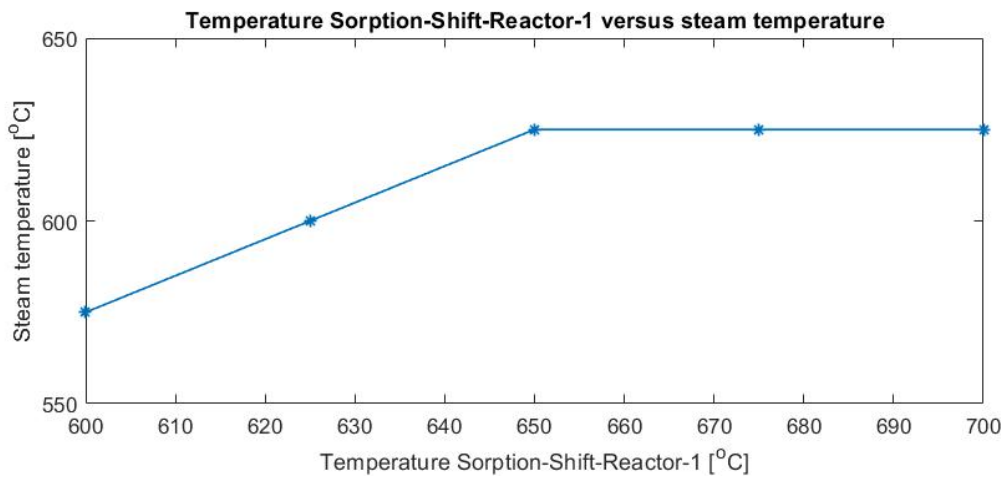


Figure .14: Temperature shift-1 versus steam temperature, obtained from Aspen Plus

Sensitivity analysis regenerator Temperature

Figure .15 shows the heating system, powered by the flue gases. The temperature distribution of the flue gases with a regenerator temperature of 900 °C are displayed in figure .16 and the temperature distribution of the flue gases with a regenerator temperature of 800 °C are displayed in figure .17. Both figures also contain the optimal temperature distribution at the regenerator maximum efficiency point.

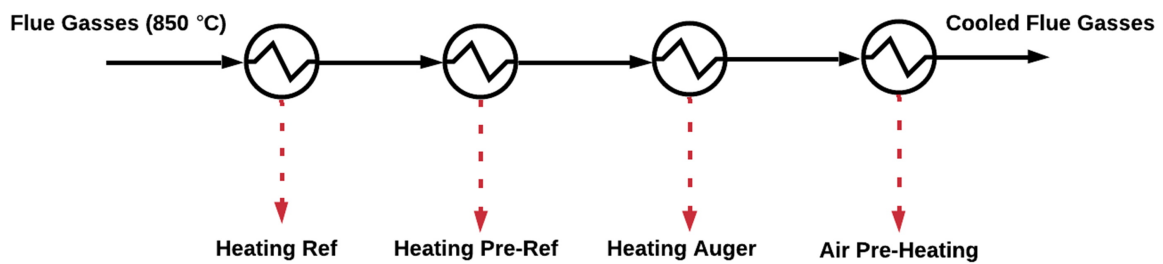


Figure .15: Overview heating using flue gases

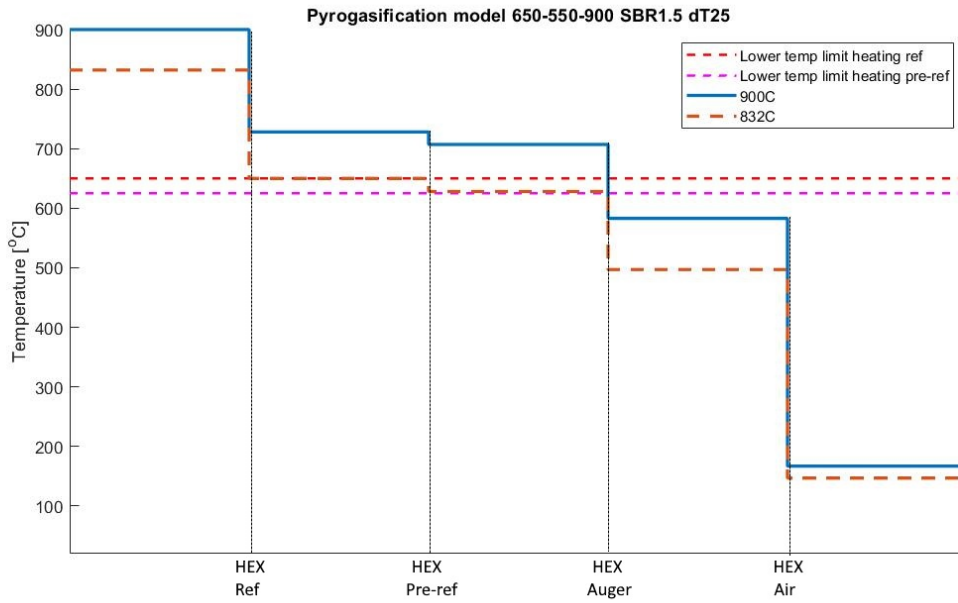


Figure .16: Temperature distribution flue gases at a regenerator temperature of 900 °C, in combination with optimum generator temperature at 832 °C

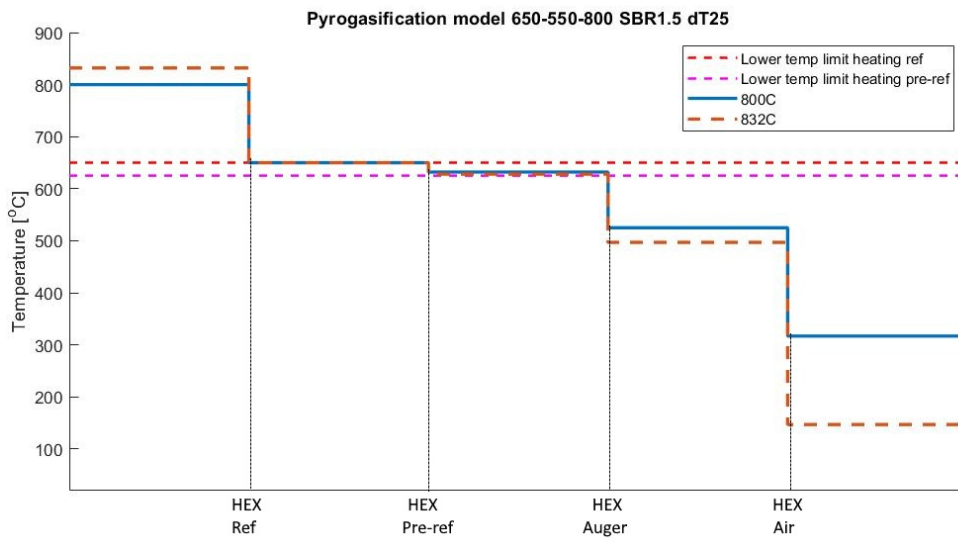


Figure .17: Temperature distribution flue gases at a regenerator temperature of 800 °C, in combination with optimum generator temperature at 832 °C

Sensitivity analysis minimum Pinch Point Heat Exchanges

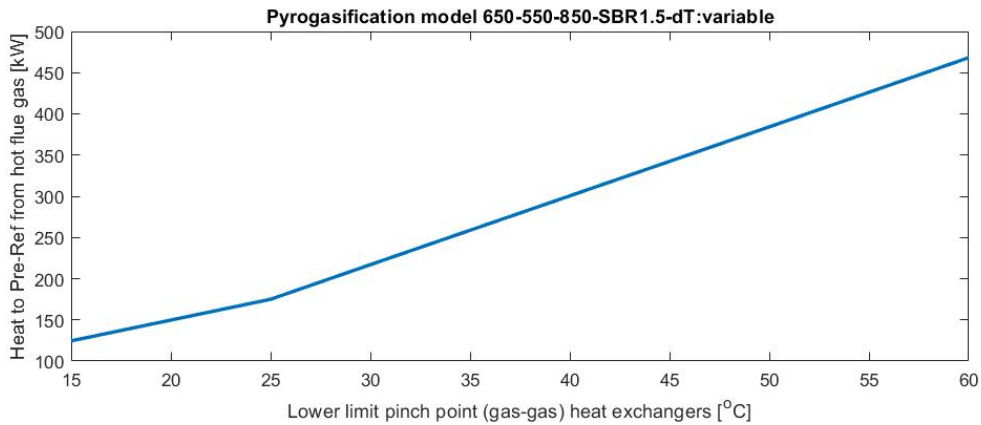


Figure .18: Heat delivered to pre-reformer from hot flue-gases as a function of lower limit pinch point of gas-gas heat exchanger and boilers

Sensitivity analysis SC ratio

Figure .19 further explains the influence of SC ratio on system efficiency. The blue line represents the hydrogen temperature after heat recovery for steam generation. It can be seen that at an SC below 4.6, the hydrogen gas leaving the system still contains a lot of heat, which is not utilized, without the loss of efficiency (even with a slight increase of efficiency), this heat can be used for additional steam generation. The orange line in figure .19 represents additional heating which is required for steam generation. In order to do so, an additional heat exchanger is placed in the model to recycle heat from the hot flue gases coming from the regenerator. In order to supply sufficient heat for steam generation, additional biomass is combusted at an SC of 5.28 and 5.99 respectively to provide the system with sufficient steam at 625 °C. An additional analysis can be performed to find the exact optimal SC, extrapolation of figure .19 results in an optimal SC of roughly 4.64-4.67. heat recovery is capped at 125 °C. Heat exchangers can be further analyzed and optimized to determine maximum (thermal and cost) efficiency operation conditions.

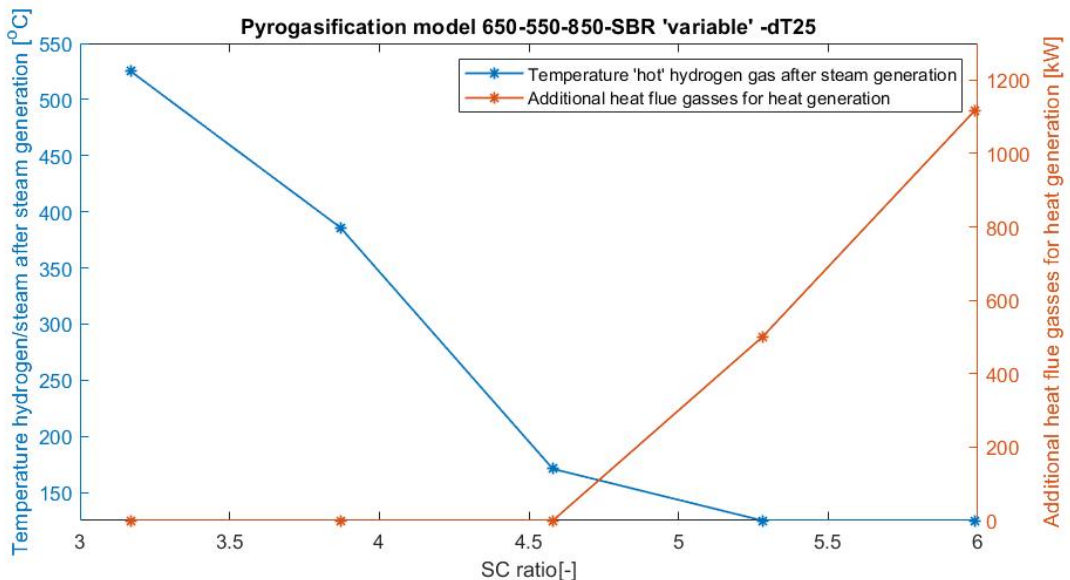


Figure .19: Temperature "hot" hydrogen gas after steam generation versus SBR (left axis) and additional heat required for steam generation versus SBR (right axis)

G Hydrogen fuel specifications for fuel cell applications

Absorption of CO_2 reduces the number of impurities in the produced hydrogen gas by capturing CO_2 directly and CO indirectly. In order to produce high-quality hydrogen fuel, the required purity of the produced hydrogen has to be 99,97 V%. The hydrogen fuel standards are displayed in table .5 [124]. The main components of interest are highlighted in the table: CH_2 , CO_2 , H_2O , and CO are expected to be the main pollutants in the produced hydrogen gas. Nitrogen (air) could also be a pollutant if the biomass is not purged with CO_2 before it enters the auger reactor.

Table .5: Hydrogen fuel quality standards for fuel cells [75]

Component	Max Pollution (PPM)
Hydrogen fuel (total)	300
Water	5
Total hydrocarbons	2
Methane	100
oxygen	5
Helium	300
Nitrogen and Argon	300
Carbon Dioxide	2
Carbon monoxide	0,2
Total Sulfur Compounds	0,004
Formaldehyde	0,2
Formic Acid	0,2
Ammonia	0,1
Total halogenated compounds	0,05

In order to clean the hydrogen gas, different techniques can be used. CO is the hardest species to remove directly. Herefore, a shift-reactor can be used, operating at around 360 C, in combination with a catalyst to "shift" the water-gas-shift reaction towards CO_2 and H_2 . CO_2 can then be removed with a scrubber. Furthermore, adsorption techniques can be required to get the hydrogen gas up to the right quality. Pressure Swing Absorption (PSA) can be one technique to get the required gas specification and to remove pollutants. PSA is used for impurity-removal in current hydrogen production methods using steam-methane reforming [125]. PSA requires elevated pressures. Increasing the pressure of hydrogen is energy-intensive.

H Additional cost analysis

Alternative cost scenario: CO2 taxation implementation

Initially, the price of €1.50 per kg hydrogen is assumed based on current (2020) market prices. But it is safe to assume that hydrogen prices will increase faster than average inflation rates due to change in policies. One of the economic models which are constructed will take CO₂ taxation's into account, with an estimated hydrogen price increase of 10% per year between 2020 and 2030 (up until 2030 CO₂ taxation in the Netherlands will increase yearly). CO₂ taxation will increase hydrogen market prices since the cheapest form of hydrogen is "grey hydrogen" produced by fossil fuels, the production of grey hydrogen results in the release of a large amount of CO₂, if this CO₂ is taxed, grey hydrogen prices increase. From 2021 it is estimated that biochar prices increase by 10 % annually using the same assumptions as for hydrogen prices due to additional CO₂ taxation of fossil fuel-based systems.

It is assumed that the installation will run at 85% at full capacity on a yearly basis, corresponding to 7446 hours per year. Assuming constant prices for the produced product (the prices are not compensated for inflation since the WACC is not inflation-adjusted). This will lead to a yearly income in 2020 as shown in table .6.

Table .6: Product prices and estimated system income in 2020

Product	production rate	price per kg	income/year
Hydrogen	276,3 kg/h	€1.50	€3.085.000 / year
Biochar	874 kg/h	€0.25	€1.627.000 / year
Total income			€4.713.000 / year

If hydrogen and biochar prices increase by 10% on a yearly basis from 2020 to 2030, due to additional CO₂ taxation, the prices and thus yearly system revenues would increase drastically up to a point in 2030 which is displayed in table .7.

Table .7: Product prices and estimated system income in 2030, assuming price increase due to CO₂ taxation's

Product	production rate	price per kg	income/year
Hydrogen	276,3 kg/h	€3.89	€8.004.300 / year
Biochar	874 kg/h	€0.25	€4.219.900 / year
Total income			€12.224.200 / year

This system will, however, still not be profitable over an operational time period of 12 years as can be seen in figure .20. Having a discounted cumulative cash flow over this time period of €-23.048.559 euro. It is important to note that the simulation starts in 2020, with still the low hydrogen prices. The break-even price of hydrogen of the current system is, however, calculated at €4.01/kg hydrogen for the (cost) optimized system, meaning that after 2030 still additional subsidies are required to make the system profitable. The annual price increase of 10% is a rough assumption. If, for example, sustainable hydrogen demand would increase drastically, the prices can increase even further.

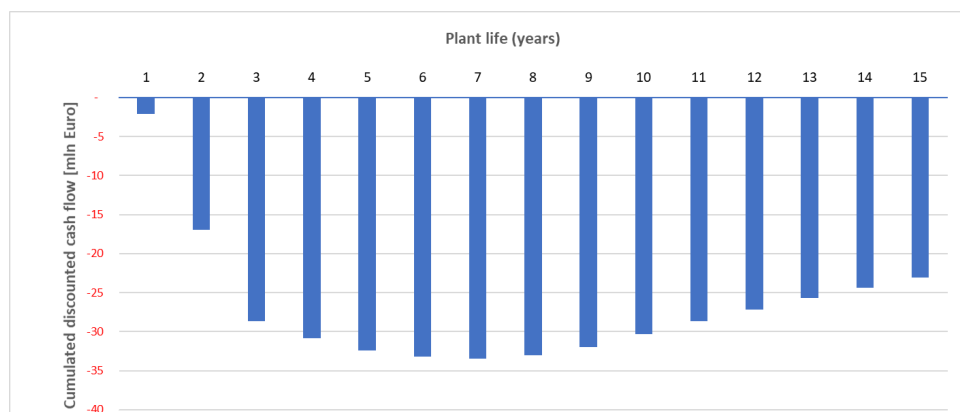


Figure .20: Discounted cumulative cash flows for scenario 2: no subsidies, with CO2 taxation

I Graphs for cost estimation

Figure .21 [69] displays the graph used for cost estimation of reactors . Figure .22 [71] displays the graph used for cost estimation of heat exchangers. Figure .23 [69] displays the graph used for cost estimation of the auger reactor.

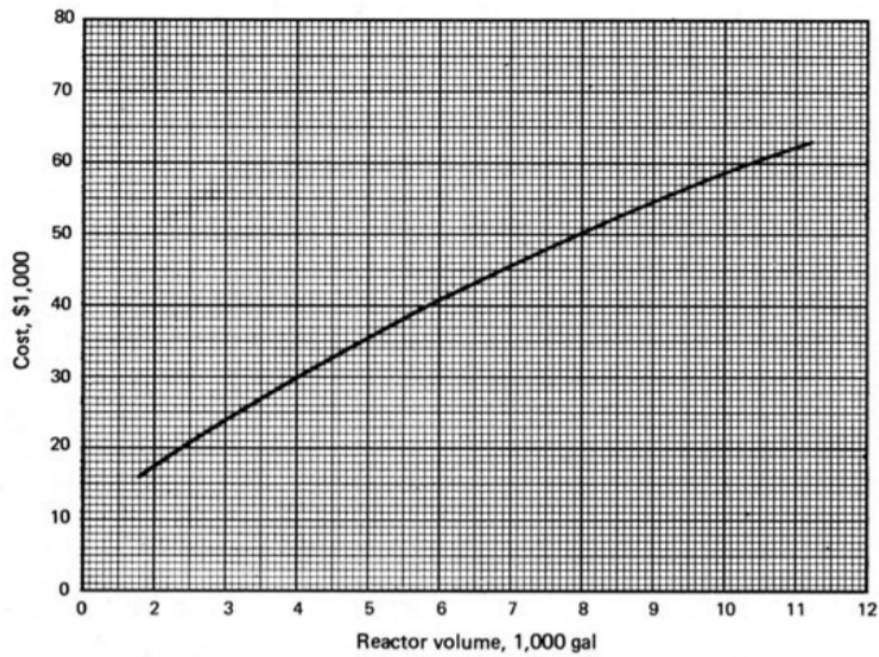


Figure .21: Cost fixed/fluidized bed reactor size dependency [69]

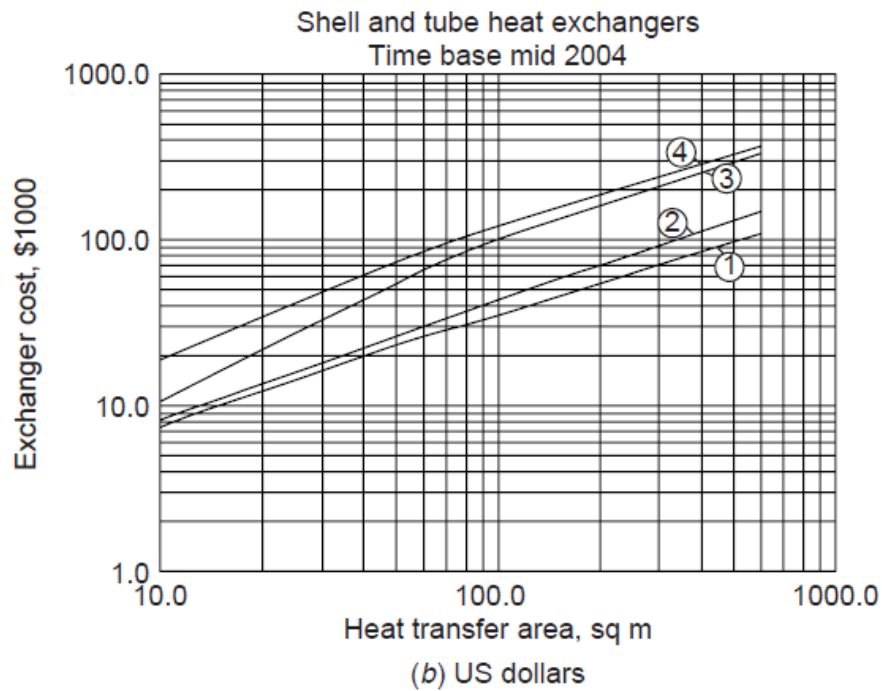


Figure .22: Cost HEX as function of steel type and required surface area [71]

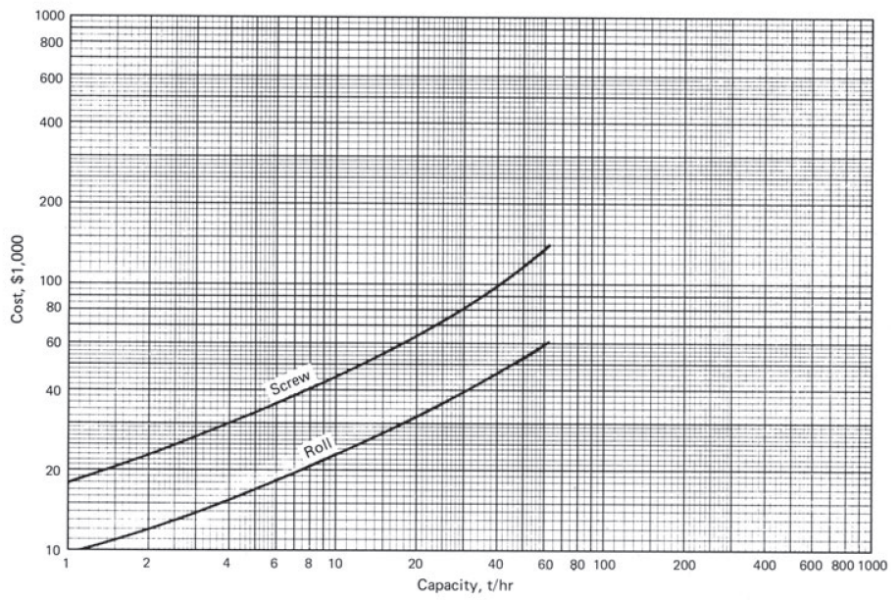


Figure .23: Cost auger reactor dependency on mass flowrate [69]

J Sensitivity analysis OPEX

This appendix will discuss the sensitivity analysis performed with respect to the large (variable) contributors to the OPEX: Biomass purchasing cost, catalyst replacement strategy, and CaO replacement strategy.

Sensitivity biomass input cost

Biomass input costs have been identified as the largest contributor to the capital expenditure: 47% of the OPEX is biomass purchasing cost. The biomass purchasing cost was set at €6.5 per GJ, which translates to 118 €/per kg for the high-quality pinewood which is used in the system, comparable to high-quality wood pallet prices in the current (2020) European market. Since an auger reactor is used for the slow pyrolysis step, lower qualities biomass can also be utilized in the pyrolysis system, also for sorbent regeneration (biomass combustion), lower qualities of biomass can be used in the SEWGS system. In order to determine the influence of biomass cost price on the break-even prices of biochar and hydrogen, a sensitivity analysis is performed where price ranges are from 2 to 8 GJ/kg biomass. Note that for different types of biomass also the simulation should be re-performed due to other compositions (different C/O and C/H ratio, other moisture content, other mineral content). This section will only focus on the variability of biomass cost on hydrogen production prices and not on the effect of different types of biomass on the overall system mechanics.

The influence on hydrogen break-even prices are displayed in figure .24. The expected subsidies on hydrogen (€5,83) + expected market price (€1,50) is displayed as a red line. Typical biomass prices are currently in the €6-8 per GJ range (€4.08 - €4.57 per kg H₂ production cost). When biomass is seen as waste (for example, municipal waste or forest residues), the purchasing cost of biomass can drop significantly, but even when there are no purchasing cost additional subsidies: €1.44 subsidies + €1.50 market price are required to reach a break-even point after 12 years. This is mainly due to the required capital investment, maintenance cost, labor cost, catalyst replacement cost of the reforming system, and overhead costs.

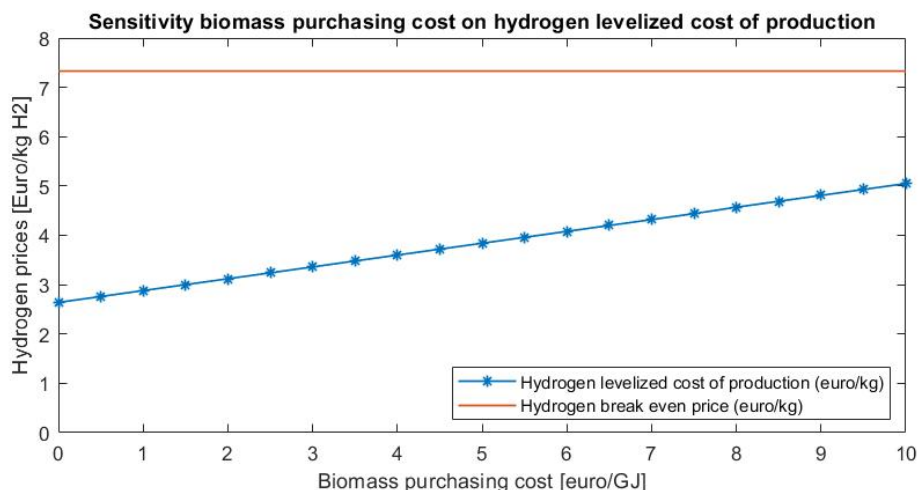


Figure .24: Influence Biomass purchasing cost (€/ GJ) on hydrogen production break even prices, including expected income/subsidies

Catalyst replacement cost

Catalysts are used in the reformer system. Ni-based catalysts are used due to their good tar tracking abilities at a relatively low-temperature range (700-800 °C). Due to heavy oils in the volatile fraction released by slow pyrolysis, coking is one of the main expected problems in the reformer system, deactivating the catalyst, resulting in a required catalyst makeup. Due to the relatively high cost for Ni-based catalyst, this can be significant costs depending on the catalyst replacement strategy. For the pyrolysis system followed by steam reforming processes, there are unknowns with respect to sorbent durability. Sorbent lifetime can be elongated by removing cokes by combustion (adding air/oxygen to the reformers for catalyst reactivation). This can, however, lead to, for example, sintering due to (locally) elevated temperatures. Other (cheaper) catalysts can also be used, for example, calcined dolomite's, which also have good tar cracking abilities.

Figure .25 shows the influence of Ni-based catalyst replacing strategies, varying from four times every month up to once every two years. From 2 times a year up to once every 2 years, there is hardly an influence of catalyst cost on the Levelized Cost of Hydrogen (LCOH): €4.04 to €3.92. It is hard to predict what kind of replacement strategy is required. Due to slow pyrolysis and secondary reactions in the auger reactor, there is a relatively small heavy oil fraction in the

produced pyrolysis oil compared to the aqueous fraction, reducing coking on catalysts. Furthermore, the catalyst of the pre-reformer can be different (with a different replacement strategy) compared to the reformer. Furthermore, there are methods to "reactivate" deactivated catalysts. Another option, when catalyst replacement costs are deemed too high is a combination with the SEWGS system: if, for example, calcined dolomite's are used in the SEWEGS system as CO_2 sorbent, spent sorbent leaving the regenerator can be used as a catalyst for the (pre) reforming system due to the reforming/tar cracking abilities of calcined dolomite's.

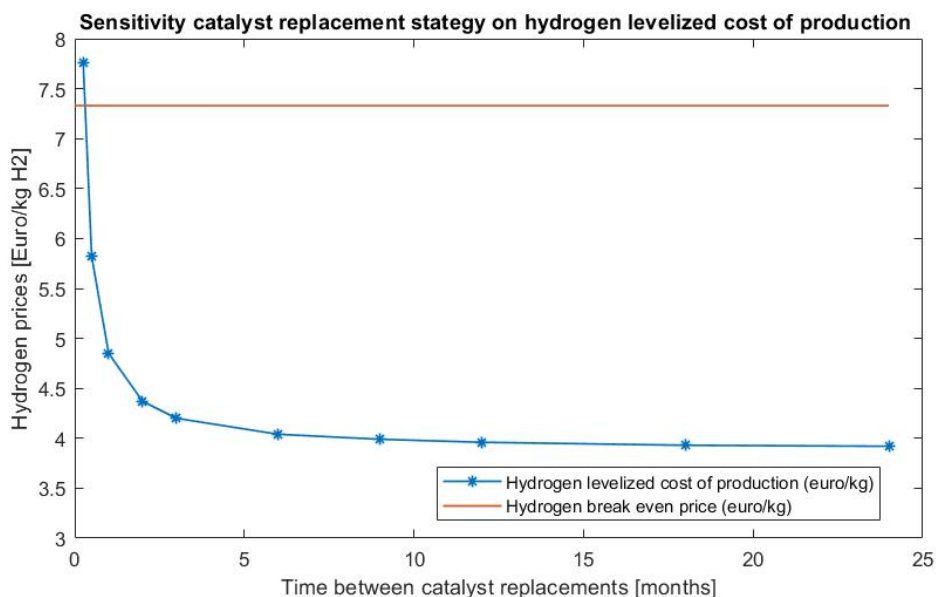


Figure .25: Influence replacement strategy of reforming (Ni-based) catalyst on hydrogen levelized cost of production, including expected income/subsidies

CaO replacement strategy and cost

Under the standard configuration. 10% of the CaO is replaced per cycle to compensate for the activity decay over the multi-cyclic performance of the sorbent. Under the standard conditions, limestone costs are only a small fraction of the operating expenditure: 2 %. This section will analyze if another replacement strategy is selected, there will be a significant change in the Levelized cost of production of hydrogen. Furthermore, limestone prices are also further analyzed. If (relatively long) transport is required from a limestone mine to the installation, limestone prices can increase due to high transportation costs over longer distances. Therefore the system is also analyzed where limestone prices are doubled (from €10 to €20). The results are displayed in figure .26, where replacement strategies are varied from 2% to 100%, the required amount of CaO is calculated according to the model designed for sorbent makeup as discussed in appendix E.

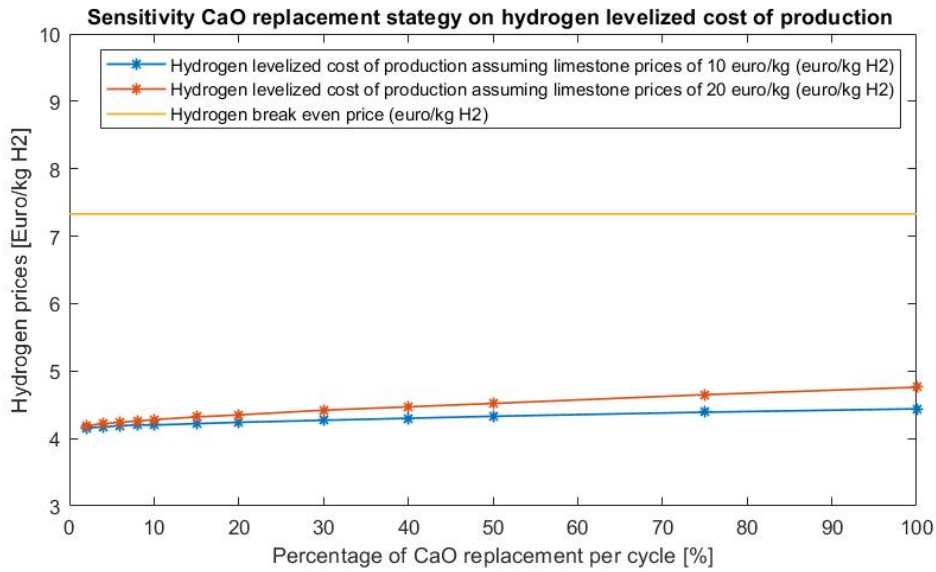


Figure .26: Influence replacement strategy of limestone on hydrogen levelized cost of production, including expected income/subsidies

The cost vary from €4.16 per kg H_2 (2% replacement, €10 per ton) €4.76€per ton (100% replacement, €20 per ton).

Note that besides purchasing cost, the system efficiency is also influenced by the replacement strategy. If more sorbent makeup is implemented, the average activity of the sorbent increases in the system, resulting in less CaO/CaCO₃ being cycled through the system, increasing efficiency and decreasing required biomass purchasing cost. Therefore the negative effect of a more intensive replacement strategy is (partly) undone by the increase in efficiency, but only if the new sorbent can be heated up by using the remaining heat in the spent sorbent. The mechanics of different replacement strategies on overall system efficiency and cost are still unknown and require additional modeling. At this moment, it can be noted, however, that limestone purchasing cost will not have a significant influence on the levelized cost of production of hydrogen in the 2%-20% replacement range, especially when compared to the variability of other variable costs (biomass and catalyst).

K Biomass characteristics related to thermal conversion

There are different types of biomass that can be utilized for waste to energy systems. The properties of woody biomass will be shortly discussed in this section. Furthermore, the effect of biomass properties on thermal conversion characteristics is discussed in this section.

Physicochemical properties and ultimate analyses

Biomass consists out of the following three main elements: Carbon (C), Hydrogen (H), and Oxygen (O). Carbon and Hydrogen have a positive influence on the heating value, while oxygen has a negative influence on the heating value of a biomass species. Compared to fossil fuels, biomass contains a lot of oxygen, resulting in lower heating values; this is shown in a Van Krevelen diagram in figure .27 where the O/C and H/C ratios of several solid fuels are plotted [126].

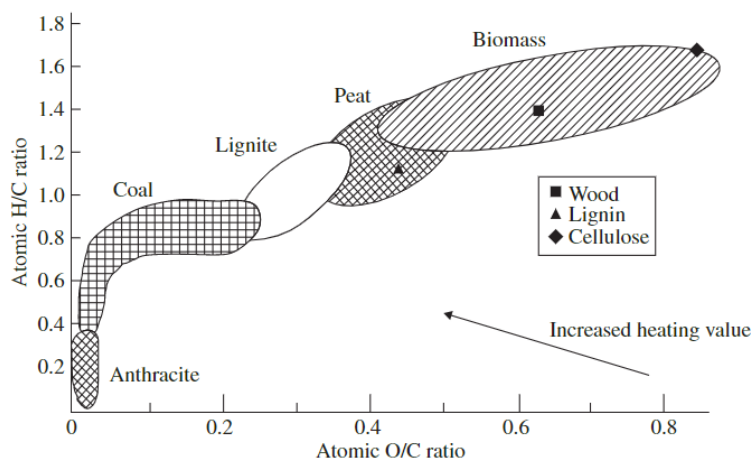


Figure .27: Van Krevelen diagram solid fuels [126]

Other elements which are in minor concentrations present in biomass are nitrogen (N), chlorine (Cl), sulfur (S), Fluor(F), potassium (K), sodium (Na), magnesium (Mg), calcium(Ca) and phosphorus(P). Nitrogen can cause NO_x emissions, and both chlorine and sulfur can cause catalyst poisoning during catalytic cracking of biomass; other minerals can be traced back in the ashes after thermal treatment of biomass [126].

An ultimate analysis is used to determine the elemental composition (H, C, O, and N) and the ash content of biomass. During an ultimate analysis, biomass is combusted using oxygen, and helium is used as a carrier gas; the produced flue gases are led over copper to ensure complete conversion of flue gases to N₂, H₂O, SO₂ and CO₂ respectively. H₂O, SO₂, and CO₂ are absorbed in columns, and nitrogen is detected by a thermal conductivity detector (TDC). Next, the absorbed gases are released and measured by the TDC to determine the H, C, and S content. Finally, the O content can be calculated assuming full conversion to H₂O, SO₂ and CO₂ [126].

Structural organic components and proximate analysis

The structural cell wall composition of biomass, which originates from plants, mainly consists out of cellulose, hemicellulose, and lignin. Cellulose is the most common material in woody biomass, which normally consists of 40-50 wt% out of cellulose. Cellulose can be represented by the chemical formula: (C₆H₁₀O₅)_n which is a homopolysaccharide of glucose (C₆H₁₂O₆) [126]. Hemicellulose makes up for about 25 -35 wt% of woody biomass and is a combination of both C₆ and C₅ sugars strung together, cell walls in woody biomass are made out of hemicellulose. Lignin makes up for about 20-30 wt% of woody biomass and forms together with hemicellulose the cell walls and cementing material between cells [126]. Lignin is relatively stable during thermal treatment of biomass and has a larger HHV compared to hemicellulose and cellulose, which indicates a lower O/C ratio, which can be seen back in the complex structure of lignin, which contains a lot of double (C=C) bonds.

A proximate analysis can be used to determine the moisture, volatile matter, fixed carbon, and ash content of biomass. Moisture is necessary to sustain life for any living organism. In biomass, both free and inherent moisture is present. To determine the moisture content of biomass, a biomass sample is put on a scale and heated for 24h at 105 °C this removes all the moisture present in the biomass. Measuring the weight before and after drying yields the moisture content. This can be both expressed relative to the dry or wet weight of biomass. To determine the volatile matter

concentration, biomass is heated to 550 °C which releases all the volatiles (in stable fuels) in the form of gases and fluids (tars), weighing the biomass before and after this process yields the volatile matter content. The ash content is determined by weighing the sample after complete combustion and comparing it to the original dry weight. Finally, the fixed carbon content can be determined by subtracting the mass of volatile matter and ash from the dry matter content.

Biomass type and characteristics

The type of biomass that is used has a large influence on the process and on the produced gas. The following biomass properties influence the gasification process significantly [13]:

- The chemical composition: the amount of cellulose, hemicellulose, and lignin, respectively
- Moisture content
- Physical qualities: Particle size, shape, and density

Other biomass properties which could also influence the pyrogasification gas yield of biomass are:

- Elemental composition
- Inherent mineral content
- Amount of volatile matter

The main cell wall structural components of biomass are cellulose, hemicellulose, and lignin. Cellulose decomposes at higher temperatures compared to hemicellulose: during a proximate analysis, cellulose decomposition peaks at around 350 °C while hemicellulose decomposition rates peak at around 275 °C [126]. Lignin is relatively stable during thermal conversion and mostly decomposes at higher temperatures. A weight-loss graph of biomass during a proximate analysis is given in figure .28 [126] where both the Derivative ThermoGravimetry (DTG), which relates to decomposition rate and ThermoGravimetry (TG), which relates to the total measured mass, are plotted. The observed peaks correspond to maximum cellulose and hemicellulose decomposition.

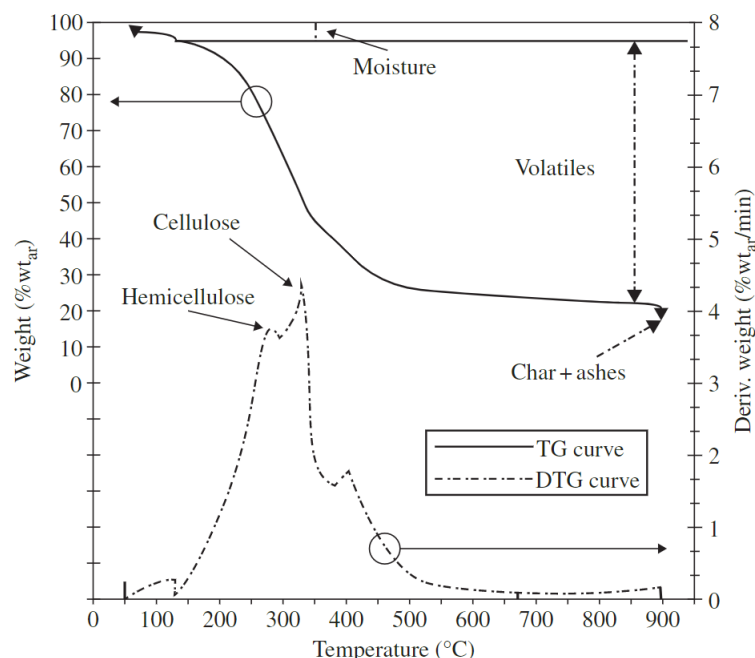


Figure .28: Proximate analysis of biomass showing DTG and TG curve and corresponding temperature regions of cellular thermal decomposition [126]

The gas yield composition is also dependent on the share of cellulose, hemicellulose, and lignin present in the biomass. Depending on the type of biomass that is used, the ratio of these components differ. The gasification of each individual component has been studied by Hanaoka et al. [127] which used steam-air gasification to gasify the isolated components. During the experiments, a temperature of 1173K, ER of 0,3, $[H_2O]/[C]$ molar ratio of 10 (can be related to SBR), and a residence time of approximately 0,7 seconds was used. No catalysts were used during the experiments. The

results are displayed in table .8. After the gasification of the pure components, the gas composition was compared to the fuel gas composition of Japanese Oak and Japanese Red Pine and concluded that it is possible to predict the gas composition based on the share cellulose and lignin, respectively.

Table .8: Gas yield in mol % from the air-steam gasification of biomass components

Component	CO	CO ₂	H ₂	CH ₄	C ₂ H ₄	1 - C ₄ H ₈
Hemicellulose	24,8	35,6	32,4	5,2	1,0	1,0
Cellulose	35,5	27,0	28,7	6,5	0,7	1,7
Lignin	25,8	35,7	32,1	5,0	0,6	0,7

The moisture content in biomass has a large influence on the LHV of biomass and has a negative influence on the efficiency of thermal treatment of biomass as can be shown in equation .30 [13]. As the amount of moisture increases, more heat needs to be added to the system for water evaporation, while both the LHV of the biomass and the amount of produced hydrogen decreases.

$$efficiency \% = \frac{nH_2 \cdot LHV_{H_2} - Q_{in}}{LHV_{biomass}} \times 100 \quad (.30)$$

The moisture which is present in biomass could, however, serve as steam, which enhances the gasification process as discussed in section 2.2.4 where an SBR of 1,5 was found to be optimal for steam reforming of biomass, tar, and methane to enhance hydrogen production. An SBR of 1,5 corresponds to a moisture content of 60% in biomass when biomass moisture is used for steam production. When "biomass moisture" is used instead of external steam, the process is called self-moisture gasification. During conventional steam gasification, biomass is dried before steam gasification; this required both heat for drying and steam production. During self-moisture gasification, these two process steps are done simultaneously, reducing the energy requirements of the system [128].

Physical qualities of biomass correspond to the sphericity and particle size of the used biomass, which both relate to the heating rate. Particle sphericity can be determined according to the ratio of the "ideal surface area/actual surface area" if a particle with a given volume were spherical surface area is divided by the actual surface area as shown in equation .31. Increasing the particle size and increasing the particle sphericity reduce the heating rate of the used biomass. Research performed by Herguido et al. [129] compared the steam gasification of sawdust particles with a mean diameter of 500 µm with wood chips of 2 x 5 x 10 mm. For gasification temperatures of 780 °C they found that sawdust yielded 1,2kg of syngas per kg of biomass compared to 0,7 kg syngas/kg biomass for the wood chips. This difference in syngas yield was mainly attributed to the amount of char conversion as a function of particle size: when small particles are used, the surface area of the produced char is large compared to the volume. When large biomass particles are used, assuming a shrinking-core model, the surface area/volume ratio is much lower compare to small particles, resulting in less char reforming. This difference in char conversion has also been measured by Herguido. et al.: ± 20 % char production for wood chips compared to ± 10% char production for sawdust particles, confirming the above theory [129].

$$\phi_s = \frac{\pi^{\frac{1}{3}} (6 \times V_p)^{\frac{2}{3}}}{A_p} \quad (.31)$$

L Alternative Hydrogen production processes out of biomass: biological and SCWG

There are different techniques to convert biomass into hydrogen. Biomass consists of roughly 6 wt % hydrogen [130] which seems relatively low, hydrogen has; however, a much larger Lower Heating Value (LHV) compared to fossil fuels: 2,4 times higher than methane and four times higher than coal [130]. There are two main routes to convert biomass into hydrogen: Thermal chemical conversion and biological conversion. Thermal conversion is based on heating and cracking biomass, while biological conversion is based on hydrogen-producing enzymes.

Thermal-chemical hydrogen production from biomass can be further split up into three subcategories: 1. Pyrolysis 2. Gasification, and 3. Supercritical water gasification (SCWG). Biological conversion methods for hydrogen production out of biomass can also be categorized into three subcategories: 1. Fermentative hydrogen production, 2. Photosynthesis processes, and 3. Biological water gas shift reaction (BWGS). Figure .29 gives an overview of the different conversion techniques to produce hydrogen out of biomass.

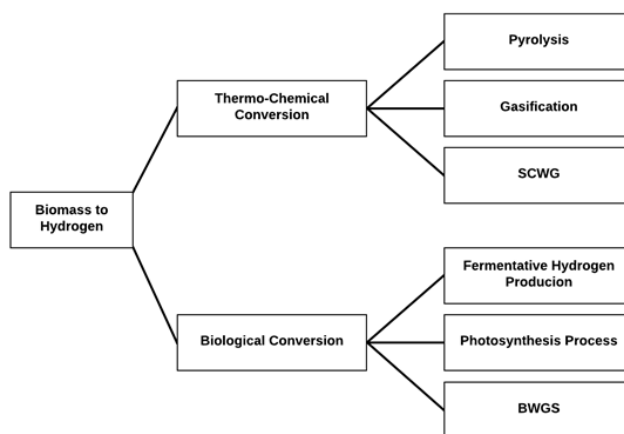


Figure .29: Biomass to hydrogen conversion techniques

Biological conversion will be discussed in this section as well as SCWG. Pyrolysis and gasification for hydrogen production are elaborately explained in the main report since this forms the basis of the pyrogasification system.

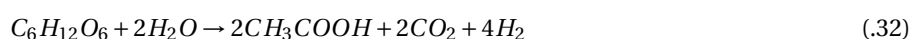
Fermentative Hydrogen Production

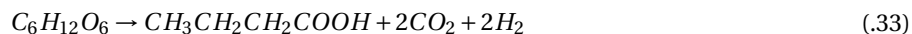
Fermentative hydrogen production can be realized in the absence of light: dark fermentation or with the help of light: photofermentative hydrogen production [130, 131]. Both processes will be discussed shortly in the next sections.

Dark fermentation has several advantages above other biological methods of hydrogen production. Dark fermentation does not require energy from light, has lower energy demands, and requires moderate process conditions (process temperatures)[131]. Furthermore, dark fermentation can be used to process a large variety of waste, varying from food industry waste (frying fat, slaughterhouse waste) to manure and sewage sludge. Dark fermentation can therefore serve a double purpose as both waste disposal and energy generation [131]

Bacteria used for dark fermentation can be categorized based on their oxygen requirement, bacteria which work strictly in an environment without oxygen are called obligate anaerobes, bacteria which can work either in an environment with or without oxygen are called facultative anaerobes [131]. The bacteria can be further classified based on their temperature requirement, which can either be ambient temperatures: mesophiles or elevated temperatures: thermophiles [131]. In practice, obligate anaerobic bacteria are used for hydrogen production because these bacteria can utilize a wide range of different types of feed (waste) and have a higher hydrogen production rate. Facultative anaerobic bacteria are, however, easier to handle and are reported can survive in higher hydrogen concentrations. In practice, mixed cultures of bacteria are used to enhance gas production and to ferment complex structures.

Fermentation is a process that does not require oxygen; several chemical processes occur in bacteria in order to regenerate ATP, as by-product alcohols and acids are formed as well as hydrogen. Since most organic matter used for fermentation are complex hydrocarbons, the first step during fermentation is hydrolysis to produce glucose. Chemical reactions that occur during dark fermentation of glucose are shown in equations .32 and .33. It is important to note that glucose first reacts to pyruvate before acetate (equation .32) or butyrate (equation .33) are formed.

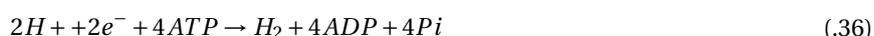




acids which are formed during dark fermentation could be further processed by photofermentative bacteria according to formula .34 in a two-stage process. It is important to note that the reaction displayed in equation .34 cannot happen simultaneously with dark fermentation, and therefore multiple reactors are required for a two-stage process.



Photofermentative hydrogen production occurs in purple non-sulphuric bacteria. Photosynthetic bacteria produce chemical energy: a proton gradient; this proton gradient can be used by the enzyme Nitrogenase which leads to the production of ammonia and the production of hydrogen [131]. In the absence of nitrogen, nitrogenase can still produce hydrogen. The chemical reactions by nitrogenase are shown in equations .35 (with nitrogen) and .36 (without nitrogen). Photofermentative hydrogen-producing bacteria converse under limiting nitrogen conditions organic acids to hydrogen almost stoichiometrically. Both processes require a lot of additional energy, which is provided by sunlight.

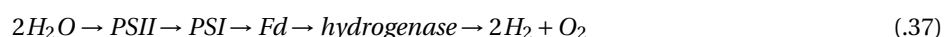


The main advantages of photofermentative hydrogen production are that the process is irreversible since a catalyst (nitrogenase) is used. Furthermore, photofermentative hydrogen production can be used as a second stage reaction step for dark fermentation where otherwise unusable substrates can be further fermented into hydrogen[131]. The disadvantages of photofermentative hydrogen production are that it requires light, resulting in problems with self-shading and leads to the requirement of transparent yet impermeable hydrogen reactors; furthermore, the light conversion efficiency is low[131].

In practice, biogas installations are operational, but not with the aim to produce hydrogen. Hydrogen is produced in these installations; however, hydrogen is then used as a product to react with CO_2 to form methane, which is the main product produced by biogas installations.

Photosynthesis process for hydrogen production

Green algae and cyanobacteria can be used for the production of hydrogen, based on the photosynthesis process [130, 132]. During photosynthesis, light can be absorbed during two different processes: PSII and PSI. PSII is a water splitting, and O_2 evolving processes [132] while PSI generates a reductant for carbon dioxide, which is then used for the formation of large carbon chains [132]. Per photosystem, a photon is used for the removal of an electron from water used for H_2 and CO_2 reduction, respectively. In conventional photosynthesis, only PSI is used due to the lack of hydrogenase enzymes, but some green algae and cyanobacteria have this enzyme and can produce hydrogen based on the photosynthesis process: biophotolysis. The reaction steps for biophotolysis are displayed in equation .37, here Fd is ferredoxin, which acts as an electron carrier.



The photofermentation process described in the previous chapter can also be classified as photosynthesis hydrogen production.

Biological water gas shift reaction

The water-gas shift reaction has already been described in the introduction, which is an equilibrium reaction between carbon monoxide (CO), water (H_2O), and hydrogen (H_2 and carbon dioxide (CO_2) according to equation .38. During thermal treatments of biomass, fuel gas is produced containing the gases necessary for the water gas shift reaction; high temperatures/pressures are, however, required for a sufficiently high conversion rate. There are some bacteria (photo heterophilic bacteria) that can produce H_2 out of CO, based on a biological water-gas shift reaction. After pyrolysis or gasification, fuel gases have, however, already a sufficiently high temperature for an efficient water-gas shift; however, this is still an equilibrium reaction resulting in a fraction of CO in the fuel gases.



Super Critical Water Gasification

Super Critical Water Gasification (SCWG) is a process that can be used for biomass feed with a high moisture content (>50 wt%), for example, sewage sludge, paper sludge, or even algae [130]. Super critically water ($T > 374\text{ }^{\circ}\text{C}$ and $P > 22,1\text{MPa}$) is completely miscible with organic substances and gases, and therefore drying of biomass can be avoided when SCWG is used [130]. The main disadvantage of SCWG is the high energy cost of the system to produce super-critical water, and therefore economic efficiency becomes a large obstacle for the technology [133].

Some advantages of SCWG are listed below [130, 133]

- High reactions rates
- No limit of interphase mass transfer resulting in fast and complete reactions
- Possibility of post-reaction separation by adjusting temperature/pressure
- During the reaction heat transfer characteristics are better compared to "conventionall" gasification with gas-solid and gas-liquid reactions.
- SCWG has a relatively low coke, tar, and char formation compared to conventional gasification

M Societal analysis bar graphs CO2 footprint

For the different analyzed systems, including and excluding greenhouse feeding of flue gases, bar charts have been made to visualize the CO_2 footprint for these scenarios.

Figure .30 shows the CO_2 footprint of the pyrogasification SEWGS system without greenhouse feeding, and figure .31 shows the CO_2 footprint of the pyrogasification SEWGS system with greenhouse feeding.

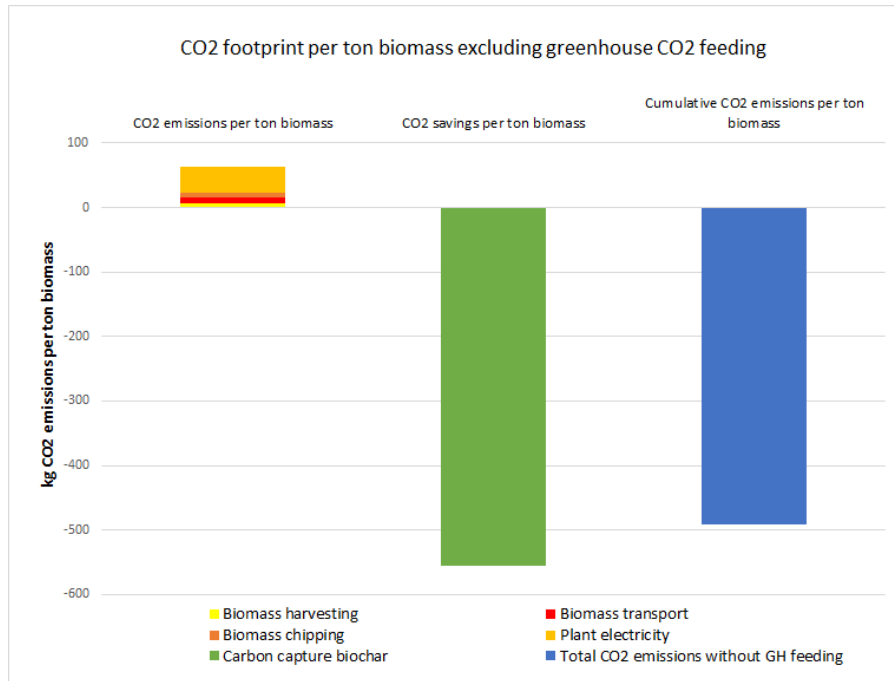


Figure .30: CO2 footprint with no greenhouse feeding

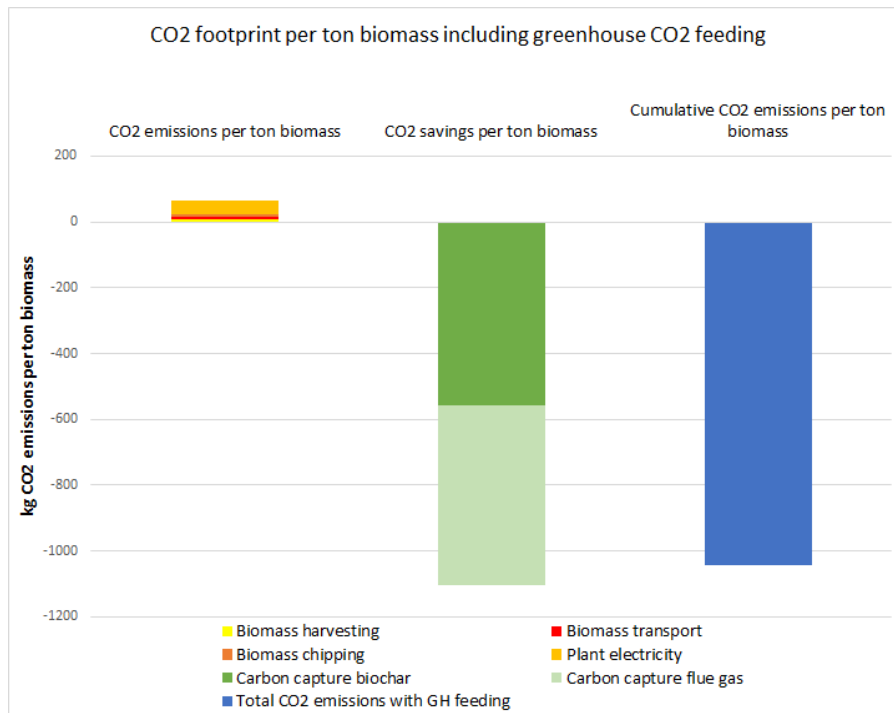


Figure .31: CO2 footprint with greenhouse feeding

N Paper draft:Techno-economic analysis of a novel pyrogasification-sorption-shift system for the production of a high purity hydrogen and high quality biochar out of biomass

This appendix contains a draft which for a research paper which has been written. The aim of this research paper is to discuss the technical and economical feasibility of the designed system, focus sing on the oxy-fuel system. This research paper helps substantiates the written research proposal for further research.

Paper (draft, to be reviewed)

University of Twente

Techno-economic analysis of a novel pyrogasification-sorption-shift system for the production of a high purity hydrogen and high quality biochar out of biomass

Jesse Buiteveld, Eddy Bramer, Gerrit Brem

University of Twente

Department of Thermal and Fluid Engineering

corresponding author – e-mail: e.a.bramer@utwente.nl

A novel system is developed for the production of high purity hydrogen and high quality biochar out of biomass. The novel system uses a combination of pyrolysis in an auger reactor for high quality biochar production, gasification and finally a system based on Calcium Looping (CaL) based Sorption-Enhanced-Water-Gas-Shift (SEWGS) for high purity hydrogen production out of syngas. In the SEWGS system CO₂ is captured using CaO, and the water-gas-shift reaction is shifted into the direction of H₂ and CO₂. Heat required for endothermic sorbent regeneration is supplied by oxy-fuel combustion of biomass to produce a concentrated stream of CO₂ suited for carbon capture and storage. The SEWGS system is uncoupled from the gasification system so that ideal process temperatures can be reached for both processes. The designed system is simulated in Aspen Plus, and a financial model is designed for cash flow simulations to determine the economic system feasibility. The analyzed system produced 202.4 kg biochar (HHV=34.2 MJ/kg) and 52.4 kg hydrogen (99.6 vol% H₂) per ton of biomass input (dry and ash free). The system efficiency based on chemical energy is 72.5%. The levelized cost of hydrogen (LCOH) of the designed system are in the €2.94-4.42 range, which are significantly lower compared to high purity hydrogen production using electrolysis. Further research is required with respect to CaL based SEWGS reactor kinetics, sorbent durability improvement and with respect to auger reactor upscaling.

KEYWORDS: Hydrogen, Biochar, Calcium Looping, Auger Reactor, Pyrolysis, Gasification, Steam Reforming, Sorption-Enhanced-Water-Gas-Shift, Heat Integration, Biomass, Pre-combustion Carbon Capture, Carbon Capture and Storage, Aspen Plus, Cash Flow Simulations, Financial Analysis

1. INTRODUCTION

The Paris agreement came into force in 2016, which currently (2021) has been ratified by 190 different parties, including the USA. The Paris agreement aims to limit global warming up to 1.5 °C compared to the pre-industrial level. In order to reach the goals set by the Paris agreement the share of renewable energy sources should increase significantly, replacing fossil fuels to reduce carbon emissions. Recent efforts to pursue climate change mitigation have resulted in a significant increased share of solar and wind energy. Solar and wind energy are intermittent renewable energy sources, when large shares of intermittent energy sources are implemented this can result in a mismatch between energy supply and demand. In order to solve this mismatch supply side management (SSM) is required.

Sustainable SSM uses sustainable dispatchable energy sources, for example: hydropower, energy storage and biomass. It is expected that in the future energy economy, hydrogen will play a large role both as energy carrier, raw material for the chemical industry and as energy storage medium: the so

called ‘hydrogen energy economy’. The most obvious route for sustainable hydrogen production is based on electrolysis using (overproduction) of solar and wind power, currently a lot of effort is put in the realization of large scale sustainable hydrogen production plants, mostly based on wind power combined with Polymer Electrolyte Membrane (PEM) electrolysis. In the future hydrogen energy economy a hydrogen gas grid can be implemented, comparable to the natural gas grid for hydrogen transportation [1].

This research focusses on an alternative method based on thermal conversion processes of biomass for the production of high purity hydrogen combined with the production of a high quality biochar and Carbon Capture and Storage (CCS). When hydrogen of similar quality compared to (PEM) electrolysis is produced, the same distribution network (gas-grid) can be used, reducing cost. A by-product of electrolysis is oxygen (O_2) which can be used as oxidant for biomass gasification processes.

Biochar can be used as soil amendment for carbon sequestration and for soil quality improvement [2,3]. Furthermore high quality biochar can be used for pollutant removal from gasses (activated carbon replacement) or even as carbon black replacement for fillers in (low quality) rubbers [2,4]. In this study a novel system is analyzed for biomass based hydrogen and biochar production based on a combination of different thermal conversion methods for biomass (derived) products. A combination of pyrolysis, gasification and sorption-enhanced water-gas-shift is analyzed to produce these high quality products.

1.1 Pyrolysis

Pyrolysis of biomass is a thermal conversion method, which processes biomass at elevated temperatures in an inert atmosphere, pyrolysis is an endothermic process. Pyrolysis produces three main products: gasses, tars and char, during pyrolysis volatiles (tars and fuel gases) as well as moisture are released from the biomass species, while fixed carbon remains solid in the form of biochar [5,6]. General pyrolysis mechanics are displayed in equation 1 [5]. This research focuses on pyrolysis, with slow to intermediate heating rates. The released volatiles by biomass pyrolysis can be further processed for the production of high purity hydrogen, produced biochar can be separated and captured. The most important key process parameters for the production of a high quality biochar are pyrolysis heating rate and pyrolysis temperature[5–7]. Under increased pyrolysis temperature gas yield increased while oil and char yield decreases, as is displayed in Fig.1. [6] Under elevated temperature the biochar quality increased resulting in an increased Higher Heating Value (HHV) and decreased O/C and H/C ratios in the biochar species as displayed in Fig.2 [6]. Under elevated heating rates biochar quality increased, Demibras et al. [7] found that under a pyrolysis heating rate of 100K/s biochar with HHV=35MJ/kg was produced out of biomass while at a heating rate of 2K/s a biochar with HHV=29 MJ/kg was produced.

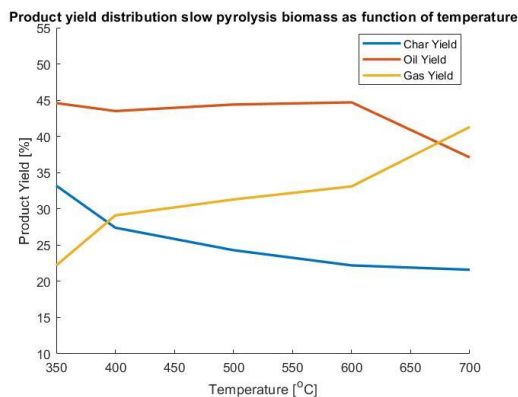


Figure 1: Slow pyrolysis temperature versus product distribution

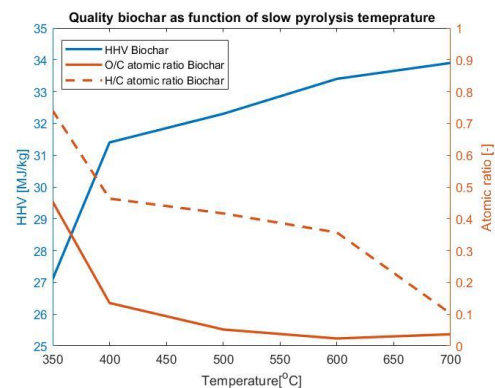
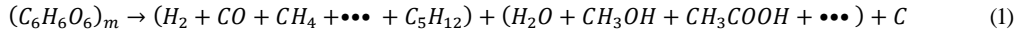
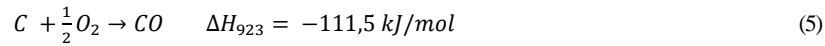
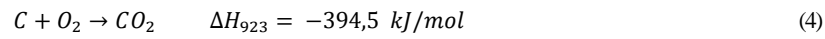
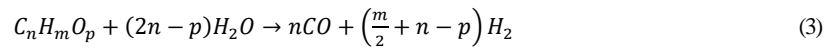
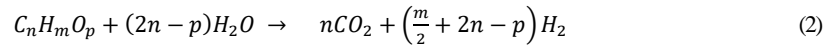


Figure 2: Slow pyrolysis temperature versus biochar quality



1.2 Gasification and steam reforming

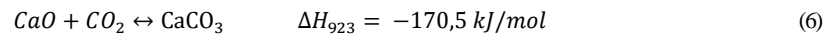
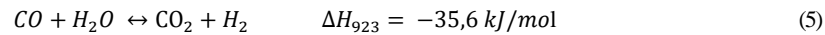
Gasses and tars produced by (slow) pyrolysis can be further processed using a reforming or gasification process in order to converge the produced volatiles into a hydrocarbon free syngas, consisting of CO, CO₂, H₂O and H₂ [8,9]. Both steam reforming and gasification are based on the same principal: introducing an oxidant (steam of oxygen) to further crack hydrocarbons into smaller molecules. General steam reforming mechanics are displayed in equations 2 and 3 [10], steam reforming is an endothermic process. General oxidation mechanics are displayed in equation 4 and 5 [10], oxidation is exothermic.



Steam reforming and gasification processes can yield a hydrogen rich syngas. The key process parameters for the production of a high purity hydrogen using reforming/gasification is temperature [8,10–14]. Elevated temperatures increase tar cracking and reforming reactions, increasing hydrogen production rate. Research by van Rossum et al.[9] on catalytic steam reforming of pyrolysis oil showed that under reforming temperatures above 750 °C a hydrocarbon free syngas can be produced. Steam to Carbon (SC) ratio is an important key process parameter for steam reforming processes influencing both hydrogen yield and system thermal efficiency, a SC ratio for reforming processes in the range off 3-4.5 results in optimal process conditions [8,15]. Catalyst selection influences tar cracking abilities of gasification/reforming processes as well, nickel based catalysts and dolomites are catalysts which can be used for gasification processes for hydrogen production, the optimal temperature range for Ni-based catalysts is in the 700-800 °C range while the optimal temperature range for dolomites is in the 800-900 °C range [16].

1.3 Sorption enhanced water gas shift system based on Calcium Looping

A combination of gasification with carbon capture can increase hydrogen yield and hydrogen purity. One of the promising methods for pre-combustion carbon capture is based on Calcium Looping (CaL) which uses calcium oxide to capture CO₂. When CO₂ is captured this increases hydrogen purity in two ways: 1. Removal of CO₂ from the syngas directly and 2. Shift the Water-Gas-Shift (WGS) reaction (equation 5), such that CO reacts to CO₂ which is then captured indirectly. The general reaction for carbon capture (carbonation) using CaO is displayed in equation 6. From a hydrocarbon free syngas, calcium looping based Sorption Enhanced Water Gas Shift (SEWGS) has the possibility to produce high purity hydrogen, comparable with hydrogen produced by PEM electrolysis [17].



The strength of CaL based system lies with the reversibility of the carbonation/calcination reaction. The CaO/CaCO₃ equilibrium pressure is dependent on temperature. When the equilibrium pressure is below the CO₂ partial pressure carbonation takes place, when the equilibrium pressure is above the CO₂ partial pressure, calcination (regeneration) of the sorbent takes place. Figure 3 displayed the CaO/CaCO₃ equilibrium pressure as well as a typical syngas partial pressure under 1 atm, and displays the temperature range for carbonation and calcination reactions respectively [10]. When the aim of the CaL SEWGS system is to produce high purity hydrogen carbonation temperatures in the 500-600°C range are required

One of the most studied process configurations for hydrogen production based on CaL is sorption enhanced gasification, with *in situ* carbon capture [8,10,13–15,18–20]. In *in situ* carbon capture both gasification and carbon captures takes place in the same reactor at a temperature of 600-750 °C. Sorption enhanced gasification has several benefits: heat released from exothermic carbonation can be used for the gasification system, CaO acts both as sorbent and as catalyst, the system requires a relative simple process configuration (dual circulating fluidized bed). In such a system the formed CaCO₃ is led to an regenerator which operates at 800-900 °C to regenerate sorbent, heat is supplied by combustion of circulated char.

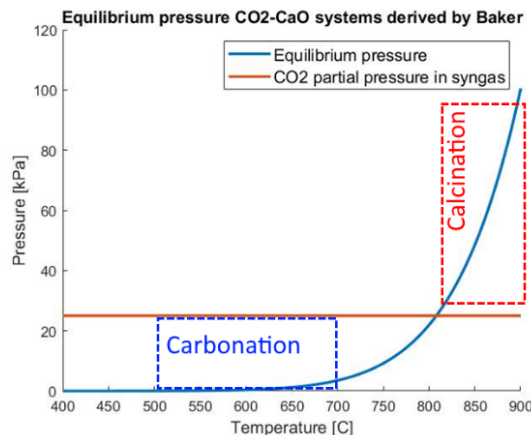


Figure 3: CaO/CaCO₃ equilibrium pressure versus CO₂ partial pressure in syngas under atmospheric pressure.

Fig.4 displayed the influence of temperature on hydrogen yield of different gasification processes [8,10–14]. Two different area's can be identified in Fig.4: 1. Sorption enhanced gasification and 2. Steam reforming.

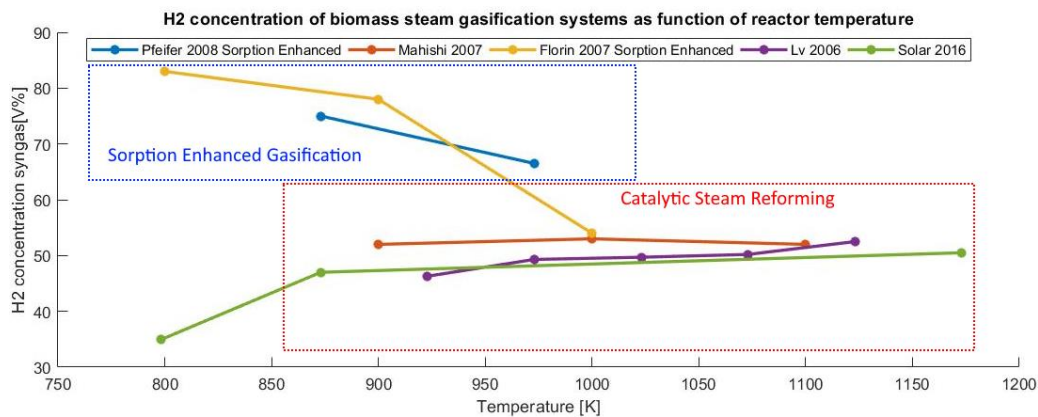


Figure 4: Hydrogen concentration syngas as function of temperature for sorption-enhanced gasification system and catalytic steam reforming systems

Steam reforming has an optimal temperature range (based on thermal efficiency) of 750-800 °C, which will lead to high hydrogen purities, but without a large energy penalty compared to temperatures in the 1000-1100 °C range (in this temperature range the process is less dependent on tar cracking catalysts). From figure 4 it can be seen that sorption enhanced gasification produces a higher purity hydrogen in the 70-80Vol% range, but this is not yet close to hydrogen purities produced by PEM electrolysis (>99,5Vol%). For sorption enhanced gasification a compromise has to be made with respect to ideal temperature for gasification (>750 °C) and ideal temperature for high purity hydrogen production based on sorbent/CO₂ equilibrium (T<600 °C). Under high temperatures, which are ideal for tar cracking no CO₂ can be captured due to high equilibrium pressures at these temperatures, at low temperatures, ideal for high CO₂ absorption rates, tars are insufficiently cracked resulting in ‘pollutants’ (tars, CH₄, C₂H₄, C₂H₆ etc.) in the hydrogen rich gas. Sorption enhanced gasification can be especially of great interest for the chemical industry, where a tailored syngas is in many cases required (instead of pure hydrogen), for example for methanol production.

In order to produce a high purity hydrogen out of syngas the system configuration is the most important process parameter of a SEWGS system. For the production of a high purity hydrogen based on a gasification SEWGS system it is recommended to uncouple the SEWGS system from the gasification system, which has been explained by Li et al[17]. In an uncoupled system both gasification and SEWGS can operate at optimal temperature, resulting in 1: Complete conversion of volatiles to a hydrocarbon free syngas and 2: Sufficiency capture of CO and CO₂ due to relative low carbonation temperatures. The main disadvantage of an uncoupled system is the energy penalty accompanied with calcination, combined with a large amount of cooling which is required at the sorption-shift reactor.

In our previous research [21] based on Aspen plus process simulations we showed the potential of such an uncoupled pyrogasification SEWGS when heat integration is implemented: heat released in the sorption-shift reactors can be efficiently used for steam production of the reforming process, a thermal efficiency of 74.6% was simulated, slightly lower compared to conventional gasification processes[22] given the high quality biomass input. The general process overview which has been proposed in this research is displayed in figure 5. Bottle necks have been identified in our previous work[21] with respect to reformer heating and the calcination reactor. Oxy-fuel combustion in the regenerator has not been analyzed up to date for the proposed system, such a system can be combined with electrolysis: where ‘waste’ oxygen can be utilized for combustion in the regenerator, the same gas infrastructure can be used and a pure steam of CO₂ can be produced for CCS.

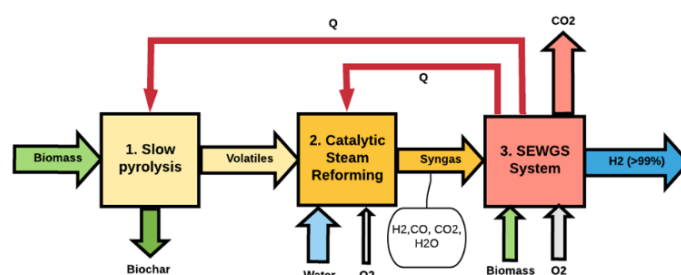


Figure 5: general system configuration pyrogasification sorption shift system

1.4 The cost of sustainable hydrogen production

This research will focus on the technical and financial feasibility of a pyrogasification SEWGS system. No financial study on such a system based on CaL has been performed up to date. In order to

determine the system feasibility, the system should be financial compatible with other high purity hydrogen production techniques such as electrolysis. Hydrogen production cost for different technologies has been the subject of different studies and estimated hydrogen production prices for different technologies are displayed in table 1.[23] . It is important to note that for conventional gasification systems, the hydrogen purity typically in the 40-50 vol% range is not a high grade (Vol %>99.5).

Tab. 1: Hydrogen production cost for different technologies

Technology	Hydrogen production cost
Steam reforming	1.92 €/kg
Gasification	1.44-1.74 €/kg
Electrolysis	8.73 €/kg

1.5 Research goal

The subject of this study is to determine the technical and economic feasibility of an uncoupled pyrogasification SEWGS system for the production of high quality biochar, high purity hydrogen and CCS. In order to do so, a system is designed based on pyrolysis, gasification/reforming and SEWGS. process simulations are performed in Aspen Plus flow process simulation software. The process simulations are performed to model heat integration, determine reactor stoichiometry and to determine system operating conditions. A financial model is constructed to determine the economic system feasibility, based on the process simulation results. Finally suggestions for further research are given.

2. MATERIALS AND METHOD

The proposed system for the production of high quality biochar and high purity hydrogen contains the following three systems: 1. Slow pyrolysis to release volatiles and to produce a high quality biochar, 2: reforming/gasification system to produce a hydrocarbon free syngas, 3: Cal based SEWGS system for the production of a high purity hydrogen and for CCS. Furthermore heat integration is modelled to transfer high quality heat from the SEWGS system to the pyrolysis and reforming system respectively. In this chapter the system design and motivation is discussed, as well as the Aspen Plus model which is constructed. Furthermore the financial model is discussed which is designed to determine the systems economic feasibility. Finally the system input is characterized.

2.1 System design

Pyrolysis is used for high quality biochar production and to maximize release of volatiles from biomass. Relative long (5-10 minutes) and controlled residence times are required, combined with high temperatures and intermediate heating rates. Using an auger reactor for pyrolysis has multiple advantages for the designed system: 1) residence time is easily controllable (dependent on rotational speed), 2) char and ash is easily removed from the auger reactor 3) promotes secondary cracking reactions due to relative long residence time of released volatiles in the auger reactor 4) good mixing and heating, especially in a dual auger configuration and 5) variable biomass input (size and quality) can be used[24,25]. Heat required for the pyrolysis system is supplied by the hot CO₂ gasses leaving the regenerator in the SEWGS system.

The volatiles released by the auger reactor are led over a two-step reforming/gasification system consisting of a pre-reformer and reformer. Two reformers are selected for energy efficiency and system robustness. Steam is added to the pre-reformer, produced by high quality heat from the sorption-shift reactors. We already identified reformer heating as one of the main system bottle necks[21], therefore a small fraction of oxygen is added to the reformer such that the desired temperature (> 750°C) is reached. Since oxygen is added to the reforming system as well as steam,

a relative low SC of 2.0 is used (measured in the pre-reformer). The hot syngas leaving the reformer is cooled, in a gas-gas Heat Exchanger (HEX), heating up the pre-reformer input. The pre-reformer is modelled as an fixed bed while the reformer is modelled as a fluidized bed.

The CaL based SEWGS system contains three fluidized bed reactors, a High Temperature Sorption-Shift (HTSS) reactor operating at 650 °C, a Low Temperature Sorption-Shift (LTSS) reactor operating at 550 °C and a regenerator operating at 900 °C . Two shift reactors are used for system robustness: if there is a blowout in the HTSS, CO₂ can still be absorbed in the LTSS. Furthermore when using two reactors thermodynamic equilibrium is better approached: at 650 °C reaction rates are relatively high compared at 550 °C, at 650 °C roughly 90% of CO₂ can be captured, and at 550°C once again roughly 90% of the remaining CO₂ can be captured. The HTSS supplies direct heat for high quality steam production (625 °C), gasses are cooled prior and after the LTS, also producing high quality steam (625°C).

CaO is cycled through the SEWGS system, regenerated sorbent (100 % CaO) leaving the regenerator (900 °C) first enters the LTSS reactor before it is cycled through the HTSS. Gas is cooled before it enters the LTSS, resulting in a reactor temperature of 550 °C . the HTSS is cooled internally, heat from the HTSS and LTSS system respectively is used for steam generation, utilized by the reforming system. A surplus of high quality steam (625 °C) is produced, this surplus can be used for example for electricity generation, or for residential/industrial heating.. The sorbent leaving the HTSS is regenerated in the regenerator, which operates at 900 °C. Biomass is combusted in the regenerator to provide energy for regeneration, pure oxygen is used at an equivalence ratio of 1.1 to ensure complete combustion. Heat is required in the regenerator to heat up the sorbent and for the endothermic calcination reaction (equation 6). A concentrated stream of hot CO₂ gas leaves the regenerator, the hot CO₂ gasses are used to heat up the auger reactor, remaining heat is used for oxygen pre-heating to increase the system energy and exergy efficiency.). A surplus of sorbent (140%) is simulated due to deactivation of sorbent over time. Sorbent deactivation has been identified as one of the main disadvantages of using CaO for SEWGS [10].

In the designed system efficient heat exchange between subsystems is required, therefore multiple heat exchangers are required for steam generation, auger reactor heating and multiple gas cooling/heating systems. The system is designed in such a way the minimum pinch point in heat exchangers is 25 °C .

An overview with reactor selection and motivation is given in table 2. Figure 6 displays the designed system configuration which is analyzed in this research. The reactor and stream numbers used in figure 6 are used throughout this research.

Tab. 2: Reactor selection and motivation

Reactor	Reactor type	Motivation
A: pyrolysis	Auger reactor	<ul style="list-style-type: none"> • Controlled residence time and heating rate • Flexible with biomass input • Promotes secondary cracking reactions • Easy ash and char removal • Good mixing and heating (dual auger configuration)
B: Pre-reforming	Fixed bed	<ul style="list-style-type: none"> • Good gas -solid contact • No blowouts • Due to gas/steam heating prior to reforming even heat distribution is expected
C: Reforming/ gasification	Bubbling fluidized bed	<ul style="list-style-type: none"> • Good heat distribution is required due to partial combustion in the gasifier • Relative small (catalyst) particles can be used
D: HTSS	Bubbling fluidized bed	<ul style="list-style-type: none"> • Good heat distribution due to particle mixing is required due to highly exothermic reaction in HTS and LTS reactor. • Relative small sorbent particles can be used
E: LTSS	Bubbling fluidized bed	
F: Regenerator	Fast fluidized bed	<ul style="list-style-type: none"> • Due to biomass oxy-fuel combustion good heat distribution is required to prevent hot spots in the reactor

Table 3 displays the reactors used in the Aspen Plus simulations accompanied with a reactor description, for the ‘‘yield reactors’’ the source is also specified.

Tab. 3: Reactor characterization Aspen Plus

Reactor	Block type	Source/Method	Description
A: Auger reactor	RYIELD	[6]	Slow pyrolysis of biomass in an auger reactor, char is separated from the auger reactor, volatiles are led to the reforming system. Auger is heated by hot flue gasses (HEX3)
B: Pre-Reformer	RYIELD	[6,12]	Catalytic steam reforming of released volatiles by the pyrolysis system. A SC of 2 is used. Pre-reformer is heated by hot syngas leaving the reformer (HEX 1). Steam is generated in the HTSS reactor
C: Reformer	RGIBBS	Thermodynamic Equilibrium Calculations	Gasification and steam reforming of fuel gases leaving the pre-reformer. Reactor is heated by partial combustion, using pure oxygen as input. An Equivalence ratio of 0.196 is used
D: HTSS	RGIBBS	Thermodynamic Equilibrium Calculations	Facilitates high temperature SEWGS reaction. Reactor is cooled using water/steam, which is used for the reforming process.
E: LTSS	RGIBBS	Thermodynamic Equilibrium Calculations	Facilitates low temperature SEWGS reaction to further increase hydrogen purity. Hydrogen gas is cooled prior and post reactor producing high quality steam.
F: Regenerator	RGIBBS	Thermodynamic Equilibrium Calculations	Regenerates CaCO ₃ back to CaO, biomass is combusted using an equivalence ratio of 1.1. Hot flue gasses are cleaned and are used for auger heating and oxygen heating to increase system efficiency.

For the RGIBBS reactors the gibs free energy is minimized according to equation 7 where μ_i is the chemical potential of component i. and n_i is the number of moles of component i.

$$dG = -SdT + v dP + \sum_{i=1}^N \mu_i dn_i = 0 \quad (7)$$

2.3 Financial model

A financial analysis is performed to determine the financial feasibility of the proposed system. The financial model can be split up into two main sections:

1. CAPEX
2. OPEX
3. Revenues

CAPEX

The total CAPEX of the system is estimated using the factorial technique by Peters and Timmerhaus [26], derived from the Lang factorial techniques for cost estimation. For this technique

only the main process equipment is required, which is multiplied by an factor (4.55) to determine the overall CAPEX

The cost for heat exchangers is determined by the type of HEX, required material and required surface area of the HEX. Required surface area can be calculated using the well-known relation between Log Mean Temperature difference (LMTD), heat transfer coefficient and required duty of the HEX. Shell in tube HEX are used in this system, plate HEX cannot be used: at high process temperatures these type of HEX are welded boxes from the outside, which makes it impossible to clean the plate heat exchangers.

The cost of fluidized bed reactors is determined by the material type, required insulation and on the required reactor volume, which is calculated based on volume flow, void fraction of the bed material and a factor corresponding the amount of "free space" required above the reactor. No information in literature can be found for industrial sized auger reactor pricing, therefore the cost of an auger reactor is based on the mass throughput rate, related to a screw press, which is then multiplied by an assumed factor 2 to compensate for increased volume and material requirements. The cost of the HEX integrated in the reactors are calculated separately, increasing total reactor cost. Because of the large unknown with respect to auger reactor cost, an additional contingency fee will be taken into account when calculating the total CAPEX.

The remaining main process equipment which is taken into account for the designed system are: 1. Cyclone for fly ash separation. 2. Biomass feeding systems (moving floors). 3. Belt conveyors for char/ash transport. 4. Denox system+ gas scrubber for gas cleaning. 5. Start up burners. 6. CaO transport system .

For the reactor vessels, HEX and the cyclone the cost are determined based on size (related to volume flows and duty), therefore widely available tables/graphs for cost estimation are used. Corrections are made to get a more accurate cost estimation: a factor 1.3 is used for HEX placed within a fluidized bed, and by a factor 3 for the reactor vessels, due to additional required insulation (concrete walls), a factor 3 has been recommended by a consulted industrial partner based on practical experience on industrial sized fluidized bed reactors for biomass processing. Furthermore price indexes and exchange rates are used to get an estimate of the current reactor cost in euro's. For the remaining process material an industrial partner is consulted to get an cost estimate of the process equipment.

An additional contingency fee of 40% is taken into account for the construction of the designed installation due to uncertainties with respect to the auger reactor, and due to the novelty of the design additional cost are expected.

The investment strategy used in the financial model is spread over 3 years. The investment strategy is displayed in tale 4 where TDC are the Total Depreciable Cost.

Tab. 4: Investment strategy

Year	Investment
1	0.08 of TDC
2	0.60 of TDC
3	0.32 of TDC+ working capital

OPEX

The OPEX is split up into three main sources: 1. Variable cost, 2. Fixed cost and 3. Company general operating expenses. The assumption made for the OPEX calculations are displayed in table 5.

Tab. 5: OPEX assumptions

	Assumed cost	Additional Assumptions
Variable cost		
Biomass	€118/ton	-
Ni-based catalyst	€5000/ton	Replaced 4 times per year
Limestone	€10/ton	10% sorbent make up is used
Process water	€0.80/m ³	-
Electricity	€80/ MWh	Installation consumes 2% electric power compared to thermal input
Miscellaneous operating material	10% of maintenance cost	-
Fixed cost		
Maintenance	3% of direct capital cost	-
Labor	€80.000 per FTE	11 FTE: 1 supervisor: 10 operators (2 per shift)
Laboratory cost	20% of labor cost	-
Plant overhead	50% of total labor cost	-
Taxes	0.2% of direct capital cost	-
Insurance	0.3% of direct capital cost + 1% of annual revenues	-
Company general operating expenses		
General overhead	10% of direct production cost ¹	¹ Direct production cost are "fixed cost + capital cost".

Revenues

The designed system produces three valuable products: a high purity hydrogen, a high quality biochar and a stream of concentrated CO₂ suitable for CCS. The current market value of these products (2021) are displayed in table 6 [27]. When the breakeven price is calculated a coupled breakeven price is calculated for all three products, multiplying the base value by the same factor.

Tab.6: Market value products pyrogasification SEWGS system

Species	Market value
Hydrogen	€1.50/kg
Biochar	€250/ton
CO ₂	€25/ton

The used Weighted Average Cost of Capital (WACC) for the system is set at 5.2%, based on the most recent KPMG cost of capital study, the WACC for the energy and natural resources is used [28].

The constructed financial model is discussed with industrial partner active in biomass processing (gasification) technology in the Netherlands. The model has been adjusted based on practical experience on industrial sized biomass processing (fluidized bed gasification) plants as well as experience on biomass powered CHP plants.

2.4 Materials

A high quality biomass is used in the process simulations both as input for the auger reactor and regenerator, pine wood is selected with a low moisture and ash content. The proximate and ultimate analysis of the uses biomass species are is displayed in table 7 and 8. The Phyllis database [29] is

used to validate the used proximate/ultimate analysis by comparing it with other similar species of pinewood. The Higher Heating Value (HHV) of the used biomass is 18.00 MJ/kg.

Tab. 7: Proximate analysis Biomass

Pinewood	[wt%]
Moisture	8,0%
Volatiles	78,7%
Ash	0,4%
Fixed Carbon	12,9%

Tab.8: Ultimate analysis Biomass (daf)

Pinewood	[wt%]
C	49,4%
H	6,0%
N	0,0%
O	44,6%

3. ASPEN PLUS SIMULATION RESULTS

Aspen plus simulations of the designed system are performed to determine system characteristics and to determine the technical feasibility of the system. The system is analyzed with a biomass input of 1 kg/s in the auger, 0.298 kg/s of biomass is required in the calcinating reactor. This results in a chemical energy input of the simulated system of 23.4 MJ. Per ton of biomass input (dry and ash free) the analyzed system produces 51.6 kg of hydrogen and 204.2kg of biochar respectively. The biochar composition is displayed in table 9 and hydrogen composition is displayed in table 10.

Tab. 9: Biochar characteristics

Pinewood	[wt%]
C	89.2
H	3.1
O	6.1
Ash	1.6
HHV	34.2 MJ/kg

Tab.10: Hydrogen product characteristics

Gas species	[Vol%]
CO	0.05
CO ₂	0.18
CH ₄	0.15
H ₂	99.62

The influence of reactor temperature of the LTSS on the final product distribution is shown in figure 8. In figure 8 the correlation between SEWGS reactor temperature and hydrogen/CO₂ concentrations as explained in section 1 (figure 4) becomes even more clear, decreased reactor temperatures will increase the hydrogen purity and decrease the CO and CO₂ concentrations.

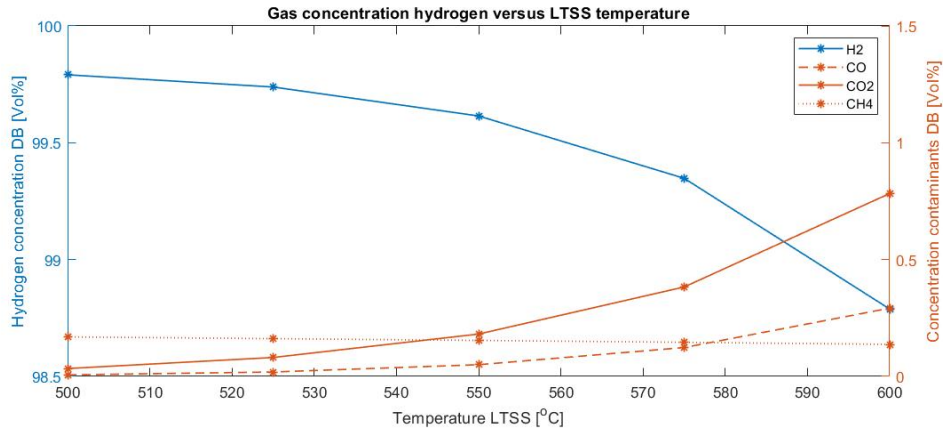


Figure 8: Temperature LTSS reactor versus gas concentrations in the product gas

The system has been simulated at a SC ratio of 2.0 and a ER of 0.196 in the reformer. The efficiency based on chemical energy is calculated at 72.5% based on equation 8. Where En represents the chemical energy of char, hydrogen, biomass ($_{bm}$) input of the auger and biomass input of the regenerator respectively.

$$\eta_{tot} = \frac{En_{char} + En_{H_2}}{En_{bm-aug} + En_{bm-regen}} \quad (8)$$

The system contains three large heat losses, these heat losses and their characteristics are displayed in table 11. It is important to note that the partial water pressure of both stream 8b and 14b is below 1 atm (water vapor/hydrogen and water vapor/CO₂ mixture respectively), resulting in latent heat released during cooling of these gasses at relatively low temperatures <100°C .

Tab.11: Min heat losses pyrogasification SEWGS system

Stream	Type	Temperature	Latent and sensible heat compared to system chemical energy input (biomass)
8b	Hydrogen/water vapor mixture	104 °C	8.5%
14b	Concentrated CO ₂ /water vapor mixture	290°C	5.6%
Q2	Steam	625°C	12.6%

4. COST ANALYSIS RESULTS

The factorial technique derived by Peters and Timmerhaus is used to determine the CAPEX of the analyzed pyrogasification SEWGS system. First the total cost of the process equipment is determined as displayed in table 12.

Tab.12: Process equipment total cost

Process Equipment	Total cost
Reactors	€1.476.000
Heat Exchangers	€849.000
Other process equipment	€928.000

The total CAPEX is displayed in detail in table 13. The method by Peters and Timmerhaus normally uses a factor of 4.55 for solid processing plants. In this case an additional 40% contingency (factor 1.55) is taken into account due to uncertainties in the system (auger cost, novel design, complexity). The chemical energy input of the simulated system is equal to 23.4 MW, resulting in investment cost of €848/kW

Tab.13: Total CAPEX

	Cost	Factor
Total equipment cost	€3.253.000	1
Direct plant cost	€8.588.000	2.64
Direct and indirect cost	€10.930.000	3.36
Total depreciable cost	€17.630.000	3.87+1.55
Total capital investment	€19.842.000	4.55+1.55

The annual OPEX of the system is €8.067.000, translating to €345/kW per year. The distribution of the OPEX is displayed in figure 9. Biomass purchasing cost is the main contributor to the OPEX (50%) followed by labor cost (19%). The cash flow simulations show that of the total cost over a total period of 15 years (12 years operation+ 3 years construction) 22.5% of the total cost is related to the CAPEX and 77.5 % of the total cost is related to OPEX.

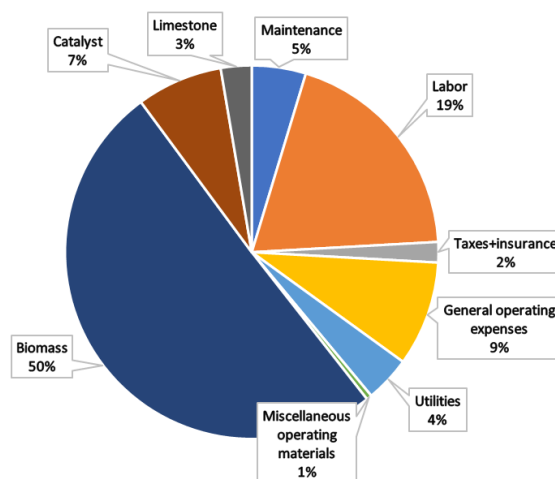


Figure 9: Overview OPEX deviation

Cash flow simulations are performed using the product market values as displayed in table 6, combined with the investment strategy (table 4), discount rates and the calculated CAPEX and OPEX. The cash flow simulations show that a system without subsidies is not profitable based on the current product market values. Based on product market value and product yield the annual expected income

is €5.003.000, while the annual OPEX is €8.067.000. Over an operational time period of 12 years the Net present value (NPV) of the designed installation (23.4MW) is €-41.755.000.

A break even analysis is performed based on cash flow simulations to determine the coupled hydrogen, biochar and CO₂ prices. Furthermore a break even analysis is performed to determine the uncoupled Levelized Cost Of Hydrogen (LCOH) (assuming the market value of biochar and CO₂ respectively as displayed in table 6). The coupled product break even prices are displayed in table 14, assuming that the price of each product proportionally increases based on the market value.

Tab.14: Breakeven prices

Product	Market price	Breakeven price (coupled)	Breakeven price (uncoupled)
Hydrogen	€1.50/kg	€3.12/kg	€4.79/kg
Biochar	€250/ton	€520/ton	€250/ton
CO ₂	€25/ton	€52/ton	€25/ton

Subsidies, or market value increase of the produced products is required in order to make the analyzed system economical feasible. This is comparable to other biomass processing techniques and high purity hydrogen production techniques based on electrolysis. The expected subsidies for high purity hydrogen are expected to be €5.83 /kg in the Netherlands based on the most current (2021) subsidy regulations (SDE++). Subsidies are also expected for CCS techniques, which are expected to be € 105.8/ton CO₂ for the Netherlands in 2021.

Cash flows are simulated based on the expected subsidies for hydrogen, and with the market value of CO₂ gas and biochar respectively. The simulation results which display the cumulative discounted cash flows are displayed in figure 10. Here the investment period (3 years) is followed by an operational period of 12 years.

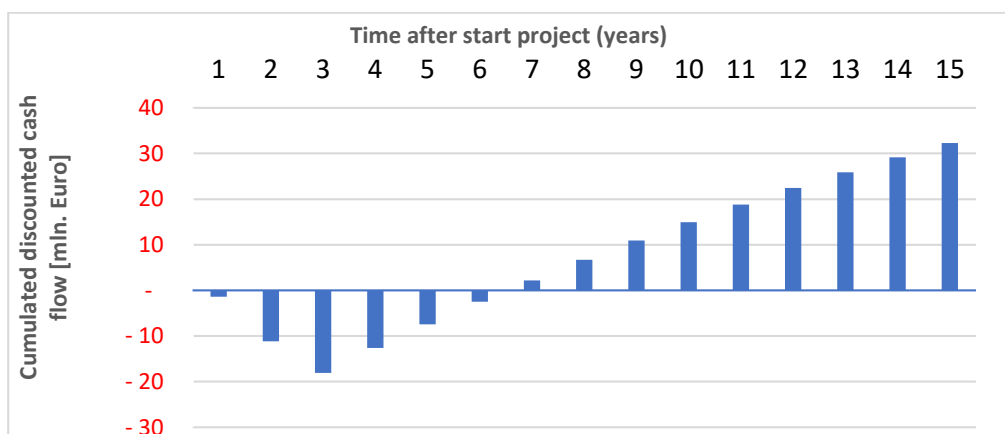


Figure 10 cumulative cash flows for the pyrogasification SEWGS system, including expected subsidies for hydrogen

The results displayed in figure 10 relate to a payback period of 3.5 years (after the installation is taken into operation) and an Initial Rate of Return (IRR) of 26.1 %. The NPV over the life time of the installation (12+3 years), assuming subsidies on the hydrogen product is equal to €32.317.000, relative to the NPV of the investment of €18.092.000.

5. DISCUSSION

The results are discussed for the process simulation followed by the financial system analysis. Results are validated and compared to literature

5.1 Process simulations

The system efficiency based on chemical energy for the analyzed system is 72.5%. Based on the biomass composition (O/C ratio of 0.68) the efficiency of conventional gasification systems is in the 76-78 % range [22]. The process simulations show that a high quality biochar (HHV=34,2 MJ/kg) can be produced, combined with a concentrated stream of CO₂ and a high purity hydrogen (H₂ vol% = 99.6%) which is comparable to industrial PEM electrolysis hydrogen products. While conventional gasification/reforming produces syngas with typical hydrogen concentrations of 40-50 vol%.

The pyrolysis system is modelled based on experimental results found by Phan et al.[6] based on slow pyrolysis of high quality (8% moisture, 0.4 % ash) pine wood at 500 °C in a batch reactor. Preferably results based on slow pyrolysis in an auger reactor are required as system input, or kinetic models based on slow pyrolysis of biomass in auger reactors. An auger reactor enhances secondary cracking reactions due to a relatively long residence times of tars and vapors in the auger reactor it is expected that the output from the auger reactor deviate slightly from the output used in this research. Furthermore an auger reactor is more flexible with respect to input (biomass quality, particle size), therefore an auger reactor is also suited for the processing of lower quality biomass (municipal solid waste, forest residues). The released volatile fraction from lower qualities of biomass can be upgraded to a hydrocarbon free syngas in the reforming/gasification system, similar to when higher qualities of biomass are used. Further experimental research is required to more accurately determine the detailed yield composition (gas, oils and char respectively) of slow pyrolysis of both high and low quality biomass in auger reactors. Implementing experimental data improves the process simulations.

The products of the reformer/gasification system are modelled at thermodynamic equilibrium. In order to validate this assumption the intermediate stream results (stream 6) are compared to results found by van Rossum et al.[9] on catalytic steam reforming of pyrolysis oil derived from pinewood. In order for a good comparison a simulation is run at similar process conditions (SC=2.7, T=777°C, ER=0.0), the results found by van Rossum et al. are compared to the simulation results in table 15. The results show large agreement, concluding that for reformer/gasification temperatures of >750 °C the assumption of thermodynamic equilibrium is justified.

Tab. 15: Reformer product validation [9]

Species	Simulation	Experimental
H ₂	0,655	0,658
CO	0,129	0,143
CO ₂	0,216	0,199
CH ₄	0,000	0,000

The results found for the SEWGS system are compared to the recently published (2020) results found by Li et al [17] on the analysis of a similar process. Li et al. performed process simulations comparable to this research using Aspen Plus. Up to date no experimental validation of a CaL based SEWGS system (without the addition of an additional shift catalyst) for the production of high purity hydrogen, combined with a gasification system is given in literature. The results found by Li et al. are

compared to the results found in this research, the results show great agreement. For the experimental validation, and for better understanding of CaL based SEWGS kinetics, further research is required.

Tab. 16: Reformer product validation [9]

Species	Simulation ¹	Validation
H ₂	0.996	0.997
CO	0.001	0.001
CO ₂	0.002	0.001
CH ₄	0.002	0.001

¹Mismtach due to rounding of concentrations

The energetic analysis of the system showed that there are two low quality heat losses, and a high quality heat loss: steam at 625 °C derived from cooling of the HTSS reactor. Both waste streams can be utilized, the high temperature waste stream can be used for power production (possibly in a CHP system). The electric power produced by a possible CHP system can supply sufficient electricity for the installation itself (roughly 2% compared to thermal input in the cost analysis) decreasing utility cost, but increasing CAPEX. The effect of a relative small CHP on cost efficiency has yet to be determined. Furthermore an incorporated CHP for the utilization of high temperature waste heat can reduce the carbon footprint of the installation. Waste heat leaving the CHP, combined with low quality waste heat present in stream 8b and 14b can be used for residential and industrial heating, or for the drying of biomass prior to the pyrolysis system when high moisture biomass is used as system input. Another application of the high quality heat (steam) produced by the SEWGS system can be for the production(steam activation) of activated carbon using the biochar product or for sorbent hydration of calcium oxide to increase the sorbent durability. When high quality waste heat leaving the SEWGS system is utilized the efficiency is however comparable to conventional gasification systems. What makes this system unique is however not the efficiency, but the high quality products which are produced.

One of the main disadvantages of an uncoupled CaL based SEWGS system are the large heat losses due to highly endothermic calcination and highly exothermic carbonation. The HTSS and LTSS require cooling in order to maintain the desired reactor temperatures. The proposed novel configuration can utilize this waste heat, and uses it for high quality steam production which is utilized in the reforming process balancing out the heat loss of the overall system since less heat input for the reforming process is required. Heat released by biomass combustion in the regenerator is transported in CaO to the SEWGS reactors, where it is released and led to the reforming system using generated steam.

The effect of SEWGS temperature on the hydrogen concentration indicate that at temperatures of 500 °C higher hydrogen purities can be obtained (based on thermodynamic equilibrium calculations). In the HTSS/LTSS calcium oxide has a double function: 1. CO₂ sorbent 2. WGS catalyst. Additional research is required to determine the effect of CaO on the WGS reaction in the 400-600 °C range to determine at which temperatures thermodynamic equilibrium is still approached In the SEWGS system. Sorbent deactivation is a large problem with respect to CaL based systems, due to decreased effective surface area (from micro pores to macro pores) the sorbent capacity of CaO decrease over multiple cycles. Enhancing sorbent durability can be done by replacement of calcium oxide by calcined dolomites, or by sorbent hydration techniques.

A configuration where this novel biomass pyrogasification system is placed parallel to a electrolysis system for hydrogen production has a large future potential: both systems produce high quality hydrogen, oxygen produced by electrolysis can be used directly for this system and a more centralized entry point for a hydrogen grid is required.

5.2 Cost analysis

The cost analysis showed that three valuable products are produced: high purity hydrogen, biochar and concentrated CO₂. Based on the current market value of these products the designed system is not cost compatible, the production cost are significantly higher (+108%) compared to the market value of these products. It is expected that, due to upcoming CO₂ taxations in Europe the market value of the products will increase relative to the inflation rate in Europe. The analysis shows that subsidies are required in order to make the system economically feasible, comparable to other biomass processing systems. A additional contingency fee of 40% was used for the CAPEX estimation, due to the novelty of the design additional unexpected cost have to be taken into account. When the technology matures, this additional contingency fee would not be necessary, resulting in the production cost as displayed in table 17.

Tab.17: Break even prices without additional contingency fee

Product	Market price	Breakeven price (coupled)	Breakeven price (uncoupled)
Hydrogen	€1.50/kg	€2.94/kg	€4.42/kg
Biochar	€250/ton	€490/ton	€250/ton
CO ₂	€25/ton	€49/ton	€25/ton

When comparing the coupled levelized cost of hydrogen with other sustainable hydrogen production methods in table 18 [23] it is shown that the analyzed system produces high purity hydrogen at significantly lower cost compared to electrolysis. The production cost are however significantly higher compared to conventional gasification, which produces a syngas. This is expected due to the increased complexity of the designed system, which contain an additional pyrolysis step for biochar production and a SEWGS system for the production of both high purity hydrogen and highly concentrated CO₂.

Tab. 18: Hydrogen production cost for different technologies

Process	Hydrogen production Cost
Gasification	1.44-1.74 €/kg
Electrolysis	8.73 €/kg
Pyrogasification SEWGS	3.12-4.79 €/kg

The main driver of the cost of hydrogen are the biomass purchasing cost, which contributes to 39% of the total expenditure over the lifetime of the installation, translating to €1.21-1.86 per kg hydrogen which is produced using the pyrogasification SEWGS system. Based on the current market price of biomass it is hard to imagine that conventional gasification can produce hydrogen at €/kg 1.44-1.74 in Europe, given the that the current European market price of biomass is in the €6.5-9 per MJ range.

6. FURTHER RESEARCH

A novel design for a pyrogasification SEWGS system has been discussed in this research. The results presented are based on process simulations in Aspen Plus and on a cost analysis derived from the process simulations based on cash flow simulations. The simulation results show positive results with respect to efficiency, product quality and production cost compared to other high purity sustainable hydrogen production methods. Further research is required to increase the accuracy of the simulations by implementing results found by experiments. Especially the CaL based SEWGS system

and the auger reactor require further analysis. Furthermore the process configuration discussed in this research can be altered in order to increase the (cost) efficiency, or reduce the complexity of the design. Subjects for further research are listed below:

- i. Perform fundamental research (using TGA experiments) to determine the catalytic effect of CaO on the WGS reaction, combined with sorption kinetics. This research should determine optimal SEWGS reactor temperatures and design (based on required residence times) .
- ii. Implement the kinetic parameters found by this study can be integrated the HTSS and LTSS reactors for more accurate simulations.
- iii. Determine the effect on sorbent kinetics of methods to increase the sorbent durability. Using calcined dolomites ($\text{MgCO}_3\text{-CaCO}_3$) and sorbent hydration are cost effective methods to increase the sorbent activity, the catalytic effect of hydrated sorbent/calcined dolomites on the reactor kinetics should be further investigated.
- iv. Analyze and model sorbent replacement strategies and implement these in process simulations, model reactor kinetics based on sorbent activity related to the replacement strategy.
- v. A proof of concept has to be given of the CaL based SEWGS reactor for the continuous production of high purity hydrogen as described in this research.
- vi. Determine the product yield of slow pyrolysis in auger reactors of both gasses, tars and solids (composition, ultimate and proximate analysis of products).
- vii. Analyze the possibilities and barriers of slow pyrolysis in an auger reactor using lower qualities of biomass, for example municipal solid waste and forest residues, which are typically characterized by a high moisture and ash content.
- viii. Analyze the possibilities and barriers for upscaling of pyrolysis in auger reactors, with the main focus on reactor heating.
- ix. Investigate possibilities for system adjustments related to integration of the high temperature waste steam. Adjustments which can be made are related to sorbent hydration and steam activation of biochar as well as electricity production using a CHP installation.
- x. Analyze possibilities for system complexity reduction: using only one reformer and/or one SEWGS reactor can be investigated as possible system improvement. The effect on produced syngas (can a hydrocarbon free syngas still be produced?) and produced hydrogen (can the high purity hydrogen still be produced?) should be investigated within these simplified systems.

7. CONCLUSION

A pyrogasification SEWGS system has been designed, modeled in Aspen Plus and has been analyzed with respect to economic feasibility. The designed system is a combination of pyrolysis, gasification and a uncoupled CaL SEWGS system. Since the SEWGS system is uncoupled from the gasification system both process can operate at ideal process conditions producing a hydrocarbon free syngas (gasification, $>750\text{ }^\circ\text{C}$) and high purity hydrogen (SEWGS, $<550\text{ }^\circ\text{C}$). Efficient heat integration is designed such that heat released by the SEWGS system (exothermic carbonation) is used for steam generation for the gasification system. Sorbent regeneration (calcination, endothermic) is performed in a biomass fueled reactor using oxy-fuel combustion, for gasification a small fraction of oxygen is used as well. The designed pyrogasification SEWGS system is suitable to operate combined with an electrolysis system for hydrogen production: oxygen is produced as byproduct from electrolysis, and

biomass distribution costs are reduced by more centralized production.

The system produced high quality products: a high purity biochar (HHV=34.2 MJ/kg) combined with high purity hydrogen (vol% = 99.6%) comparable to hydrogen purity produced by industrial sized electrolysis plants. Per ton of biomass input (dry and ash free) the designed system produced 204.2 kg biochar and 51.6 kg of hydrogen respectively, furthermore a concentrated stream of CO₂ is produced suitable for CCS. The system efficiency based on chemical energy is equal to 72.5 %, slightly lower compare to conventional gasification systems, the product quality produce by the pyrogasification SEWGS system is however significantly higher. High temperature waste heat from the SEWGS system (625°C, 12.6% compared to chemical energy system input) can still be utilized.

The financial model shows that the main contributor to levelized cost of hydrogen is OPEX with 77.5%, within the OPEX biomass purchasing cost contributes 50% to the OPEX. The calculated hydrogen breakeven price is in the €2.94-€4.42 range, assuming system maturity. The calculated breakeven price is significantly lower compared to expected hydrogen break even prices from electrolysis using sustainable energy. Low purity hydrogen production using conventional gasification has a lower LCOH compared to the analyzed system which is expected due to reduced complexity. When subsidies are assumed for hydrogen, the system becomes economical feasible, having a payback period of 3.5 years (after construction) and a IRR of 26.1%.

Further research is required with respect to kinetics of CaL based SEWGS reactors, sorbent durability improvements and auger reactor upscaling possibilities and barriers. The designed models in this research are dynamic and can easily be altered and improved using newly found data or alternative process designs.

LITERATURE

1. Rosen, M. A. & Koohi-Fayegh, S. The prospects for hydrogen as an energy carrier: an overview of hydrogen energy and hydrogen energy systems. *Energy, Ecol. Environ.* **1**, 10–29 (2016).
2. Oliveira, F. R. *et al.* Environmental application of biochar: Current status and perspectives. *Bioresour. Technol.* **246**, 110–122 (2017).
3. Majumder, S., Neogi, S., Dutta, T., Powel, M. A. & Banik, P. The impact of biochar on soil carbon sequestration: Meta-analytical approach to evaluating environmental and economic advantages. *J. Environ. Manage.* **250**, 109466 (2019).
4. Peterson, S. C. Utilization of low-ash biochar to partially replace carbon black in styrene-butadiene rubber composites. *J. Elastomers Plast.* **45**, 487–497 (2013).
5. Tripathi, M., Sahu, J. N. & Ganesan, P. Effect of process parameters on production of biochar from biomass waste through pyrolysis: A review. *Renew. Sustain. Energy Rev.* **55**, 467–481 (2016).
6. Phan, A. N., Ryu, C., Sharifi, V. N. & Swithenbank, J. Characterisation of slow pyrolysis products from segregated wastes for energy production. *J. Anal. Appl. Pyrolysis* **81**, 65–71 (2008).
7. Demirbas, A. Determination of calorific values of bio-chars and pyro-oils from pyrolysis of beech trunkbarks. *J. Anal. Appl. Pyrolysis* **72**, 215–219 (2004).
8. Mahishi, M. R. & Goswami, D. Y. Thermodynamic optimization of biomass gasifier for hydrogen production. *Int. J. Hydrogen Energy* **32**, 3831–3840 (2007).
9. Rossum van, G. *Steam reforming and gasification of pyrolysis oil.* (2009).
10. Florin, N. H. & Harris, A. T. Enhanced hydrogen production from biomass with in situ carbon dioxide capture using calcium oxide sorbents. *Chem. Eng. Sci.* **63**, 287–316 (2008).

11. Lv, P. *et al.* Bio-syngas production from biomass catalytic gasification. *Energy Convers. Manag.* **48**, 1132–1139 (2007).
12. Solar, J. *et al.* Influence of temperature and residence time in the pyrolysis of woody biomass waste in a continuous screw reactor. *Biomass and Bioenergy* **95**, 416–423 (2016).
13. Pfeifer, C., Puchner, B. & Hofbauer, H. In-situ CO₂-absorption in a dual fluidized bed biomass steam gasifier to produce a hydrogen rich syngas. *Int. J. Chem. React. Eng.* **5**, (2007).
14. Mahishi, M. R. & Goswami, D. Y. An experimental study of hydrogen production by gasification of biomass in the presence of a CO₂ sorbent. *Int. J. Hydrogen Energy* **32**, 2803–2808 (2007).
15. Florin, N. H. & Harris, A. T. Hydrogen production from biomass coupled with carbon dioxide capture: The implications of thermodynamic equilibrium. *Int. J. Hydrogen Energy* **32**, 4119–4134 (2007).
16. Anis, S. & Zainal, Z. A. Tar reduction in biomass producer gas via mechanical, catalytic and thermal methods: A review. *Renew. Sustain. Energy Rev.* **15**, 2355–2377 (2011).
17. Li, B. *et al.* Simulation of sorption enhanced staged gasification of biomass for hydrogen production in the presence of calcium oxide. *Int. J. Hydrogen Energy* **45**, 26855–26864 (2020).
18. Hanaoka, T. *et al.* Hydrogen production from woody biomass by steam gasification using a CO₂ sorbent. *Biomass and Bioenergy* **28**, 63–68 (2005).
19. Pfeifer, C.; Puchner, B., Proll, T.; Hofbauer, H. H₂-Rich Syngas from Renewable Sources by Dual Fluidized Bed Steam Gasification of Solid Biomass. *12th Int. Conf. Fluid.* 889–895 (2007).
20. Hanak, D. P., Michalski, S. & Manovic, V. From post-combustion carbon capture to sorption-enhanced hydrogen production: A state-of-the-art review of carbonate looping process feasibility. *Energy Convers. Manag.* **177**, 428–452 (2018).
21. Buiteveld, J., Bramer, E., Brem, G. & Buiteveld, J. Design of a novel biomass pyrogasification sorption-shift system for high purity hydrogen and biochar production. *NOTES POWER Eng. VOL VII* (2020).
22. Prins, M. J., Ptasinski, K. J. & Janssen, F. J. J. G. From coal to biomass gasification: Comparison of thermodynamic efficiency. *Energy* **32**, 1248–1259 (2007).
23. Shiva Kumar, S. & Himabindu, V. Hydrogen production by PEM water electrolysis – A review. *Mater. Sci. Energy Technol.* **2**, 442–454 (2019).
24. Brassard, P., Godbout, S. & Raghavan, V. Pyrolysis in auger reactors for biochar and bio-oil production: A review. *Biosyst. Eng.* **161**, 80–92 (2017).
25. Campuzano, F., Brown, R. C. & Martínez, J. D. Auger reactors for pyrolysis of biomass and wastes. *Renew. Sustain. Energy Rev.* **102**, 372–409 (2019).
26. van Amsterdam, M. F. Factorial Techniques applied in Chemical Plant Cost Estimation : A Comparative Study based on Literature and Cases. 158 (2018).
27. Campbell, R. M., Anderson, N. M., Daugaard, D. E. & Naughton, H. T. Financial viability of biofuel and biochar production from forest biomass in the face of market price volatility and uncertainty. *Appl. Energy* **230**, 330–343 (2018).
28. Castedello, M. & Schöniger, S. Cost of Capital Study 2019: The Calm Before the Storm-Rising Profits and Deflated Values? (2019).
29. Phyllis2 - Database for the physico-chemical composition of (treated) lignocellulosic biomass, micro- and macroalgae, various feedstocks for biogas production and biochar. <https://phyllis.nl/?nr=ECN-M--07-024> (2020).

O Research proposal for further research

This appendix contains the complete research proposal for further research, with the main focus on CaL based SEWGS for high purity hydrogen out of syngas.

Research proposal
Pyrogasification sorption enhanced water gas shift system for the
production of high purity hydrogen and carbon sequestration

Jesse Buiteveld
University of Twente

January 2021

1 Introduction

This document contains a research proposal for the further development of a pyrogasification sorption enhanced water gas shift system: a system to produce high quality biochar and hydrogen out of waste (biomass). First the general system concept is introduced, which is designed at the University of Twente, as well as the societal relevance and the possible positive impact his system can have on the future sustainable energy economy. Next simulation results by research up to date performed at the University of Twente is discussed as well as other research up to date on similar processes. Based on research up to date subjects for further research are identified and stated in the research goals and deliverables of this study. Finally a global planning and required resources for this study is discussed.

1.1 System introduction

At the University of Twente a biomass processing concept is designed to produce a high quality biochar, high purity hydrogen and a pure stream of CO_2 suitable for carbon capture and storage. Producing high quality bio-based raw materials like biochar and hydrogen out of biomass is desirable above heat and/or power production out of biomass. This is in accordance with long-term biomass policies of Western countries where a shift is made from biomass for heat/power to biomass to high quality raw materials. The proposed novel system uses biomass as input and consists of several thermal processing steps: pyrolysis followed by gasification (pyrogasification) and sorption enhanced water gas shift. A novel system is developed using a Sorption Enhanced Water Gas Shift (SEWGS) based on Calcium Looping (CaL) to produce a high purity hydrogen: 99% + out of biomass, produce a pure stream of CO_2 for Carbon Capture and Storage (CCS) as well as to supply heat for the gasification process prior to the SEWGS system. In the designed concept slow pyrolysis of biomass is performed in an auger reactor for the production of high quality biochar. Using an auger reactor for pyrolysis makes handling of lower quality biomass easier due to easy gas/solid separation and controlled residence times. The proposed system which requires further analysis is displayed in figure 1. Slow pyrolysis is used to produce a high quality bio-char and to release volatiles from the processed biomass. The steam reforming/gasification system is used to converge the released volatiles to a hydrocarbon free syngas. Finally the SEWGS system removes CO_2 directly and CO indirectly from the syngas. Resulting in a high purity hydrogen gas (>99% H_2). The SEWGS system uses a calcium looping (CaL) for pre-combustion carbon capture. CaO reacts with CO_2 forming $CaCO_3$, $CaCO_3$ is regenerated using heat from oxy-fuel biomass combustion, resulting in a pure stream of CO_2 after condensation. High quality heat released by the SEWGS is integrated to supply heat for the gasification and pyrolysis systems.

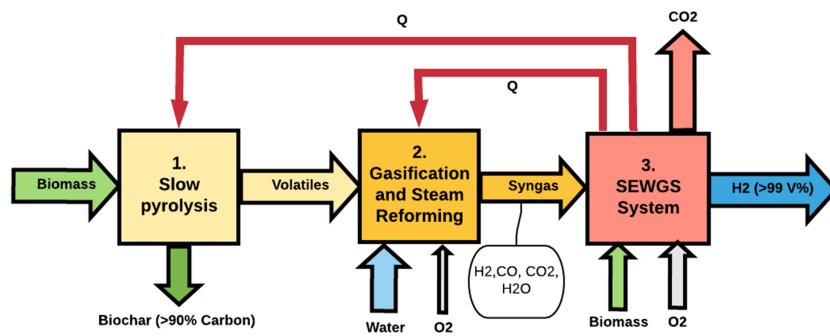
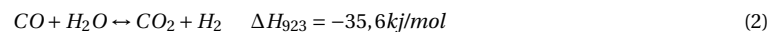
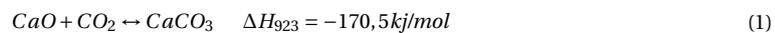


Figure 1: General overview proposed system for biomass processing: the pyrogasification sorption-shift system

A better understanding of the mechanics and kinetics of the CaL based SEWGS system is required. One of the disadvantages of CaL pre-combustion carbon capture is the large energy penalty accompanied with regeneration of $CaCO_3$ to CaO as displayed in equation 1. While regeneration requires energy (heat), the same amount of heat is released in the sorption shift reactor when CO_2 is captured, efficient heat integration can balance out this energy penalty. Capturing CO_2 will shift the Water Gas Shift (WGS) reaction (equation 2) which will also release heat. In order to maintain the SEWGS reactors at the desired temperature continuous cooling is required. This cooling is used to produce steam for the pyrogasification system.



A SEWGS system based on calcium looping is selected because of the possibility of high quality heat integration when CaL is used. Research on the designed concept, based on process simulations have shown that sufficient heat is released during carbonation (650 °C), combined with residual high quality heat in flue gasses from sorbent regenerating(900 °C) to power the biomass gasification/pyrolysis processes. When other sorption materials are used, for example hydrotalcites, operating temperatures are significantly lower reducing the possibility of high quality heat integration.

1.2 Technology implementation and future perspective

In order to reach the climate goals as stated in the Paris Agreement: prevent global temperature rise to exceed 2 °C compared to the pre-industrial level, fossil fuels need to be replaced by sustainable energy sources. Greenhouse gas emissions need to be reduced significantly in the next 30 years, resulting in a carbon neutral society in 2050 as set in the Paris Agreement. Currently large investments are made for intermittent sustainable energy sources: solar energy and wind energy, which brings a mismatch with respect to energy supply and demand. In order to solve this mismatch, energy storage and sustainable dispatchable energy sources are required, which can be utilized when there is no wind/solar energy available.

Hydrogen and biomass are two dispatchable sustainable energy sources with a large (future) potential. Hydrogen can be produced using (PEM) electrolysis when sustainable electricity supply exceeds electricity demand utilizing the electricity surplus for energy storage in the form of hydrogen. In order to distribute large quantities of hydrogen from production side (for example close to the north-sea) to the end user a hydrogen gas-grid is required for transportation. Biomass can be used for sustainable energy production combined with CCS, resulting in systems with a CO₂ negative footprint. Thermal conversion techniques like pyrolysis and gasification are able to produce fuels and bio-based raw materials from biomass: biochar, bio-oil and syngas. Hydrogen purity in syngas does not exceed 50-60 V% using conventional gasification systems. The proposed novel design for biomass processing, using a combination of pyrolysis, gasification and Sorption Enhanced Water Gas Shift (SEWGS) has the potential to produce high purity hydrogen however (>99.5%), together with a high quality biochar and a highly concentrated CO₂ for CCS.

A change is noticed in European policies for the utilization of biomass energy sources: from the utilization of biomass for electricity and heat to utilization of biomass for bio-based. Biomass is available in many forms, ranging from "high quality biomass": for example wood pallets to lower quality biomass: forest residues or municipal waste. These lower quality types of biomass are in many cases already produced as waste, and are in many cases not utilized and landfilled. Due to the combination of pyrolysis in an auger reactor followed by the gasification system The proposed system is able to process both high quality and low quality (with high moisture and ash content) biomass, while maintaining high quality bio-based raw materials as output .

The proposed biomass pyrogasification SEWGS system produces a high quality biochar, high purity hydrogen and provides a means of carbon sequestration by producing a highly concentrated stream of CO₂. Biochar has many applications ranging from replacement of coal, soil amendment (fertilizer), pollutant removal (both organic and inorganic), replacement of active coals and as possible carbon black replacement. The proposed system fits in European policies for biomass resource utilization from 2020 forward, producing high quality products from waste. The added value of the pyrogasification SEWGS system becomes especially clear when it is combined with hydrogen production based on electrolysis as displayed in figure 2. Oxygen produced as by-product of electrolysis can be used for sorbent regeneration (oxy-fuel combustion) and gasification. Furthermore high quality hydrogen of the same quality of hydrogen produced from commercial PEM electrolysis is produced(99.5-99.9V%) meaning it can be distributed using the same gas grid.

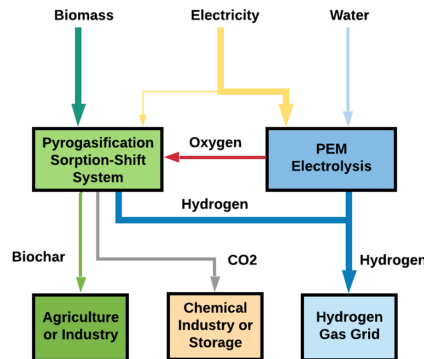


Figure 2: Overview combined pyrogasification SEWGS system with electrolysis

2 Preliminary results proposed system

In order to determine the system feasibility the proposed concept for a pyrogasification SEWGS system has been designed and modeled using Aspen Plus process simulating software at the University of Twente. A system analysis based on process simulations has been performed based on the entire system to determine the technical, economical and sustainable feasibility. The results of the reforming system and SEWGS system are based on thermodynamic equilibrium simulations, combined with experimental results from other authors [1, 2] on slow pyrolysis and pyrolysis in auger reactors followed by catalytic reforming.

Reactor stoichiometrics and heat integrating of the proposed concept for pyrogasification SEWGS system is simulated. The simulation results show an overall system energy efficiency of 72.5 %, which is comparable to conventional gasification systems. The big difference lies however in the high product quality produced by the pyrogasification SEWGS system, the analyzed system produced per ton of biomass input 47 kg of high purity hydrogen (see table 2) and 187 kg of high quality biochar (see table 1)

Table 1: Characteristics biochar product

Biochar	
C	89,2%
H	3,1 %
O	6,1 %
Ash	1,6 %
HHV	34,2 MJ/kg

Table 2: Hydrogen product quality (dry)

Hydrogen	Concentration
CO	0,05%
CO ₂	0,18 %
CH ₄	0,14 %
H ₂	99,63 %

The production cost of produced hydrogen are simulated and calculated at €2.94/kg combined with biochar break even cost are calculated to be €490.4/ton. Hydrogen production cost using electrolysis is estimated at €8,44 per kg [3]. Hydrogen production cost using conventional gasification are estimated to be €1.60 per kg [3], conventional gasification do not produce high quality products however, have fluctuating hydrogen purity's and do not have an integrated CCS solution. The proposed system shows a better alternative with respect to cost efficiency for high purity hydrogen production. Besides hydrogen production the system produces a high quality biochar and offers a means for carbon sequestration. The carbon footprint of the system is calculated when both biochar and a pure stream of CO₂ from the regenerator is captured and stored, resulting in a negative CO₂ footprint of -1591 kg CO₂ per ton of biomass input.

Preliminary results using process simulations are validated using research by van Rossum et al. [4] and by Li et al. [5]. Van Rossum et al. performed experimental research in a two-stage catalytic steam reformer, with pyrolysis oil as input. The results after the reforming system in this research, using a simulation run with similar process conditions are compared with experimental results found by van Rossum et al. in figure 3. The results are in close agreement. Li et al. also performed simulations on a CaL based SEWGS system. The results found in this research are compared to the results found by Li et al. in table 4. These results also show similar results compared to the simulation results found by us.

Table 3: Simulation results and experimental results found by van Rossum et al.

Gas species	simulation results	experimental results
CO_2	21.6%	19.9 %
CO	12.9%	14.3 %
H_2	65.5 %	65.8 %
CH_4	0.0 %	0.0 %
C_2H_4	0.0%	0.0 %
C_2H_6	0.0%	0.0 %

Table 4: Simulation results validation by results found by Li et al.

Gas species	simulation results	Results Li et al. (2020)
CO_2	0.18 %	0.1 %
CO	0.05%	0.1 %
H_2	99.63 %	99.7 %
CH_4	0.14 %	0.1 %

The process simulations show a system which can compete with other sustainable hydrogen production methods while also providing a means for carbon sequestration. Further research is required with respect to auger pyrolysis mechanics and upscaling possibilities and with respect to the SEWGS system based on CaL to validate the process simulations and a better understanding of the system.

3 Research up to date on CaL and SEWGS

Producing high purity hydrogen from biomass feedstock using a calcium looping based SEWGS system has not been the subject of many studies up to date. Li et al. [5] published in October 2020 process simulation results of a CaL looping based SEWGS system combined with biomass gasification, of which results were very similar to the results discussed in section 2. Both CaL and SEWGS have been studied in the last 20 years, but a combination for high quality hydrogen production using syngas from biomass gasification in a separate reactor has not been experimentally validated. In order to determine the system technical and economical feasibility and to give proof of concept further research of this proposed novel system is required. This section discusses most relevant research up to date on both SEWGS and CaL and discusses research subjects which have not been studied yet, which are required to better understand the system.

CaL looping has been the subject of many studies, in the last 20 years CaL is mainly studied for two types of applications:

1. Sorption enhanced hydrogen production [6, 7]
2. Post combustion carbon capture [8, 9]

In recent years research is focused towards CaL systems for post combustion carbon capture for coal and gas fired power plants [8]. Due to relative high carbonation (500 °C - 700 °C) and calcination temperatures (800 °C - 900 °C) there is the possibility of high quality heat integration [8]. The downside of calcium based sorbent is reduced sorbent multi-cycle activity, as has been described by many authors [9–11] and has been identified as the main bottleneck of CaL based CO_2 capture techniques. Due to reduced surface area of CaO particles over multiple cycles the structure of the particles changes: micro pores are replaced by macro pores, which decreases effective surface area. Furthermore sintering of CaO particles also causes a reduction in effective surface area over multiple cycles. Multiple methods for sorbent multi cycle activity enhancement have been proposed: sorbent hydration, using calcined dolomite's ($MgCO_3$ - $CaCO_3$), using nano-sized particles, introducing mild calcination conditions (700 °C) and using tailored sorbents which incorporate CaO in an inert porous matrix (Al_2O_3 -3, $CaTiO_3$) [7]. Out of cost considerations using calcined dolomite or sorbent hydration are the most promising techniques to increase sorbent durability for the proposed novel CaL SEWGS system. Especially since preliminary simulation results show the potential of steam generation for sorbent hydration without additional energy cost due to exothermic carbonation reactions.

SEWGS is a subject of some ongoing studies, but with the main focus on "low temperature" applications, which in many cases uses both a sorbent and catalyst to shift the WGS reaction [12, 13]. : Boon et al. [14] analysed potassium-promoted hydrotalcite (K-HTC) as CO_2 sorbent in the 300-500 °C domain. 400 °C steam is used to regenerate the sorbent. Potassium promoted sorbents have been the subject of many recent studies up to date [12, 14, 15]. The big advantage of using K-HTC is durability: while CaO deactivates fast over multiple cycles, potassium promoted sorbent have demonstrated to operate stable in over 4.000 carbonation/calcination cycles. Cost are however significantly higher of the sorbent and regeneration requires a relative low temperature steam compared to CaL, which results in an energy/cost penalty when high quality heat for pyrolysis/gasification is required. The main focus of current research is not on biomass processing but on processing of gas from blast furnaces and CCS in general [14].

Zivkovic et al. [13] designed kinetic models for CaO based SEWGS system. In this research experimental results at a relative low temperature range (250 °C - 525 °C) were validated with the designed kinetic model. Due to the low carbonation temperatures a catalyst was used (iron-chromium based) in order for a sufficiently fast WGS reaction. Li et al. [16] showed that under high temperature operating conditions (500-700 °C) CaO has an enhancing effect on the WGS, acting as both a catalyst and sorbent. Further kinetics of CaO and (partly) deactivated CaO/CaCO₃ should be further investigated to obtain accurate dynamic models for CaL based SEWGS systems. Zivkovic et al. used a shrinking core model to model CO_2 absorption kinetics of CaO. A shrinking core model was proposed to cope with increased diffusion residence of CO_2 through the formed CaCO₃ layer. Using a regression analysis on experimental data kinetic parameters were found. This research shows a good framework for further fundamental research, where increased temperatures (with no catalyst) and sorbent deactivation and sorbent hydration on catalytic function is further analyzed and modeled.

4 Research goals

Additional understanding of the CaL SEWGS system is required as described in the previous sections. Further fundamental research and proof of concepts are required. The gained insights by fundamental research can be implemented in the already designed model.

- **Fundamental:** Obtain a better understanding of kinetics of CaL SEWGS system, including multi cyclic sorbent deactivation, sorbent hydration strategies, and alternative calcium based sorbents.
- **Applied:** Provide proof of concept of the proposed pyrogasification sorption-shift system.
- **Applied:** Improve process simulations and use process simulations for further technology upscaling.

The proposed system operates at relative high temperatures (500-650 °C). Both limestone and calcined dolomite's kinetics can be further investigated for high temperature SEWGS due to wide availability and low cost of these materials. Fundamental research is required to analyse the effect of sorbent deactivation and sorbent hydration on WGS kinetics. Furthermore experiments should be used to design a dynamic model for CaL based SEWGS systems for CaO/calcined dolomite's including sorbent hydration as a possible reactivation step. After the construction of this kinetic model a proof of concept should be given for a pyrogasification SEWGS system on lab scale, prove of concept of heat integration should also be given for the SEWGS reactor. Finally the already designed simulations should be revisited and fitted to newly found (experimental) data to more correctly simulate the total process and give a more accurate estimation of system cost.

More concrete research goals of the proposed research are listed below:

1. Construct a kinetic model of CaO and calcined dolomite's to predict CO_2 absorption and WGS reaction kinetics based on TGA test results of sorbents to determine kinetic parameters based on a regression analysis
2. Design and build a fluidized bed based SEWGS reactor, validate kinetic models for CaL based SEWGS
3. Test and optimize different sorbents with respect to durability: test different hydration strategies for CaO and calcined dolomite's.
4. Expand kinetic model to also account for sorbent deactivation
5. Provide proof of concept of continuous operating SEWGS system
6. Gain insight in heat transport in a SEWGS reactor due to exothermic carbonation and WGS
7. Design operating conditions and dimensions for a continuous operating SEWGS reactor, based on heat/mass transport requirements as well as sorbent kinetics

8. Use results to simulate the SEWGS in more detail in Aspen Plus by incorporating the newly found kinetic models.

If this research yields positive results the system can be tested and build as a semi industrial scale installation to upgrade flue gasses and provide carbon capture. This is however outside the scope of the proposed research.

5 Deliverables

The proposed research has the following deliverables:

1. Improved kinetic model for CaL SEWGS, taken into account sorbent deactivation to accurately predict cycling operating conditions
2. Proof of concept for continuous high quality hydrogen production using a CaL based SEWGS reactor
3. Improved process simulations Incorporated with kinetic models
4. Advise and suggestions for technology upscaling possibilities to an (semi) industrial scale

6 Required resources

The research described in this report consists of experimental research on two different test set ups. The first set of experiments should be performed using a TGA to analyse kinetics of a SEWGS system. A TGA system is already present at the university of Twente. The second set of experiments should be performed in a lab scale fluidized bed. A lab scale bed is already present at the University of Twente, but this test set up is used intensively for other research. A proposed test set up for experimental research is displayed in figure 3.

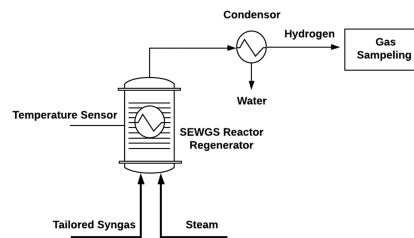


Figure 3: Test set up for fluidized bed SEWGS reactor

With respect to required materials it is recommended that a new (lab scale) fluidized bed, including a heater for the bed is purchased. Furthermore sample gasses (tailored syngases) are required as well as different sorbent materials. The most important resource which is required for this research are human resources. The purposed research is well suited for a PhD project of 4 years. An associate professor needs to supervise the PhD candidate and lab assistance is also required. It is estimated that the project required 2 FTE per year at €60.000 per FTE/year. The main required resources, with estimated cost are displayed in table 5.

Table 5: Total CAPEX sorption-shift-system for the oxy-fuel based system

Resource	estimated Cost
Human resources	€480.000
New equipment purchasing	€100.000-€200.000
Material (sorbents/syngas)	€50.000-€100.000
Depreciation equipment	€50.000-€100.000
Total Estimated cost	€680.000-€880.000

7 Planning

It is recommended for the proposed research to make it a PhD project, corresponding with an duration of 4 years. A planning for this research is shown in figure 4.

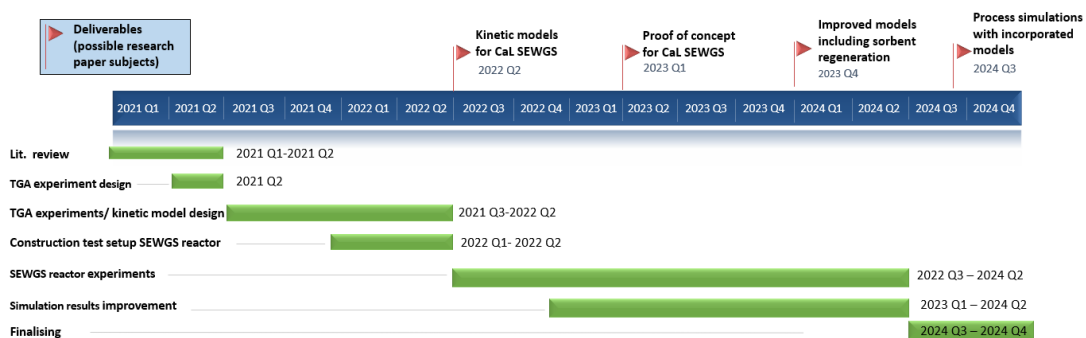


Figure 4: Planning

Bibliography

- [1] Anh N Phan, Changkook Ryu, Vida N Sharifi, and Jim Swithenbank. Characterisation of slow pyrolysis products from segregated wastes for energy production. *Journal of Analytical and Applied Pyrolysis*, 81(1):65–71, 2008.
- [2] J Solar, I De Marco, BM Caballero, A Lopez-Urionabarrenechea, N Rodriguez, I Agirre, and A Adrados. Influence of temperature and residence time in the pyrolysis of woody biomass waste in a continuous screw reactor. *Biomass and Bioenergy*, 95:416–423, 2016.
- [3] S Shiva Kumar and V Himabindu. Hydrogen production by pem water electrolysis—a review. *Materials Science for Energy Technologies*, 2(3):442–454, 2019.
- [4] G. van Rossum. *Steam reforming and gasification of pyrolysis oil : Reactor and process development for syngas production from biomass*. PhD thesis, University of Twente, Netherlands, 10 2009.
- [5] Bin Li, Christian Fabrice Magoua Mbeugang, Dongjing Liu, Shu Zhang, Shuang Wang, Qian Wang, Zhixiang Xu, and Xun Hu. Simulation of sorption enhanced staged gasification of biomass for hydrogen production in the presence of calcium oxide. *International Journal of Hydrogen Energy*, 45(51):26855–26864, 2020.
- [6] Charles C Dean, John Blamey, Nicholas H Florin, Mohamad J Al-Jeboori, and Paul S Fennell. The calcium looping cycle for co2 capture from power generation, cement manufacture and hydrogen production. *Chemical Engineering Research and Design*, 89(6):836–855, 2011.
- [7] Nicholas H Florin and Andrew T Harris. Enhanced hydrogen production from biomass with in situ carbon dioxide capture using calcium oxide sorbents. *Chemical Engineering Science*, 63(2):287–316, 2008.
- [8] Dawid P Hanak, Sebastian Michalski, and Vasilije Manovic. From post-combustion carbon capture to sorption-enhanced hydrogen production: A state-of-the-art review of carbonate looping process feasibility. *Energy Conversion and Management*, 177:428–452, 2018.
- [9] Isabel Martinez, Gemma Grasa, Jarno Parkkinen, Tero Tynjälä, Timo Hyppänen, Ramon Murillo, and Matteo C Romano. Review and research needs of ca-looping systems modelling for post-combustion co2 capture applications. *International Journal of Greenhouse Gas Control*, 50:271–304, 2016.
- [10] Ronald Barker. The reversibility of the reaction $\text{CaCO}_3 \rightleftharpoons \text{CaO} + \text{CO}_2$. *Journal of applied Chemistry and biotechnology*, 23(10):733–742, 1973.
- [11] Li Zhen-shan, Cai Ning-sheng, and Eric Croiset. Process analysis of co2 capture from flue gas using carbonation/calcination cycles. *AIChE journal*, 54(7):1912–1925, 2008.
- [12] ER Van Selow, PD Cobden, RW Van den Brink, JR Hufton, and A Wright. Performance of sorption-enhanced water-gas shift as a pre-combustion co2 capture technology. *Energy Procedia*, 1(1):689–696, 2009.
- [13] Luka A Živković, Andrej Pohar, Blaž Likozar, and Nikola M Nikačević. Kinetics and reactor modeling for cao sorption-enhanced high-temperature water–gas shift (se-wgs) reaction for hydrogen production. *Applied Energy*, 178:844–855, 2016.
- [14] Jurriaan Boon, Kai Coenen, Eric van Dijk, Paul Cobden, Fausto Gallucci, and Martin van Sint Annaland. Sorption-enhanced water–gas shift. In *Advances in chemical engineering*, volume 51, pages 1–96. Elsevier, 2017.
- [15] Hyun Min Jang, Ki Bong Lee, Hugo S Caram, and Shivaji Sircar. High-purity hydrogen production through sorption enhanced water gas shift reaction using k2co3-promoted hydrotalcite. *Chemical engineering science*, 73: 431–438, 2012.
- [16] Bin Li, Liangyuan Wei, Haiping Yang, Xianhua Wang, and Hanping Chen. The enhancing mechanism of calcium oxide on water gas shift reaction for hydrogen production. *Energy*, 68:248–254, 2014.

P Proceedings "Young Professionals in Power Engineering" conference, Wroclaw University, Poland

During the "Young professionals in Power Engineering" conference on 9-11 December (Wroclaw University, Poland), preliminary simulation results have been presented. At the conference, the process simulation results have been discussed as well as the results of the parametric study for pyrogasification SEWGS systems. This section contains the abstract which has been submitted and published for the book of abstracts, which has been published prior to the conference. Furthermore, a conference paper is written, which is submitted to be published in the "post-conference monography", at the time of writing, the paper is not yet peer-reviewed.



Design of a novel biomass pyrogasification process with an integrated sorption-shift system for hydrogen and carbon production

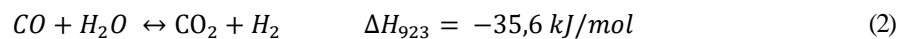
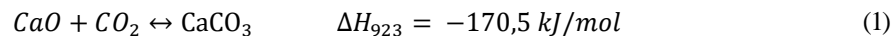
*Jesse Buiteveld, Eddy Bramer, Gerrit Brem
 University of Twente¹
 Departement of Thermal and Fluid Engineering*

Abstract

A novel system for the production of a high quality biochar and high purity hydrogen out of biomass is developed and simulated in Aspen Plus. The proposed system uses a combination of slow pyrolysis, steam reforming and a novel sorption-shift-system based on Calcium Looping (CaL): a Sorption-Enhanced-Water-Gas-Shift (SEWGS) system to increase hydrogen yield and purity.

The reactor configuration of the SEWGS system was identified as a key parameter for high quality hydrogen production [1]. In this study the reforming process and SEWGS system are decoupled: a post-reforming SEWGS system is proposed to ensure both complete tar conversion in the reformer at standard reforming conditions (750°C) and a high quality hydrogen production in the SEWGS system at 550°C.

This system uses calcium oxide (CaO) for carbon capture according to Equation 1 and to shift the Water-Gas-Shift (WGS) reaction (Equation 2) into the direction of hydrogen. The developed system contains two sorption-shift reactors in series and a regenerator heated by biomass combustion for the calcination of the CaCO₃. An efficient heat integration is developed which gives a double function to the SEWGS system: hydrogen production of high purity and steam generation for heat integration.



The overall process is shown in Figure 1. The first process step is slow pyrolysis for biochar production [2], then a two-stage steam reforming process is used for syngas production to produce a hydrocarbon (tar) free syngas [3], and the final step is the novel SEWGS system for CO₂ capture and hydrogen production [4].

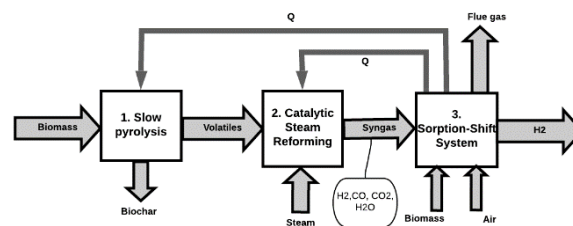


Fig. 1 General system configuration Pyrogasification sorption-shift system

An Aspen plus model is developed for process simulations to optimize the key process parameters for hydrogen production and to maximize heat integration. The designed system operates at a reformer temperature of 750°C, a final sorption shift temperature of 550°C and a Steam to Carbon (SC) ratio of 4.87 in the pre-reformer. Process simulations show an overall energy efficiency of 74.4 % and a cold gas efficiency of 42.2%, a high quality biochar is produced: HHV=34.18 MJ/kg as well as high quality hydrogen: 99.67% purity. A system sensitivity analysis is

¹ Corresponding author: E-mail address e.a.bramer@utwente.nl

performed for process optimization by heat integration and to identify energy shortages in subsystems. The sensitivity analysis identified heat integration of regenerator waste heat for (pre-) reformer heating as the main bottleneck in the system. Further process optimizations is recommended with respect to biomass feed and (pre-) reformer heating to increase the system sustainability and decrease system complexity and cost.

Literature

- [1] Florin, N. H., & Harris, A. T. (2008). Enhanced hydrogen production from biomass with in situ carbon dioxide capture using calcium oxide sorbents. *Chemical Engineering Science*, 63(2), 287-316. <https://doi.org/10.1016/j.ces.2007.09.011>
- [2] Phan, A. N., Ryu, C., Sharifi, V. N., & Swithenbank, J. (2008). Characterisation of slow pyrolysis products from segregated wastes for energy production. *Journal of Analytical and Applied Pyrolysis*, 81(1), 65-71. <https://doi.org/10.1016/j.jaap.2007.09.001>
- [3] van Rossum, G. (2009). *Steam reforming and gasification of pyrolysis oil*. Enschede: University of Twente. <https://doi.org/10.3990/1.9789036528894>
- [4] Pfeifer, C. (2013). Sorption-enhanced gasification. In *Fluidized bed technologies for near-zero emission combustion and gasification* (pp. 971-1001). Woodhead Publishing . <https://doi.org/10.1533/9780857098801.4.971>



Design of a novel biomass pyrogasification sorption-shift system for high purity hydrogen and biochar production

Jesse Buiteveld, Eddy Bramer, Gerrit Brem

University of Twente

Department of Thermal and Fluid Engineering

corresponding author – e-mail: e.a.bramer@utwente.nl

ABSTRACT

A novel system for the production of high quality biochar and high purity hydrogen out of biomass is developed. The proposed system uses a combination of slow pyrolysis, steam reforming and a novel sorption-shift-system based on Calcium Looping (CaL). This system uses calcium oxide (CaO) for carbon dioxide capture and to shift the Water-Gas-Shift (WGS) reaction into the direction of hydrogen. An Aspen Plus model is constructed for process simulations, analysis and process optimization. The designed system operates at a reformer temperature of 750°C, a final sorption shift temperature of 550°C and a Steam to Carbon (SC) ratio of 4.57 in the pre-reformer. Process simulations show an overall energy efficiency of 74.4 % and a cold gas efficiency of 42.2%, a high quality biochar is produced: HHV=34.18 MJ/kg as well as high quality hydrogen: 99.67% purity. A sensitivity analysis identified (pre-) reformer heating as the main bottleneck in the system. Further process optimizations and development is recommended with respect to cost efficiency optimization, (pre-) reformer heating and implementation of oxy-fuel combustion for CaO regeneration.

KEYWORDS: Pyrolysis, steam reforming, CO₂ absorption, water gas shift, hydrogen, biochar, calcium oxide, CaL, pre-combustion carbon capture, biomass, heat integration, Aspen Plus modelling

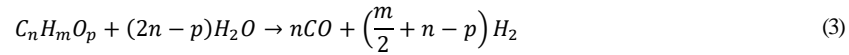
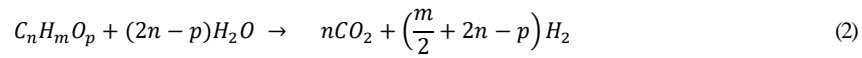
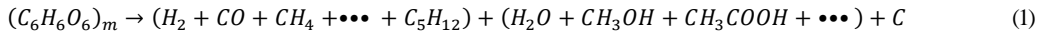
1. INTRODUCTION

The demand for sustainable energy sources is rising globally. There are limited fossil fuel resources available which are depleting fast and CO₂ emissions from the combustion of fossil fuels cause climate change. In order to prevent global temperature rise to exceed 2°C compared to the pre-industrial level as stated in the Paris agreement, fossil fuels need to be replaced by sustainable energy sources. Implementing large shares of intermittent renewable energy sources like solar and wind energy brings a mismatch with respect to energy supply and demand. In order to cope with this mismatch sustainable dispatchable energy sources are required. One of the promising options with respect to sustainable Supply Side Management (SSM) are biomass gasification and pyrolysis systems, within these processes biomass is converted into either sustainable gas, oil and char which can easily be stored and utilized when required.

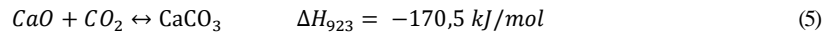
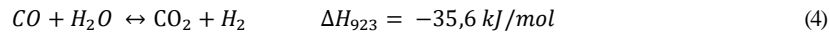
Two high quality products which can be produced by pyrolysis/gasification processes are biochar and hydrogen. Hydrogen is expected to play a large role in the energy transition, and is seen as one of the big energy carriers of the future, in the “hydrogen energy economy” hydrogen can serve as transportation fuel, energy storage medium, raw material for the chemical energy but also as

replacement for natural gas: replacing the natural gas grid by a sustainable hydrogen gas grid[1]. Biochar can serve as material for carbon sequestration resulting in a carbon negative system, biochar can also be used for the removal of pollutants from soil and as fertiliser when it used in agriculture as soil amendment[2]. High quality biochar's also have the potential to replace active carbons and carbon black [2].

Slow pyrolysis of biomass is a thermal conversion method to produce high quality biochar and to release moisture and volatiles (tar and fuel gas) from biomass [3,4]. General pyrolysis mechanics are displayed in equation 1[3], pyrolysis is an endothermic process. Volatiles produced by pyrolysis can be further reformed/cracked using catalytic steam reforming or gasification processes to produce a hydrocarbon (tar, methane) fee syngas (H_2 , CO , CO_2 , H_2O) [5,6]. General biomass steam reforming mechanics are displayed in equation 2 and 3[7], steam reforming is an endothermic process.



Coupling a gasification system with carbon capture can increase hydrogen yield and purity: by removing CO_2 directly and CO indirectly by shifting the Water-Gas-Shift reaction (equation 4) [7]. A sorbent which can be used for CO_2 capture is calcium oxide (CaO) which is abundantly available in the form of limestone and has a desired operation temperature range when sorption is combined with gasification: 550-650 °C for carbonation. For calcination: $CaCO_3$ to CaO (equation 5), a temperature of 800-900 °C is required [7,8]. Combining these two reaction mechanisms results in a Sorption Enhanced Water-Gas-Shift (SEWGS) reaction which captures CO_2 and increases hydrogen purity. The sorption reaction is exothermic, being able to supply most of the heat required for gasification[6]. Regeneration of $CaCO_3$ to CaO is endothermic and is accompanied with a large energy penalty.



The advantage of carbon capture using calcium oxide lies within the reversibility of calcination and carbonation[8,9]. Calcium carbonate can be regenerated using a system based on calcium looping (CaL). In a CaL system $CaO/CaCO_3$ is continuously cycled and $CaCO_3$ is regenerated to CaO under elevated temperatures [7-9]. Such a CaL system is a form of pre-combustion carbon capture and storage which can result in the removal of atmospheric CO_2 .

Slow pyrolysis, steam reforming and SEWGS are all processes which contribute to the production of high quality energy carriers (hydrogen and biochar). Combining these processes, in combination with heat integration is the subject of this study. Slow pyrolysis, steam reforming and SEWGS have been studied individually, but in almost all cases separately. The novelty of this research lies within the integration of these 3 systems. Combining these systems can result in:

- Increased product quality
- Increased system efficiency

The aim of this study is to model a pyrogasification-sorption-shift system in combination with heat integration using Aspen Plus process simulation software. In order to do so key process parameters of the individual processes have to be determined and are used to design a system configuration for both the production of high quality hydrogen and biochar out of biomass in combination with a SEWGS system. Aspen Plus simulations are used to determine reactor stoichiometry, heat integration, system optimization and to identify heat shortages in subsystems using a sensitivity analysis. The model discussed in this research forms a basis for further research. This paper discusses preliminary simulation results and gives recommendations for further research.

2. MATERIALS AND METHOD

The analysed system contains three subsystems, each with a different function: 1) pyrolysis system for the production of biochar, 2) steam reforming system to produce a hydrocarbon free syngas, 3) sorption-shift system to increase hydrogen purity and capture CO₂. The key process parameters of each subsystem will be discussed in this chapter which are used to formulate and design an integrated system. This design is discussed as well as the constructed Aspen Plus model. Finally biomass (system input) is characterized.

2.1 SUB SYSTEM ANALYSIS

Pyrolysis. The key system parameters for (slow) pyrolysis are reactor temperature and heating rate [3,4,10]. Increasing system temperature leads to: 1) production of a higher quality biochar and 2) the production of more fuel gasses. The influence of pyrolysis temperature on product distribution and char quality is displayed in Fig.1 and Fig.2 as found by experimental research by Phan et al. [4], using a heating rate of 10 K/min and product residence time of 120min. Demirbas et al. [10] showed that under increasing pyrolysis heating rates biochar quality improved, at a pyrolysis temperature of 527 °C biochar quality improved from 29MJ/kg at 2K/s to 35 MJ/kg at 100K/s.

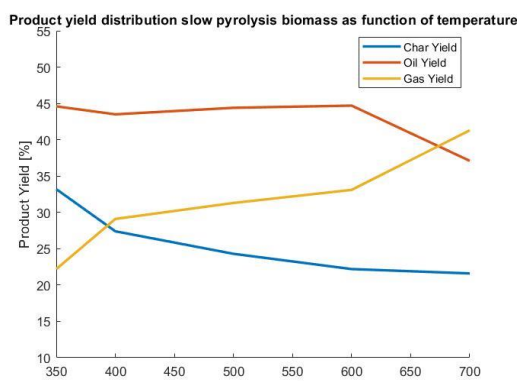


Figure 1: Slow pyrolysis temperature versus product distribution

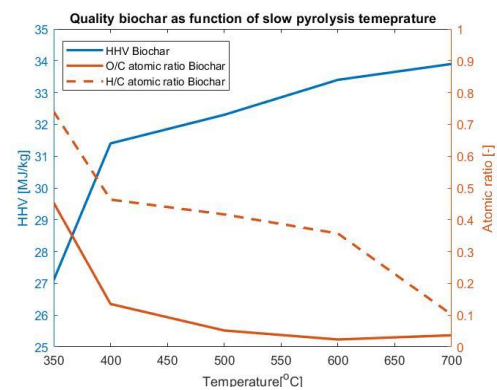


Figure 2: Slow pyrolysis temperature versus biochar quality

Using an auger reactor for pyrolysis has multiple advantages when high quality biochar production is the main purpose of pyrolysis [11,12]. 1) Easy char/ash separation at the auger exit. 2) Good material mixing/heating, especially in a duel auger configuration. 3) Promotes secondary reactions for higher gas production and tar reduction due to long residence times. 4) Controllable residence times and heating rates. 5) Variable auger input with respect to particle size and biomass quality. Depending on the desired char quality, process conditions in an auger reactor can be varied:

residence time (rotational speed) and temperature as well as biomass particle size and biomass quality [11].

Steam reforming. The aim of the steam reforming system is to produce a hydrocarbon free syngas. Key process parameters which influence gas quality are temperature and Steam to Carbon ratio (S/C), furthermore catalyst selection and reactor configuration influence product yield and purity. Figure 3 shows the influence of reactor temperature on gas quality (hydrogen concentration) found by different authors [6,7,13–16], two different areas can be identified in figure 3: 1) Sorption enhanced gasification and 2) Catalytic steam reforming. Sorption Enhanced Gasification (SEG) produces a gas with a significantly higher hydrogen purity compared to catalytic steam reforming, fuel gas produced by SEG contains hydrocarbons however, mostly methane, but also C_2H_4 , C_2H_6 and tars caused by lower reactor temperatures [7,13]. Catalytic steam reforming in a two-stage reactor system can produce a tar free syngas, resulting in complete carbon to gas conversion and higher absolute gas yield [5,17]. Optimal S/C ratio for steam gasification with respect to system efficiency were given by Mahishi et al. [6] at a S/C ratio of 4,12 using thermodynamic equilibrium modeling, van Rossum et al. [5] found complete tar conversion in an experimental two-stage reforming system at S/C ratios as low as 2.2.

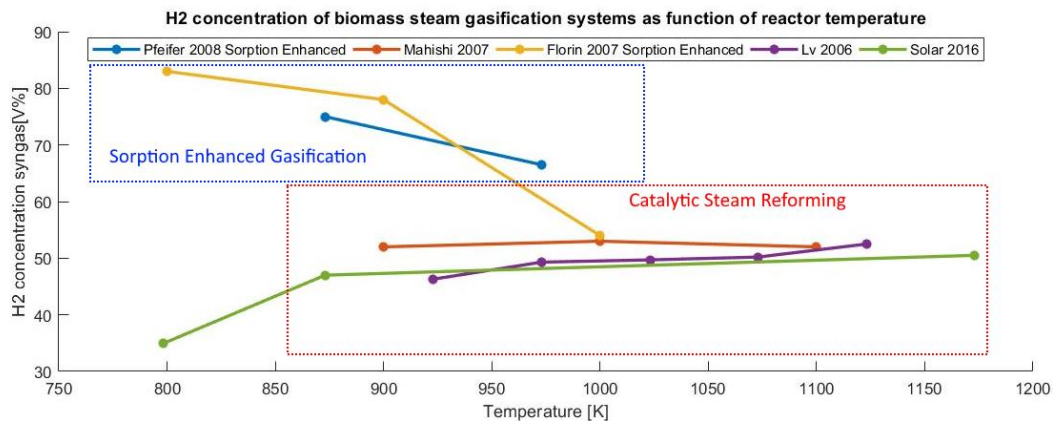


Figure 3: Hydrogen concentration syngas as function of temperature for sorption-enhanced gasification system and catalytic steam reforming systems

Sorption-Shift System. The most important key parameter for a sorption-shift system is the system configuration, since this dictates reactor temperature which determines the product gas hydrogen purity. There are two ways sorption shift can be implemented using Calcium Looping (CaL): coupled SEWGS, also called sorption enhanced gasification where *in situ* carbon capture takes place in the reformer/gasifier and sorbent regeneration (calcination) in a regenerator. This system has been the subject of several studies [6,7,13,16,18–20] where the main objective is to produce a tailored syngas with increased hydrogen purity, but also with significant fractions of CO and CO_2 and hydrocarbons, such a tailored syngas could be used in the chemical industry. A widely analyzed system configuration for SEG is a dual fluidized bed configuration for SEG: a reactor operating at $\approx 650^\circ C$ for sorption enhanced gasification, the bed material (sand with newly formed $CaCO_3$ and char) is led to a regenerator, here heat is supplied for regeneration at $850-900^\circ C$. The high temperature CaO is recycled to the gasifier/reformer, heat in the bed material, in combination by heat released by carbonation supplies the heat for gasification, as well as for steam generation within the reactor.

Another option to implement a sorption-shift system is in a uncoupled system, as recently (2020) discussed by Li et al. [21]. In such a system steam reforming reactions take place at optimal temperature ($750-850^\circ C$) producing a hydrocarbon free syngas, the gas is led to a separate SEWGS system operating at significantly lower temperatures ($550-650^\circ C$) due to the significantly lower CO_2 equilibrium pressure of CaO/ $CaCO_3$ at these temperatures [7] a high purity hydrogen can be obtained

with minimal contamination of CO and CO₂ due to efficient carbon capture at these temperatures. Such a separate SEWGS system comes with a high energy penalty, since the reformer can no longer be heated by hot regenerated CaO and by heat released by carbonation. When a high purity hydrogen is desired, for example for fuel cell applications or when hydrogen is fed to a hydrogen gas grid an uncoupled system is desired since this eliminates/reduces downstream post-processing steps. Regeneration of CaCO₃ to CaO and CO₂ provides a possibility for pre-combusting carbon capture. A uncoupled SEWGS system releases a lot of high quality heat which can be integrated and used for reactor heating.

2.2 SYSTEM DESIGN

A pyrogasification-sorption-shift system is designed, the general process configuration is given in figure 4. Slow pyrolysis is used for the removal of volatiles from the biomass input and for char production. Heat to the pyrolysis system is delivered by the Sorption-Shift System. Volatiles are led to a catalytic steam reforming system to be reformed into a hydrocarbon free syngas, which is also heated by the sorption-shift system. Finally an uncoupled sorption-shift-system captures CO

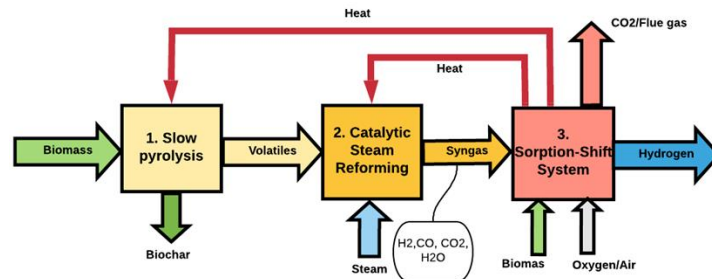


Figure 4: general system configuration pyrogasification sorption shift system

indirectly and CO₂ directly. Biomass is combusted in the regenerator for heat supply for calcination of CaCO₃, next to that also to supply sufficient heat for the pyro-gasification system.

Biomass can either be combusted with air or with oxygen (oxy-fuel combustion). Using air for combustion leads to a relative low partial CO₂ pressures in the regenerator due to large quantities of nitrogen being added, resulting in efficient regeneration at lower temperatures[7], furthermore air is abundantly available while oxygen is relative expensive. Using oxygen for combustion brings safety issues, but provides a pure stream of CO₂ instead of flue gas. Pure CO₂ has much more applications compared to flue gasses, flue gasses can be fed to for example greenhouses for carbon capture, but pure CO₂ has next to that also applications in the food and chemical industry. The model which will be further discussed in this paper will use air for biomass combustion in the regenerator. Using oxygen instead of air can become especially interesting when a pyrogasification-sorption-shift system is combined with a hydrogen electrolysis system which produces oxygen as by-product.

A more detailed process configuration is displayed in figure 5. Table 1 displays the reactor selection and motivation. Heat integration is also included in the reactor design. A pyrolysis temperature of 500 °C is selected, but depending on the required biochar specifications pyrolysis temperature can be changed (increased for higher quality biochar). A two-stage reforming system has been selected because of 1) energy efficiency: a lower quality heat is required for the pre-reformer which can largely be provided by cooling of the hot gasses leaving the reformer and 2) a two-stage reforming system has proven to provide a hydrocarbon-free syngas, reaching thermodynamic equilibrium [5,17]. The reason why a two-stage sorption-shift system is selected is for the same reasons: 1) Energy efficiency, the High Temperature Shift (HTS) system operates at 650 °C, here roughly 90% of CO₂ is captured, releasing most of the heat of reaction in the HTS reactor. The HTS

reactor also acts as steam generator, providing steam for the reforming system at 625 °C. The Low Temperature Shift (LTS) reactor operates at 550 °C, capturing roughly the 10% of the remaining CO₂, the H₂ gas is cooled prior and post-reaction for the LTS reactor, such that steam of the same quality (625 °C) can also be produced, the reason why cooling is not implemented directly in the LTS reactor is because direct cooling would result in a lower quality steam (525 °C). The other reason why a LTS and HTS system are used in series is because a two-stage system will result in a gas composition closer to thermodynamic equilibrium due to relative fast reaction rates in the HTS. For both the sorption-shift system as for the reforming systems applies that a two stage system is more robust.

The flue gasses leaving the regenerator contain a lot of sensible heat, this heat is utilized for additional reactor heating, especially for bringing the reformer to 750 °C and providing heat for the pyrolysis system. Remaining low quality sensible heat in the flue gasses is used for air-pre-heating prior to combustion.

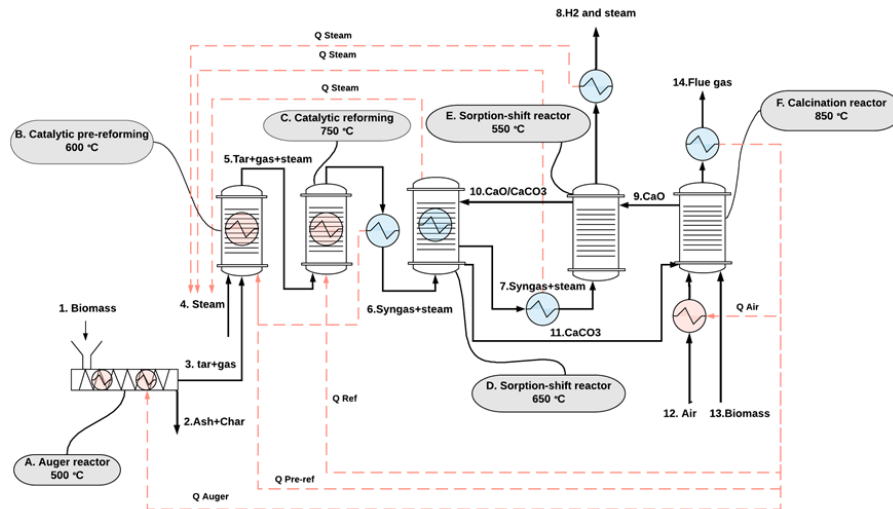


Figure 5: Design pyrogasification-sorption-shift system

Tab. 1: Reactor selection and motivation

Reactor	Reactor type	Motivation
A: pyrolysis	Auger reactor	<ul style="list-style-type: none"> Controlled residence time and heating rate Flexible with biomass input Promotes secondary cracking reactions Easy ash and char removal
B: Pre-reforming	Fixed bed	<ul style="list-style-type: none"> Good gas -solid contact No blowouts Due to gas/steam heating prior to reforming even heat distribution is expected
C: Reforming	Fixed bed	
D: HTS	Fluidized bed	<ul style="list-style-type: none"> Good heat distribution due to particle mixing is required due to highly exothermic reaction in HTS and LTS reactor and combustion in the regenerator Easy bed material transport (overflow)
E: LTS	Fluidized bed	
F: Regeneration	Fluidized bed	

2.3 ASPEN PLUS MODEL

An Aspen Plus model is constructed to simulate the above described process, the constructed flowsheet is displayed in figure 6. Figure 6 is a simplified overview which only displays mass flows, for clarity heat flows are left out, but are explained in the section below. UNIQUAC is selected as physical property method due to non-ideal behaviour of tars (for example phenol), an activity coefficient based model like UNIQUAC can cope with this unideal behaviour. ReTRAN statements are used to decompose biomass into the elemental composition in the pyrolysis reactor and regenerator respectively, this is done for simulation purposes.

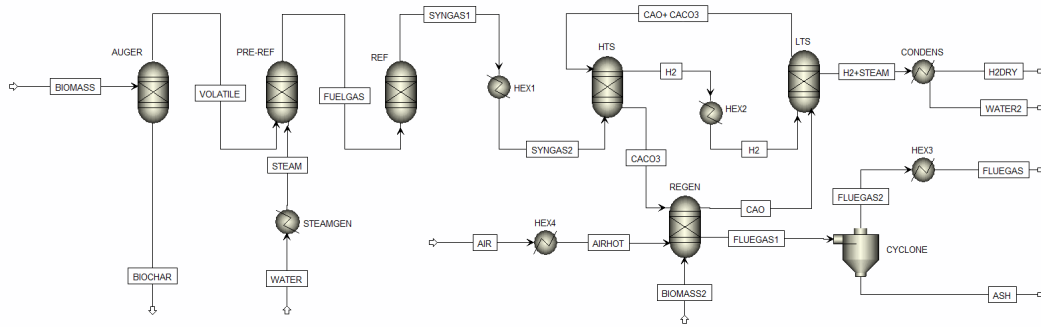


Figure 6: Aspen plus flowheet pyrogasification-sorption-shift-system

The pyrolysis system is modelled using RYIELD reactors based on results found by Phan et al. on slow pyrolysis of pinewood at temperatures of 500 °C [4], three RYIELD reactors are used to model each product accurately and to close elemental balances within the simulation. It is important to note that multiple reactors are used for simulation purposes, the pyrolysis system consists of one auger reactor, with biomass input, char and volatiles as output and requires one heat supply, figure 6 already displays the simplified flowsheet. The Pre-reformer is also modelled as RYIELD reactor based on results found by Solar et al. [15] on slow pyrolysis of pine wood followed by catalytic processing of produced volatiles for increased gas yield. The reformer, HTS, LTS regenerator are all modelled at thermodynamic equilibrium, based on minimization of the Gibbs free energy as shown in Eq. 6. where n_i is the number of moles of component i , and μ_i is the chemical potential of component i .

$$dG = -SdT + vdP + \sum_{i=1}^N \mu_i dn_i = 0 \quad (6)$$

For heat transport, a design specification (boundary condition) is implemented with respect to the minimum pinch point in Heat Exchangers (HEX) which should be at least 25K. HEX 1 cools the produced syngas leaving the reformer (750 °C), this heat is used to heat the pre-reformer (600 °C). Heat for steam generation is taken from the HTS reactor directly, and from HEX2 and the LTS reactor. HEX 3 supplies heat for the reformer, pre-reformer and auger reactor respectively. The remaining heat in the flue gas is used for air pre-heating in HEX 4.

Per 1kg of biomass input at the auger 1.5 kg of steam is generated in the standard system, translating to a S/C ratio of 4.57 in the pre-reformer. This high S/C ratio is caused because char is removed from the auger, the modelled biomass contains moisture and produced low quality pyrolysis oils has a large aqueous fraction. The maximum steam temperature which can be obtained in the system is capped at 625 °C based on temperature limitations for high quality steel alloys for high temperature steam production[22]. The hot flue gasses are used to heat the reformer, pre-reformer and auger reactor respectively. The air ratio is modelled at 2.5 at the regenerator, to increase air inlet

temperature, low temperate heat integration is implemented using flue gasses for air pre-heating. The regenerator is modelled in such a way that sufficient heat can be provided to the pyrogasification system and so that the required regenerator temperature (850 °C) is reached, this is done by adding extra biomass for combustion to the regenerator.

2.4 MATERIALS

Pine wood is selected as biomass input, the proximate and ultimate analysis of the used pinewood for process simulations is displayed in table 2 and 3 [4]. The proximate and ultimate analysis are checked with comparable pinewood species in the Phyllis database [23] to validate the composition. The HHV of the used biomass species is 18,00MJ/kg.

Tab. 2: Proximate analysis Biomass

Pinewood	[wt%]
Moisture	8,0%
Volatiles	78,7%
Ash	0,4%
Fixed Carbon	12,9%

Tab.3: Ultimate analysis Biomass (daf)

Pinewood	[wt%]
C	49,4%
H	6,0%
N	0,0%
O	44,6%

The process is modelled in Aspen Plus under the described process temperatures and conditions: pyrolysis at 500 °C, reforming at 750 °C, HTS at 650 °C, LTS at 550 °C, regenerator temperature at 850 °C and a S/C ratio in the reformer of 4,57.

3. RESULTS

The simulation results are given in this section as well as the results of the sensitivity analysis.

3.1 SIMULATION RESULTS

The system input and system output are displayed in table 4 and table 5 for the standard system simulation. The process is modelled with a biomass input for the auger reactor of 1,00 kg/s, resulting in 1,5 kg/s of steam generation given a S/C ratio of 4,57. The amount of additional combusted biomass in the regenerator is a model output based on heat requirements on subsystems, the amount of supplied air to the regenerator is calculated using a or ratio of 2.5. Per ton of biomass input (dry and ash free) the system produces 186 kg biochar and 59 kg hydrogen. Given the standard process conditions discussed in section 2, the overall system energy efficiency is 74,4% (equation 7), the cold gas efficiency is 42,2% (equation 8) and the "biomass to char" energy efficiency is 32,2% (equation 9). The energy flowrate (En) of biomass, char and hydrogen (chemical energy) is calculated by multiplying mass flow (table 4 and 5) with the higher calorific value of biomass, char and hydrogen respectively. For total biomass energetic input determination, both auger and regenerator biomass input is used.

$$\eta_{tot} = \frac{En_{char} + En_{H_2}}{En_{bm-aug} + En_{bm-regen}} \quad (7)$$

$$\eta_{cold-gas} = \frac{En_{H_2}}{En_{bm-aug} + En_{bm-regen}} \quad (8)$$

$$\eta_{char} = \frac{En_{char}}{En_{bm-aug} + En_{bm-regen}} \quad (9)$$

Tab. 4: System input

Material	Reactor(in)	Mass flow
Biomass	Auger	3,60*10 ³ kg/h
Biomass	Regenerator	1,54*10 ³ kg/h
Air	Regenerator	2,03*10 ⁴ kg/h
Water	Boiler (HTS/LTS)	5,40*10 ³ kg/h

Tab.5: System output

Material	Reactor(out)	Mass flow
Biochar	Auger	8,74*10 ² kg/h
Hydrogen	Condensor	2,94*10 ² kg/h
Flue gas	Regenerator	2,50*10 ⁴ kg/h
Water	Condensor	4,74*10 ³ kg/h
Ash	Cyclone	5,90 kg/h

The biochar and hydrogen product are further analysed and characterized displayed in table 6 and 7.

Tab. 6: Biohar characteristics[4]

Biochar	
C	89,2 %
H	3,1 %
O	6,1%
Ash	1,6%
HHV	34,2MJ/kg

Tab.7: Hydrogen gas characteristics

Hydrogen rich gas	Mass flow	V% (dry)
CO	1,4 kg/h	0,038%
CO ₂	15,9 kg/h	0,266%
CH ₄	0,6 kg/h	0,028%
H ₂	276,3 kg/h	99,67%

3.2 SENSITIVITY RESULTS

A sensitivity analysis is performed with respect to LTS temperature, regenerator temperature and S/C ratio.

Figure 7 displays the hydrogen purity as well as the concentration of containments (CO, CO₂ and CH₄) in the produced hydrogen gas (dry) as function of LTS reactor temperature.

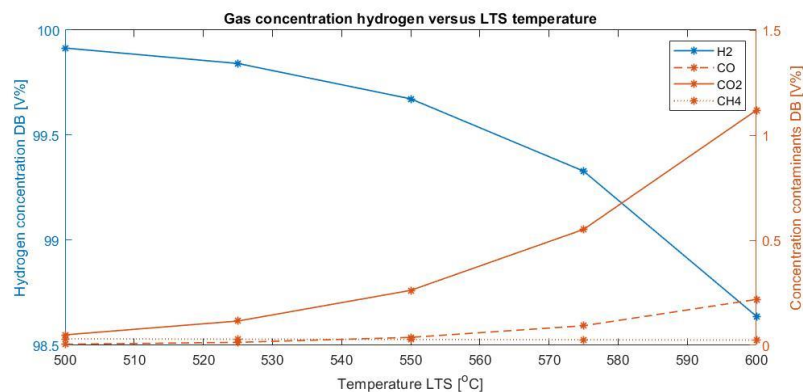


Figure 7: LTS temperature versus gas concentrations product gas

Efficiency calculations show no significant increase/decrease of the overall system efficiency as function of the LTS temperature: 74,4% at 500 °C to 74,6% at 600 °C. LTS temperature influences hydrogen purity: 99,91% at 500 °C to 98,64% at 600 °C, based on thermodynamic equilibrium calculations.

Figure 8 shows the impact of regenerator temperature on overall energy efficiency. The maximum efficiency point is determined at a regenerator temperature of 832 °C at 74,7%. Below this temperature there is a large drop in energy efficiency: 69,52% at 800 °C. At increasing temperatures form 832 °C up a light decrease in energy efficiency is noticed: 73,7 % at 900 °C.

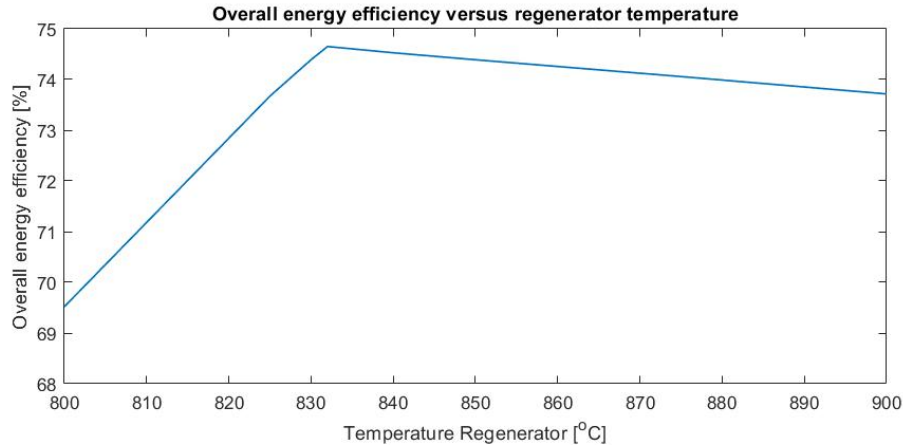


Figure 8: Regenerator temperature versus overall system efficiency

Figure 9 shows the impact of S/C ratio on total energy efficiency. An optimal S/C ratio is determined at S/C = 4.6 (74,4%). At increasing S/C there is a large drop in overall energy efficiency: 71.4% at S/C=6, while at lower S/C ratios there is no significant change in energy efficiency: 74.1% at S/C =3.2.

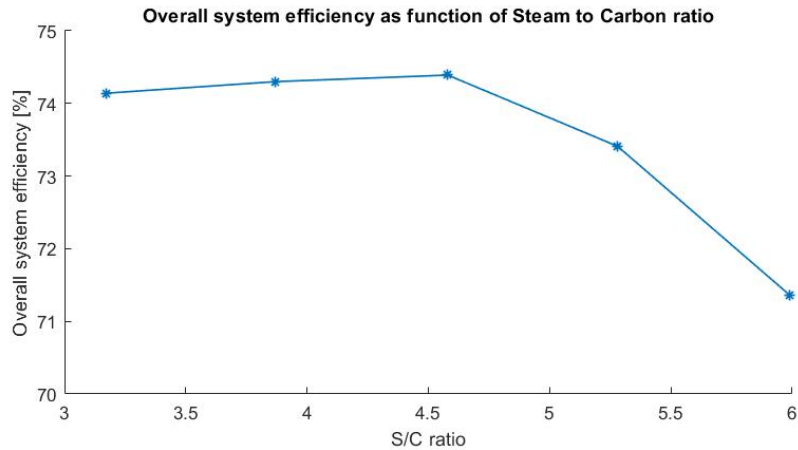


Figure 9: Overall system efficiency as function of S/C ratio

4. DISCUSSION

Simulation results show an overall energy efficiency of the system of 74,4% which is comparable to conventional gasification system given the biomass O/C ratio(0.68) which is in the 76-78% range for the given operating temperature [24]. The main difference between conventional gasification and the pyrogasification sorption-shift is product quality: the analysed system produces a high quality biochar (HHV= 34 MJ/kg) and high purity hydrogen (99,67%) compared to conventional gasification systems.

The results from the pyrolysis system are modelled in a RYIEL reactor, where experimental results are used as model input, therefore the pyrolysis model does not require validation. The results of the steam reforming system are validated using experimental research by van Rossum et al. [5] The hydrogen quality is validated using research by Li. et al.[21] as displayed in table 9. The results after reforming (stream nr.6 as displayed in figure 5) are displayed in table 8, as well as results found by van Rossum et al. both results are obtained from a reformer temperature of 777 °C and S/C of 2,7. Validation of the simulation results show that simulation results are in agreement with prior research on similar(sub) systems.

Tab. 8: Reformer product validation [5]

Species	Simulation	Experimental
H2	0,655	0,658
CO	0,129	0,143
CO2	0,216	0,199
CH4	0,000	0,000

Tab.9 Final product validation [21]

Hydrogen rich gas	Simulation	Validation
CO	0,038%	0.1%
CO ₂	0,266%	0.1%
CH ₄	0,028%	0.1%
H ₂	99,67%	99,7%

Flue gasses leaving the regenerator have relative high mass flow due to air used for combustion in the regenerator. The advantage of using air is that regeneration at lower temperatures is possible (due to lower CO₂ partial pressure). The downside is the large mass flow and relative low CO₂ concentration, resulting in increasing reactor size and limiting the possibilities for carbon capture. In order to decrease mass flow rates, and increase CO₂ concentration combustion with pure oxygen: ‘oxy-fuel combustion’ is a subject for further research. Oxy fuel combustion in the regenerator limits the heating potential of flue gasses due to lower mass flow: a system using pure oxygen most likely requires other reformer/pyrolysis heating mechanics, which can also be a subject for further research.

A novel feature of the sorption-shift reactors is the double function as both reactor and boiler, the sorption-shift system has enough capacity, given exothermic carbonation in the reactor to supply the system with steam of 625 °C up to a S/C ratio of 4,6 (measured in the pre-reformer). 30,0% of the supplied biomass is combusted in the regenerator, this heat is mostly cycled to the endothermic steam reforming processes and is either used for steam production or to heat the reforming process itself.

The gas quality as displayed in figure 7 is influenced by LTS reactor temperature, as is expected due to decreased CO₂ equilibrium pressures in the reactor at lower process temperatures, resulting in a more pure hydrogen stream. Depending on the required hydrogen purity process conditions can be tuned within the 500-600 °C without a significant efficiency loss. The hydrogen purity which is obtained in the analyzed process is significantly higher (99,67V%) compared to traditional catalytic steam reforming (60-65V% max) or sorption enhanced gasification (80-85V% max). Such a high purity hydrogen could be implemented in a hydrogen-grid without further downstream upgrading. Fuel cell applications require hydrogen of 99,97% purity (max 300ppm pollutants), in order to reduce pollutants eve more downstream upgrading is required: temperature and pressure swing absorption can be used to obtain a fuel cell graded hydrogen.

The sensitivity analysis with respect to regenerator temperature identified an energy shortage in the reformer when regenerator temperatures dropped below 832 °C resulting in a large

energy penalty in the system. The energy shortage is caused by the high quality heat which is required at the reformer. No problems with respect to auger heating and steam generation have been identified, reformer heating is identified as a system bottle neck.

By providing a double function to the shift reactors steam can be generated without additional heat requirements. Figure 9 shows even a small decrease in overall system efficiency when the S/C ratio drops below 4.6. This decrease is caused by the fact that hot steam provides heat for the pre-reformer, when less steam is added, additional heat from the regenerator is required. When the S/C ratio drops below 4.6 the shift reactors require additional cooling to maintain their temperature, this heat is lost and cannot be utilized in the system. Hot flue gasses are recirculated for reformer and auger reactor heating. Within the simulations a boundary condition for minimal pinch point: 25 °C is introduced. The heating system increases system complexity and cost, determining and optimizing HEX cost is of high importance when determining the financial system feasibility.

5. FURTHER RESEARCH

This article discusses the design of a novel pyrogasification sorption-shift system. The system is analysed and modelled in Aspen plus in order to determine the technical feasibility of the process. The designed system requires further optimization due to identified bottlenecks: pre-reformer/reformer heating and limited flue gas carbon capture applications. Furthermore there are unanswered questions with respect to cost and biomass input variation which are not discussed in this research. Further research is recommended with respect to the following topics:

- i. Cost efficiency optimization of the current design with respect to heat exchanger optimization. Increasing pinch points in heat exchangers reduces heat integration and thus system efficiency, but increases the LMTD in heat exchanger resulting in lower required HEX surface area which reduces capital cost. A cost model needs to be designed to optimize sizing of heat transfer equipment.
- ii. Cost efficiency optimization of the current design with respect to reactor size. S/C ratio has a direct influence on flow rate and thus reactor size, as well as the ER and type of oxidant. If for example oxygen is used for combustion flue gas volume/mass flows reduce significantly reducing size and cost of the regenerator.
- iii. Cost efficiency optimization of the current design with respect to LTS temperature, this temperature can be optimized taking into account reaction rates and downstream gas upgrading cost.
- iv. It is recommended to analyse an alternative system which uses oxygen for combustion in the regenerator and adds a small fraction of oxygen to the reformer. Such a system will have reduced efficiency, since part of the product is combusted in the reformer, but system complexity reduces significantly, especially with reformer heating identified as bottleneck. Furthermore adding oxygen in the regenerator makes it possible to capture a pure stream of CO₂ leaving the regenerator.
- v. Model the system with lower quality biomass types which contain more moisture and ash. Ash is separated prior to the reformer in an auger reactor and steam is required for the reformer process. Using a lower quality biomass can contribute to lower operation expenses and increased sustainability due to the relative wide availability of lower quality biomass, for example as logging residues or as landscape care residues.
- vi. Analyse and model CaO replacement strategies. CaO has a decreasing activity over multiple recycles[7]. The designed aspen plus model can be extended to analyse different

replacement strategies with respect to system efficiency, reactor sizing and operational expenditure.

6. CONCLUSIONS

A pyrogasification sorption-shift system for the production of high purity hydrogen (99,67%) and high quality biochar(HHV=34MJ/kg) out of biomass has been analysed and modelled in Aspen Plus. The analysed system uses an auger reactor for pyrolysis for the production of a high quality biochar. A two-stage reforming system produces a hydrocarbon free syngas. Finally a SEWGS system is designed and modelled for the production of high purity hydrogen and for pre-combustion carbon capture. Heat integration is modelled, which shows a large potential for implementation of waste heat from the SEWGS system. Sorption-Shift reactors have a double function in the designed system: increase hydrogen purity and act as steam generator providing steam for the reforming processes. Simulation results are validated and shown an overall system energy efficiency of 74,4% and cold gas efficiency of 44,2%. The overall system efficiency is comparable to conventional biomass gasification systems. Higher quality products are obtained with much more versatile high-end applications. Sensitivity analysis show robustness with respect to auger reactor heating and S/C ratio's up to 4.6, reformer heating is identified as a system bottleneck. Further research is required with respect to cost optimization (reactor and HEX sizing) and a simplified system configuration should be analysed using oxy-fuel combustion in the regenerator as well as oxygen addition in the reformer for heat supply by partial combustion.

LITERATURE

1. Rosen, M. A. & Koohi-Fayegh, S. The prospects for hydrogen as an energy carrier: an overview of hydrogen energy and hydrogen energy systems. *Energy, Ecol. Environ.* **1**, 10–29 (2016). <https://doi.org/10.1007/s40974-016-0005-z>
2. Oliveira, F. R. *et al.* Environmental application of biochar: Current status and perspectives. *Bioresour. Technol.* **246**, 110–122 (2017). <https://doi.org/10.1016/j.biortech.2017.08.122>
3. Tripathi, M., Sahu, J. N. & Ganesan, P. Effect of process parameters on production of biochar from biomass waste through pyrolysis: A review. *Renew. Sustain. Energy Rev.* **55**, 467–481 (2016). <https://doi.org/10.1016/j.rser.2015.10.122>
4. Phan, A. N., Ryu, C., Sharifi, V. N. & Swithenbank, J. Characterisation of slow pyrolysis products from segregated wastes for energy production. *J. Anal. Appl. Pyrolysis* **81**, 65–71 (2008). <https://doi.org/10.1016/j.jaap.2007.09.001>
5. Rossum van, G. *Steam reforming and gasification of pyrolysis oil.* (2009). <https://doi.org/10.3990/1.9789036528894>
6. Mahishi, M. R. & Goswami, D. Y. Thermodynamic optimization of biomass gasifier for hydrogen production. *Int. J. Hydrogen Energy* **32**, 3831–3840 (2007). <https://doi.org/10.1016/j.ijhydene.2007.05.018>
7. Florin, N. H. & Harris, A. T. Enhanced hydrogen production from biomass with in situ carbon dioxide capture using calcium oxide sorbents. *Chem. Eng. Sci.* **63**, 287–316 (2008). <https://doi.org/10.1016/j.ces.2007.09.011>
8. Hejazi, B., Grace, J. R., Bi, X. & Mahecha-Botero, A. Steam gasification of biomass coupled with lime-based CO₂ capture in a dual fluidized bed reactor: A modeling study. *Fuel* **117**, 1256–1266 (2014). <https://doi.org/10.1016/j.fuel.2013.07.083>

9. Pfeifer, C. *Sorption-enhanced gasification. Fluidized Bed Technologies for Near-Zero Emission Combustion and Gasification* (2013). <https://doi.org/10.1533/9780857098801.4.971>
10. Demirbas, A. Determination of calorific values of bio-chars and pyro-oils from pyrolysis of beech trunkbarks. *J. Anal. Appl. Pyrolysis* **72**, 215–219 (2004). <https://doi.org/10.1016/j.jaap.2004.06.005>
11. Brassard, P., Godbout, S. & Raghavan, V. Pyrolysis in auger reactors for biochar and bio-oil production: A review. *Biosyst. Eng.* **161**, 80–92 (2017). <https://doi.org/10.1016/j.biosystemseng.2017.06.020>
12. Campuzano, F., Brown, R. C. & Martínez, J. D. Auger reactors for pyrolysis of biomass and wastes. *Renew. Sustain. Energy Rev.* **102**, 372–409 (2019). <https://doi.org/10.1016/j.rser.2018.12.014>
13. Mahishi, M. R. & Goswami, D. Y. An experimental study of hydrogen production by gasification of biomass in the presence of a CO₂ sorbent. *Int. J. Hydrogen Energy* **32**, 2803–2808 (2007). <https://doi.org/10.1016/j.ijhydene.2007.03.030>
14. Lv, P. *et al.* Bio-syngas production from biomass catalytic gasification. *Energy Convers. Manag.* **48**, 1132–1139 (2007). <https://doi.org/10.1016/j.enconman.2006.10.014>
15. Solar, J. *et al.* Influence of temperature and residence time in the pyrolysis of woody biomass waste in a continuous screw reactor. *Biomass and Bioenergy* **95**, 416–423 (2016). <https://doi.org/10.1016/j.biombioe.2016.07.004>
16. Pfeifer, C., Puchner, B. & Hofbauer, H. In-situ CO₂-absorption in a dual fluidized bed biomass steam gasifier to produce a hydrogen rich syngas. *Int. J. Chem. React. Eng.* **5**, (2007). <https://doi.org/10.2202/1542-6580.1395>
17. Anis, S. & Zainal, Z. A. Tar reduction in biomass producer gas via mechanical, catalytic and thermal methods: A review. *Renew. Sustain. Energy Rev.* **15**, 2355–2377 (2011). <https://doi.org/10.1016/j.rser.2011.02.018>
18. Florin, N. H. & Harris, A. T. Hydrogen production from biomass coupled with carbon dioxide capture: The implications of thermodynamic equilibrium. *Int. J. Hydrogen Energy* **32**, 4119–4134 (2007). <https://doi.org/10.1016/j.ijhydene.2007.06.016>
19. Hanaoka, T. *et al.* Hydrogen production from woody biomass by steam gasification using a CO₂ sorbent. *Biomass and Bioenergy* **28**, 63–68 (2005). <https://doi.org/10.1016/j.biombioe.2004.03.009>
20. Pfeifer, C.; Puchner, B., Proll, T.; Hofbauer, H. H₂-Rich Syngas from Renewable Sources by Dual Fluidized Bed Steam Gasification of Solid Biomass. *12th Int. Conf. Fluid.* 889–895 (2007).
21. Li, B. *et al.* Simulation of sorption enhanced staged gasification of biomass for hydrogen production in the presence of calcium oxide. *Int. J. Hydrogen Energy* **45**, 26855–26864 (2020). <https://doi.org/10.1016/j.ijhydene.2020.07.121>
22. Raj, B., Choudhary, B. K. & Singh Raman, R. K. Mechanical properties and non-destructive evaluation of chromium - Molybdenum ferritic steels for steam generator application. *Int. J. Press. Vessel. Pip.* **81**, 521–534 (2004). <https://doi.org/10.1016/j.ijpvp.2003.12.010>
23. Phyllis2 - Database for the physico-chemical composition of (treated) lignocellulosic biomass, micro- and macroalgae, various feedstocks for biogas production and biochar. <https://phyllis.nl/?nr=ECN-M--07-024> (2020).
24. Prins, M. J., Ptasiński, K. J. & Janssen, F. J. G. From coal to biomass gasification: Comparison of thermodynamic efficiency. *Energy* **32**, 1248–1259 (2007). <https://doi.org/10.1016/j.energy.2006.07.017>